NOVEL POLYELECTROLYTE COMPLEXES FOR ORAL INSULIN DELIVERY

CHIDINMA O. IBIE

PhD **2013**

NOVEL POLYELECTROLYTE COMPLEXES FOR ORAL INSULIN DELIVERY

CHIDINMA O. IBIE

A thesis submitted in partial fulfilment of the
requirements of the
Robert Gordon University
for the degree of Doctor of Philosophy

November 2013

ACKNOWLEDGEMENTS

I would like to acknowledge the immense support and expertise provided by my supervisors Drs Colin Thompson and Rachel Knott during the course of this research. Their immeasurable and unequalled mentorship comes highly appreciated. I would also want to acknowledge the continuous encouragement and professional support provided by Dr. Kerr Matthews my former MRes supervisor and mentor, without whom I probably may not have had the opportunity to do my PhD in this area.

Special thanks to all members of the technical staff, in particular Mrs Liz Hendrie, Laurie Mearns, Chris Fletcher, Tina Lowes, Margaret Brown, John Wood, Brian DeJonckheere, Maureen Byres and Raymond Reid who provided assistance to me at critical stages of the data collection process. I also have to thank Margaret Mullin and Denise Gilmour of the University of Strathclyde, Glasgow who were responsible for TEM and elemental analysis respectively.

I also acknowledge my friends and former colleagues in PD1 Drs V. Paudyal, M. Dapar and E. Medu as well as Okey Ndu and Caroline McLeod who made the long hours of work pass quickly. I would also like to express immense gratitude to my husband and daughter Davies and Michelle Ibie and parents Prof. and Mrs R. I. Udegbunam for their love and emotional support through the turbulent PhD experience.

Finally, I want to acknowledge the Institute for Health and Welfare Research, Robert Gordon University and the Scottish Overseas Research Scholarship Awards Scheme for providing the funding for my PhD.

ABSTRACT

Oral delivery of insulin used for the management of Type 1 Diabetes could be referred to as one of the major long term goals of diabetes research. However, the bioavailability of orally administered insulin is significantly compromised by enzymatic degradation in the GI tract and poor enteral absorption of the protein due to its macromolecular size and hydrophilicity. Nano-sized polymer-protein polyelectrolyte complexes (PECS) formed by electrostatic interactions between insulin and Polyallylamine-based polymers at pH 7.4 have been adapted to facilitate oral insulin delivery.

Polyallylamine (15kDa) was quaternised by methylation of its primary amines using methyl iodide to yield quaternised Paa (QPaa). Average level of polymer quaternisation was determined by elemental analysis and was found to be 72 ± 2mol%. Subsequent thiolation of Paa and QPaa using two different thiolation procedures involving carbodiimide mediated conjugation to N-acetylcysteine (NAC) and modification of the polymers using 2-iminothiolane hydrochloride yielded their respective NAC and 4-thiobutylamidine (TBA) conjugates: Paa-NAC/QPaa-NAC and Paa-TBA/QPaa-TBA. Estimation of the free thiol content of these thiomers by iodometric titration showed that both Paa-NAC and QPaa-NAC displayed 60 ± 1.2 and 60 ± 4.3µmol free thiol groups per gram polymer, while Paa-TBA and QPaa-TBA conjugates displayed 490 ± 18 and 440 ± 21µmol free thiol groups per gram polymer respectively.

Mixing optimal mass ratios of each polymer and insulin in Tris buffer at pH 7.4 resulted in the formation of soluble nanocomplexes. Complexes were characterised by transmittance measurements, particle size analysis, zeta potential, complexation efficiency, and transmission electron microscopy (TEM). Stable polymer-insulin complexes were observed to have hydrodynamic sizes between 50-200nm, positively charged zeta potential values ranging between 20-40mV and high insulin complexation efficiency (> 90%). Complexation of insulin with TBA conjugates however appeared to alter insulin conformation affecting the detection of complexed insulin by HPLC. TEM analysis revealed the formation of bilayered nanovessicles as well as conventional single-layered nanoparticles on complexation of insulin with QPaa and thiolated Paa/QPaa derivatives. *In-vitro* assessments of enzyme-protective effect of QPaa, Paa-NAC and QPaa-NAC insulin complexes showed that when compared to a free insulin control, all the aforementioned complexes could protect insulin from degradation by trypsin and α-chymotrypsin, but not from pepsin. *In-vitro* mucin adsorption assays showed that all polymers exhibited a similar mucoadhesive profile with their corresponding insulin PEC, with thiolated Paa derivatives adsorbing >20% more mucin than Paa. Thiolation of QPaa did not result in a

noticeable improvement in its mucoadhesive capacity indicating that polymer-mucin thiol-disulphide interactions may be hindered by the presence of quaternary groups.

The IC_{50} of each polymer was determined by MTT assays carried out on Caco-2 cells with or without the inclusion of a 24-hour cell recovery period. An MTT assay conducted without a recovery period indicated that quaternisation of Paa was associated with a 6-fold improvement in its IC_{50}; also cells subjected to a 24-hour recovery period following treatment with QPaa (0.001-4mgml^{-1}) showed no signs of toxicity. Thiolation of Paa resulted in slight (≤ 2 fold) improvements in IC_{50}, while thiolation of QPaa resulted in a decrease in IC_{50} values obtained both with and without a cell recovery period. Each polymer was subsequently labelled with rhodamine B isothiocyanate (RBITC) and complexed with fluorescein isothiocyanate (FITC)-insulin. Monitoring uptake of these complexes by Caco-2 cells using fluorescence microscopy with DAPI staining indicated that uptake of QPaa and QPaa-TBA complexes was mainly intracellular being localised within the perinuclear area of cells highlighted by DAPI. Hence, intracellular uptake of PECS by Caco-2 cells was enhanced by Paa quaternisation and TBA-based thiolation of QPaa.

Keywords: Polyelectrolyte complexation, insulin, polyallylamine, mucoadhesion, thiolation, quaternisation, nanoparticles, transmucosal transport.

1. INTRODUCTION

The regulation of blood glucose supply in the body is mediated by the hormone insulin [1]. Insulin is a peptide hormone secreted by the beta-cells of the pancreatic islets, on stimulation by an influx of glucose into the cells [2]. Secreted insulin is conveyed directly to the liver via the portal vein, from where it maintains glucose homeostasis by stimulating the hepatic anabolism of glucose and storage compounds like glycogen depending on the energy requirements of the peripheral tissues [2]. When the body is in the fasting state, insulin concentrations are low stimulating hepatic glucose production (by gluconeogenesis and glycogenolysis) and subsequent release of glucose into the circulation while post-prandial insulin concentrations are high suppressing hepatic glucose synthesis and facilitating the entry of glucose into peripheral tissues [1].

Acute insulin deficiency in humans caused by auto-immune destruction of pancreatic beta-cells results in Insulin Dependent Diabetes Mellitus (IDDM or Type I diabetes), a condition characterised by chronic hyperglycaemia resulting in physiological anomalies such as polyuria (excretion of large volumes of dilute urine), polydipsia (marked thirst), polyphagia (difficulty in swallowing) and weight loss in sufferers [2]. Other types of diabetes include Non-insulin Dependent Diabetes Mellitus (or Type II diabetes) which is due to insulin resistance and gestational diabetes which is induced by pregnancy [3].

Generally, diabetes is irreversible and treatment is normally geared towards maintaining glucose concentration within safe/healthy limits, normally between 3.5-8mmol/L [1]. Maintaining adequate glycaemic control in people suffering from IDDM, requires the administration of exogenous insulin [3]. The use of exogenous insulin therapeutically is limited by the fact that due to the proteinous constituents of the hormone, insulin is only effective if administered parenterally. This is because the body's digestive processes have been designed to breakdown any ingested protein/peptide without undue differentiation between normal dietary proteins and therapeutic ones. Therefore, oral administration of insulin is currently not feasible and exogenous insulin formulations are often given subcutaneously [4]. The availability of only the invasive route for insulin delivery is a major constraint in the management of IDDM, because the chronic nature of the condition implies that patients require insulin therapy for relatively long periods of time. Single daily doses of parenteral insulin have also been found to be inadequate in sustaining glycaemic control and most patients require at least two to three injections of insulin daily for optimum control of blood glucose levels [5]. This treatment procedure predisposes diabetics to physiological stress and pain due to multiple injections, risk

of infections and local reactions at injection sites and complications in the administration process like precipitation of insulin in the injection pump [3].

Also, parenteral administration of insulin creates a significant difference in the normal physiological distribution of insulin in the body [6, 7]. Normally, insulin concentrations are much higher in the portal circulation than in the systemic circulation as opposed to parenterally administered insulin which brings the concentration of systemic insulin up to that in the portal circulation. This non-physiological insulin distribution has been associated with the occurrence of peripheral hyperinsulinaemia which causes hypoglycaemia, weight gain, neuropathy, retinopathy, atherosclerosis and hypertension due to insulin resistance in diabetics [7]. The need to eliminate these drawbacks as well as offer diabetics a better quality of life has prompted researchers to explore other routes of delivering insulin without compromising the therapeutic effects of the drug. The oral route offers an excellent alternative being the easiest and most convenient route of drug administration and also demanding less time and effort from medical personnel and carers [8]. Exogenous insulin distribution on oral administration also mimics the natural physiological fate of insulin in the body, closely replicating the direct delivery of endogenous insulin to the liver, where its effects of suppressing or facilitating hepatic glucose production are fundamental in sustaining glucose homeostasis [9].

Therefore, research in the past years has been focused on the development of novel formulations of insulin that can deliver therapeutic doses of the drug in its active form to its site of action through the oral route.

1.1. PROBLEMS ASSOCIATED WITH ORAL INSULIN DELIVERY

The achievement of a suitable oral insulin formulation is mitigated by the susceptibility of insulin to proteolytic digestion in the gut and difficulties in the systemic absorption of hydrophilic macromolecules like proteins from the GIT. Insulin is degraded in the GIT by pepsin in gastric juice and proteases (carboxypeptidase, chymotrypsin and trypsin) in the intestinal lumen [3, 5, 6, 7]. Fragments from the above process are further broken down by brush border peptidases and a cytosolic enzyme referred to as insulin-degrading enzyme (IDE) [10, 11]. IDE is a neutral thiol metalloproteinase involved in intracellular metabolism of insulin in hepatocytes, adipocytes, kidney, muscle cells, enterocytes and other cells [12].

Insulin absorption from the gut is limited by the GIT epithelium, a semipermeable lipoidal sieve consisting of a layer of columnar epithelial cells tightly held together by tight junctions or zona occludens [11, 13]. The GIT membrane only permits the transcellular passage of lipophilic molecules across it or paracellular transport of small hydrophilic molecules through the

numerous aqueous pores between the cells [13]. Insulin being a hydrophilic macromolecule with logP values < 0, is therefore unable to permeate the GIT epithelium unaided either transcellularly or paracellularly [14, 15], considering the molecular weight cut-off for the paracellular pathway is estimated to be 200Da [14]. The presence of the glycocalyx, a layer of mucus consisting of sulphated mucopolysaccharides which lies above the intestinal mucosa also constitutes a further permeation barrier (figure 1) which must be overcome before ingested drugs can be absorbed [3, 5].

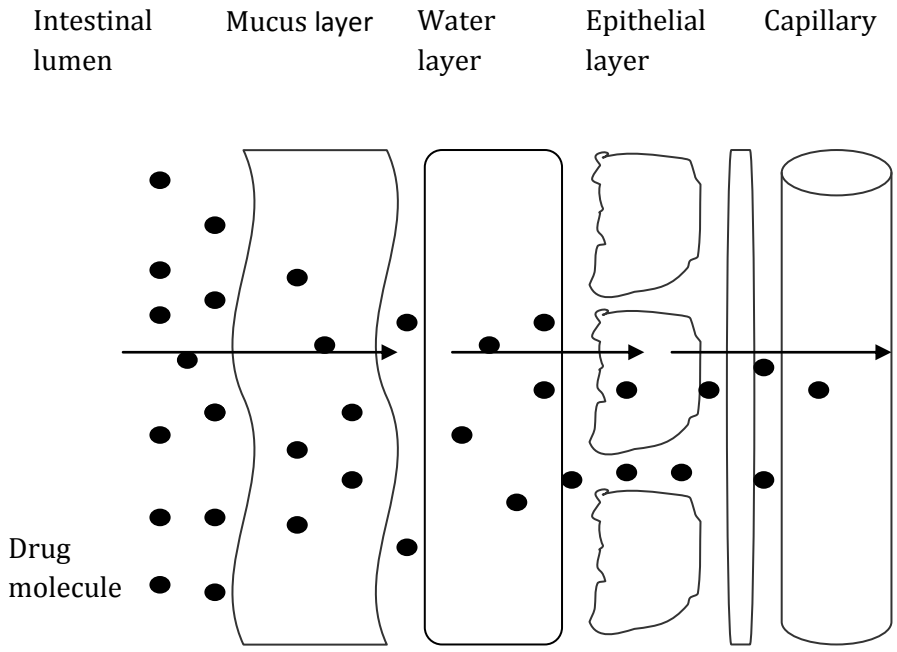

Fig. 1: Barriers to intestinal drug absorption.

Digestive enzymes that degrade proteins can also be found in the intestinal microvilli, mucus or glycocalyx [5, 14]. Consequently, the bioavailability of insulin given orally is markedly low, estimated to be less than 1% [16].

Another problem encountered in the development of oral insulin formulations is retaining the integrity and bioactivity of insulin during formulation and manufacturing procedures. Insulin like all proteins has a fragile and complex internal structure that defines its biological activity [5]. Disturbances of the primary, secondary, tertiary or quarternary structure of insulin can lead to deactivation and/or denaturation leading to loss of pharmacological activity [5]. Key determinants of protein stability include the intrinsic conformational stability of the protein native, bioactive state and colloidal stability of the protein molecules in solution governed by the extent of repulsive forces between the molecules. Physical degradation of insulin may involve unfolding into its biologically inactive conformation and aggregation into oligomers at

concentrations above 0.1μM aqueous solution and hexamers with different absorption characteristics than the monomer [17]. Aggregation also has the detrimental effect of producing larger structures which exhibit poor membrane permeability. Insulin can also undergo chemical degradation involving the formation of covalent modifications like deamidation, oxidation and disulphide bond shuffling.

Process conditions can affect the integrity of the protein structure. Insulin is prone to thermally induced denaturation. High temperatures lead to a disruption of its native conformation leading to unfolding, aggregation and loss of activity. The pH of the insulin solution affects the charge density on the molecule. Excessive charge repulsion caused by the presence of highly charged insulin molecules in solution tends to destabilize its folded conformation causing a loss of activity. While, at pH values close to the isoelectric point (pI) where proteins have both positively and negatively charged constituents, protein-protein interactions that favour the formation of aggregates are possible. The presence of cosolutes in an insulin solution also affects its conformational stability and equilibrium solubility. These solutes can be differentiated into protein denaturants like urea and guanethidine chloride that prefer to weakly bind to the unfolded state of the protein favouring unfolding and protein stabilisers like high concentrations of sugars, polyols and ammonium sulphate that enhance the stability of insulin by binding to the bioactive conformation. Solutes like salts and electrolytes affect the intramolecular electrostatic interactions between protein molecules as well interact with charged groups on the surface of the insulin molecule. Other formulation excipients that may affect the stability of insulin in solution include preservatives and surfactants.

In spite of these militating factors, the development of oral formulations of insulin that can overcome these barriers and maximise the bioavailability of orally administered insulin is still ongoing. Various strategies focused mainly on designing stable formulations that can protect insulin from enzymatic degradation in the gut as well as facilitate its absorption from the GIT have been attempted with varying levels of success. Some approaches involve the use of known absorption enhancers like fatty acids, while others involve the use of more recent and smart polymers or carrier systems that can protect insulin from proteolytic digestion while also mediating its absorption across the GIT epithelium. Subsequent sections of this review highlight the different pharmaceutical technologies and formulations that have been developed and evaluated for oral insulin delivery.

1.2. APPROACHES IN THE DEVELOPMENT OF ORAL INSULIN FORMULATIONS

Attempts to design an efficient oral delivery system for insulin are numerous with each concept focusing on the need to ensure that sufficiently therapeutic concentrations of the active drug

gets to the target sites. In order to achieve this, oral insulin delivery systems need to be stable in the GIT environment, protect the drug from enzymes that cause its inactivation and also enable enteral absorption of insulin. So far, research has indicated that only formulations that are able to efficiently and simultaneously fulfil all of the above requirements can lead to any significant improvement in the bioavailability of orally administered insulin. A detailed review of various formulations investigated for oral delivery of insulin is carried out in subsequent sections below.

1.2.1. Co-administration with functional excipients

Enzyme-protective, stabilising and absorption-enhancing agents have been administered concurrently with oral insulin in a bid to enhance bioavailability.

The concurrent use of protease inhibitors with insulin was shown to improve its bioavailability by limiting the rate of proteolytic degradation [18, 19, 20] and maximising the amount of oral insulin available for absorption. Incorporating a trypsin inhibitor into gelatine microspheres containing insulin was observed to yield an enhanced hypoglycaemic effect [21]. The bioavailability of insulin loaded into alginate/chitosan microspheres was also found to be improved by the use of betacyclodextrins which reduce hydrolysis and enzymatic degradation [22]. Examples of protease inhibitors that have been used as described include sodium glycocholate, aprotinin, bacitracin, soybean trypsin inhibitor and camostat mesilate. Studies have however indicated that protease inhibitors may be more effective in curtailing enzymatic degradation of insulin if the drug is released in the large intestine, due to the lower enzymatic activity of that region relative to the small intestine [20, 23, 24]. However, the long term effects of enzyme inhibitors on the body which include disruption of the digestion of dietary proteins, risk of absorption of unwanted or toxic proteins and the potential stimulation of protease secretion due to feedback regulations [25] could outweigh the benefits of these protease inhibitors.

Facilitating the absorption of insulin across the intestinal epithelium have resulted in the use of permeation enhancers like bile salts, salicylates, long chain fatty acids and surfactants which enhance insulin absorption by increasing the permeability of the lipid bilayer cell membranes of the epithelial cell lining [5]. It has been shown that oral insulin dispersed in different fatty acids (lauric, palmitic and stearic acid) emulsified using sodium glycocholate was capable of inducing hypoglycaemia in rabbits, with the greatest hypoglycaemic effect being observed with palmitic acid [26]. Unsaturated fatty acids containing the same number of carbon atoms were found to be unable to produce a similar effect. This difference was ascribed to the presence of double

bonds within the structure of unsaturated fatty acids causing the formation of fluid micelles that are capable of initiating minimal disruption at the lipid bilayers, when compared to the rigid micelles formed by their saturated counterparts. Surfactants like the polysorbates and chelating agents have also been included in oral insulin formulations as absorption enhancers, but relatively high concentrations of these chemicals were needed to produce cell membrane disruption and their use associated with cell membrane solubilisation and intestinal wall damage [27, 28]. The use of these absorption enhancing agents is also limited by their lack of specificity, as they compromise the integrity of the mucosal surface allowing harmful contents of the intestine like toxins and biological pathogens access to the systemic circulation.

Paracellular transport of insulin across the GIT epithelium has also been investigated. Some agents have been found to mediate the reversible and controlled opening of the tight junctions between adjacent epithelial cells increasing tight junction permeability. Zonula occludens toxin (ZOT), a protein produced by Vibrio cholera has been found to be able to effect safe, reversible and dose-dependent increase in tight junction permeability by acting specifically on the actin filaments of the zona occludens found at the jejunum and ileum only [5]. *In vivo,* ZOT has been shown to elicit a 10-fold increase in the absorption of insulin from the ileum and jejunum of rabbits, with no effect observed in the colon [29]. Diabetic animals given a combination of ZOT and insulin orally have also been shown to demonstrate survival rates and reduction in blood glucose concentration similar to those treated with parenteral insulin [5]. Other agents that have been found to be able to mediate reversible opening of the tight junctions include chitosan, thiolated polymers and some alkylglycosides [14]. However, increasing the bioavailability of oral insulin by only paracellular transport has been criticised by many researchers, who insist that this pathway is still limited by the large size of the insulin molecule [30, 31].

Studies into the beneficial effects of stabilising agents in oral insulin delivery have been carried out with results showing documented improvements of hypoglycaemic effect and insulin bioavailability when co-administered with excipients that enhance insulin stability. Peptides and proteins have a delicate and complex three-dimensional structure that is difficult to stabilise. The tendency of insulin to self-associate and aggregate has been linked to the presence of a hydrophobic segment near the beta-chain terminus [32, 33]. This destabilisation and aggregation can lead to either loss of bioactivity due to denaturation/deactivation or reduction in paracellular absorption due to association of insulin into hexameric or dimeric aggregates too large to access the paracellular route. The ability of polyol-surfactants and polymeric surfactants to offer steric stabilisation of insulin has been shown [34], while saccharides, amino acids and urea were observed to stabilise insulin by increasing the

intramolecular hydrophobic interaction of the protein [35]. Recent studies have also shown that alkylmaltosides like dodecylmaltoside have the ability to limit insulin aggregation by the formation of a complex with the drug [36]. Though, negligible improvements in bioavailability (0.5-1%) were observed after coadministration of insulin and dodecylmaltoside to diabetic rats. The Chinese plant exudate, Sanguis draxonis which has been found to stabilise oral insulin formulations by promoting disaggregation in insulin formulations elicited significant hypoglycaemic effect when co-administered with insulin in streptozocin-induced diabetic rats [37].

1.2.2. Chemical modification of insulin

Another approach employed by scientists to enhance oral absorption of insulin entails the chemical attachment of functional moieties like polymers, targeting ligands and recognition sites to the insulin molecule creating altered chemical entities with physicochemical properties that promote absorption of insulin from the GIT. Basically, the nature of the linkage used should be such that the regeneration of the insulin molecule on reaching the target site is assured. Therefore most functional moieties are attached to insulin by means of covalent or hydrolysable bonds that can be cleaved off after absorption. In cases where the active drug is to be delivered to the target site and systemic circulation as the conjugate, the pharmacological activity, pharmacokinetics, biocompatibility and renal clearance of the new entity must be well-defined.

The different types of chemically modified insulin developed for oral delivery are given below.

1.2.2.1. Polymer-insulin conjugation

Polymer-drug conjugation technology was pioneered by Jatzkewitz in 1955, who developed a depot formulation for mescaline by attaching the alkaloid to poly (N-vinylpyrrolidone) using a dipeptide spacer (glycyl-L-leucine) [38]. Abuchowski and Davis extended this concept to peptide and protein delivery by demonstrating that site-specific attachment of polyethyleneglycol (PEG) to proteins shielded digestible portions of the protein from enzymatic attack [39], yielding conjugates with improved solubility, reduced immunogenicity and allergenicity and retained bioactivity[40,41].

Recently NOBEX Corporation have developed an oral insulin delivery system comprising an amphiphillic oligomer (consisting of a short chain hydrophilic PEG unit linked to a lipophillic alkyl group) covalently bound to the lysine-29 of the ß-chain of human recombinant insulin [42]. The conjugated derivative called Hexyl-Insulin Monoconjugate 2 (HIM-2) achieves improved resistance against enzymatic degradation by steric hindrance, preventing attacking enzymes from getting to their target sites. Also the improved solubility of the drug conjugate

enhances its compatibility with most formulation excipients while the presence of an amphiphillic oligomer with both lipophillic and hydrophilic components enhances permeation, by facilitating the passage of the drug through aqueous and lipid barriers of the GIT epithelium. The attachment of oligomers to insulin also minimises the risk of the aggregation into multiple self-association forms.

However, the overall effects of the attachment of protective oligomers on insulin have to be properly evaluated and optimised. This is because the presence of these amphiphiles may interfere with the ability of the drug to bind to cell receptor sites resulting in loss of activity or they may alter the pharmacokinetics of the drug due to hindered systemic degradation and clearance [42]. Results of oral administration of HIM-2 to normal volunteers and both Type I and II diabetics showed that the conjugate elicited substantial hypoglycaemic action and a rapid absorption profile. Bioavailability studies are yet to be carried out in humans, but results of the clinical trials suggest an apparent bioavailability of 5%. The low bioavailability of this formulation indicates that more work needs to be done before this conjugate can be used therapeutically.

1.2.2.2. Conjugation of insulin to Receptor-recognisable ligands

Improving transcellular insulin absorption by conjugation of insulin to endogenous receptor-recognisable ligands to induce endocytotic internalisation of the conjugate, on binding of the ligand to its specific receptor sites has been attempted. This method of receptor mediated transcytosis has the advantage of not compromising the integrity of the cell membrane and is also unlimited by the size of the molecule being transported [14].

Endogenous cellular transport systems exploited for this purpose include the covalent attachment of cobalamin to insulin, utilising the normal Vitamin B_{12} absorption pathway for oral insulin uptake. On oral administration, the conjugated cobalamin binds to intrinsic factor (released in the stomach) in the duodenum, after which this complex subsequently travels down to the ileum and binds to the intrinsic factor receptor located on GI epithelilal cells initiating uptake of the bound insulin [43]. The cobalamin-insulin conjugate is absorbed into the bloodstream by an intrinsic factor receptor-mediated transcytotic process. The efficacy of this system is however limited by the minimal amount of intrinsic factor receptors available in the gut, hence significantly limiting the amount of insulin that can be absorbed [44].

Another receptor-recognition based oral insulin formulation is based on the conjugation of insulin to transferrin (the transport protein for iron) via disulphide linkages promoting absorption of insulin via transferrin receptor-mediated transcytosis [45, 46]. This transferrin-

conjugation based system may be more advantageous than the cobalamin-based system due to the high density of transferrin receptors in the GIT and the stability of transferrin against tryptic and chymotryptic digestion [47, 48]. Oral administration of the insulin-transferrin conjugate elicited a slow but prolonged dose-dependent hypoglycaemic effect in fasted streptozocin-induced diabetic rats [49]. Transport of insulin by transferrin-receptor mediated transcytosis was observed to be enhanced by the use of brefeldin A, a fungal metabolite toxic to intestinal epithelial cell organelles and Tryphostin-8, a GTPase inhibitor [50, 51].

The use of receptor-mediated endocytotic processes to facilitate oral absorption of insulin and improve bioavailability is limited by the fact that at high concentrations of the drug, the carrier systems become saturated [52]. Absorption can also be limited by metabolic inhibitors like dinitrophenol and by the presence of competing substrate analogs [13].

1.2.2.3. Use of Cell-Penetrating Peptides (CPPs)

These are also referred to as Protein Transduction Domains, a class of short peptides (less than 30 residues) known to translocate across the cell membrane into the cytoplasm in a receptor and energy independent manner [52, 53]. Most cell-penetrating peptides were derived from sequences of membrane interacting proteins like fusion proteins, signal peptides, transmembrane domains and antimicrobial peptides [54].

Cell-penetrating peptides transport their cargo into the intracellular compartment by directly disrupting the lipid bilayer structure or mediating cellular internalisation by endocytosis or direct translocation [55, 56]. Also, the presence of a net positive charge on these peptides has been reported to be directly related to their ability to translocate across cell membranes by the formation of electrostatic interactions with phospholipid head groups [53].

The exact mode of action of CPPs is still not clear, but investigations indicate that the pathway for cellular uptake may depend on the specific sequence of each peptide.Examples of cell-penetrating peptides used to facilitate cellular uptake of various molecules include the drosophila homeotic transcription factor antp, transcription factor VP22 from Herpes simplex virus type-1, HIV-1 transactivating transcriptional factor (TAT) and penetratin from the third helix of the homeodomain of antennapedia [52, 53]. The use of CPPs in oral delivery of insulin has however been limited to the conjugation of insulin to TAT. Conjugation of insulin to TAT has been reported to significantly increase its uptake across Caco-2 cells [57]. Penetratin has also been shown to be ineffective in the transfer of large proteins, thereby limiting its use in the formulation of oral insulin delivery systems [58]. The majority of the data obtained from the use of CPPs has indicated that they cause no toxicity in-vivo or cell membrane damage [54, 59]. The

use of CPPs as oral delivery systems is affected by the availability of relatively limited data on their use.

1.2.2.4. Protein Lipidization

Lipid modification of insulin by covalent conjugation or non-covalent complexation with hydrophobic lipid moieties increases the lipophilicity of the drug, making it more easily absorbed through the GIT epithelium and increasing its stability to enzymatic degradation [44]. Lipidization of macromolecules often results in a reduction in biological activity, therefore reversible lipidization techniques that ensure the post-absorptive regeneration of the active drug from their lipid conjugates are currently the focus of research groups developing such systems [60].

Reversible Aqueous Lipidization (REAL) technology involves the conjugation of peptide drugs to lipid moieties by attaching hydrophobic groups covalently to the drug molecule through the use of lipidizing reagents. This lipidization technique is yet to be extended to the development of insulin for oral delivery, although the system has been successfully used for oral delivery of salmon calcitonin [60]. A significant disadvantage of peptide lipidization is efflux from intestinal epithelial cells by P-glycoprotein and multidrug resistance protein 2, an effect observed with lipophillic cyclopeptides [44].

Another formulation which enhances enteral insulin absorption by increasing lipophilicity has been developed by Emisphere Technologies. This system comprises a set of carrier molecules, called Eligen carriers that are small, hydrophobic molecules that bind non-covalently to insulin, altering the tertiary structure of insulin and exposing internal hydrophobic amino acid residues that are in a complex with improved lipophilicity, increased flexibility and better absorption profile [61]. On getting into the systemic circulation, the dilution effect of the bloodstream causes the complex to dissociate leading to regeneration of insulin. Then, insulin is postulated to fold back to its normal bioactive conformation, exerting its pharmacological effect on target cells. These suggested conformational changes of insulin have been supported with data from near-UV spectroscopy which monitors alterations in the tertiary structure of the molecule.

Eligen carrier molecules that have been taken through preclinical studies and clinical trials include N-8-[2-(hydroxyl-benzoyl) amino] caprylate sodium (SNAC) and 4-[(2-hydroxy-4-chlorobenzoyl) amino]butanoate sodium (4-CNAB). Preclinical studies and clinical trials have shown that co-administration of Eligen carriers with insulin increase the resistance of insulin to enzymatic degradation in GI fluids, improves absorption of insulin through the GIT epithelium and normalizes blood glucose levels. The potential effect of long term use of high

concentrations of these Eligen molecules contained in a dose of this formulation have to be clarified.

1.2.3. Use of mucoadhesive systems

The immobilization of an oral dosage form at the absorption site can enhance uptake of the drug by creating a concentration gradient that leads to increased uptake of the drug from the dosage form [14]. Mucoadhesion is mediated primarily by the ability of certain materials to interact with mucin residues present in the intestinal mucosa either chemically or by the formation of non-chemical bonds [62]. Different theories of mucoadhesion have been put forward to explain the diverse range of possible mucoadhesive interactions observed experimentally [63]. One of the earliest theories of mucoadhesion was the **wetting theory** which described the ability of low viscosity liquid adhesives to spread and penetrate into the surface irregularities of a mucosal surface, overcoming interfacial tension to create adhesive bonds [64, 65]. Others include the **electrostatic theory** which emphasizes that the creation of mucoadhesive bonds involves the transfer of electrons and requires the presence of an electrical double layer across the adhesive interface [66]. While the **diffusion theory** takes into consideration the ability of polymeric chains to interpenetrate into mucin chains attaining sufficient depth within the glycoprotein matrix to sustain a permanent mucoadhesive bond [67]. This depth attained has been found to be dependent on the polymer molecular weight, cross-linking density and diffusion coefficient, with minimum depth for good mucoadhesive bonds being estimated to be within the range of 0.5-2μm [68]. The **adsorption theory** of mucoadhesion places emphasis on the nature of the different chemical groups present at the interacting surfaces which results in an interplay of different types of forces (covalent, hydrophobic association, electrostatic, van der Waals interaction) facilitating the mucoadhesion process [69, 70].

Mucoadhesion has been applied in the promotion of enteral insulin absorption by incorporating insulin in materials that adhere tightly to the intestinal mucosa, prolonging the residence time of the drug at its absorption site and maximising uptake of the drug [71]. The attachment of mucoadhesive dosage forms containing insulin to the intestinal mucosa also limits enzymatic degradation, as the close interaction of the carrier to the mucosal surface reduces the exposure of the drug to proteolytic enzymes in the intestinal lumen [71]. Mucoadhesive materials found to be useful in the delivery of oral insulin include mucoadhesive polymers and lectins. Polymers with uniquely mucoadhesive properties include chitosan, polyethyleneglycol (PEG) and cross-linked polyacrylic acid [3, 72]. Chitosan is a naturally occurring polysaccharide obtained from chitin found in the shells of crustaceans [62]. Chitosan has been widely used in the development of different forms of oral insulin delivery systems due to its absorption enhancing capability and

strong mucoadhesive properties which are believed to be due to the presence of positively charged groups on its structure (Fig. 2) that interacts with negatively charged mucin groups forming a tightly bound complex [62].

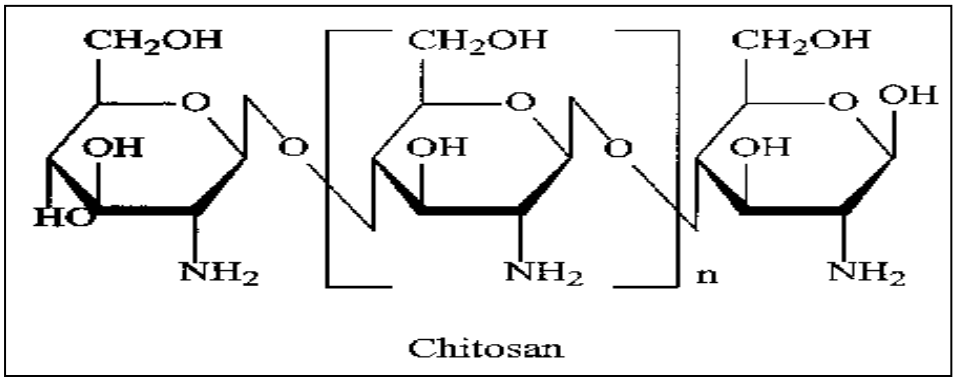

Fig. 2: Chemical structure of Chitosan

The administration of different types of chitosan-based dosage forms has been associated with significant hypoglycaemic effect in-vivo. The ability of polyethylene glycol chains to interpenetrate and entangle with the mucosa layer, facilitates the adhesion of dosage forms containing PEG to the intestinal mucosa improving uptake of insulin [73].

Thiolated polymers have also been observed to be strong mucoadhesives [74]. This has been linked to the availability of reactive thiol groups within their structure, which are capable of forming disulphide bonds with cysteine-rich domains of mucus glycoproteins which significantly promotes the retention of high concentrations of the drug at the absorption site enhancing intestinal absorption of insulin. Some thiomers have also been found to maximise the amount of insulin available for absorption by chelating the metal ions of endogenous proteases thereby curtailing their activity [75]. Examples of thiolated polymers useful for oral insulin delivery include thiolated chitosan and thiolated polycarbophil [74, 76]. The use of thiolated polymers must be carefully evaluated to prevent polymer thiol-disulphide interactions with insulin which may result in loss of activity. Mucoadhesive patches containing insulin, carbopol 934, pectin and sodium carboxymethylcellulose compressed into a 1-4mm radii disc designed for enteral insulin absorption was able to induce dose-dependent hypoglycaemia in healthy rats [77]. Micropatches small enough to travel between intestinal villi have also been developed using silicon oxide, porous silicon or poly (methyl methacrylate) for oral insulin delivery [77].

Lectins are proteins or glycoproteins of nonimmunological origin that specifically recognise sugar molecules and can bind to glycosylated domains/mucins present in the mammalian mucosa [78]. Lectins therefore promote mucoadhesion by a specific biointeraction process with sugars present in glycolipids and glycoproteins of mammalian mucosa. Non-toxic plant lectins include Solanum tuberosum lectin (STL), Dolichos biflorus agglutinin (DBA), Ulex europaeus isoagglutinin I (UEAI) and Wheat germ agglutinin (WGA) [79]. WGA has a molecular weight of 36KDa and binds to N-acetylglucosamine and sialic residues [80]. WGA has been shown to exhibit the highest mucin binding capability to human intestinal cell lines and human colonocytes, but minimal mucoadhesive properties at low pH and would not be highly bound to the stomach mucosa lining [81]. WGA is therefore the most commonly used lectin in oral insulin delivery, where it has been used to functionalize different oral insulin delivery systems enabling site-specific adhesion of these carrier systems to the intestinal mucosa. WGA conjugated alginate microparticles were observed to promote the intestinal absorption of insulin in diabetic rats [80]. pH-sensitive hydrogels functionalized with WGA have also been developed for oral insulin delivery [81].

One major problem associated with the use of mucoadhesive systems is that the body carries out a continuous turnover of the GI mucus layer every 12-24 hours [82]. This therefore limits the time for drug absorption site through the mucosa to this timeframe, irrespective of the mucoadhesive capacity of the carrier system. Hence, ideally drug release from the mucoadhesive system should have taken place prior to the body's mucus turnover cycle.

1.2.4. Use of particulate carrier systems

Oral insulin delivery systems featuring encapsulation or entrapment of the drug in particulate structures of various sizes, morphology and functionality can be designed to respond to a variety of environmental stimuli. The post-absorptive fate of a drug is often dictated by its unique physicochemical and pharmacokinetic profile. Therefore the introduction of a polymeric wall enclosing the drug molecule may modify its pharmacokinetic profile altering parameters such as drug absorption, drug distribution within subcellular/cellular compartments, transport across biological barriers and also metabolism and degradation of the drug [83]. Different particulate structures employed as carrier systems for oral insulin are discussed below.

1.2.4.1. Nanoparticles

These are polymeric, submicron (<1μm), colloidal systems that can be used to encapsulate and deliver drug moieties into the systemic circulation. These nanoparticles can be in form of nanospheres, which contain the drug dispersed throughout a polymer matrix (figure 3A), or as

vesicular structures called nanocapsules made up of a fluid drug-loaded core surrounded by a singular polymeric wall (figure 3B) [84].

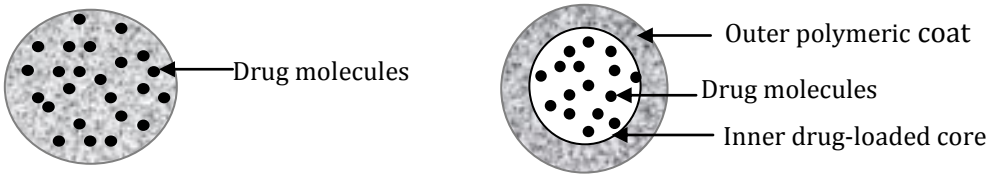

A) Nanosphere B) Nanocapsule

Fig. 3: Different types of nanoparticulate structures A) nanosphere B)nanocapsule .

Nanoparticulate carriers are more readily transported across the intestinal mucosa than micro scale carrier systems [85].

Entrapment of insulin in nanoparticles has also been observed to lead to increased insulin bioavailability and enhanced hypoglycaemic effect when administered orally [86, 87]. The outer polymeric membrane of nanocapsules has also been shown to serve as a protective coat for encapsulated insulin preventing enzymatic degradation. *In-vitro* incubation of insulin-loaded poly(alkylcyanoacrylate) nanoparticles in media containing gastric and pancreatic proteolytic enzymes showed retention of least 75% of incorporated insulin, while free insulin in the media was largely degraded [86, 87].

Nanoparticles can be taken up by the membraneous epithelial cells (M cells) located on the specialized epithelium covering the aggregates of lymphoid follicles known as Peyer's patches [88]. M cells are specialised cells involved in the transport of macromolecules, particles and organisms from the gut by endocytosis. Research has indicated that this route is favoured for the transport of smaller hydrophobic nanocapsules which seem to have a higher affinity for M cells than absorptive cells [89]. Nanoparticles (with diameters below 150nm) also translocate across the intestinal epithelium via the paracellular pathway, poly (isobutylcyanoacrylate) nanocapsules have been detected in the intercellular spaces between intestinal absorptive cells and lumen of the capillaries [45, 90]

The mechanism of absorption of nanoparticles from the GIT varies depending on the physicochemical properties of the constituent polymer and the surface properties of the particle. Nanoparticles having different functionalities can be tailor-made by careful selection of

parent polymers that possess the target properties. For example, nanoparticles with prolonged activity and long-circulating half-lives can be created by coating them with PEG, which provides a coat of hydrophilic chains that repel plasma proteins and prevent degradation [84]. This effect has also been achieved by the addition of poloxamer 188 to insulin loaded chitosan – tripolyphosphate nanoparticles, which on oral administration elicited a prolonged hypoglycaemic effect in diabetic rats due to delayed clearance [91]. Chitosan has also been shown to improve paracellular transport of insulin by mediating the reversible opening of tight junctions between cells. Insulin-loaded chitosan nanoparticles given orally to diabetic rats normalised glucose levels for several hours [92, 93].

pH-sensitive nanoparticles containing methacrylic acid grafted with PEG have been shown to curtail the release of insulin in the stomach, facilitating its release at near neutral pH [94]. These particles exhibited hypoglycaemic effects that lasted for about 6 hours in diabetic rats. Insulin loaded nanoparticles bearing receptor-recognisable ligands like Vitamin B_{12} on their surfaces have also been used to facilitate internalisation of insulin by receptor-mediated endocytosis [95]. Vitamin B_{12} functionalised nanoparticles counter the aforementioned problems of low loading efficiency inherent in the direct conjugation of cobalamin to insulin by initiating active uptake of nanoparticles. A significant advantage of the use of nanoparticles in the delivery of oral insulin is that nanoparticles tend to concentrate mostly in the liver irrespective of their composition [96]. The uptake of nanoparticles by the liver enhances glycaemic control by suppressing hepatic glucose production using insulin encapsulated within the nanoparticles, when they are taken up to be degraded. Problems associated with the use of nanoparticles in oral insulin delivery include the risk of disruption of the delicate insulin structure during the intense processing conditions required for the production of some types of nanoparticles [97].

1.2.4.2. Microspheres

Insulin intended for oral administration can be encapsulated within the core of polymer particles with dimensions within the micron range (about 1-500 μm) known as microspheres or microparticles. Microspheres are often prepared using a water-in-oil-in-water (w/o/w) technique to incorporate the protein, and drug release from microsphere is normally through bulk or surface degradation of the polymeric structure [98]. These polymeric microspheres have been shown to be capable of protecting encapsulated proteins from degradation, while also enhancing their absorption by translocating through the Peyer's patches or absorptive epithelium of the intestine [5, 99, 100]. Oral insulin delivery by encapsulation in microspheres also encourages better hypoglycaemic control because microspheres concentrate in the liver thereby effectively supplying insulin required for the suppression of hepatic glucose production.

Different designs and fabrications of microspheres have been employed for oral insulin delivery. Enteral absorption and transport of microspheres has been shown to be favoured by making the microsphere sizes smaller [101]. Insulin-loaded pH-sensitive microspheres composed of poly(methacrylic acid) and polyethylene glycol have been shown to well absorbed from the ileum and elicited a marked hypoglycaemic effect in healthy rats [102]. These microspheres exhibited good mucoadhesive properties due to the presence of the PEG moiety and pH-modulated insulin release by pH-dependent swelling of interpolymer complexes formed between protonated components of the microsphere. The microspheres were also observed to demonstrate marked inhibition of tryptic activity, which may be ascribed to the ability of the matrix polymer to bind to calcium ions required for initiation of enzymatic activity.

Another novel formulation of insulin microspheres consists of charge-interaction complexes containing negatively charged insulin loaded poly(lactic-co-glycolic acid) microparticles coupled with positively charged micromagnets [103]. These charge-interaction complexes are localized at the intestinal region through the application of an external magnetic field to the subjects ingesting the formulation. Only the microparticles are absorbed from the intestine. Mice fitted with a magnetic belt were given the complex and the amount of insulin retained in the intestinal tract was compared to that retained in a control group. The mice given the charged complex were observed to retain 32.5% of administered insulin while the control group only retained 5.4% of administered insulin.

Other formulations of microspheres observed to be useful in enhancing oral insulin delivery include mucoadhesive chitosan microspheres and microspheres enclosing absorption enhancers and protease inhibitors along with insulin [104, 105]. The problem associated with the use of microspheres in oral insulin delivery is the risk of inactivation or denaturation of insulin during the intensive processing conditions often encountered in the preparation of microsphere formulations.

1.2.4.3. Liposomes

These are tiny, vesicular self-assembly systems formed when phospholipids are dispersed in aqueous media [106]. Liposomes consist of hydrophobic and hydrophilic domains with the ability to encapsulate or solubilise different types of drugs based on their polarity. Liposomes have been shown to be able to protect insulin from enzymatic degradation. Insulin loaded liposomes coated with chitosan and chitosan-EDTA conjugates were observed to protect insulin

from degradation by pepsin and trypsin resulting in a bioavailability of 8.91% on oral administration to rats [107].

Liposomes bearing targeting moieties and functional coatings have been developed to enhance the bioavailability of orally administered liposomal insulin. For example, insulin has been incorporated within the core of liposomes equipped with an outer envelope of Sendai virus (SEV) enables the delivery of insulin directly into the cell cytoplasm by the process of membrane fusion [108]. This type of liposomes termed fusogenic liposomes can effect intracellular insulin delivery, though the presence of insulin-degrading enzyme in the cytosol can effectively limit the usefulness of this technique if an enzyme inhibitor is not co-administered with the liposome formulation. The use of these fusogenic liposomes have been linked with marked improvements in the absorption of insulin. An American company, Diasome have also encapsulated insulin within Hepatic-Directed Vesicles (HDV) which are basically liposomes of about 150nm in diameter featuring a hepatic targeting moiety in their lipid bilayer [7]. This delivery system facilitates the direct transport of liposomal insulin to the liver greatly reducing the amount of insulin required for the induction of significant hypoglycaemic effect. Chitosan coated liposomes reduced tryptic digestion of insulin and improved enteral insulin absorption, exhibiting a marked hypoglycaemic effect for four hours on oral administration to diabetic mice [109]. However the use of liposomes in insulin delivery is challenging due to the inability of lipid-based systems to entrap sufficient quantities of hydrophilic drugs resulting in low drug loading efficiency [14]. Other disadvantages include low GIT stability and leakage of entrapped drug [106].

1.2.5. Hydrogels

A hydrogel consists of a three-dimensional network of hydrophilic polymer chains that do not dissolve but swell up in water, absorbing large amounts of water within their structure [110]. This makes them similar to natural tissue and possibly contributes to their good biocompatibilty profile [111]. Hydrogels retain their physical integrity in solution due to the presence of numerous cross linkages between consituent polymer groups within their structure [112]. These cross linkages may be in form of covalent bonding or non-chemical bonds like hydrogen bonding, hydrophobic interaction, crystallinity, stereocomplex formation and ionic association. The physical properties of a hydrogel are often determined by the nature of these cross-linkages as well as the characteristics of the polymers used for constructing the hydrogel.

Smart hydrogels that are designed to facilitate drug release in response to specific stimuli peculiar to the disease in question have been found to be very useful in drug delivery. Hydrogels can be made to respond to changes in pH, temperature, light and the presence of microbes. This type of intelligent self-regulated drug delivery systems are well suited for the delivery of insulin for the management of Type I diabetes because they can be designed to recognise fluctuations in blood glucose concentration initiating an adequate response.

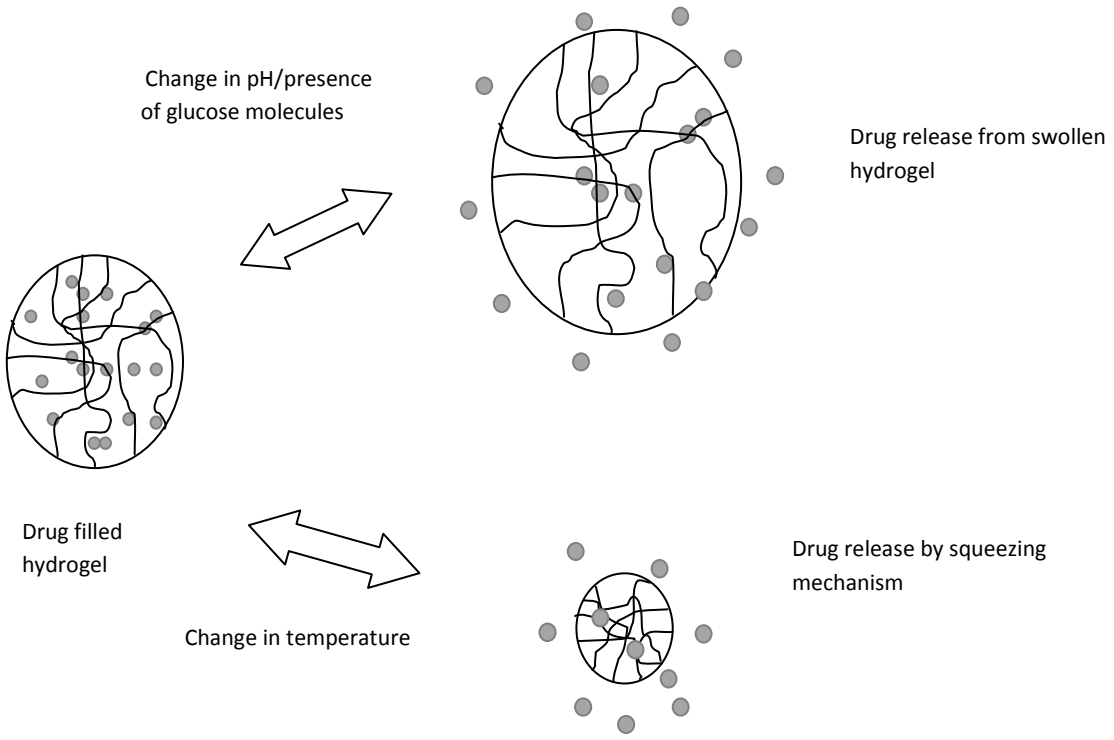

Fig. 4: Diagrammatic representation showing release of drug molecules from hydrogels using the swelling mechanism (adapted from Jeong, S.H., Huh, K.M. and Park, K. (2006) Hydrogel drug delivery systems. In I. F. Uchegbu and A.G. Schatzlein [Ed] Polymers in drug delivery. Taylor and Francis group, Boca Raton, 49-61.

Hydrogels which show pH-responsive swelling behaviour can be used to protect insulin from acid-catalysed degradation in the stomach by hindering its release from the dosage form. Reversible pH-dependent swelling is induced by the presence of polymers bearing side groups that are prone to protonation or deprotonation based on the pH of the surrounding medium. Grafting another suitable polymer onto such pH-sensitive polymers can lead to complexation by formation of temporary crosslinks such as hydrogen bonding or ionic interactions when the polymer is protonated thereby favouring the retention of structural integrity and hindering the release of any incorporated drug when the hydrogel is in media with pH values below its pKa.

When such hydrogels are in contact with medium above their pKa values, the side groups become deprotonated exhibiting interchain repulsion and decomplexation which leads to swelling and water absorption promoting the release of the incorporated drug (figure 4 above). Hydrogels that modulate drug release based on the formation of hydrogen bonds are known as complexation hydrogels [111]. Hydrogels that exhibit pH-dependent complexation are referred to as pH-responsive complexation hydrogels [111].

An example of a complexation hydrogel that has been used for oral insulin delivery is poly (methacrylic acid) (MAA) grafted with polyethyleneglycol (P (MAA-g-EG)) [113, 114]. The carboxylic acid groups of MAA (pKa 4.9) are responsible for facilitating pH-dependent formation of hydrogen bonds with the oxygen moiety of the polyethyleneglycol chains. P(MAA-g-EG) complexation hydrogel confines insulin release to the small intestine and enables localization of the drug at the absorption site due to the mucoadhesive properties of PEG chains which penetrate into the mucosal layer. The oral administration of insulin-loaded P(MAA-g-EG) hydrogel in Wistar rats resulted in a decrease in membrane resistance of Caco-2 monolayer and a bioavailability of 12.8% [115]. Insulin was also protected in simulated gastric fluid and released in simulated intestinal fluid. Other monomers used in the formation of hydrogels for protein delivery include N-isopropyl acrylamide, acrylic acid, 2-hydroxyethyl methacrylate, ethylene glycol dimethacrylate and polyvinylalcohol [111].

Glucose-sensitive hydrogels have also been developed for oral insulin delivery. The addition of glucose oxidase to pH-sensitive hydrogels enables them further sensitivity to the presence of glucose. Decrease in the pH of the surrounding medium due to the conversion of glucose to gluconic acid by glucose oxidase within the hydrogel triggers hydrogel swelling and corresponding insulin release on entry of glucose into the hydrogel [116]. Concanavalin A (Con A), a glucose binding protein can be used to physically cross-link glucose-attached polymer chains [117]. The incorporated insulin needs to be modified with glucose to foster association with Con A, which is a gel in the absence of free glucose transforms to the sol state in the presence of free glucose enabling rapid release of insulin. Phenylboronic acid and its derivatives have also been shown to be good glucose complexing agents useful for the formation of glucose-sensitive insulin delivery systems as described above [118].

Superporous hydrogels with mucoadhesive properties made up of poly (acrylic acid-co-acrylamide)/O-carboxymethyl chitosan have also been shown to be effective in oral delivery of insulin [119]. These are enteric, super-absorbent and fast-swelling hydrogels that adhere to the intestinal mucosa when swollen, facilitating paracellular insulin transport by opening up the tight junctions using the mechanical pressure exerted by the swollen hydrogel. Insulin-loaded

superporous hydrogels were shown to multiply transport of insulin across rat intestine and colon ex vivo by 2 to 3 folds. Other hydrogel systems that have been used for oral insulin delivery include microflora –activated colon-targeted hydrogels made up of amidated calcium pectinate/calcium pectinate and molecular weight modulated hydrogel beads containing N-isopropylamide, butyl methacrylate and acrylic acid [120, 121].

Although the use of hydrogels in drug delivery has been largely successful, ensuring faster release of insulin by hastening the response of the hydrogel to environmental stimuli can be achieved by minimising the dimensions of the hydrogel [122].

A review of the data from the use of these different oral insulin delivery systems indicates that successfully delivering a therapeutic concentration of active insulin to target organs will require a combination of efficient carrier and targeting technologies to overcome the overwhelming barriers present at different phases of the delivery process. Invariably, the achievement of a functional oral delivery system for insulin will involve innovative optimisation of pre-existing macromolecular carriers to enable effective GI peptide stabilisation and delivery.

1.3. POLYELECTROLYTE COMPLEXATION

Recent advances in the design of functional polymeric drug delivery systems have led to the utilisation of association complexes formed by non-chemical bonding of one polyelectrolyte to another as novel carriers for the delivery of drugs. These polymers are held together by forces such as that due to electrostatic interaction, hydrophobic association, hydrogen bonding and van der Waals forces. Polyelectrolyte complexes (PECS) formed spontaneously from the electrostatic interaction between oppositely charged polyelectrolytes through the process of polyelectrolyte complexation have gained attention in the pharmaceutical industry due to their potential applications in the formulation of protein delivery systems. Polyelectrolytes are polymers that have a net negative (polyanions) or positive charge (polycations) at near neutral pH values [123]. They are normally soluble in water due to electrostatic interactions with water molecules and mixing oppositely charged polyelectrolytes in aqueous media may result in the formation of water-soluble, stable, nano-sized PECS as shown in figure 5 below.

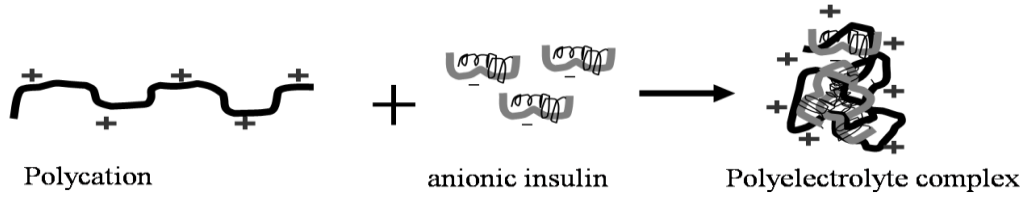

Fig. 5: Polyelectrolyte complex formation between an oppositely charged polymer and protein.

Polyelectrolyte complexation is an equilibrium process stabilised not only electrostatically, but also sterically through the presence of hydrophilic chains which repulse each other stabilising the PECS [124,125]. The nature of the complexes formed varies with the stoichiometry of the mixture .The process can be described as occurring in three phases [126]. The first phase involves the formation of a primary complex stabilised by coulombic forces, while the second phase entails the stabilisation of the primary complex either by the creation of new bonds within the complex and/or rectifying the distortions of the polymer chains. The final step involves spontaneous intercomplex aggregation mainly by hydrophobic association. The nature of the complexes formed varies with the stoichiometry of the mixture [127] and factors that affect the formation and stability of PECS include polyelectrolyte concentration, polymer molecular weight, pH and ionic strength of the solution, solvents, ion site, charge density and temperature [128].

Formulation parameters like solvent composition, polyelectrolyte concentration and mixing ratio affects the type and stability of complexes obtained. Interpolymer chain repulsion dominates at low charge ratios causing a macroscopic phase separation with each phase mostly containing separate polymers, while high charge ratios lead to complex precipitation due to maximum electrostatic interaction reducing solvent interaction [128, 129]. Intermediate charge ratios optimise the effects of interchain repulsion, electrostatic interaction and solvent interaction to create a stable dispersion [130]. pH has a marked effect on complexation, especially with polyampholytes which may be polycationic or polyanionic depending on if the pH of the solution is below or above their pI [131]. pH also influences the degree of ionisation of charged groups and may hence affect charge density [131, 132]. High charge density facilitates high complexation efficiency and consequently drug loading and also enhances PEC stability [133]. Ionic strength of the solvent affects PEC stability, at high ionic strength electrical double layer screening by counterions may diminish the influence of electrostatic forces and allow short-range inter-complex interactions to dominate increasing the potential for PEC aggregation [129, 134]. Research conducted on chitosan-Lignosulfonate PECS, showed that the type of complexes obtained may also vary with temperature [135]. High temperatures (100˚C) facilitated the formation of compact complexes, with a positive change in enthalpy driving the release of bound small molecules like water and counter ions resulting in an increase in entropy favouring complexation. Polymer characteristics like molecular weight affect chain conformation and flexibility and influence the morphology of complexes produced [136].

Investigative techniques employed in PEC characterisation include turbidimetric measurements to monitor precipitation, viscosity measurements, Fourier Transform Infrared Spectroscopy (FTIR), Thermal analysis, Nuclear Magnetic Resonance Spectroscopy, powder X-ray diffraction, Static Light Scattering, Circular Dichroism and other analytical procedures [137]. The spontaneous formation of nano-sized complexes by polyelectrolyte complexation has the advantage of being a more benign process than other methods of manufacturing nanoparticles, which usually require the use of aggressive processing/manufacturing conditions, toxic organic solvents, excessive heat, sonication and agitation thereby reducing the risk of protein deactivation/denaturation.

1.4. THE USE OF POLYELECTROLYTE COMPLEXATION FOR ORAL INSULIN DELIVERY

The concept of polyelectrolyte complexation has been applied to the development of oral formulations of therapeutic macromolecules by electrostatic linkage to a polymeric carrier molecule. However tailoring its use to oral protein delivery involves rational optimisation of polymer structure to provide a robust network to facilitate optimum complexation, enzymatic protection and GI absorption of proteins. Polyelectrolyte complexation conveniently creates a platform where various functionalities shown to improve oral protein bioavailability can be imparted into the delivery system by modification of the carrier polymer rather than the protein molecule intended for oral administration. This serves the purpose of preserving the original structure and/or activity of the drug while attempting to improve its therapeutic efficacy.

In oral insulin delivery, polyelectrolyte complexes containing insulin have been the subject of extensive research. Proteins and peptides are ampholytes, hence based on the pH of their solution they can exist as either polycations or polyanions in aqueous media [131]. Insulin for example is negatively charged above its pI of 5.5; polymer-protein PEC formation can therefore occur spontaneously in aqueous/buffer solutions at neutral pH containing insulin and polycations/positively charged polymeric carriers (Fig. 5). Cationic polymers which at physiologic pH feature protonable amine groups that can undergo electrostatic complexation with negatively charged insulin are often suitable in the design of polymer-insulin PECS [11]. These complexes are often positively charged, spherical nanoparticles, with hydrodynamic sizes between 100-400nm in aqueous or buffer solutions [124]. Incorporating insulin intended for oral administration into a dosage form of the size range described above enhances uptake by transcytotic transport of nanoparticles through Peyer's patches (aggregates of lymphoid follicles partly covered by the highly specialized M cells which have the ability to transport macromolecules, particles and organisms from the gut by endocytosis) [23, 24, 25].

In addition, the presence of a positive charge on these nanocomplexes implies that at physiological pH, they are capable of interacting electrostatically with negatively charged groups present at epithelial tight junctions causing them to open transiently allowing the paracellular transport of insulin across the epithelium [26]. These positively charged complexes also promote transmucosal insulin absorption by interacting with negatively charged components of the intestinal mucosa like sulphate residues and sialic acid (which by virtue of its pK_a of 2.6 is completely ionised at intestinal pH). Insulin–loaded polyelectrolyte nanocomplexes can be designed to be mucoadhesive, tight-junction modulating, amphiphillic and enzymatically protective by associating insulin with polymers that possess such abilities. Polyelectrolyte complexes applied for oral delivery of insulin are discussed below.

1.4.1. Amphiphillic polyelectrolytes

Improving the bioavailability of oral insulin requires absorption of the drug through both aqueous and lipid layers/barriers in the body. Data obtained from various research groups suggests that achieving this may entail the use of formulations that impart an optimum balance of both hydrophilic and lipophilic properties to the delivery system. Amphiphillic polymers which contain hydrophilic and hydrophobic components can exist naturally or can be synthesized by grafting a hydrophobic pendant group/polymer onto a hydrophilic backbone. Complexation of amphiphillic polyelectrolytes (AP) with insulin molecules has been reported to promote uptake of insulin by Caco-2 cell monolayers [136].

A series of positively charged AP consisting of polyallylamine (Paa) made amphiphillic by hydrophobic substitution with various lipid pendant groups (palmitoyl, cetyl and cholesteryl groups) has been attempted for use in oral insulin delivery [136, 137,138]. The Paa backbone was also further modified by quaternising its primary amines resulting in a permanently charged AP (QPaa) with enhanced aqueous solubility [136]. Complexation with negatively charged insulin was carried out in tris(hydroxymethyl)aminomethane (Tris) buffer resulting mostly in spherical nano-sized PECS , although the palmitoyl-substituted AP yielded fluffy aggregates. These quaternised Paa-based PECs exhibited good insulin loading efficiency, protect insulin from peptic and tryptic degradation [137, 138].

Another AP system that has been used to facilitate oral insulin delivery is hydrophobic poly(lactic-co-glycolic acid) (PLGA) or poly(lactic acid) (PLA) grafted onto a hydrophilic poly(vinyl alcohol) backbone yielding an AP termed ‘PVA-g-PLA’ [139]. The AP was made cationic and more water-soluble by the attachment of amino groups, diethylaminopropylamine (DEAPA) to the PVA backbone [140]. The stability of the resultant PECs was observed to be

modulated solely by level of hydrophilic modification (DEAPA), while increase in hydrophobic substitution was observed to facilitate insulin loading efficiency.

These PVA-g-PLA-insulin PECs were capable of limiting tryptic degradation of insulin, reducing transepithelial electrical resistance (TEER) of Caco-2 cell monolayers and promoting cellular internalisation of insulin. All these effects were shown to be significantly enhanced by increase in the level of PLA grafting, indicating the importance of hydrophobic interactions in facilitating oral insulin delivery. Further work defining the exact mechanisms of the actions of these APs and their hypoglycaemic effect and bioavailability in-vivo would still be required before they can be used.

1.4.2. Polycations and their derivatives

Currently, the most common polycation used in the formulation of PECS containing insulin for oral administration is chitosan. Chitosan is very useful in the oral delivery of hydrophilic macromolecules due to its ability to facilitate paracellular transport via the reversible opening of the tight junctions. This is mediated by electrostatic interactions between the protonated amino groups of chitosan and negatively charged groups present in mucus, tight junction proteins and glycoproteins on cell surfaces [140, 141]. The role of chitosan in the promotion of enteral insulin absorption is however limited by its pKa of 5.5, which makes it soluble in only acidic pH conditions at which chitosan is cationic and in an uncoiled state but unfavourable for the release of proteinous drugs or peptides [140, 141]. This also means that at intestinal pH conditions at which the permeation effects of chitosan are required, it will be insoluble and ineffective.

Therefore derivatives of chitosan which are soluble at neutral or alkaline pH conditions have been developed and applied as polyelectrolytes for enhancing oral absorption of insulin. This includes different forms of quaternised chitosan which are produced by methylation of the primary amines on C-2 using methyl iodide [140, 141]. The presence of a quaternary ammonium moiety on these chitosan derivatives imparts a permanent pH-independent positive charge to the polymer that fosters electrostatic interaction with tight junction sites to enhance paracellular transport of insulin [144]. The most commonly used quaternised chitosan is trimethyl chitosan (TMC). Optimisation of the level of quaternisation has been found to be vital in facilitating paracellular transport and mucoadhesion using quaternised chitosan [140, 141]. High levels of quaternisation have been associated with decreased mucoadhesivity due to reduced chain flexibility, interpenetration and steric hindrance [145, 146] while lower levels of quaternisation reduce interactions with mucus, also causing corresponding decreases in mucoadhesion.

Quaternised chitosan has been shown to be able to elicit its tight junction modulating effect when administered either as a macromolecular dispersion or as a polymer-insulin PEC. However, research favours the use of quaternised chitosan-insulin PECs which encourage both transcellular and paracellular insulin transport, while also enabling close interactions of the dosage form with mucus [133]. This mucoadhesive effect promotes the permeation enhancing effect of chitosan on the intestinal mucosa and retains high amounts of the drug at the absorption site creating a concentration gradient that increases uptake of the drug. Consequently, the administration of insulin-loaded TMC PECS to rats was observed to cause a greater increase in insulin transport across the ex-vivo mucosa and a larger drop in blood glucose than was observed on administration of insulin with quaternised chitosan solutions. TMC PECs have been observed to reduce tryptic degradation of insulin considerably [31].

Also used in the formation of PECs are thiolated chitosan derivatives which contain chitosan conjugated to thiol-containing compounds via amide or amidine bonds. As described earlier thiolated chitosan derivatives are strongly mucoadhesive and mediate their absorption promoting effect via localization of the drug at the absorption site thereby enhancing drug uptake [147]. Thiolated trimethyl chitosan/ insulin PECS have been reported to show a higher degree of mucoadhesiveness and permeation enhancing effect than trimethylchitosan PECS, resulting in a more potent hypoglycaemic effect on ileal and oral administration in normal rats [147].

However, PECs are largely unstable in the gastric fluid due to the fact that electrostatic interactions may be lost by fluctuations in the charge of the insulin moiety at acidic pH [148]. Hence APs may perform better as PECS due to the presence of hydrophobic as well as electrostatic interactions in the formation and stabilisation of AP PECs. The formulation of PECs as part of an enteric-coated solid dosage form may also be a viable approach to countering their instability in gastric fluid.

1.5. OBJECTIVES OF THE WORK

Polyallylamine (Paa) (available as the hydrochloride salt) is a cationic polymer composed of free primary amine groups attached to a hydrocarbon backbone. The work reported herein entails optimising the structure of Paa through quaternisation and thiolation for the formulation of polymer-insulin polyelectrolyte complexes intended for oral administration. Subsequent chapters of the thesis report the impact of the aforementioned modifications on the physical characteristics, insulin complexation efficiency, morphology, enzyme-protective capacity, mucoadhesive capacity, cytotoxicity and cellular uptake of the resultant insulin PECS.

2. POLYMER SYNTHESIS AND CHARACTERISATION

2.1. INTRODUCTION

This chapter focused on chemical alteration of the structure of Paa aimed at improving its function in the areas of complexation, enzymatic protection and transmucosal/transepithelial transport of insulin intended for oral delivery. The chemical procedures applied in optimising the structure of Paa includes methylation of the primary amines of Paa using methyl iodide to yield QPaa and immobilisation of different types of reactive thiol groups on both QPaa and Paa to yield novel Paa and QPaa based thiomers. As mentioned in chapter one, quaternisation stabilises polycationic charge thereby enhancing processes like tight junction opening, insulin complexation and mucoadhesion that benefit from charge-based interactions. Thiolation is primarily geared towards improving the mucoadhesive properties of each polymer by facilitating polymer-mucin thiol-disulphide bonding.

Thiolation of Paa/QPaa was possible either through carbodiimide mediated coupling of the primary amine groups of the polymer to N-acetylcysteine (NAC) creating a stable amide bond or by reacting the polymers with 2-iminothiolane which yields the 4-thiobutylamidine derivatives of the parent polymer. The success of the synthesis process was evaluated by determining the level of polymer substitution using elemental analysis and iodometric titration to determine free thiol content for thiomers. Further structural characterisation was carried out by Nuclear Magnetic Resonance (^{1}H NMR) and Fourier Transform Infrared Spectroscopy (FTIR). Other characterisation techniques used include zeta potential determination to quantify surface charge of the different polymers and Differential Scanning Calorimetry (DSC) to assess thermal properties of the polymers. The mucoadhesive profile of thiolated derivatives was also evaluated in comparison to that of their parent polymers by comparing the results of a mucin adsorption assay.

2.2. MATERIALS AND METHODS

2.2.1. MATERIALS

Poly(allylamine hydrochloride) (average Mw = 15kDa), tris(hydroxymethyl)aminomethane (Tris base) (≥ 99%), iodomethane, amberlite IRA-96 resin (20-50 mesh), sodium iodide, N-(3-Dimethylaminopropyl)-N'-ethyl carbodiimide hydrochloride (EDAC), sodium hydroxide, N-hydroxysuccinimide (NHS), N-acetylcysteine, 2-iminothiolane hydrochloride, sodium borohydride, phosphate buffer saline (PBS), iodine solution (0.5M), starch solution (2%) and

Porcine gastric mucin (crude type II) were all purchased from Sigma-Aldrich UK. Other solvents used were of HPLC grade and were obtained from Fisher Scientific, UK.

2.2.2 SYNTHESIS OF POLYMERS

The methods used for the purification and quaternisation of Paa were adapted from previous work of Thompson et al [136].

2.2.2.1. Production and purification of Paa free base

Polyallylamine hydrochloride (10g) was dissolved in 100ml distilled water and the solution titrated with sodium hydroxide pellets up to pH 13. The mixture was stirred continuously at 500rpm for 1 hour and then dialysed (molecular weight cut-off - 7kDa) against 5L distilled water with six water changes carried out over 24 hours. The purified polyallylamine was obtained by lyophilising the dialysate for 48 hours with a freeze drier (VirTis adVantage, Biopharma Process Systems, UK).

2.2.2.2. Quaternisation of Paa

Polyallylamine (0.6g, 0.04mmol) was dissolved in 100ml methanol in a round bottomed flask. Sodium hydroxide (0.56mg) and Sodium iodide (0.25mg) were stirred into the mixture until all solutes were completely dissolved. The flask was placed in an oil bath maintained at 36°C under a fume hood, after which methyl iodide (3.51ml, 56mmol) was subsequently added into the reaction mixture. The reaction was carried out for 3 hours under nitrogen. The white precipitate formed at the base of the reaction flask was collected, while the supernatant was added dropwise into 400ml of diethylether. Diethylether (200ml) was added into the flask containing the white precipitate and both ether suspensions left standing overnight at room temperature. The diethylether was then decanted and the white precipitates left to dry under the fumehood.

The dried precipitates were dissolved in a 1:1 mixture of ethanol and water (100ml) and the solution dialysed (molecular weight cut-off - 7kDa) for 24hours with six water changes. The dialysate was then passed through an Amberlite 93 exchange resin column, previously washed with HCl (2M 100ml) and titrated to neutral pH using distilled water. QPaa was obtained after freeze drying the column eluent for 48 hours.

2.2.2.3. Synthesis of Paa and QPaa N-acetylcysteine conjugates

Thiolation of Paa/QPaa by conjugation to N-acetylcysteine via an amide bond was carried out separately using a similar method to Yin et al. [147] (Fig. 6). N-acetylcysteine (250mg;

1.53mmol) was dissolved in 100ml of deionised water into which EDAC and NHS were added consecutively up to a final concentration of 200mM to activate the carboxylic acid groups of N-acetylcysteine. The mixture was adjusted to pH 4-5 using 2M HCl and left stirring at room temperature for 1 hour, after which Paa/QPaa (250mg) was added into the reaction mixture and the pH of the mixture readjusted to between pH 4-5. The reaction was carried out under nitrogen at room temperature for 5 hours without exposure to light. A control experiment containing equivalent concentrations of N-acetylcysteine and Paa without EDAC/NHS was also set up in the same way and allowed to run simultaneously.

The reaction mixtures for the test and control experiments were then dialysed (molecular weight cut-off - 7kDa) in the dark at 4°C, once against 5mM HCl, twice against 5mM HCl containing 1% NaCl, once again against 5M HCl and finally against 0.4mM HCl. The polymer conjugates were isolated by dialysis and then freeze dried. The lyophilised product obtained was characterised and stored at -20°C.

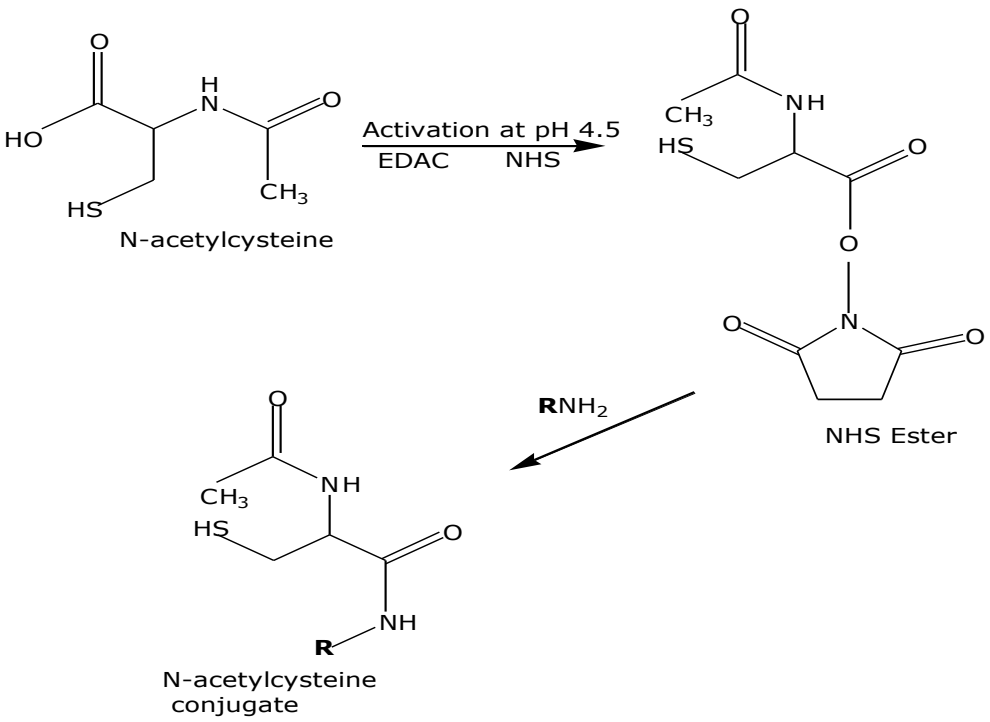

Where '**R**' represents Paa/QPaa

Fig. 6: Thiolation reaction for EDAC/NHS mediated coupling of N-acetylcysteine to Paa/QPaa.

2.2.2.4. Modification of Paa and QPaa using 2-iminothiolane

The thiolation of Paa and QPaa using amidine linkages was carried out separately following the method previously described by Bernkop Schnurch et al. [149] (Fig. 7 below). Paa/QPaa

(500mg) was dissolved in 50ml deionised water and the pH adjusted to 6.5 using 5M HCl. 2-iminothiolane hydrochloride (400mg) was added into the flask, and the reaction left stirring under nitrogen. The experiment was conducted at room temperature in the dark for 14 hours. The polymer conjugates were then isolated by dialysis and freeze dried as described in 2.2.2.3, after which they were also characterised and stored at -20°C.

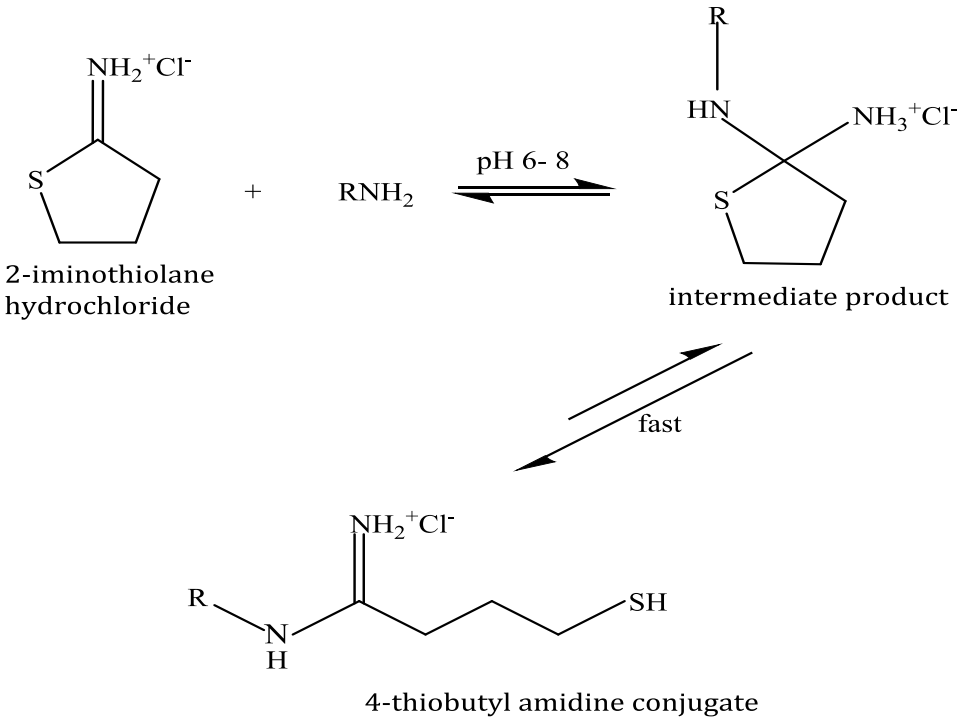

Where '**R**' represents Paa/QPaa

Fig. 7: Reaction scheme for Paa/QPaa thiolation using 2-iminothiolane

2.2.3. STRUCTURAL CHARACTERISATION OF POLYMERS

2.2.3.1. Elemental analysis

The relative abundance of carbon, hydrogen, nitrogen and chlorine in samples (1mg) of each polymer was estimated using a Perkin Elmer series 2 elemental analyser (Perkin Elmer, UK). Elemental analysis was used to determine the average degree of polymer quaternisation as shown in the calculation below. Elemental analysis results are expressed as the percentage content of each element in the sample. Subtracting the number of mols of carbon in Paa from that in QPaa gives the additional moles of carbon added onto the Paa backbone after quaternisation. Expressing this difference as a percentage of the total number of additional mols of carbon expected if full quaternisation was obtained (which is equal to 3) gives the degree of polymer quaternisation (in mol %) [136]. The quaternisation process was done in triplicate and the average degree of quaternisation was determined for each sample.

2.2.3.2. Determination of free thiol content

The amount of free thiol groups immobilised on each thiolated conjugate was estimated by iodometric titration using a 2% starch solution as indicator. Each thiomer (10mg) was dissolved in 1ml of deionised water acidified with a drop of 2M HCl. 1% starch indicator (300µl) was added into the polymer solution before titrating the solution with a 1mM iodine solution until a permanent blue colour characteristic of the iodine-starch complex was observed [150]. The amount of thiol groups (in mols) per gram of polymer was estimated from a calibration plot prepared from titrating iodine against increasing concentrations (2-100mgml^{-1}) of an N-acetylcysteine reference standard (R^2= 0.99). Iodometric titrations for each polymer as well as the controls were carried out in triplicate.

2.2.3.3. Determination of disulphide bond content

The total amount of thiol substituents per gram of polymer was obtained by reducing the disulphide bonds formed during the thiolation reaction using sodium borohydride ($NaBH_4$) via the reaction below, followed by determination of free thiol content as described above.
A 1ml solution (1mgml^{-1}) of each thiomer in tris buffer pH 7.4 was prepared in a glass vial and mixed with 4% sodium borohydride solution (2ml) and the reaction incubated at 37°C for 1hour in a shaking water bath. The reaction was then stopped by slowly adding 400µl of 5M HCl with gentle stirring. Each reaction mixture was subsequently subjected to iodometric titration as described above and the free thiol content obtained used to obtain the total thiol substitution. The disulphide bond content of each thiomer was estimated by subtracting free thiol content obtained for each polymer prior to the reduction process from the total thiol content which was obtained after treatment with the reducing agent. This was done in triplicate.

Total thiol substitution was also determined by carrying out elemental analysis on all thiolated polymers using the method described in section 2.2.3.1. to obtain sulphur content (%).

2.2.3.4. FT-IR

Structural elucidation was carried out by obtaining FTIR spectra of dry lyophilised polymer samples. Each spectra was obtained by collecting 28 scans per spectrum between 4000-600cm^{-1} at a resolution of 4cm^{-1} using a Thermo-Nicolet FTIR spectrophotometer (Thermo Fisher Scientific, USA). Wavenumbers for identified peaks were obtained using the in-built OMNIC software attached to the equipment.

2.2.3.5. Zeta potential

The zeta potential (mV) of 1mgml^{-1} polymer solutions in tris buffer pH 7.4 contained in folded capillary cells was determined at 25°C by photon correlation spectroscopy (PCS) (Zetasizer Nano-ZS, Malvern Instruments, UK).

2.2.3.6. Thermal analysis (DSC)

Polymer samples (2-3mg) were placed in hermetic aluminium pans and then subjected to DSC analysis within -90°C to 370°C at a heating rate of 20°Cmin^{-1} under nitrogen using a Q100 differential scanning calorimeter (TA instruments, UK) precalibrated with an indium reference standard [138, 151].

2.2.4. *IN-VITRO* EVALUATION OF MUCOADHESIVE CAPACITY OF POLYMERS

Serial dilutions (0.1-1mgml^{-1}) of mucin in tris buffer were prepared from a 1mgml^{-1} stock solution of porcine mucin in tris buffer pH 7.4 obtained by probe sonication. The absorbance of each diluted mucin sample at 251nm was obtained by UV spectrometry (Agilent G1103A photo diode array, Agilent Technology, China) and the values plotted against the equivalent sample concentration to obtain a standard calibration curve (R^2= 0.99).

Assessment of the mucoadhesive capacity of each polymer was determined by measurement of the amount of mucin adsorbed by each polymer using a similar method to that described by Modi. et al. [152]; 0.25ml of a 0.5mgml^{-1} solution of each polymer in tris buffer pH 7.4 was mixed with 1mgml^{-1} mucin in tris buffer pH 7.4 and the mixture incubated at 37°C in a shaking water bath for 5 hours. Control samples were also prepared by mixing the aforementioned mucin in tris buffer solution with only 0.25ml tris buffer at pH 7.4 and then incubated as described above. All control and test samples were subsequently transferred into separate eppendorf tubes and centrifuged at 10,000rpm for 30minutes, and the concentration of mucin in each supernatant measured by UV spectrometry at 251nm as described earlier. Percentage (%) of total mucin adsorbed to each sample of polymer was calculated as shown below:

$$\% \text{ mucin adsorption } (M_{ad}) = [M_o - M_s] / M_o \times 100$$

Where,

M_O = concentration of free mucin in control supernatant

M_S = concentration of free mucin in the sample supernatant

2.2.5. *IN-SITU* CROSSLINKING AND REDUCTION IN FREE THIOL CONTENT OF THIOMERS

Samples (4mg) of each thiomer were hydrated in 1ml of tris buffer and buffered to pH 8 using 0.1M tris base, after which 3ml of PBS was added into each thiomer solution. The samples were incubated at 37°C in a shaking water bath and the change in the free thiol content of each sample with time estimated over 8 hours, by withdrawing 1ml of each sample every 2hours and titrating with iodine solution as described in 2.2.3.2. (any solids formed were separated out by centrifuging the sample at 10,000rpm for 10minutes, prior to titration).

2.3. RESULTS AND DISCUSSION

2.3.1. VALIDATION OF POLYMER SYNTHESIS

The average degree of quaternisation of QPaa as estimated by elemental analysis was found to be 72 ± 2 mol% (mean ± S.D; n=3) at an average yield of 76.2 ± 5% (mean ± S.D; n=3). Immobilisation of reactive thiol groups on primary amino groups on the Paa/QPaa backbone was carried out using two types of covalent bonds. Paa and QPaa were coupled via a stable amide bond to N-acetylcysteine using a water-soluble carbodiimide cross-linker (EDAC) and NHS to form Paa/QPaa-N-acetylcysteine conjugates as shown in fig. 8.

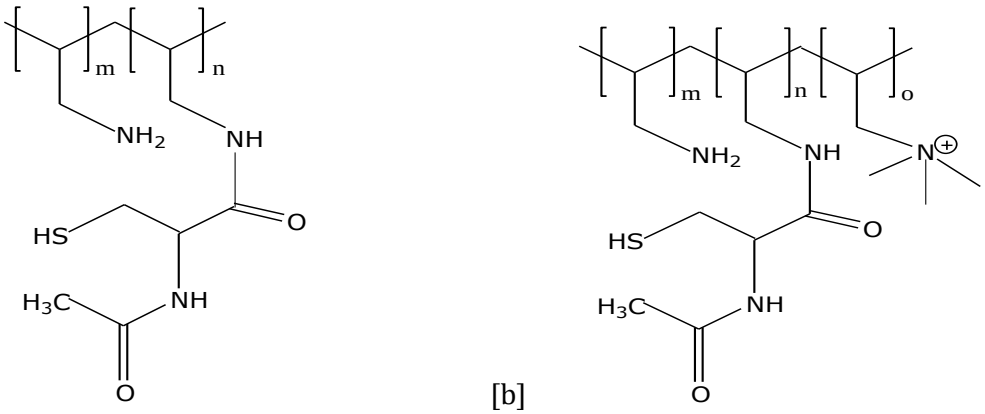

Fig. 8: Presumptive structure of repeating units of NAC conjugates of a) Paa: Paa-NAC b) QPaa:QPaa-NAC.

Paa and QPaa were also coupled to 4-thiobutylamidine via a reaction with 2-iminothiolane hydrochloride, a thiol-containing imidoester forming Paa/QPaa-4-thiobutylamidine conjugates. These TBA conjugates have a protonated amidine bond which bears an extra positive charge on the thiol constituent at pH 7.4 as can be seen in fig. 9 below [74, 153].

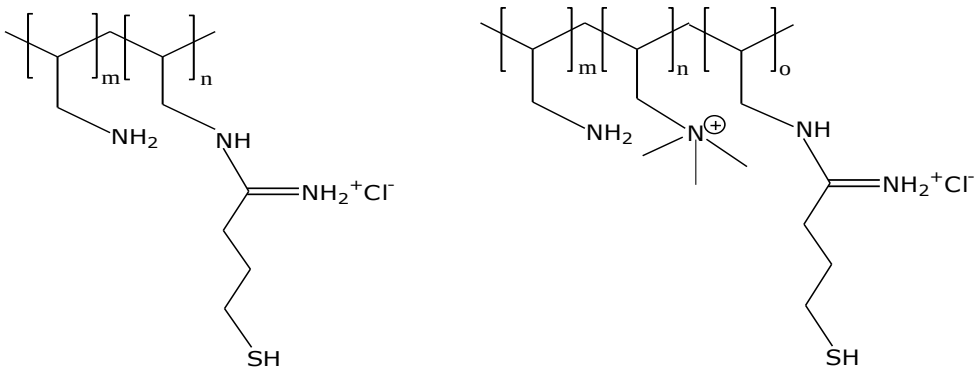

[a] [b]

Fig. 9: Presumptive structure of repeating units of thiobutylamidine conjugates of a) Paa: Paa-TBA b) QPaa:QPaa-TBA.

Optimisation of the coupling reaction between the polymers and N-acetylcysteine necessitated the inclusion of NHS in the cross-linking reaction as shown in figure 6 to stabilise the O-acylisourea intermediate product of the EDAC-carboxylic acid reaction which is susceptible to hydrolysis and consequently has a short life span in aqueous media [154]. The reaction was also carried out under nitrogen and at pH 4.5 to limit air or pH-induced oxidation of thiol groups to the reactive thiolate anion S^- resulting in the formation of intramolecular disulphide bond formation [155]. An N-acylated amino acid was used during the reaction to prevent the occurrence of unwanted side reactions resulting in the formation of oligo/poly cysteine conjugates [150]. After lyophilisation, all polymer conjugates appeared as white, powders of fibrous structure which were readily soluble over a wide pH range (3-8). The mean percentage yield (n=3) of Paa-NAC and QPaa-NAC conjugates was found to be 68.8 ± 2.8% and 73.6 ± 2.3 % respectively, while the percentage yield of the Paa-TBA and QPaa-TBA conjugates was calculated as 73.1 ± 4.4% and 83.6 ± 7.7 % respectively.

The total sulphydryl group content of each conjugate as well as the amount available as free thiols (SH) and disulphide (S-S) bonds was estimated by iodometric titration as described in section 2.2.3.2. and the results shown in Table 1 below.

Table 1: Total thiol content, free thiol and disulphide bond content of thiomers (indicated values are mean ± S.D.) (n = 3).

Polymer	Free SH content ($\mu molg^{-1}$)	S-S bond content ($\mu molg^{-1}$)	Total thiol Substitution ($\mu molg^{-1}$)
Paa-NAC	60 ± 1.2	280	340 ± 4.1
QPaa-NAC	60 ± 4.3	220	280 ± 3.3
Paa-TBA	490 ± 18	590	1080 ± 28
QPaa-TBA	440 ± 21	560	1000 ± 31

The negligible amount of thiol groups (0.2 ± 0.06$\mu molg^{-1}$ polymer) detected in control samples obtained from similar NAC conjugation experiments carried out without the addition of EDAC/NHS into the reaction mixture showed that EDAC/NHS was essential in the synthesis of NAC-based thiomers.

The coupling efficiency of the EDAC/NHS mediated thiolation process was relatively low resulting in the attachment of fewer molecules of the sulphydryl-containing moiety on the polymer backbone than polymer conjugates obtained using 2-iminothiolane. This contributed to the relatively low levels of thiolation observed in Paa/QPaa-NAC conjugates as can be seen from Table 1 above. The relatively low coupling efficiency of the EDAC-mediated thiolation process has previously been reported by other research groups [147, 150] working on the thiolation of similar polycations using EDAC concentrations ranging between 25-200mM and has been attributed to a side reaction of EDAC with the nucleophilic thiolate anion that results in the formation of an adduct that is subsequently hydrolysed to one of the reaction by-products, urea [156]. In contrast, the reaction of Paa/QPaa with 2-iminothiolane was observed to proceed with greater efficiency considering the relatively high levels of sulphydryl groups substitution obtained for Paa-TBA conjugates shown in table 1 .

Elemental analysis results confirmed the presence of sulphur within thiolated samples. Sulphur content of NAC conjugates (n=2): Paa-NAC and QPaa-NAC was found to be **334 ± 9** and **319 ± 12$\mu molg^{-1}$** respectively. The sulphur content of Paa-TBA and QPaa-TBA was **1,143± 15** and

1,109 ± 9µmolg^{-1} respectively. These results were found to be similar to the total thiol content obtained by iodometric titration shown in table 1 above.

2.3.2. FTIR SPECTROSCOPY

Results of FTIR analysis of polymer samples are shown in figures 10 and 11 below.

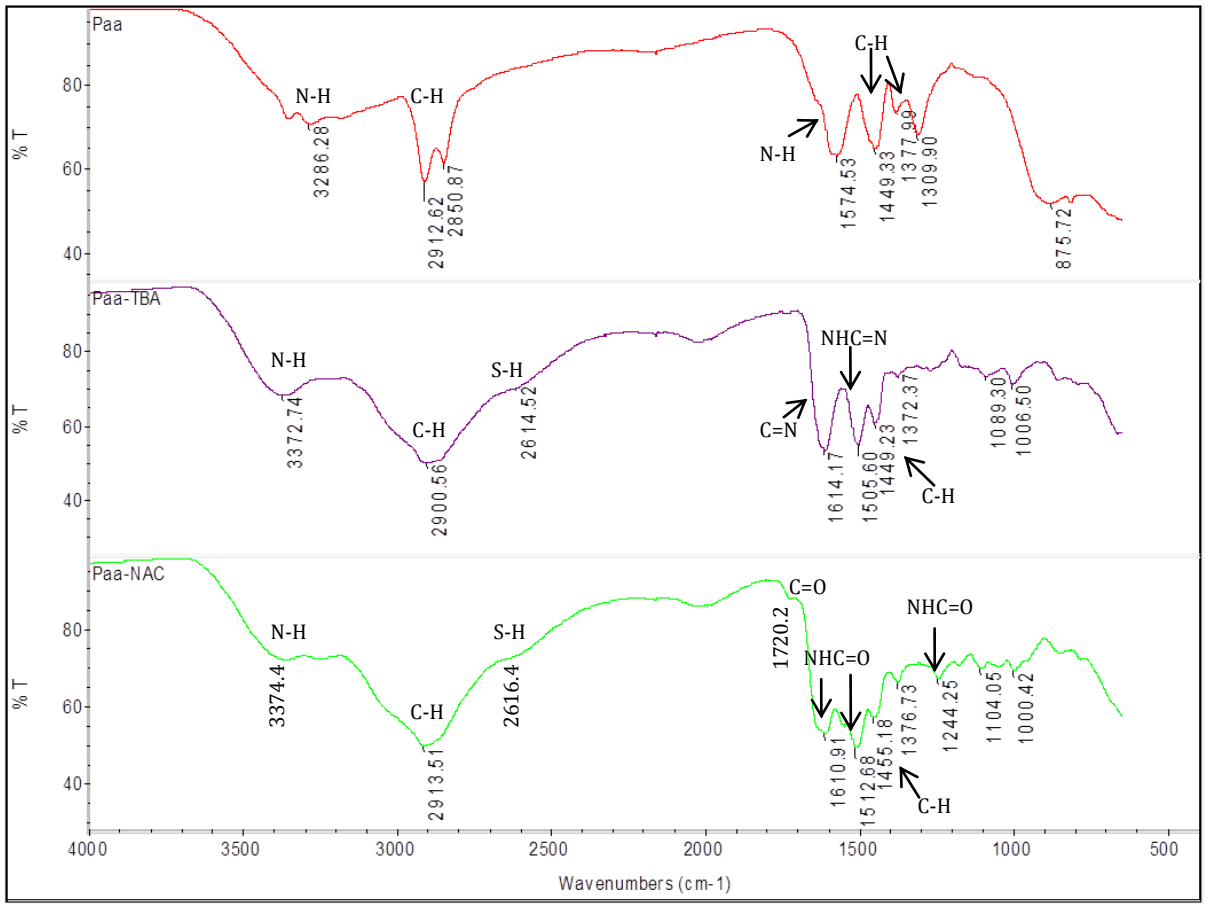

Figure 10: FTIR spectra of Paa and thiolated Paa derivatives

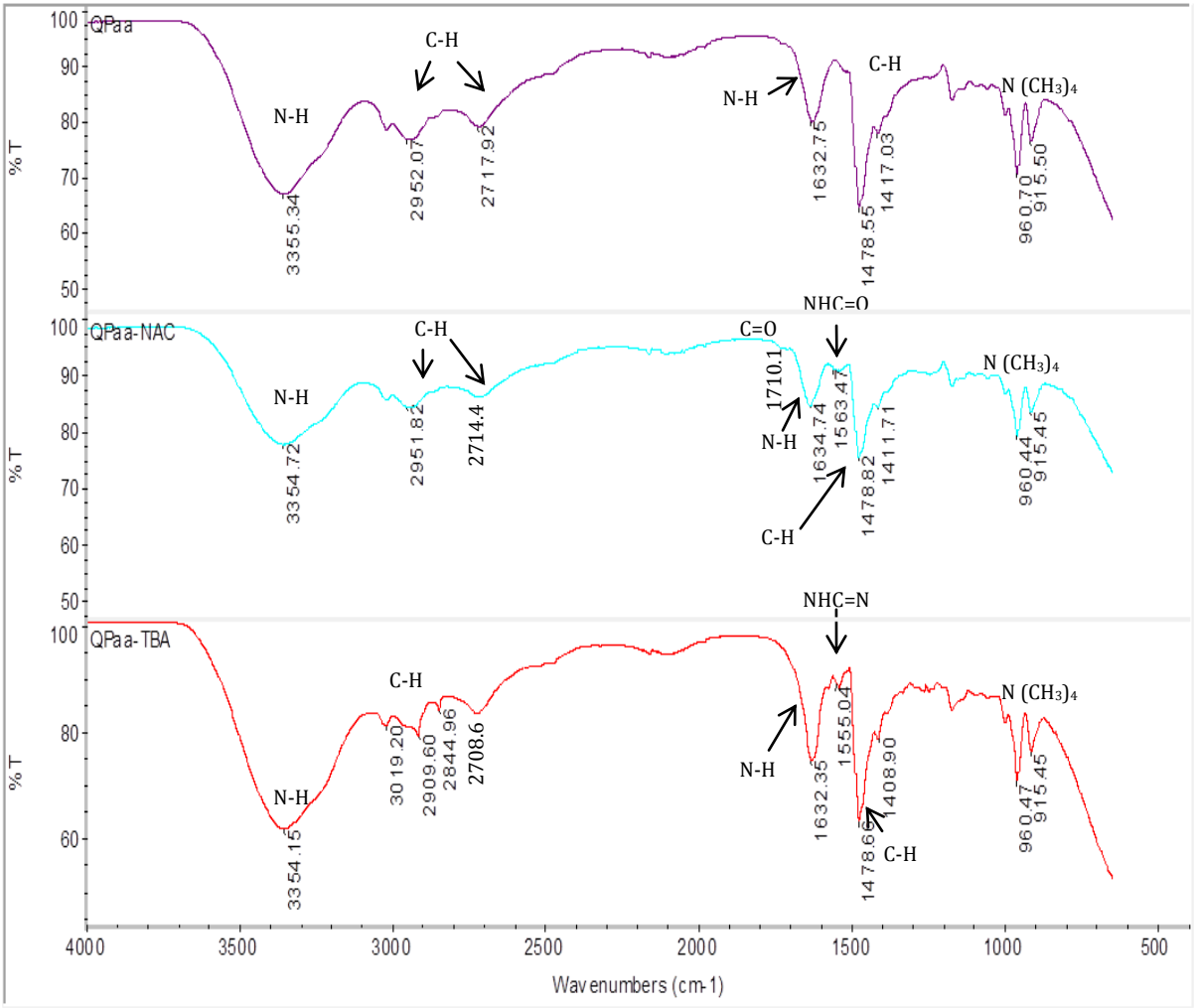

Figure 11: FTIR spectra of QPaa and thiolated QPaa derivatives

The FTIR spectra obtained after analysis of dry lyophilised polymer samples showed that the Paa backbone exhibited characteristic amine stretch and bending vibrations at 3286cm^{-1}and 1574cm^{-1} respectively, while peaks corresponding to –CH stretching vibrations were observed at approximately 2850cm^{-1}, 2912cm^{-1}, 1449cm^{-1} and a weak band at 1378cm^{-1} (figure 10). FTIR spectra of Paa-based thiomers were similar in appearance exhibiting several new peaks in addition to most peaks associated with the Paa backbone except for the Paa amine stretch peak at 1574cm^{-1} which appears to be absent suggesting substitution. Amongst the new peaks, the SH stretch vibration at 2614/2616cm^{-1} could be identified on both Paa-NAC and Paa-TBA spectra confirming successful thiolation [157, 158]. Paa-NAC showed characteristic amide absorption bands at 1610 cm^{-1} (amide I), 1512 cm^{-1} (amide II) and 1244 cm^{-1}(amide III) as well as a weak band corresponding to the carbonyl group at approximately 1720 cm^{-1}[157, 158]. The amidine bond present in Paa-TBA which has similar conjugation effects as the amide bond also exhibited

a strong band at 1614 cm^{-1} corresponding to the C=N group and another peak at 1505 cm^{-1} which correlates with the C-N stretch/N-H bend of the amide II band [159].

Quaternised Paa derivatives were characterised by N-H stretching vibration at approximately 3355 cm^{-1}, C-H stretching vibrations at 2717 cm^{-1} and 2952 cm^{-1}, N-H absorption band at 1632 cm^{-1} (figure 11). Quaternised samples also showed a C-H deformation band at 1479 cm^{-1} and a peak corresponding to the quaternary nitrogen at approximately 960 cm^{-1}[160]. In addition to the above features, thiolated QPaa samples also displayed new peaks at about 1560 cm^{-1} which could be attributed to the C-N stretch/N-H bend found in thiolated Paa samples at approximately 1500 cm^{-1}. QPaa-NAC also exhibited a weak band at 1700 cm^{-1} associated with the C=O group of the amide bond, while QPaa-TBA showed relatively stronger bands at 3019 and 2844 cm^{-1} assigned to CH_2 stretching mode probably resulting from its relatively higher level of side chain substitution [158, 161].

FTIR analysis of thiolated derivatives showed that NAC and TBA conjugates from the same parent polymer (Paa or QPaa) were largely similar in microstructure.

2.3.3. THERMAL ANALYSIS (DSC)

DSC gives information on melting point temperature (T_m) and glass transition temperature (T_g) of polymers. T_g is a kinetic transition which defines the point (temperature) at which the molecules of the polymer display a significant change in mobility [162]. Both parameters define the solid state physical and mechanical properties of polymers at ambient or body temperature and also guides their final application in biological systems [163]. Below the T_g, amorphous polymers are glassy or brittle, while above this T_g value the polymer becomes rubbery [163]. Factors related to polymer structure that may affect their thermal properties include chain stiffness, chain polarity and chain architecture. [162]

The impact of variations in the structure of different Paa derivatives on their physical and mechanical properties was reflected by DSC. Paa has no bulky side groups attached to it and hence has a relatively streamlined shape. This facilitates packing of the polymer molecules into crystallites increasing T_m [162, 163]. The DSC thermogram of Paa (figure 12) showed a sharp T_m occurring at about 138°C suggesting a semi-crystalline structure. The T_m appeared to occur simultaneously with decomposition of the polymer chains and may imply that the temperature required to disrupt the polymer crystallites also led to degradation of polymer chains. The T_g of Paa was found to be -12°C which implies that the polymer is rubbery at ambient or body temperature (consistent with experimental observations). Thiolation of Paa was found to be associated with a slight increase in T_m from approximately 138 to about 150°C. However, while

Paa-TBA which contains the amidine bond appears to have retained a semi-crystalline structure exhibiting a sharp T_m at about 140°C -150°C, Paa-NAC exhibited a shallow, broad endotherm at about the same temperature. This difference could likely be due to the fact that the amidine group exhibits relatively less branching than N-acetyl cysteine and the protonated amidine bond is also more likely to partake in intermolecular bonding strengthening the crystal lattice. Although both thiolated Paa samples showed no T_g on their DSC thermograms, Paa-TBA samples were observed to change from glassy to rubbery at room temperature, indicating that this polymer may have a T_g which was too subtle to be observed in the DSC thermograms.

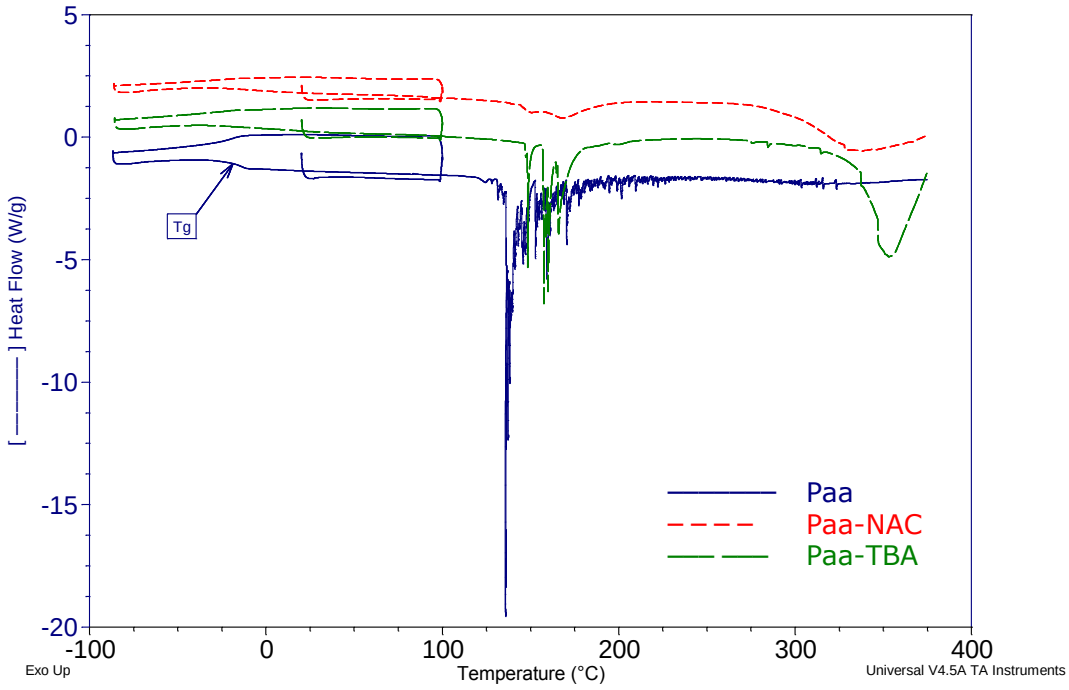

Figure 12: DSC thermograms of Paa and thiolated Paa derivatives

The attachment of bulky side groups to polymers increases the stiffness of the chain raising T_g [162]. Quaternisation which involves the attachment of bulky quaternary groups to the Paa/thiolated Paa backbone may hinder close packing of the crystallites and limit intermolecular hydrogen bonding thereby increasing system disorder [164]. This could be seen by the broad endothermic peaks exhibited by quaternised samples (figure 13). The quaternary group also creates steric bulk limiting chain flexibility and mobility of the polymer molecules. Hence, all quaternised polymers remained partially amorphous and brittle at ambient temperature except for QPaa-NAC which was soft but not rubbery. Quaternised derivatives

exhibited no T_g and the T_m of quaternised samples was much higher than their non-quaternised counterparts (290-300°C). This is similar to the thermal profile of QPaa-based AP, which showed similarly higher T_m than their non-quaternised Paa-based AP and no T_g [136].

The relatively higher T_m exhibited by quaternised polymers may be because these polymers are already in an extended conformation in their crystallite as a result of the increased stiffness of the polymer chain caused by the bulky quaternary group [164, 165]. This reduces their entropy of melting (ΔSm) or "gain in randomness" during their melting transition. According to the equation which defines T_m as ΔHm/ΔSm (where ΔHm represents the enthalpy of melting), this reduction in ΔSm will lead to an increase in T_m [164, 165]. The increase in T_m of quaternised polymers has also been attributed to a possible ionic interaction between $CH_2N^+(CH_3)_3$ and Cl^- facilitating packing of the chains into a crystal structure restoring some degree of order to the polymer structure [136]. QPaa also appeared to show decomposition of polymer chains occurring alongside its T_m. The disappearance of the sharp endothermic peaks seen in Paa and Paa-TBA indicated substitution of their primary amine groups.

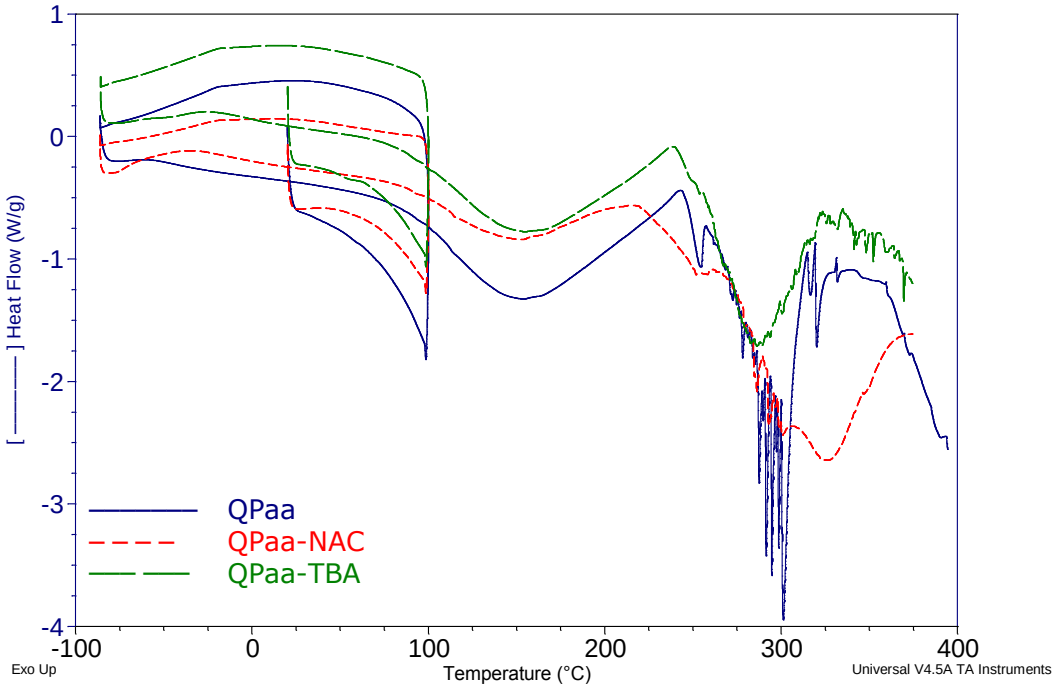

Figure 13: DSC thermograms of QPaa and thiolated QPaa derivatives.

Thermal analysis carried out on the various polymers and conjugates by DSC also confirmed the synthesis of novel derivatives of Paa/QPaa.

2.3.4. ZETA POTENTIAL

The surface charge of the each polymer was analysed by zeta potential measurement. The results of the zeta potential measurements carried out on sample solutions of each polymer in tris buffer pH 7.4 are detailed in table 2 below.

Table 2: Zeta potential (mV) of 1mgml^{-1} solutions of polymers in tris buffer pH 7.4. Values indicated are mean ± S.D. (n=3)

Polymer	**Paa**	**QPaa**	**Paa-NAC**	**QPaa-NAC**	**Paa-TBA**	**QPaa-TBA**
Zeta potential	41.9 ± 2	45.0 ± 3	35.7 ± 1	37.4 ± 1	46.9 ± 1	48.4 ± 1

Results shown in table 2 above shows that the surface charge of the polymers was found to vary with the nature of the substituting group. Quaternisation enhanced the cationic charge of both Paa and thiolated Paa derivatives. However, while thiolation using 2-iminothiolane resulted in retention of cationic charge of both parent polymers (Paa and QPaa), conjugation of Paa/QPaa to NAC resulted in a reduction of cationic surface charge. This difference is probably related to the substitution of protonable primary amine groups with the uncharged amide bond present in NAC-based thiomers while the cationic substructure of the amidine group (figure 8 and 9) facilitates the retention of cationic charge in TBA-based thiomers. The marked variation in the surface charge of the thiomers obtained could have significant implications on the capacity of the polymer to complex with insulin as well as promote processes like tight junction opening and mucoadhesion that benefit from charge-based interactions. Polymer surface charge could also influence the biodistribution and cellular uptake of insulin PECS formed from the polymers [30, 166].

2.3.5. *IN-VITRO* EVALUATION OF MUCOADHESIVE PROPERTIES

Evaluation of the mucoadhesive capacity of each polymer based on their *in-vitro* mucin adsorption profile indicated that both quaternised and thiolated polymers showed better mucoadhesive properties than the unmodified Paa backbone as can be seen in figure 14.

Thiolated Paa (Paa-NAC and Paa-TBA) exhibited the highest level of mucin adsorption amongst the different polymers tested performing better than their quaternised counterparts exhibiting similar levels of thiolation. This brings into view the fact that mucoadhesive interactions are dependent on the ability of the functional groups present on the backbone of the carrier

polymer to access and efficiently interact with compatible components of the mucin glycoproteins [167]. Thus polymer-mucin interactions are governed by multi-factorial mechanisms which determine the nature and strength of the mucoadhesive bonds and consequently, the mucoadhesive performance of the polymer [167]. A high level of polymer charge density and substitution (quaternisation, hydrophobic or thiolation) could result in a greater degree of interchain repulsion resulting in conformational changes which may decrease chain flexibility and limit interpenetration/entanglements between polymer-mucin molecules [145, 146]. Also, steric hindrance created by the presence of a high proportion of attached groups on the polymer backbone which may limit access to compatible groups by shielding charged groups thereby reducing mucoadhesive interaction [168].

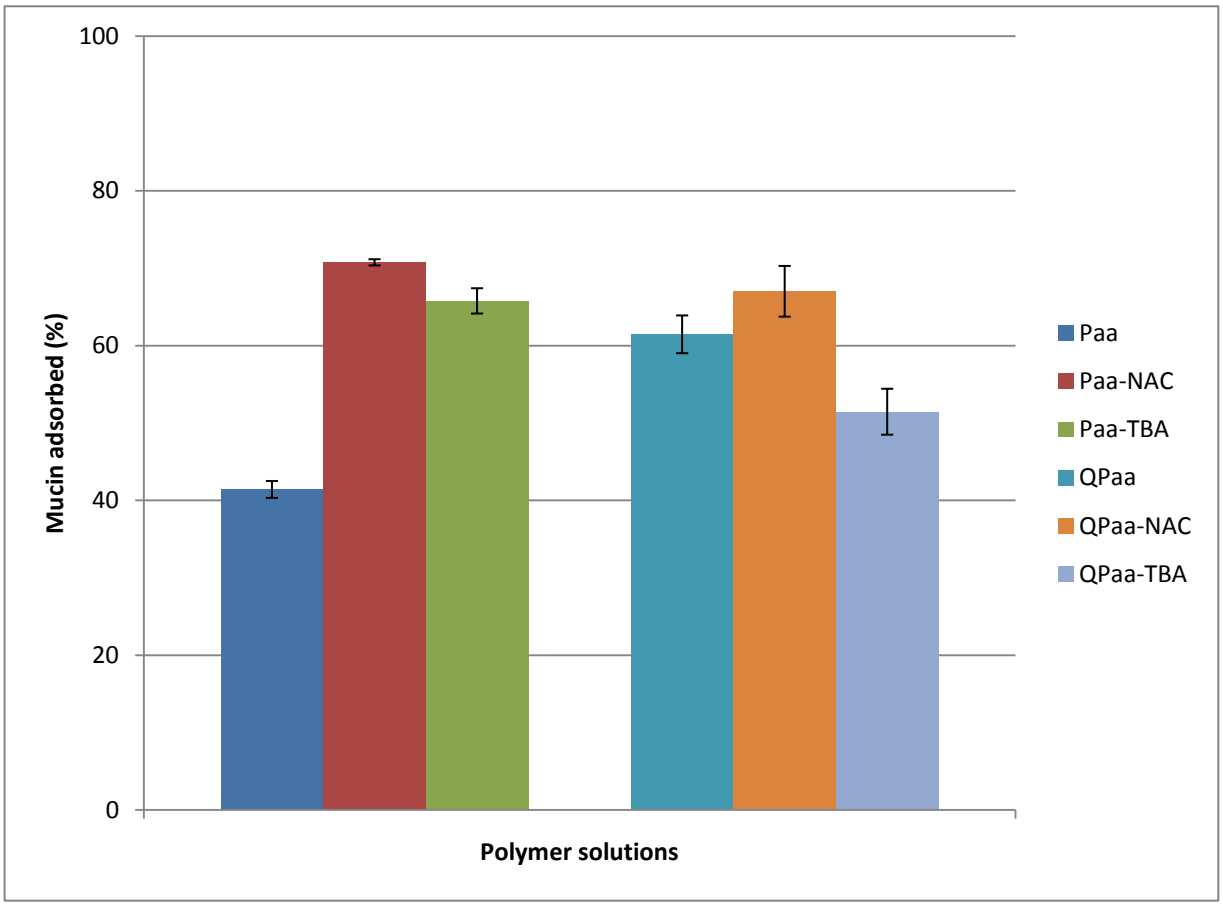

Fig. 14: Mucoadhesive capacity (% mucin adsorption) of the polymers and thiolated conjugates. (mean ± S.D.; n=3)

Hence in consideration of the aforementioned facts, assessing the mucoadhesive performance of the various thiomers as a function of level of thiol substitution indicated that although the thiol

content of Paa-TBA greatly outweighs that of Paa-NAC, Paa-TBA was slightly less mucoadhesive than Paa-NAC.

This could be associated with the high level of thiol substitution of Paa-TBA influencing polymer conformation and affecting mucin interaction or could also be as a result from the polymer thiol groups being more reactive with themselves (intra-chain thiol-disulphide crosslinking) than with those of the mucin glycoproteins. However, it appears steric effect becomes more pronounced with the QPaa-based thiomers which were already substituted with quaternary groups as can be seen from figure 14, here only QPaa-NAC which had a low level of thiolation exhibited better mucoadhesive properties than QPaa as a result of thiolation. On the contrary, QPaa-TBA showed reduced mucoadhesive properties, as this thiomer exhibited similar levels of mucoadhesion with the unmodified backbone which signifies a noticeable loss in the mucin-interaction facilitating effects of both quaternisation and thiolation. This was probably caused by steric hindrance as well as reduced chain flexibility as a result of the high degree of both quaternary and thiol substitution present in QPaa-TBA, therefore resulting in a cumulative inhibition of effective polymer-mucin interactions realised with both Paa-TBA and QPaa. This effect has been observed by other groups working with similar quaternised thiomers.

Therefore, although the mucoadhesion facilitating effects of polymer thiolation can be clearly seen by the marked increase in mucin adsorption of Paa due to thiolation, the results also highlight the need to optimise levels of substitution/quaternisation of the parent polymer to obtain the beneficial effects of these alterations on mucoadhesion.

2.3.6. EVALUATION OF *IN-SITU* CROSSLINKING PROPERTIES

Oxidation of free thiol groups above pH 5 results in the formation of intermolecular and intramolecular disulphide bonds [169] as shown in the reaction scheme below.

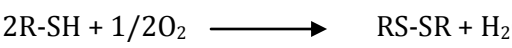

This means that thiolated polymers are capable of forming in-situ crosslinked gel networks above pH 5. The change in free thiol content of the different thiomers in phosphate buffer pH 8 was monitored by iodometric titration. It was observed that with the exception of Paa-TBA all other thiomers did not show any drop in level of free thiol content over the 8 hour incubation period and their solutions remained clear. Paa-TBA solutions on the other hand became cloudy in 1 hour and at the 2 hour time period, a visibly crosslinked network was observed within the vial as shown in figure 15 below. Centrifugation of this sample and analysis of the supernatant for the presence of free thiol by iodometric titration indicated that no free thiols could be

detected. This confirms the crosslinking of free thiols to disulphides at pH 8 occurred simultaneously with the formation of this network structure, a characteristic exhibited by thiolated polymers.

The crosslinking process was observed to be initiated by the addition of PBS into the solution of Paa-TBA in Tris buffer, implying that the process of thiol oxidation to disulphides may have been catalysed by the metal ions present in the buffer solution. This ability of metal ions to catalyse such oxidative processes has been previously documented by other research group [170]. The presence of tris in the buffer mixture was also observed to play a role in the formation of the swollen or expanded crosslinked network shown in figure 15 below

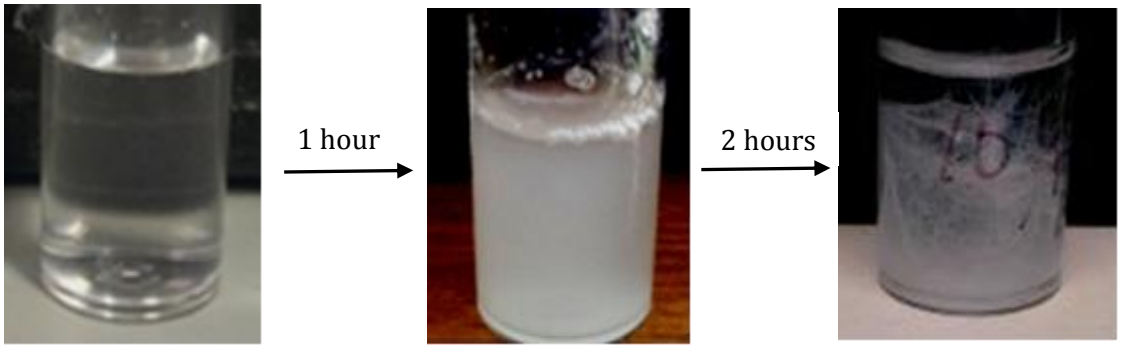

Fig. 15*: In-situ* crosslinked network formed by Paa-TBA after 2 hours incubation in tris/phosphate buffer solution.

Hydration of the dry polymer sample (Paa-TBA) with PBS was observed to lead to the formation of a collapsed gel, so the expanded network observed when PBS is added into a solution of Paa-TBA in tris buffer could be a direct effect of the increase in cationic charge of the polymer in tris buffer pH 7.4 (protonation of the primary amine group of tris base by HCl creates more positive charges within the system) resulting in increased interpolymer chain repulsion and consequent swelling [111, 171]. Such crosslinked polymer networks that undergo volume phase transitions like shrinking/swelling in response to external environmental conditions have been used in the design of hydrogels and bioadhesive systems that control the release of incorporated drugs based on changes in the porosity of the dosage form in response to different stimuli [111].

The disparity in the crosslinking behaviour of Paa-TBA and Paa-NAC could be associated with the difference in the nature (charge) of the linkage bearing the thiol substitutents. Paa-NAC thiol groups are attached via an uncharged amide bond while the amidine linkage through which the thiol groups of Paa-TBA are attached to the Paa backbone is cationic, hence creating a significant electrostatic difference in the local environment of the respective thiol moieties of Paa-TBA and Paa-NAC. Such differences in the charge density of neighbouring attached groups have been

shown to greatly influence thiol-disulphide exchange reactions [172, 173]. The formation of disulphide crosslinks by thiolated groups attached to the quaternised thiomers could have been impeded by the bulky quaternary ammonium groups present on the polymer backbone sterically limiting inter-chain thiol-disulphide interactions, as the close proximity of interacting thiol groups has been shown to improve the crosslinking process [174]. This steric effect may however be beneficial in limiting unwanted disulphide bond formation occurring between the thiomer and insulin.

The tendency of Paa-TBA to form an *in-situ* crosslinked network at physiological pH would be considered advantageous as such crosslinked systems have been used in various drug delivery applications due to their ability to offer controlled (pH-dependent) release of incorporated materials as well as extend the residence of dosage forms at the site of application [153, 161, 175].

2.4. CONCLUSION

Thiolation of Paa and QPaa was possible either through EDAC/NHS mediated coupling of the primary amine groups of the polymer to N-acetylcysteine or by modifying the polymers with 2-iminothiolane yielding the N-acetyl cysteine and 4-thiobutylamidine derivatives respectively. Thiolated derivatives from the same parent polymer were observed to be similar in structure despite differences in the thiol substituent used. DSC results showed that unlike the Paa backbone, no T_g was observed for Paa derivatives. Quaternisation of polymers also resulted in an upward shift in T_m.

Thiolated Paa derivatives were shown to have improved mucoadhesive qualities, with Paa-TBA also exhibiting *in-situ* crosslinking properties. However, thiolation of QPaa did not yield thiomers with significant improvements in mucoadhesive properties when compared to the parent polymer possibly due to their high level of quaternisation/substitution.

3. FORMULATION, CHARACTERISATION AND EVALUATION OF Paa-BASED POLYMER-INSULIN POLYELECTROLYTE COMPLEXES

3.1. INTRODUCTION

This chapter gives an overview of the processes involved in the development of optimal formulations of polymer-insulin PECS using Paa, QPaa and their thiolated derivatives by characterisation of the complexes obtained using techniques like Photon Correlation Spectroscopy (PCS) (for determination of particle size, polydispersity index (PDI) and zeta potential), UV spectroscopy (for turbidity measurements) and Transmission electron microscopy (TEM) amongst others. The section also evaluates the *in-vitro* capacity of polymer, insulin PECS prepared from different polymers to protect complexed insulin from enzymatic degradation. The mucoadhesive properties of PECS were also evaluated using the mucin adsorption method.

3.2. MATERIALS AND METHODS

3.2.1. MATERIALS

Insulin (27 units per mg/Umg^{-1}, from bovine pancreas), tris(hydroxymethyl)aminomethane (Tris base) (≥ 99%), pepsin (3640 Umg^{-1}, from porcine gastric mucosa), α-chymotrypsin (TLCK treated, Type VII from bovine pancreas, ≥ 40 Umg^{-1}), trypsin (TPCK treated, from bovine pancreas, 11,004 Umg^{-1}) and Porcine gastric mucin (crude type II) were all purchased from Sigma-Aldrich UK. Mercodia Bovine insulin ELISA kit and sample buffer were obtained from Diagenics Ltd. UK.

Trifluoroacetic acid (TFA) and Acetonitrile (HPLC grade) were all purchased from Fischer Scientific, UK. Other chemicals used were of analytical grade.

Polymers used for the formulation of test insulin PECS include Paa, Paa-TBA, Paa-NAC, QPaa, QPaa-TBA and QPaa-NAC.

3.2.2. PREPARATION OF POLYMER, INSULIN COMPLEXES

A series of test formulations of PECS were prepared at room temperature by mixing equal volumes (2ml) of separate solutions of each polymer with insulin in a glass vial while varying polymer:insulin (P : I) mass ratio between 0.2-2:1 and insulin stock solution concentration at two different concentration levels (0.5 and 2mgml^{-1}). For the parent polymers (Paa and QPaa), the complexation process was also carried out with different buffer systems (sodium hydroxide

or Tris buffer both at pH 7.4), while complexation of insulin with thiolated Paa/QPaa derivatives was carried out in tris buffer pH 7.4 only. After mixing the polymer and insulin solutions, the pH of each formulation was adjusted to pH 7.4 (using either 0.1M Tris base or 0.01M HCl as required) and the complexes were left to stand for 2 hours at room temperature before characterisation [137].

3.2.3. CHARACTERISATION OF POLYMER, INSULIN COMPLEXES

The identification and selection of optimal formulations of polymer, insulin PECS from each polymer was based on the assessment of the physical properties, stability and insulin complexation efficiency of each test PEC formulation using the parameters described below. All measurements were carried out as complexes were made (day 0) and after the formulations were left standing at room temperature for 72 hours (day 3).

3.2.3.1. Particle size analysis

The average hydrodynamic diameter (H. diameter) and polydispersity index (PDI) of insulin complexes formed by each polymer was analysed at 25°C by PCS (Zetasizer Nano-ZS, Malvern Instruments, UK) after 1ml of each complex formulation had been transferred into a plastic cuvette. The PDI of the sample gives an indication of the mean size distribution of the particles present in a sample of the PEC suspension.

3.2.3.2. Zeta Potential Measurements

The zeta potential of complexes formed within each test sample was determined by filling a folded capillary cell with a sample of each complex formulation and analysing at 25°C by PCS.

3.2.3.3. Transmittance studies

In order to evaluate the colloidal stability of complexes formed and objectively define macroscopic appearance of each test formulation, the turbidity of 2ml samples of each PEC suspension was measured by determining the percentage transmittance of each complex suspension at 630nm using an Agilent G1103A photo diode array (Agilent Technology, China). Tris buffer pH 7.4 and insulin stock solutions were used as controls.

3.2.3.4. Complexation efficiency

The amount of insulin present in each complex formulation and the corresponding control stock solution was quantified by HPLC analysis using a Shimadzu HPLC system composed of a DGU-20As degasser attached to an LC-20AD pump with a SIL-20A autosampler, a CTO-10ASvp

column oven (at 25°C) and a RF-10Axl fluorescence detector ($\lambda_{excitation}$ = 276 nm; $\lambda_{emission}$ = 600 nm).

The stationery phase was an XBridge™ BEH 130 C18 Column (150mm x 4.6mm) (Waters, U.K.) and the mobile phase was water/acetonitrile (68.5:31.5) buffered to pH 2 with TFA at a flow rate of 1mlmin^{-1}.

The insulin peak was detected at 5 minutes and the insulin concentration detected calculated from a calibration curve prepared from dilutions of a standard stock solution (0.015-1.5 mgml^{-1}; R^2 = 0.992; n=3). For Paa, QPaa and their NAC conjugates, complexation efficiency (%) of each PEC was obtained by expressing the amount of insulin detected as mentioned above as a percentage of the total amount of insulin incorporated in the sample. Complexation efficiency of PECS prepared from TBA-conjugates was obtained by first subtracting insulin concentration detected by HPLC from total amount of insulin incorporated and then expressing this value as a percentage of total insulin. Complexation efficiency of these complexes was also calculated using insulin concentrations detected by a Mercodia bovine insulin ELISA kit (Diagenics Ltd., UK). Briefly, Paa-TBA insulin complexes prepared at 0.8:1 P : I ratio were diluted down to 2.5µg/L using ELISA sample buffer and the amount of insulin contained in equivalent lml samples of complex and control was obtained following the method outlined in the assay kit. The insulin content of both control and complex samples were determined using the values obtained from a calibration plot (R^2 = 0.98) prepared from insulin standards provided in the kit (0.05-3µg/L). Results were obtained in triplicate.

3.2.3.5. Transmission Electron Microscopy (TEM)

The morphology of polymer, insulin complexes was visualised using a LEO 912 energy filtering transmission electron microscope at 100/120kV. Formvar/Carbon-coated 200 mesh copper grids were glow discharged and complex solutions dried down to a thin layer onto a hydrophilic support film. Aqueous methylamine vanadate (1%) (Nanovan; Nanoprobes, Stony Brook, NY, USA) was applied and the set-up air dried before imaging [137].

Subsequent to the optimisation process described above, stable PEC formulations were identified for each type of polymer tested. These optimal formulations were used for further evaluation processes detailed below.

3.2.4. *IN-VITRO* ENZYMATIC DEGRADATION STUDIES

Trypsin (6.4mgml^{-1}, 2.7 x 10^{-4}M), test complex suspensions and insulin control (0.25mgml^{-1}) (each 4.5ml) solutions were prepared separately in pH 8 Tris buffer and incubated in a water

bath at 37°C for 2 hours. Trypsin (0.05ml) was then added into each complex solution. Aliquots of the mixture (0.2ml) were withdrawn every 30 minutes and mixed with ice cold TFA solution (0.015ml, 0.1% v/v) to stop enzymatic activity. The experiment was conducted for 4 hours at 37°C with samples being analysed by the HPLC process described earlier. Results obtained were compared with an insulin control subjected to similar conditions as the complexes. The same process was repeated with α-chymotrypsin (5mgml^{-1}, 2.0 x 10^{-4} M) in pH 8 Tris buffer.

Peptic degradation studies were carried out by dissolving pepsin (0.1mgml^{-1}, 2.8 x10^{-6}M) in 0.01M HCl after which both complex and enzyme solutions were then buffered to pH 2 with a drop of 5M HCl and incubated in a water bath at 37°C for 2 hours. Pepsin (0.016ml) was added into the complex solutions and samples (0.15ml) were drawn from each mixture every 30 minutes and put into ice cold Tris base (0.15ml, 0.1M) to halt enzyme activity. This experiment was also conducted for 4 hours at 37°C with samples being analysed by HPLC. Results obtained were compared with insulin controls (0.25mgml^{-1}) subjected to similar conditions as the complexes. HPLC analysis was subsequently carried out on each sample to determine the amount of non-degraded insulin remaining as a function of time.

3.2.5. *IN-VITRO* EVALUATION OF MUCOADHESIVE CAPACITY OF COMPLEXES

Assessment of the mucoadhesive capacity of each polymer, insulin PEC formulation was determined by measurement of the amount of mucin adsorbed by the complexes using the mucin adsorption assay described in section 2.2.4. [152]. PEC formulations composed of 0.5:0.25 mgml^{-1} P: I mass ratio were prepared for each test polymer as described earlier. Experiments were carried out by mixing 1ml of mucin in tris buffer pH 7.4 solution (1mgml^{-1}) with a 0.25ml sample of each test PEC formulation. Controls were prepared by mixing 0.25ml of Tris buffer pH 7.4 with 1ml (1mgml^{-1}) mucin solution and incubated as described for test samples An additional test sample containing a similar mixture of mucin and 0.25ml of insulin in tris buffer pH 7.4 (0.25mgml^{-1}) was also prepared. These mixtures were subsequently incubated at 37°C on a shaking water bath for 5 hours.

All control and test samples were subsequently transferred into separate Eppendorf tubes and centrifuged at 10,000rpm for 30minutes, and the concentration of mucin in each supernatant measured by UV spectrometry at 251nm. Percentage (%) of total mucin adsorbed to each sample of polymer was calculated as described in section 2.2.4.

3.2.6. STATISTICAL ANALYSIS

All results are expressed as the mean ± standard deviation of three experiments.

3.3 RESULTS AND DISCUSSION

3.3.1. FORMULATION DEVELOPMENT AND OPTIMISATION

Developing stable formulations of polymer, insulin PECS involved evaluating the impact of varied polymer: insulin (P: I) mass ratios, insulin stock concentration level and different buffer systems on the physical properties and stability of complexes formed.

Parameters used in the evaluation and subsequent selection of optimal formulations included: insulin complexation efficiency which shows the proportion of incorporated insulin available as nano-sized PECS; particle size analysis comprising measurements of hydrodynamic diameters as well as the size distribution (PDI) of complexes formed and turbidity measurements (expressed as %transmittance) which reflects the stability and macroscopic properties of the formulation. The average zeta potential of each formulation was determined and used alongside the aforementioned properties to evaluate the overall stability profile of the test formulation. TEM imaging was also carried out on both stable and unstable samples of selected complexes.

Good formulations of these PECS should contain discrete, nano-sized complexes exhibiting hydrodynamic diameters between 50-200nm and PDI values between 0.1-0.3 showing a uniform particle size distribution. These complexes should also exhibit high insulin complexation efficiency and high transmittance values indicating minimal aggregation of PECS.

3.3.1.1. Evaluation of Paa, insulin complexation in Tris buffer pH 7.4

Paa, insulin PECS were prepared in Tris buffer pH 7.4 using both 0.5 and 2mgml^{-1} insulin stock solutions at mass ratios between 0.2-2:1 and analysed as described above at Day 0 (2 hours after PEC preparation) and at day 3 (72 hours after PEC preparation). Zeta potential of complexes was carried out only at day 0. Results are shown in figures 16-19 and Table 3 below.

Table 3: Zeta potential (mV) of Paa, insulin PECS prepared in Tris buffer pH 7.4 using 0.5 and 2mgml^{-1} insulin stock at day 0 (n=3; mean ± S.D).

	0.5mgml^{-1} insulin stock				**2mgml^{-1} insulin stock**			
Mass ratios	**0.2:1**	**0.8:1**	**1:1**	**2:1**	**0.2:1**	**0.8:1**	**1:1**	**2:1**
Zeta (mV)	29.8 ± 2	31.2 ± 1	33.9 ± 1	34.2 ± 3	29.9 ± 2	36.1 ± 1	38.6 ± 4	35.3 ± 2

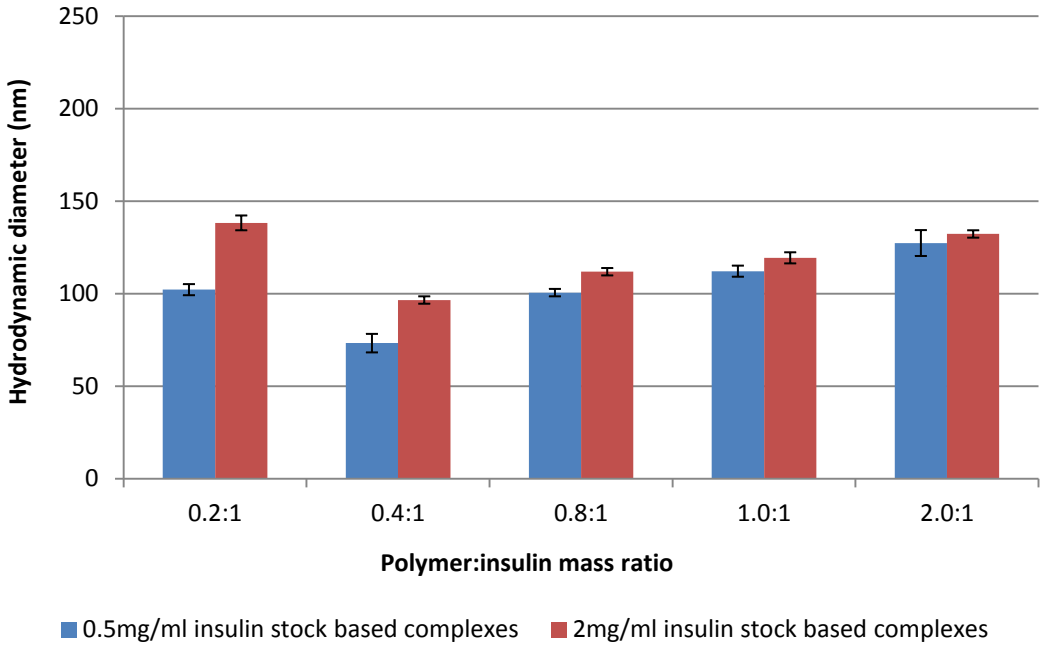

A)

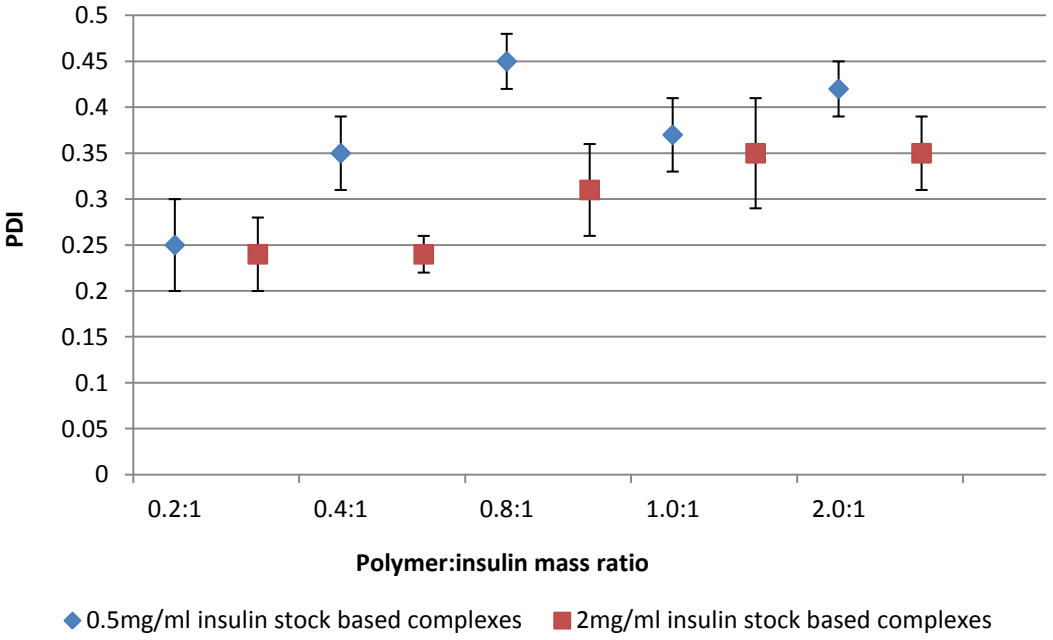

B)

Fig. 16: Particle size analysis of Paa, insulin complexes in Tris buffer pH 7.4 at day 0. Results show A) Hydrodynamic diameter B) PDI of PECS prepared at varied P: I mass ratios using 0.5 and 2mgml^{-1} insulin stock. (n=3; mean ± S.D.)

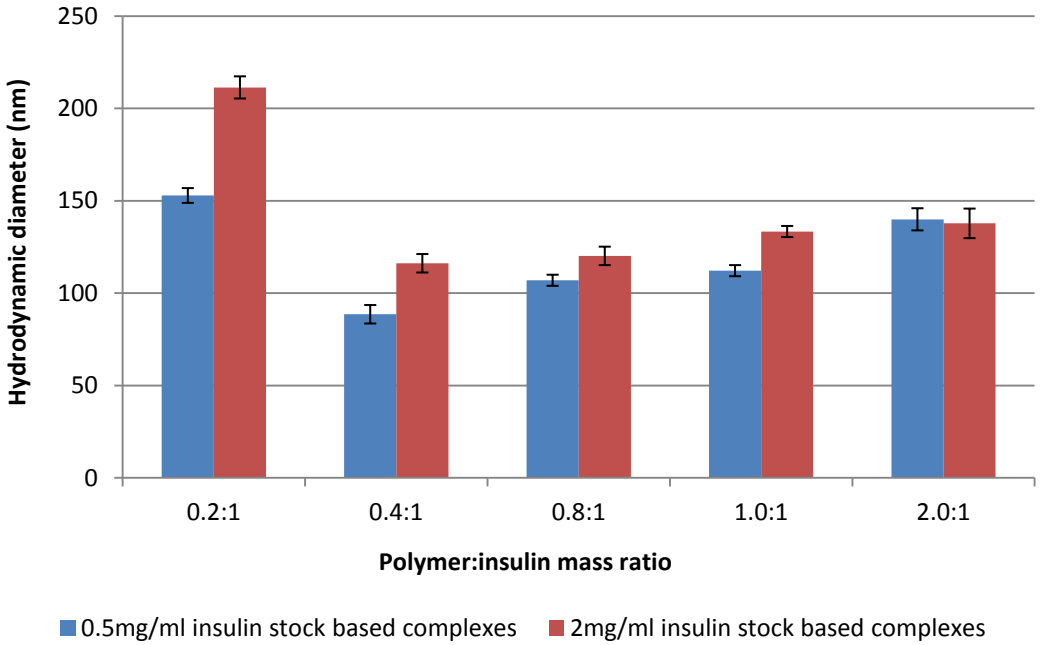

A)

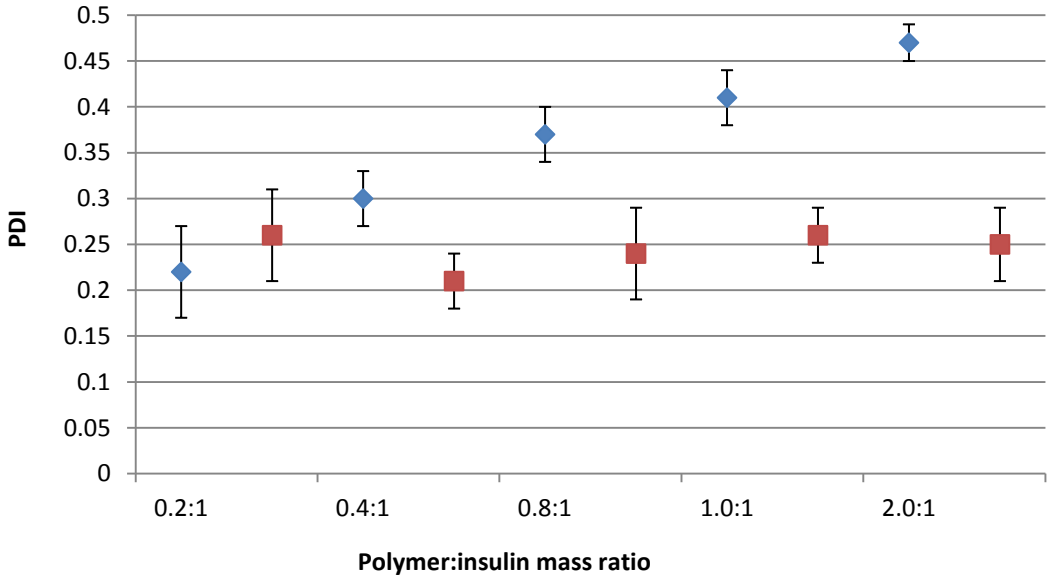

B)

Fig. 17: Particle size analysis of Paa, insulin complexes in Tris buffer pH 7.4 at day 3. Results show A) Hydrodynamic diameter B) PDI of PECS prepared at varied P: I mass ratios using 0.5 and 2mgml^{-1} insulin stock. (n=3; mean ± S.D.)

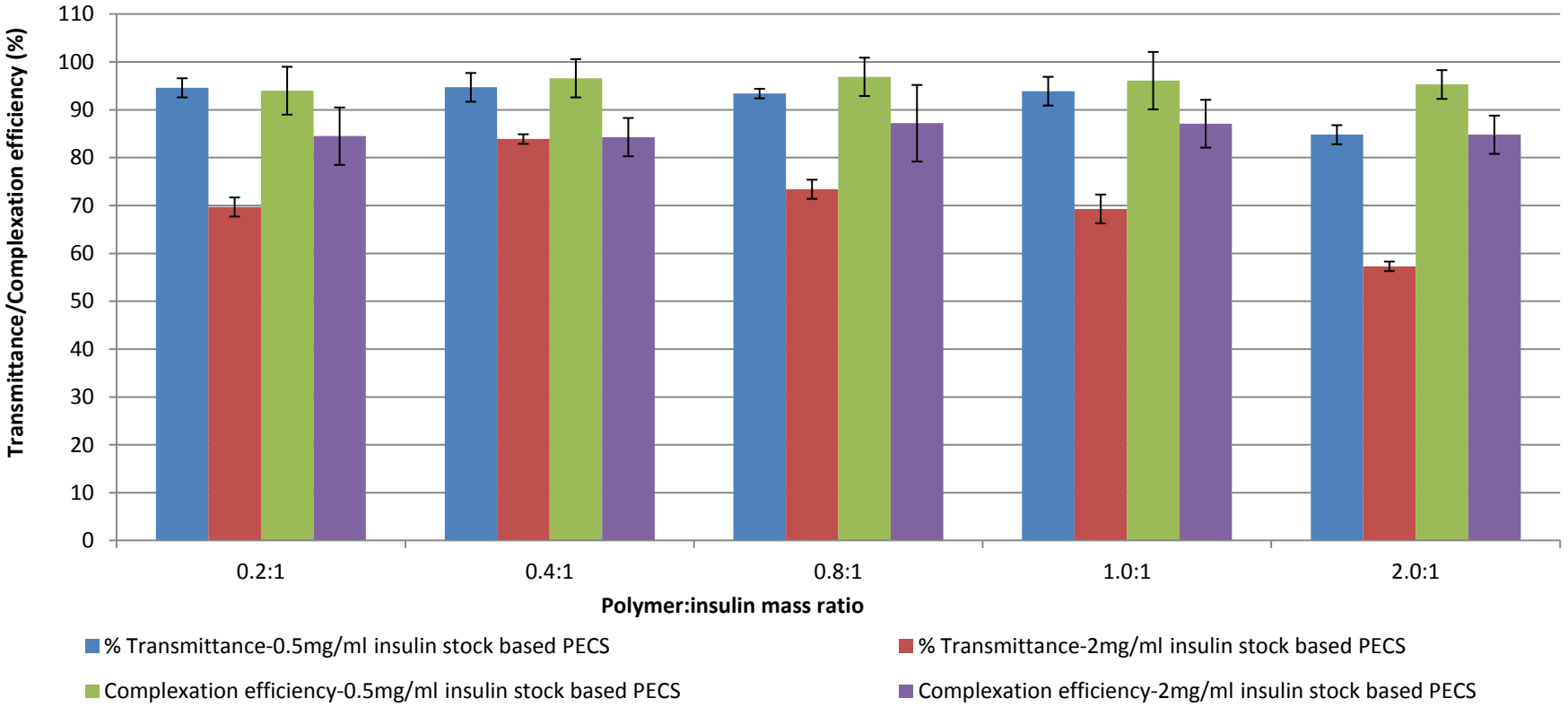

Fig. 18: % Transmittance and Complexation efficiency of Paa, insulin PECS prepared in Tris buffer pH 7.4 at different P: I mass ratios using 0.5 and 2mgml^{-1} insulin stock solution (Day 0) (n=3; mean ± S.D.)

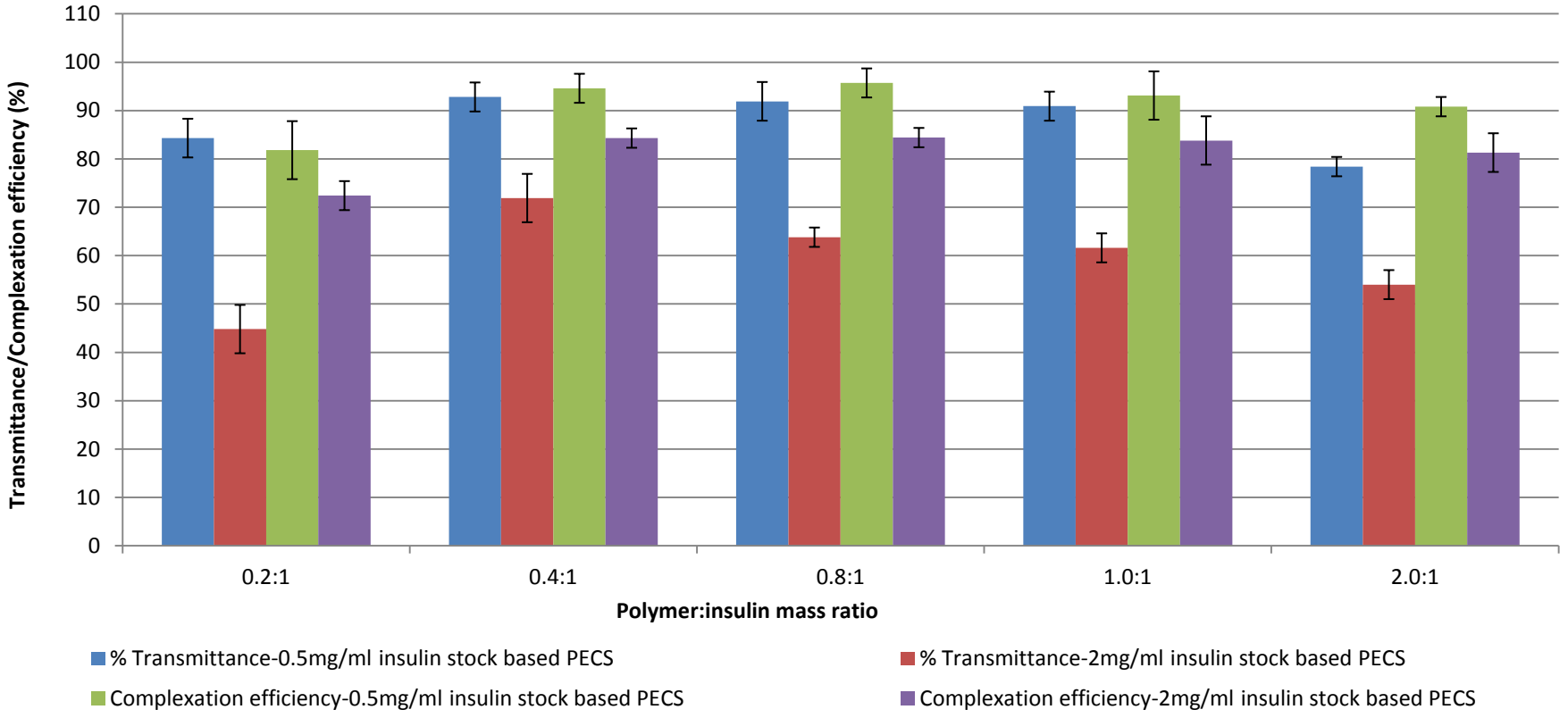

Fig. 19: % Transmittance and Complexation efficiency of Paa, insulin PECS prepared in Tris buffer pH 7.4 at different P: I mass ratios using 0.5 and 2mgml^{-1} insulin stock solution (Day 3) (n=3; mean ± S.D.)

Complexation of Paa with insulin was carried out initially in Tris buffer pH 7.4 using the 0.5mgml^{-1} insulin stock solution. Results at day 0 show that at P: I mass ratio between 0.2-1:1, Paa complexes yielded clear formulations with corresponding high transmittance values (figure 18). However, complexes exhibited relatively larger particle sizes at P:I mass ratios of 0.2:1 suggesting the existence of weaker P: I interaction at this ratio although the formulation appeared stable. Particle sizes increased again at P : I mass ratio of 2:1 and PECS turned translucent displaying a corresponding decrease in transmittance. Increasing P : I mass ratio to 2:1 may result in compression of the electrical double layer around suspended particles reducing the magnitude of the repulsive barrier between PECS (figure 20) and increasing the chances of aggregation consequently elevating particle sizes.

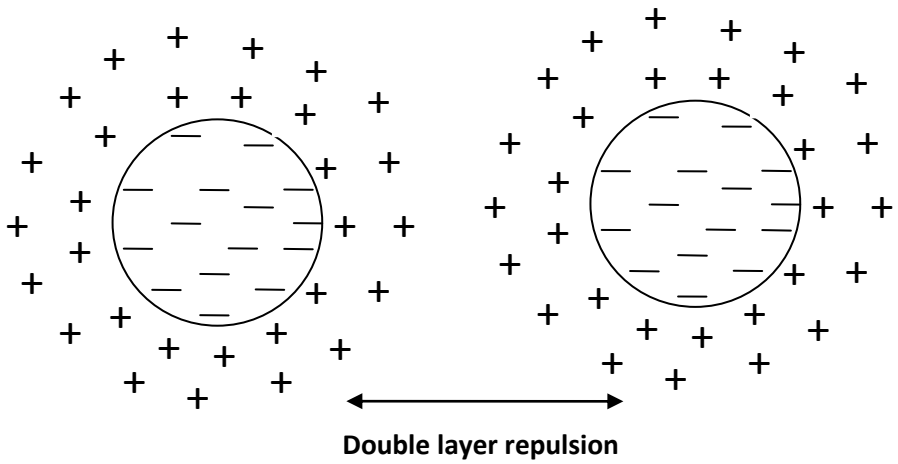

Fig. 20: Representation of Electrostatic double layer repulsion between polyelectrolyte particles.

However, formulations at higher P : I mass ratios (2:1) showed no sign of precipitation or phase separation suggesting the zeta potential of the complexes formed was sufficient to keep the particles suspended in the system. However, the PDI value for these complexes was high (> 0.3) indicating a broadening in the size distribution of complexes formed.

Raising the concentration level of the insulin stock used to 2mgml^{-1} resulted in translucent formulations (as shown in figure 21B below) with relatively larger particle sizes and lower transmittance values. Across the different mass ratios used, the stability profile of complexes followed a similar trend with that obtained at 0.5mgml^{-1} with PECS at the upper and lower margins of the mass ratio combinations (0.2:1 and 2:1) exhibiting much larger particle sizes as can be seen in figure 16.

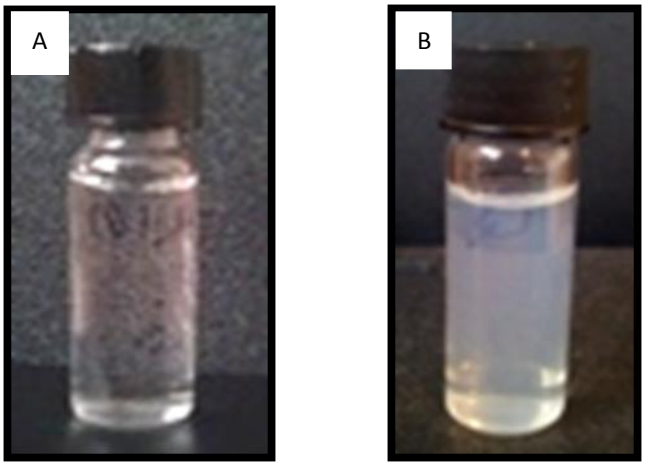

Fig. 21: Paa, insulin complex formulations A) Clear PEC formulation obtained from the 0.5mgml^{-1} insulin stock at P : I mass ratios between 0.2-1:1 B) translucent PEC formulation obtained from the 2mgml^{-1} insulin stock

The translucent appearance of complexes could be a direct effect of the higher concentration of complexes in the suspension and/or as a result of intercomplex associations as interparticulate distances fall allowing attractive forces to predominate. Hence complexes exhibit large particle sizes as they probably exist as aggregates not discrete units. PDI values for complexes prepared at the higher insulin stock concentration level appeared to be generally lower (< 0.3) than was observed with PECS prepared using the 0.5mgml^{-1} insulin stock, suggesting that the complexation process was more uniform with increase in polyelectrolyte concentration. Insulin complexation efficiency was observed to be high (≥ 90%) at all P: I mass ratios for both insulin stock concentration levels.

Paa, insulin complexes were left standing for 72 hours at room temperature and characterised. Results of analysis at day 3 indicate that for both 0.5 and 2mgml^{-1} insulin stock, complexes prepared at P: I mass ratio of 0.2:1 showed visible signs of precipitation causing an increase in particle sizes and fall in transmittance and complexation efficiency values (figures 17 and 19). The instability observed at 0.2:1 could be as a result of the lower zeta potential (<30mV) of complexes at this mass ratio, as zeta potential values above 30mV have been found to be important in stabilising dispersions of colloidal particles [176]. This is in agreement with the results of similar work which reports the formation of unstable aggregates at low P: I mass ratios presumed to be as a result of excess of the interacting protein [140].

PEC formulations at P: I mass ratios of 2:1 appeared more turbid at day 3, than formulations at P: I mass ratios between 0.4-1:1 which retained high transmittance and insulin complexation

efficiency values with slight increases in particle size. These results indicate that in Tris buffer pH 7.4, P : I mass ratios between 0.4-1:1 were optimal formulations for the preparation of Paa, insulin PECS.

3.3.1.2. Evaluation of QPaa, insulin complexation in Tris buffer pH 7.4

Characterisation of QPaa, insulin PECS prepared in Tris buffer pH 7.4 was also carried out at day 0 and day 3. Zeta potential values were carried out only at day 0. Results are displayed in figures 22-25 and Table 4 below.

Table 4: Zeta potential (mV) of QPaa, insulin PECS prepared in Tris buffer pH 7.4 using 0.5 and 2mgml^{-1} insulin stock at day 0 (n=3; mean ± S.D.).

	0.5mgml^{-1} insulin stock				**2mgml^{-1} insulin stock**			
Mass ratios	**0.2:1**	**0.8:1**	**1:1**	**2:1**	**0.2:1**	**0.8:1**	**1:1**	**2:1**
Zeta (mV)	27.8 ± 4	30.4 ± 1	34.2 ± 3	30.4 ± 3	29.8 ± 1	32.6 ± 2	33.0 ± 1	33.8 ± 1

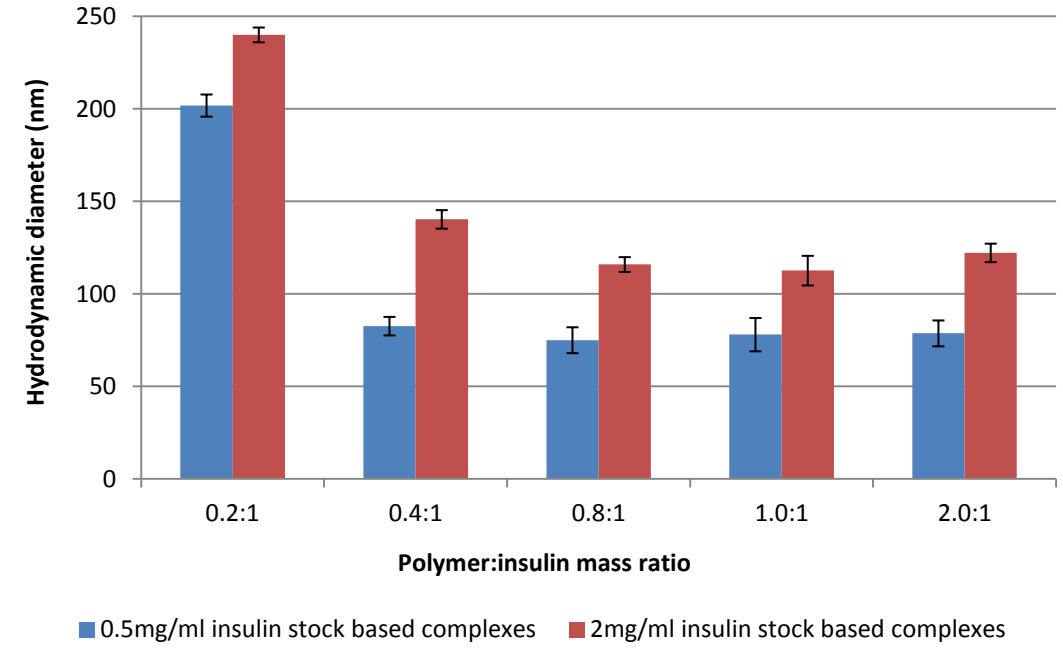

A)

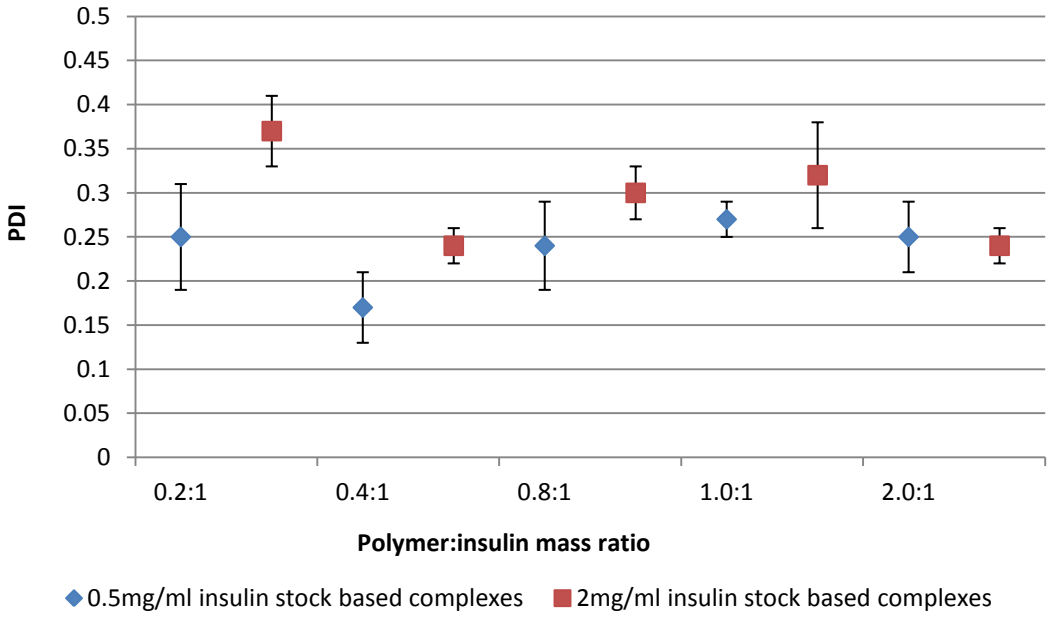

B)

Fig. 22: Particle size analysis of QPaa, insulin complexes in Tris buffer pH 7.4 at day 0. Results show A) Hydrodynamic diameter B) PDI of PECS prepared at varied P: I mass ratios using 0.5 and 2mgml^{-1} insulin stock. (n=3; mean ± S.D.)

Day 3 size analysis results showed that QPaa, insulin PECS prepared at 0.2:1 P: I mass ratio were above 1µm. Hence results were not included in figure 23 below.

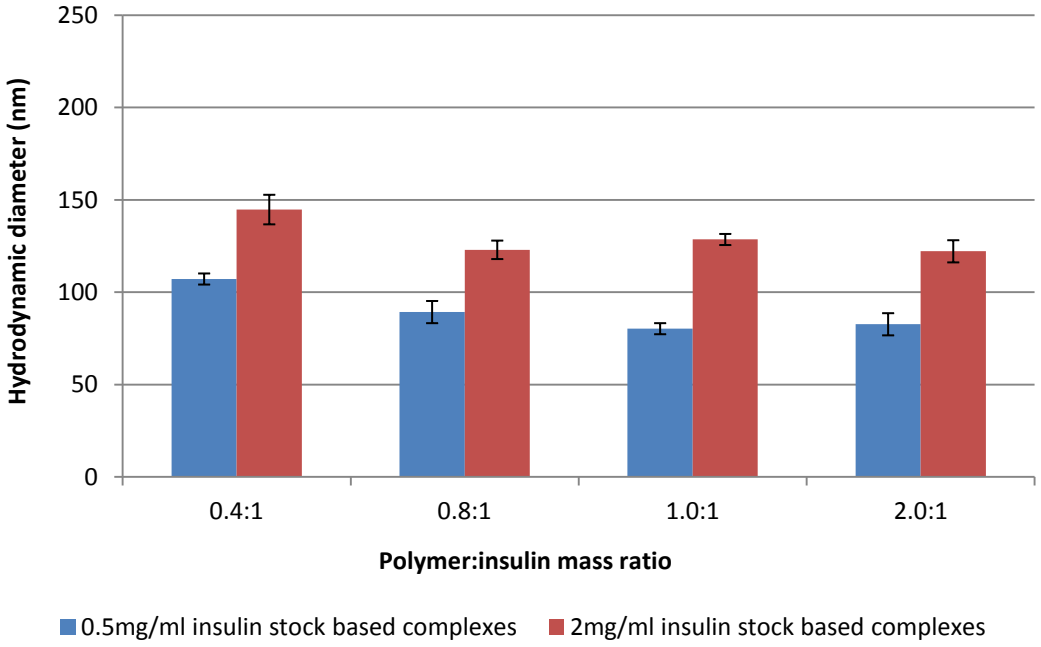

A)

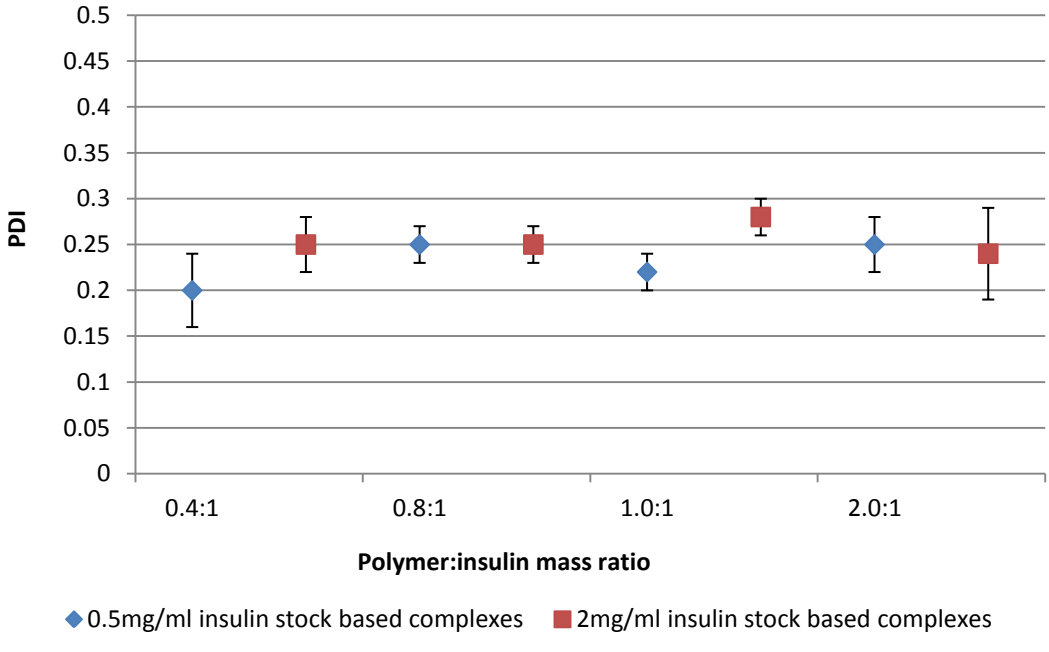

B)

Fig. 23: Particle size analysis of QPaa, insulin complexes in Tris buffer pH 7.4 at day 3. Results show A) Hydrodynamic diameter B) PDI of PECS prepared at varied P: I mass ratios using 0.5 and 2mgml^{-1} insulin stock. (n=3; mean ± S.D.)

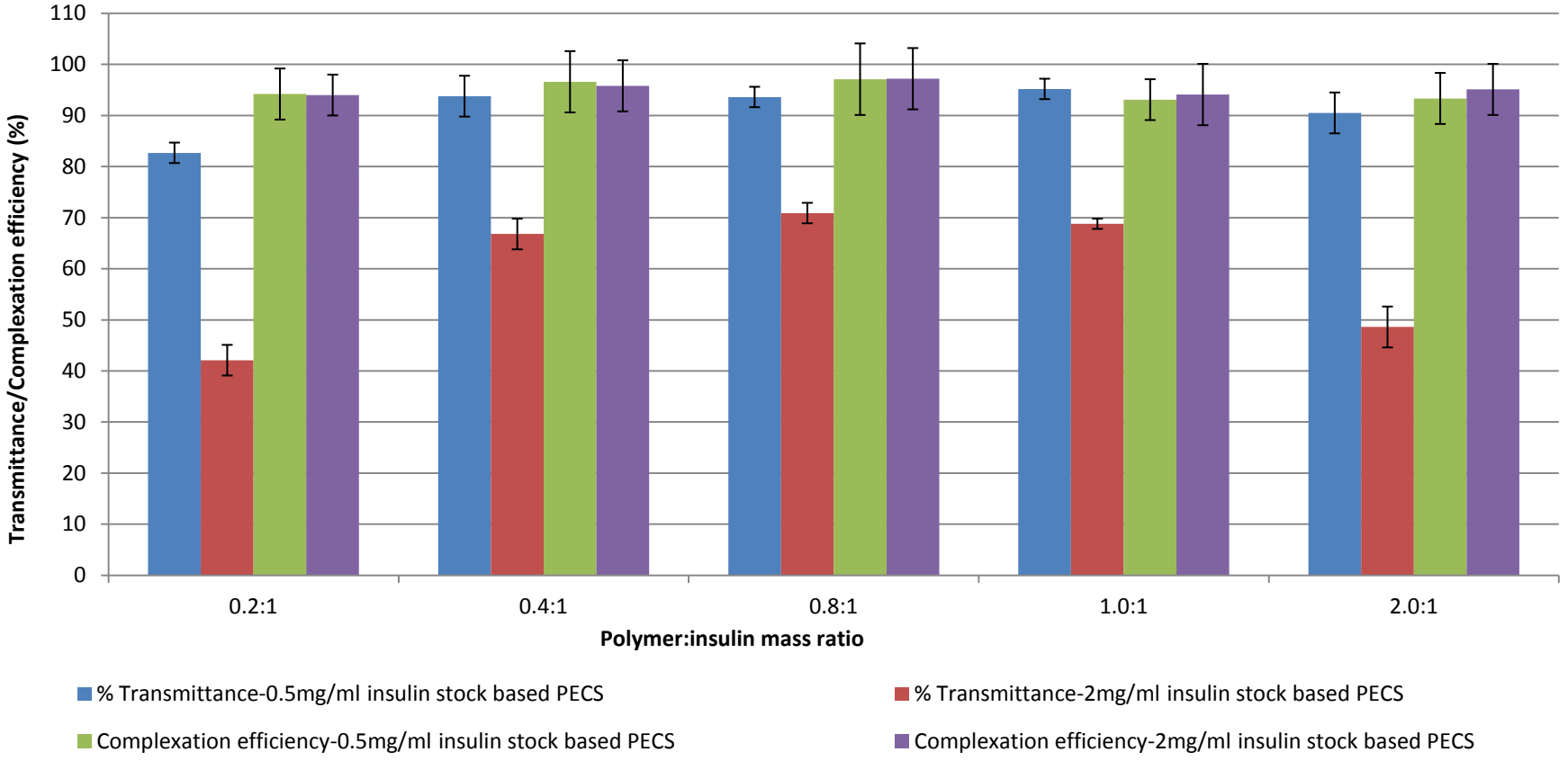

Fig. 24: % Transmittance and Complexation efficiency of QPaa, insulin PECS prepared in Tris buffer pH 7.4 at different P: I mass ratios using 0.5 and 2mgml^{-1} insulin stock solution (Day 0) (n=3; mean ± S.D.)

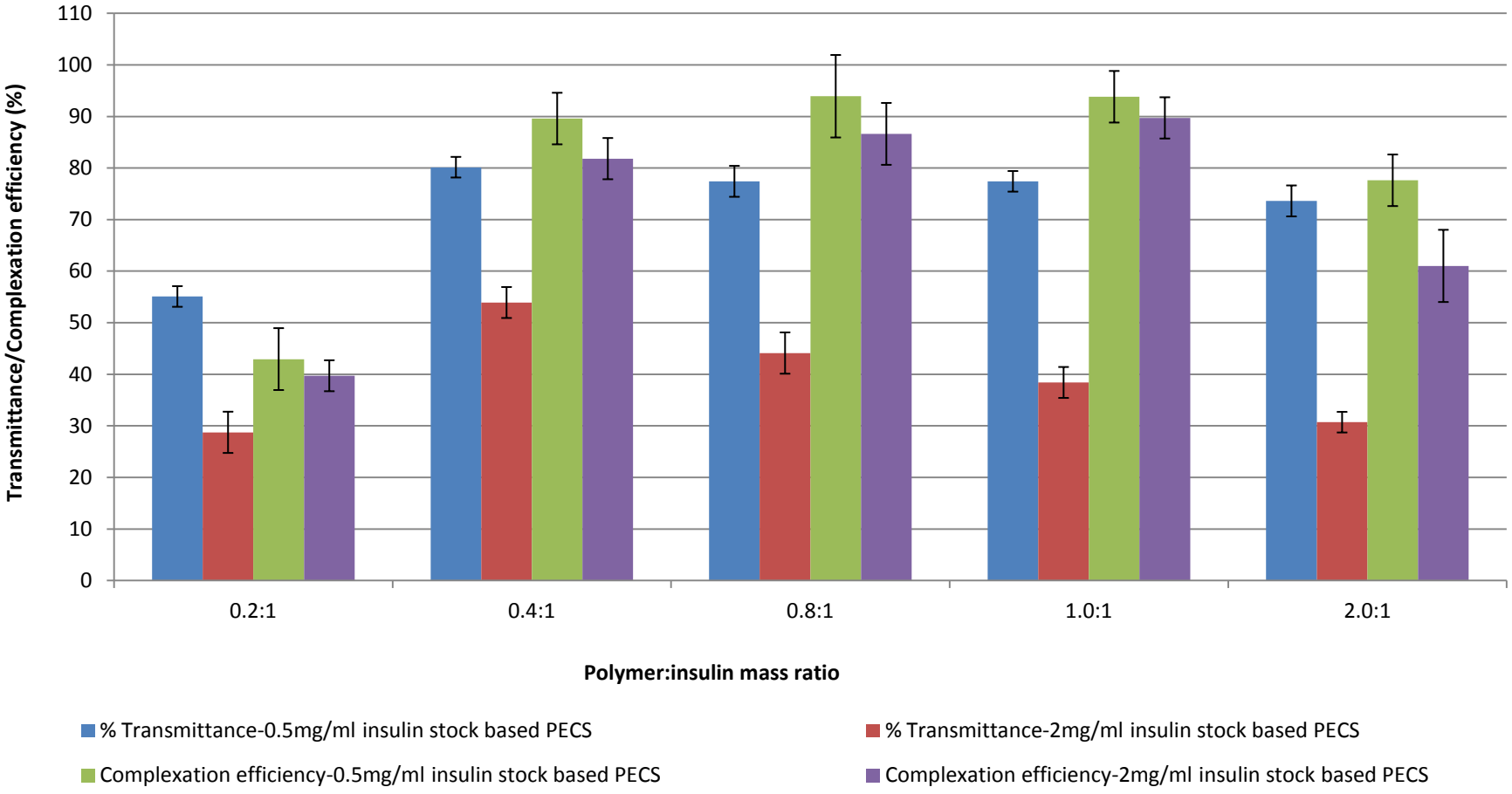

Fig. 25: % Transmittance and Complexation efficiency of QPaa, insulin PECS prepared in Tris buffer pH 7.4 at different P: I mass ratios using 0.5 and 2mgml^{-1} insulin stock solution. (Day 3) (n=3; mean ± S.D.)

In Tris buffer pH 7.4, results show that QPaa insulin PECS prepared using the 0.5mgml^{-1} insulin stock at low P: I mass ratio of 0.2:1 contained flocculated precipitates which settled at the bottom of the vial, creating a two-phased system composed of a clear supernatant layer and a flocculated bottom layer as shown in figure 26 below.

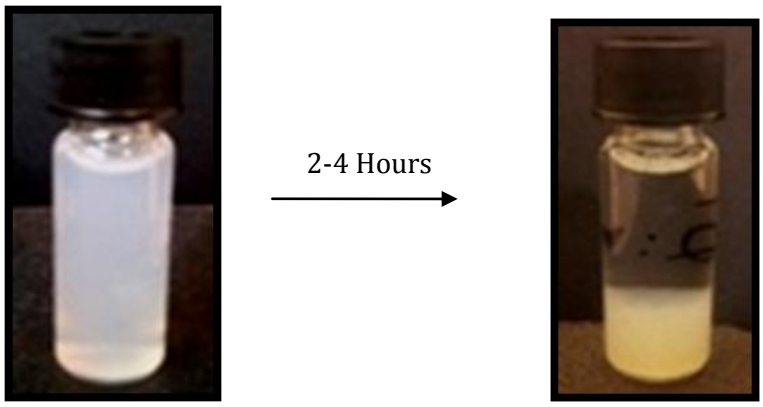

Fig. 26: QPaa, insulin PECS in Tris buffer pH 7.4 at P: I mass ratio 0.2:1 showing flocculated precipitation at the bottom of the vial after 2-4 hours of preparation.

Therefore, QPaa PECS at low P: I mass ratio (0.2:1) exhibited large particle sizes, low transmittance values and low insulin complexation efficiency (figure 22 and 24) as most of the incorporated insulin was present within this flocculated structure rather than as nano-sized PECS. The flocculation effect observed at low P: I mass ratio may suggest that polymer chains could adsorb onto multiple insulin complexes at high interparticulate distances creating a bridge between individual complexes and causing flocculation (figure 27) [177].

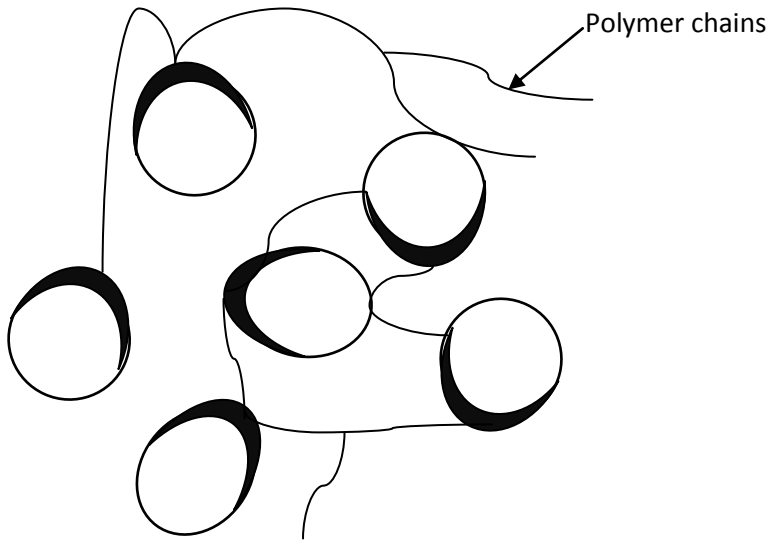

Fig. 27: Schematic illustration of polymer bridges initiating the formation of flocculated particles

Rapid phase separation was evident at Day 0 in QPaa PEC formulations made at 0.2:1 P: I mass ratios, while the onset of precipitation for similar Paa-based formulations started at day 3. This difference in the nature of interaction of Paa and QPaa with insulin at low P: I ratio could be associated with the variations in their chemical composition. N-methylation in QPaa may facilitate more intracomplex (QPaa-insulin) hydrophobic interactions at the expense of hydrophilic interactions with the bulk aqueous phase. However, increasing the P: I mass ratio to values between 0.4-1:1 stabilised the system enhancing the formation of small nano-sized complexes (<100nm) of uniform size distribution which displayed high transmittance values (>90%). The formulations were stable showing no visible signs of precipitation or phase separation. This increase in complex stability may arise from increase in repulsive forces between individual particles and/or steric forces as the surface area of particles covered by hydrophilic polymer chains increases as illustrated in figure 28 below.

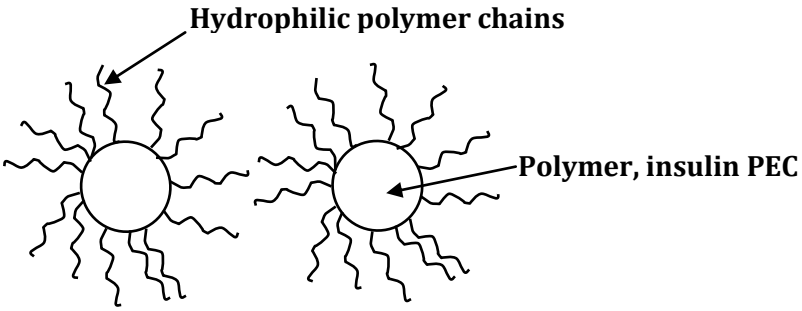

Fig. 28: Diagrammatic representation of steric repulsion between hydrophilic polymer chains.

However, a slight increase in PEC size and reduction in transmittance values at 2:1 P: I ratio showed that further increase in P:I ratio/polyelectrolyte concentration may result in compression of the double layer, reducing the magnitude of the repulsive barrier between individual complexes and increasing the chances of aggregation consequently elevating particle sizes [177, 178]. QPaa, insulin complexes displayed a more uniform size distribution (PDI values were < 0.3) than Paa complexes. This suggests that at the lower insulin stock concentration level (0.5mgml^{-1}), P : I interaction was more efficient and uniform with quaternised than non-quaternised Paa.

With the exception of complexes prepared at 0.2:1 which exhibited turbidity and precipitation/flocculation (figure 29A below), raising the concentration level of the insulin stock used in the preparation of QPaa, insulin PECS to 2mgml^{-1} also resulted in the formation of translucent but stable formulations with relatively larger particle sizes and lower transmittance values than similar PECS prepared using the 0.5mgml^{-1} insulin stock. PEC formulations were

however free from precipitation indicating PECS may be in the form of aggregates of complexes which still remain suspended in the system (figure 29C below) because of their high zeta potential. Except for the 0.2:1 P: I mass ratio, insulin complexation efficiency was observed to be high (> 90%) for all other QPaa, insulin PEC formulations. Complexation efficiency of stable QPaa, insulin complexes was observed to be higher than equivalent Paa, insulin complexes suggesting that P: I interaction was strengthened by quaternisation.

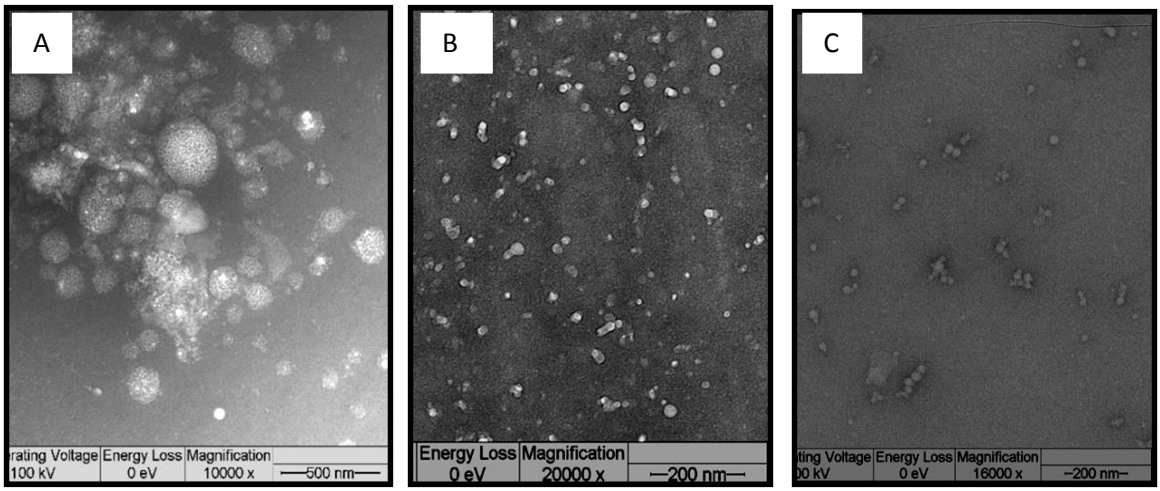

Fig. 29: TEM images of QPaa, insulin complexes prepared in Tris buffer pH 7.4 A) large precipitates obtained using the 0.5mgml^{-1} insulin stock at 0.2:1 P: I mass ratio B) small discrete spherical complexes obtained using the 0.5mgml^{-1} insulin stock at 0.8:1 P: I mass ratio C) complexes prepared at 0.8:1 P : I mass ratio using the 2mgml^{-1} insulin stock showed aggregates of spherical complexes.

Results of analysis at day 3 suggest that QPaa, insulin complexes prepared between P : I mass ratios of 0.4-1:1 were stable formulations exhibiting minimal changes in particle size, complexation efficiency and transmittance values. While, PEC formulations at 0.2:1 P : I mass ratio contained precipitates exceeding the nano-range by day 3. Therefore, optimal P : I mass ratio for the formulation of QPaa, insulin PECS was observed to range between 0.4-1:1.

3.3.1.3. Evaluation of Paa/QPaa, insulin complexation in sodium hydroxide buffer

Preparation of Paa and QPaa, insulin PECS was carried out as described in section 3.1.1. using sodium hydroxide buffer at pH 7.4 instead of Tris buffer and the formulations characterised at day 0 and day 3. Results are shown in tables 5-6 and figures 30-37 below.

Table 5: Zeta potential (mV) of Paa, insulin PECS in NaOH buffer pH 7.4 at day 0 (n=3; mean ± S.D.).

	0.5mgml^{-1} insulin stock				2mgml^{-1} insulin stock			
Mass ratios	**0.2:1**	**0.8:1**	**1:1**	**2:1**	**0.2:1**	**0.8:1**	**1:1**	**2:1**
Zeta (mV)	29.8 ± 3	27.0 ± 1	22.9 ± 1	28.5 ± 2	24.6 ± 4	22.4 ± 3	21.5 ± 3	20.1 ± 2

Size analysis showed 2mgml^{-1} insulin stock-based Paa, insulin PECS in sodium hydroxide buffer were precipitated with sizes above 1µm. Results were not included in figures 30 and 31 below.

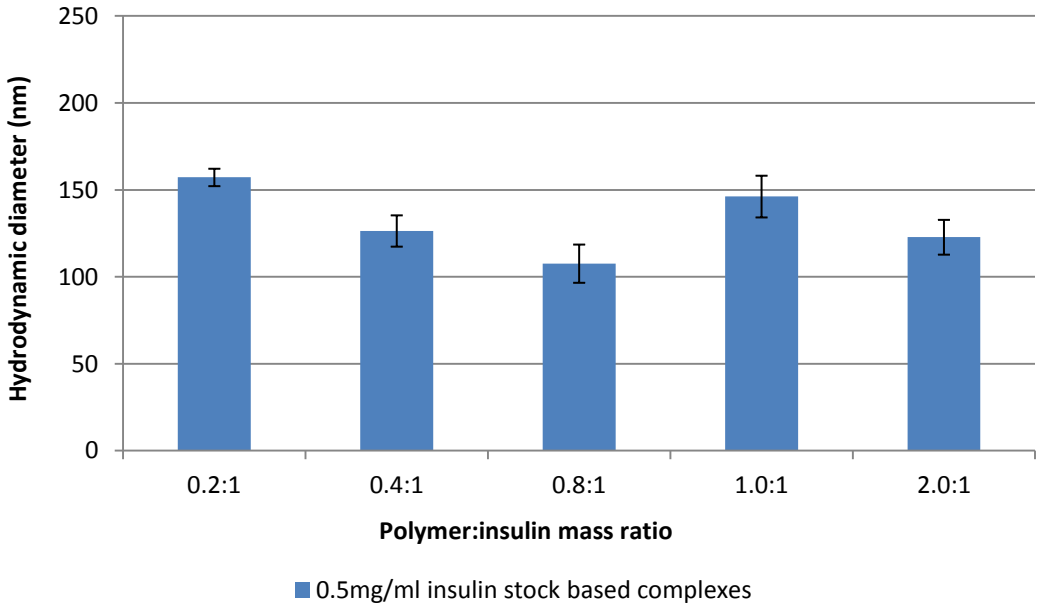

A)

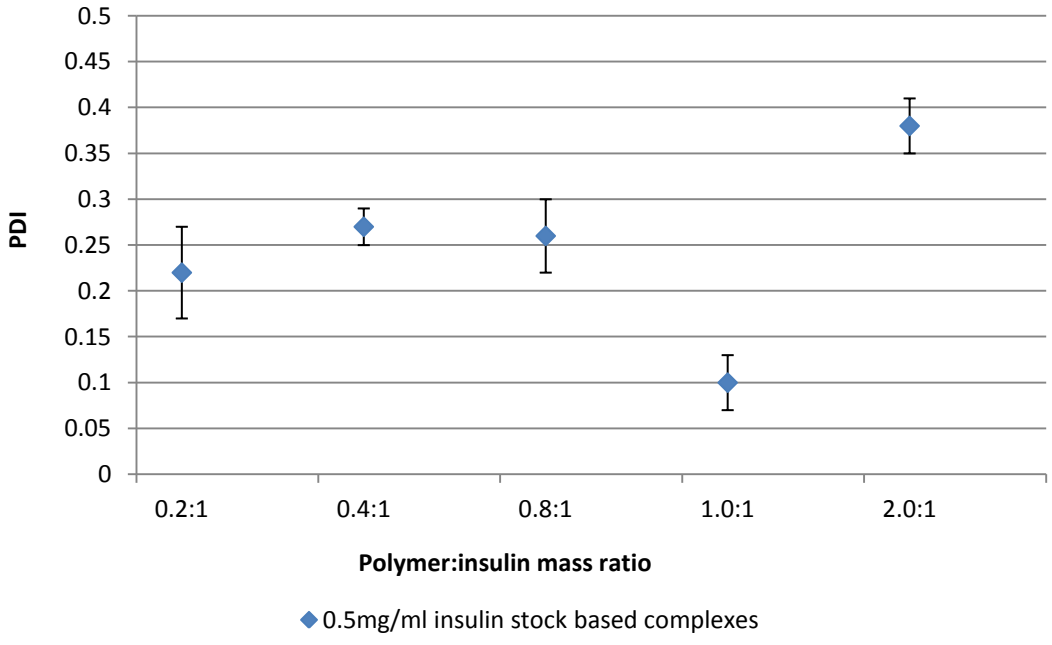

B)

Fig. 30: Size analysis of Paa, insulin PECS in NaOH buffer pH 7.4 at day 0. Results show A) Hydrodynamic diameter B) PDI of PECS at varied P: I mass ratios (n=3; mean ± S.D.)

Size analysis showed PECS prepared at 0.2:1 P: I mass ratio were precipitated with sizes above 1µm, hence these results were also not included in figure 31 below.

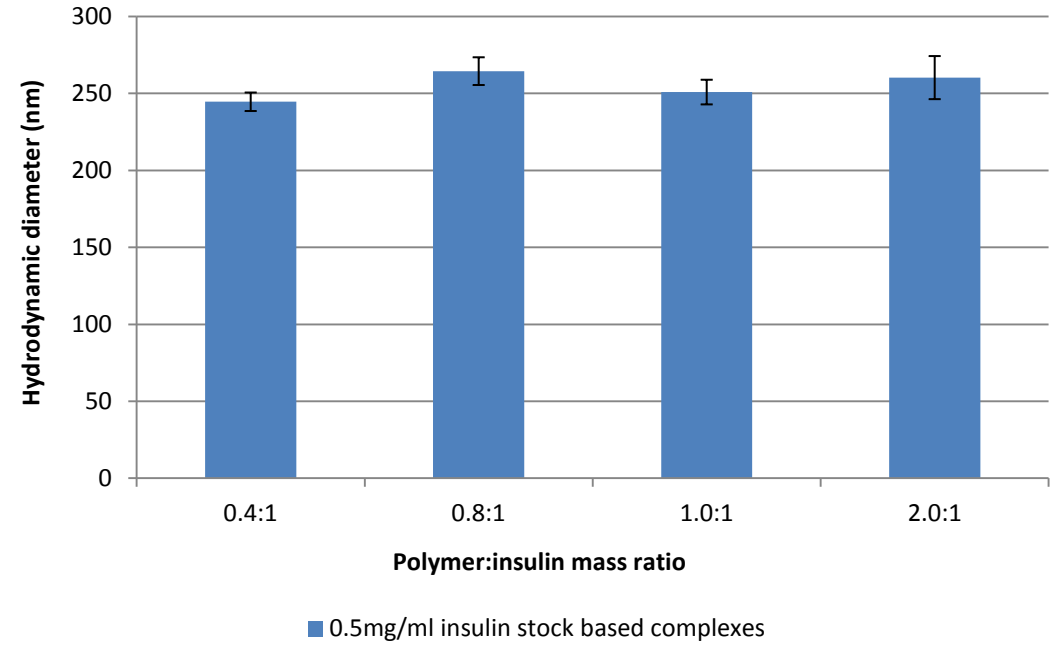

A)

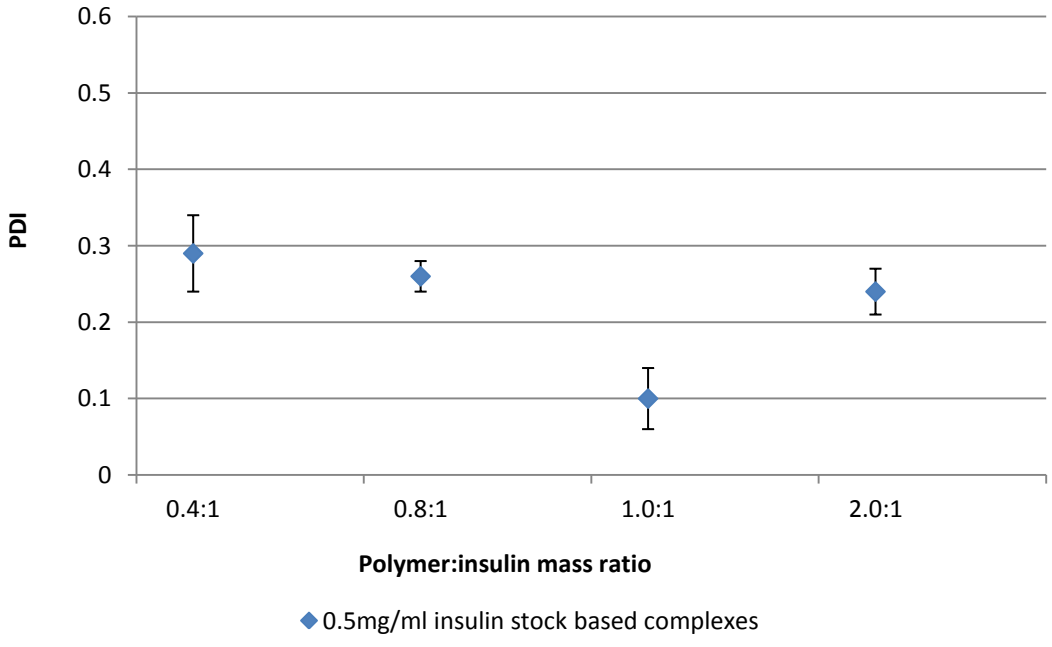

B)

Fig. 31: Size analysis of Paa, insulin PECS in NaOH buffer pH 7.4 at day 3. Results show A) Hydrodynamic diameter B) PDI of PECS at varied P: I mass ratios. (n=3; mean ± S.D.)

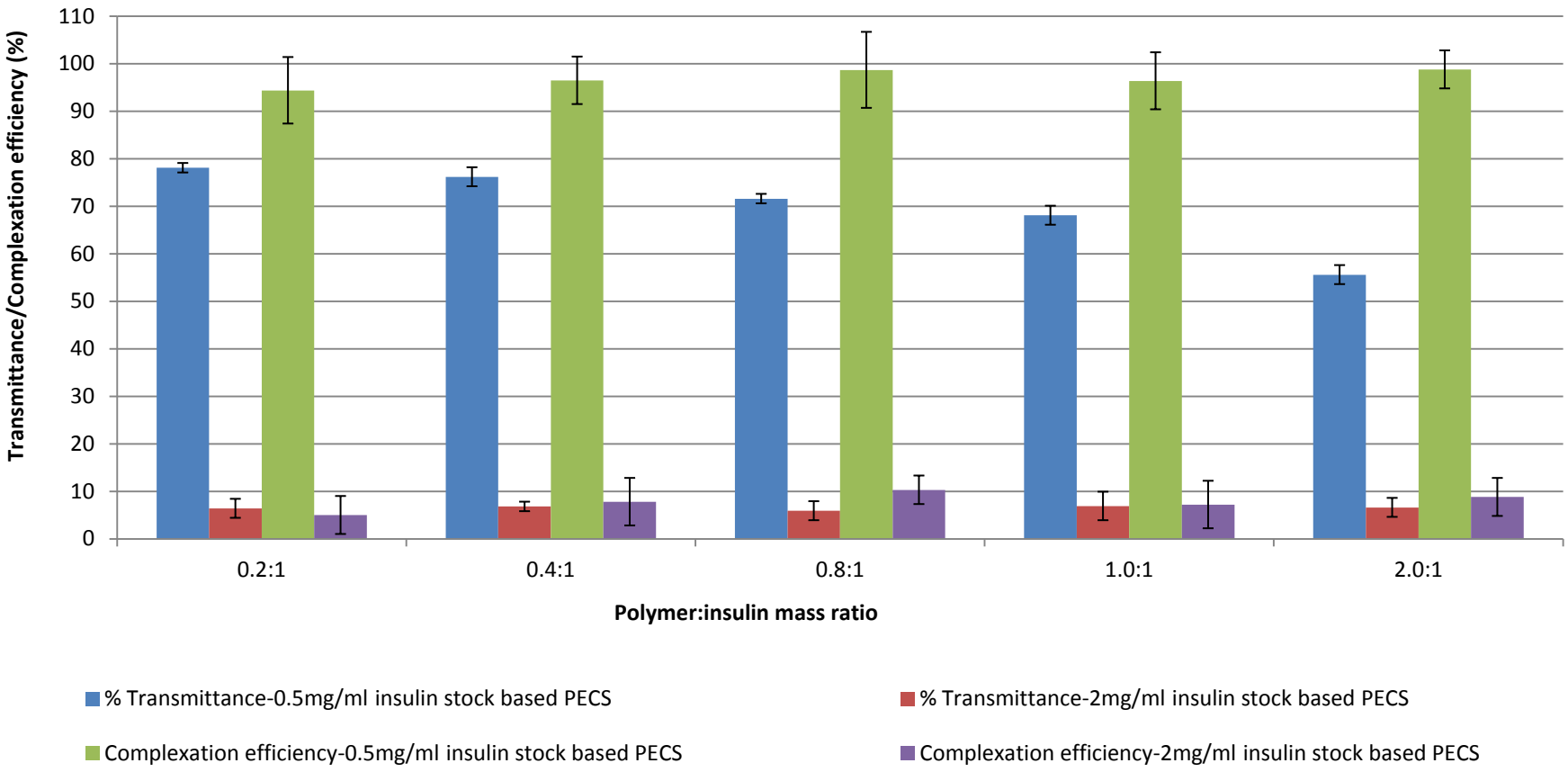

Fig. 32: % Transmittance and Complexation efficiency of Paa, insulin PECS prepared in NaOH buffer pH 7.4 at different P: I mass ratios using 0.5 and 2mgml^{-1} insulin stock solution. (Day 0) (n=3; mean ± S.D.)

Complexation efficiency and % Transmittance of 2mgml^{-1} insulin stock based Paa, insulin complexes in sodium hydroxide buffer was not repeated at 72 hours due to excessive precipitation.

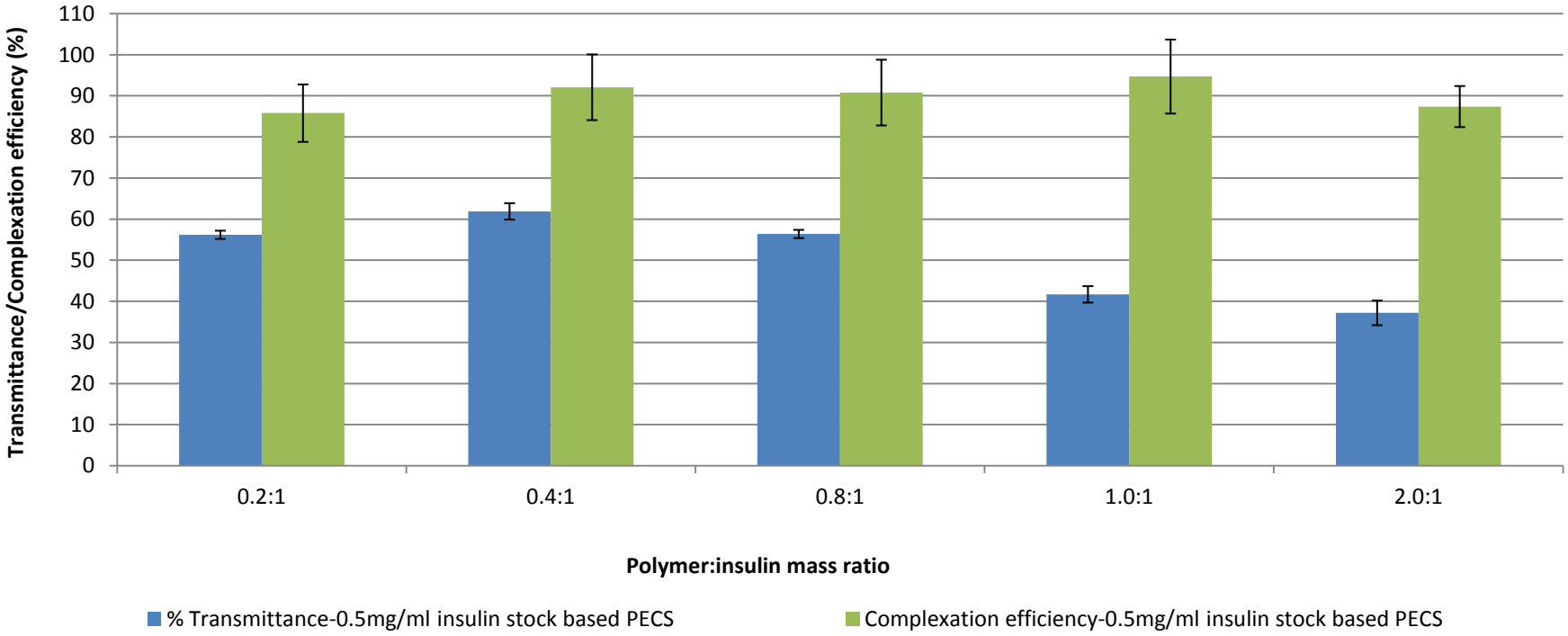

Fig. 33: % Transmittance and Complexation efficiency of Paa, insulin PECS prepared in NaOH buffer pH 7.4 at different P: I mass ratios using 0.5mgml^{-1} insulin stock solution. (Day 3) (n=3; mean ± S.D.)

Table 6: Zeta potential of QPaa, insulin PECS in NaOH buffer pH 7.4 at Day 0 (n =3; mean ± S.D.)

	0.5mgml^{-1} insulin stock				2mgml^{-1} insulin stock			
Mass ratios	**0.2:1**	**0.8:1**	**1:1**	**2:1**	**0.2:1**	**0.8:1**	**1:1**	**2:1**
Zeta (mV)	22.3 ± 3	28.3 ± 1	27.8 ± 2	28.7 ± 2	29.8 ± 1	31.8 ± 1	31.9 ± 3	33.0 ± 2

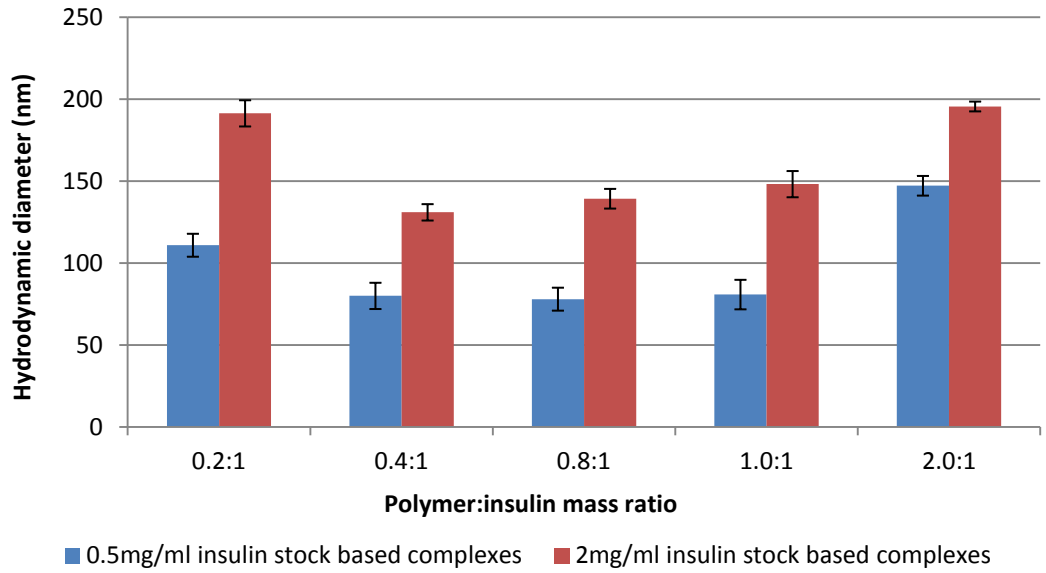

A)

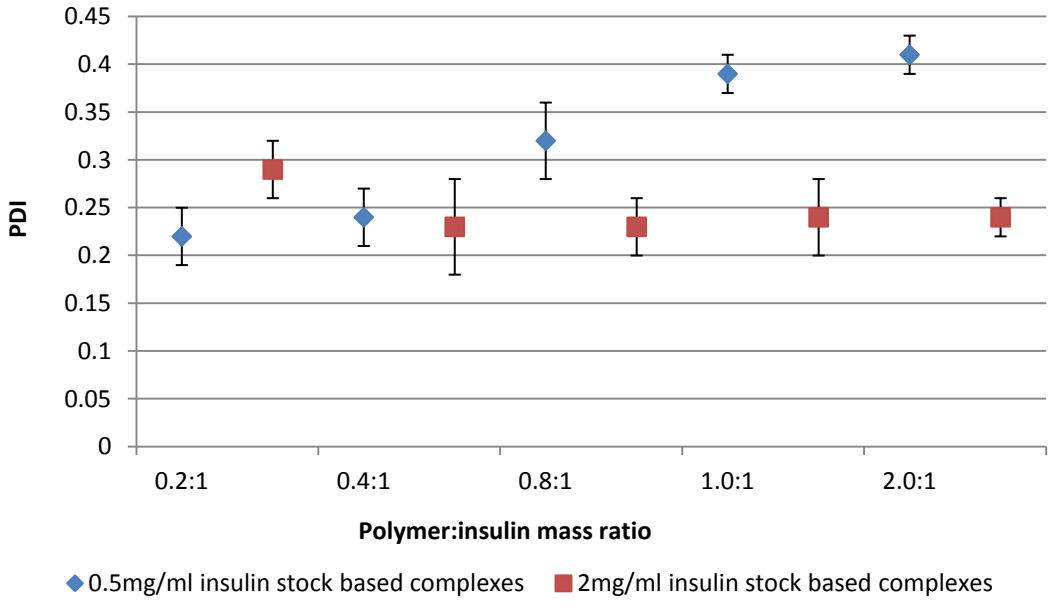

B)

Fig. 34: Size analysis of QPaa, insulin PECS in NaOH buffer pH 7.4 at day 0. Results show A) Hydrodynamic diameter B) PDI of PECS at varied P: I mass ratios. (n=3; mean ± S.D.)

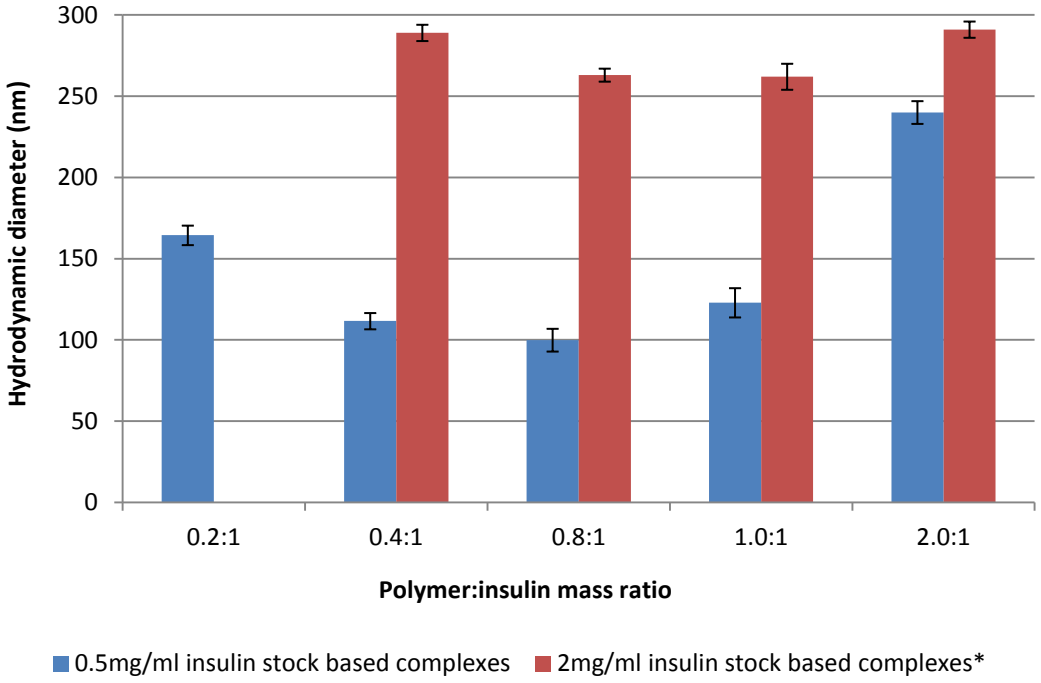

A)

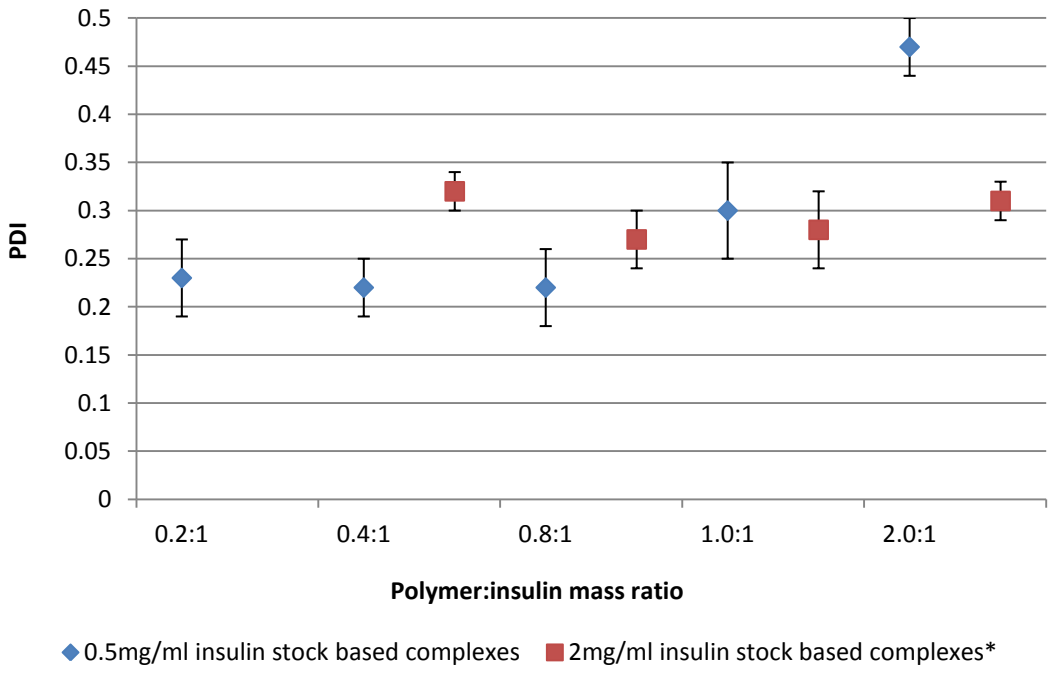

B)

* Size analysis showed 2mgml^{-1} insulin stock-based PECS prepared at 0.2:1 P: I mass ratio were precipitated with sizes above 1µm.

Fig. 35: Size analysis of QPaa, insulin PECS in NaOH buffer pH 7.4 at day 3. Results show A) Hydrodynamic diameter B) PDI of PECS at varied P: I mass ratios. (n=3; mean ± S.D.)

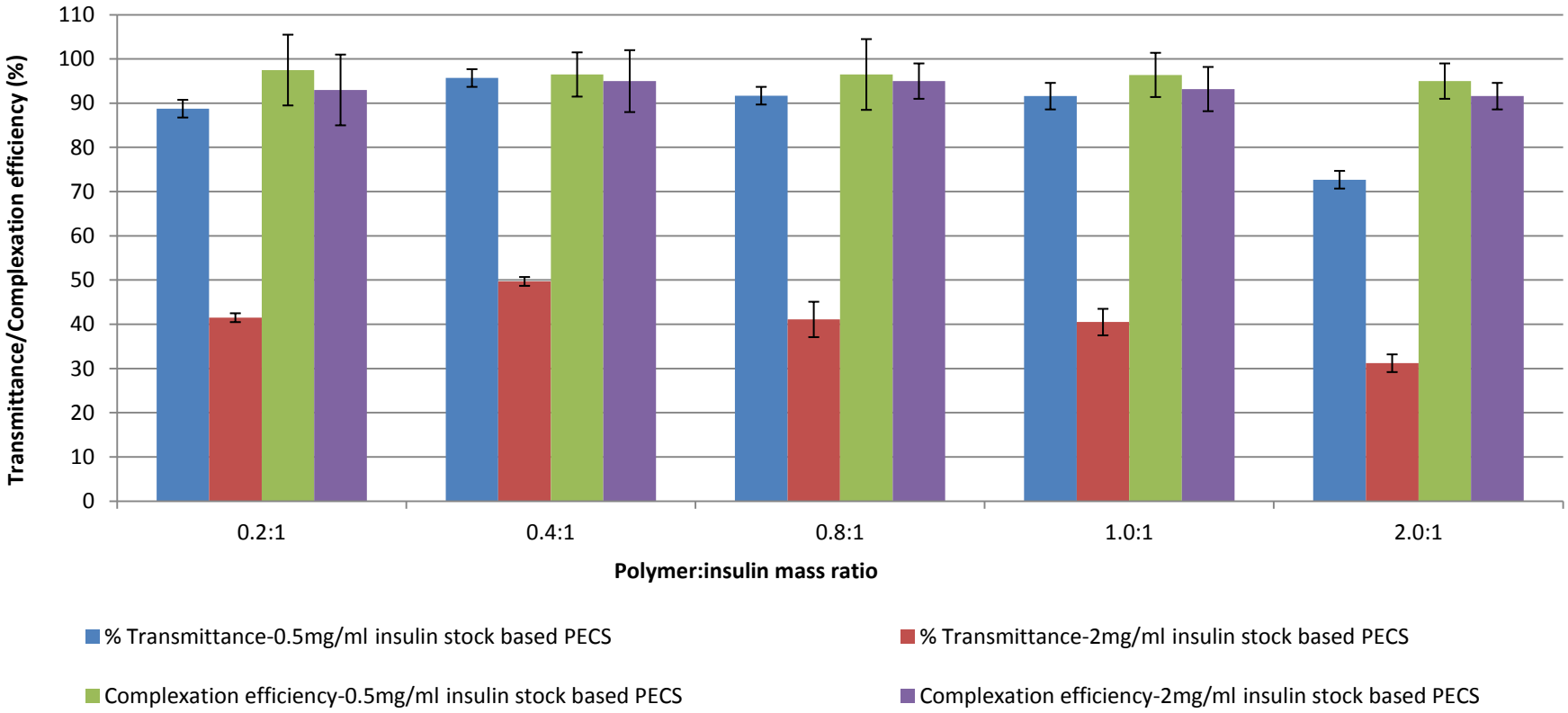

Fig. 36: % Transmittance and Complexation efficiency of QPaa, insulin PECS prepared in NaOH buffer pH 7.4 at different P: I mass ratios using 0.5 and 2mgml^{-1} insulin stock solution. (Day 0) (n=3; mean ± S.D.)

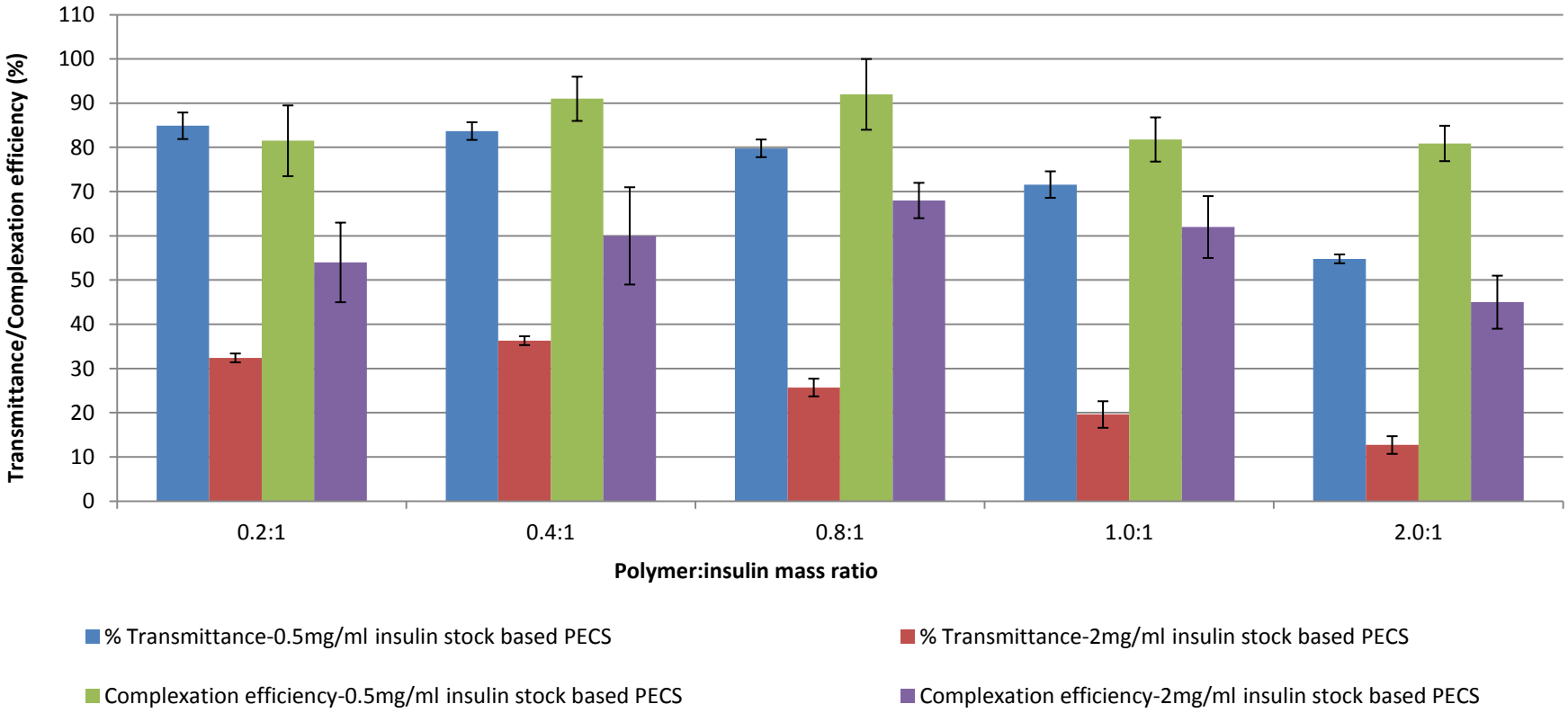

Fig. 37: % Transmittance and Complexation efficiency of QPaa, insulin PECS prepared in NaOH buffer pH 7.4 at different P: I mass ratios using 0.5 and 2mgml^{-1} insulin stock solution. (Day 3) (n=3; mean ± S.D.)

Changing the buffer system from Tris to sodium hydroxide resulted in an overall reduction in the stability and insulin complexation efficiency of all formulations as can be seen in figure 30-37 above.

Paa, insulin complexes were observed to be more adversely affected by this change to sodium hydroxide buffer than QPaa, insulin complexes. At the 0.5mgml^{-1} insulin stock concentration level, P : I complexation was still evident for both polymers. However at this concentration level, while QPaa, insulin interaction was sufficient to result in the production of small compact complexes at P : I ratios of 0.8-1:1, the particle size of corresponding Paa, insulin complexes was observed to be noticeably larger than average particle sizes of any other set of 0.5mgml^{-1} insulin stock –based complexes. This suggests that although complexation took place, P : I interaction was weak resulting in loosely held complexes and the low transmittance values obtained indicated that these complexes were also more susceptible to aggregation than those prepared in Tris buffer. The effect may be more pronounced in Paa than in QPaa complexes which benefit from the stabilising effect of the quaternary ammonium group on polymer charge.

Increasing insulin stock concentration level to 2mgml^{-1} allows for other factors like reduction in interparticulate distances (allowing attractive forces to dominate) and double layer compression which initiates further destabilisation of the system to occur. Hence, QPaa, insulin PECS displayed increased particle size, more turbidity and reduced complexation efficiency with increase in insulin stock concentration level (figures 34-37). However, Paa, insulin PECS completely precipitated out of the system resulting in very turbid formulations which displayed particle sizes outside the nano-range and negligible insulin complexation efficiency.

This destabilising effect of sodium hydroxide buffer on P : I complexation could be attributed to the screening effect of the salt ions on the repulsive charges exhibited by dispersed particles; this could compress the double layer and reduce the charge barrier to the point at which precipitation sets in [179].The difference in the dynamics of the complexation process in sodium hydroxide buffer and Tris buffer pH 7.4 may be related to the fact that sodium hydroxide is neutralised by HCl in the buffer solution producing neutral sodium chloride salt. On the other hand, Tris base is protonated by HCl creating a higher balance of positive charges when the polyelectrolytes are dissolved in Tris buffer [171]. This may explain the higher zeta potential of complexes in Tris than sodium

hydroxide buffer at pH 7.4 (Tables 3-6) with negative effects on P : I interaction and complex stability in sodium hydroxide buffer.

3.3.1.4. Evaluation of insulin complexation with NAC conjugates

Insulin PECS were prepared in Tris buffer pH 7.4 using both Paa-NAC and QPaa-NAC. Complexes were prepared using both thiomers and 0.5 and 2mgml^{-1} insulin stock at mass ratios of 0.2:1, 0.8:1 and 2:1. Complexes from each thiomer were characterised as in section 3.2 at Day 0 (2 hours after PEC preparation) and at day 3 (72 hours after PEC preparation). Zeta potential of complexes was carried out only at day 0 (table 7).

Table 7: Zeta potential (mV) of Paa-NAC, insulin PECS and QPaa-NAC, insulin complexes prepared in Tris buffer pH 7.4 using 0.5 and 2mgml^{-1} insulin stock at day 0 (n=3; mean ± S.D.).

	0.5mgml^{-1} insulin stock			**2mgml^{-1} insulin stock**		
Mass ratios	**0.2:1**	**0.8:1**	**2:1**	**0.2:1**	**0.8:1**	**2:1**
Paa-NAC	23.8 ± 1	29.2 ± 3	30.8 ± 3	23.3 ± 2	30.4 ± 4	32.9 ± 4
QPaa-NAC	19.5 ± 3	28.7 ± 3	29.0 ± 2	18.7 ± 2	31.4 ± 0	32.9 ± 2

Paa-NAC, insulin and QPaa-NAC, insulin complexes prepared at 0.2:1 P : I mass ratio were excessively precipitated and particle sizes were outside the nano-range. Results were therefore not included in figures 38 and 39 below.

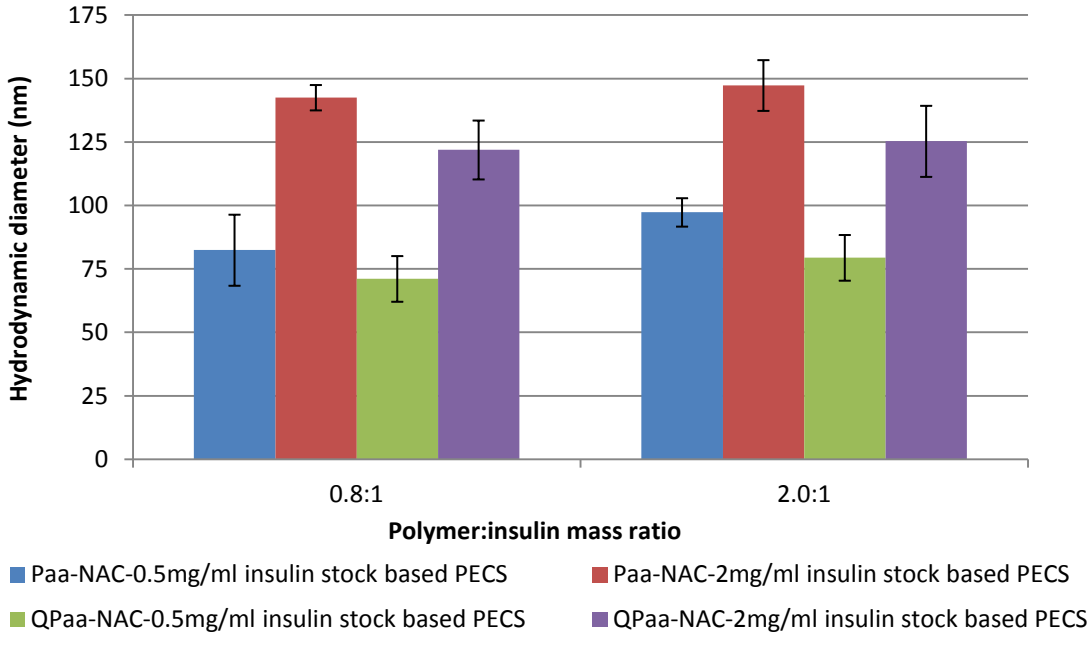

A.

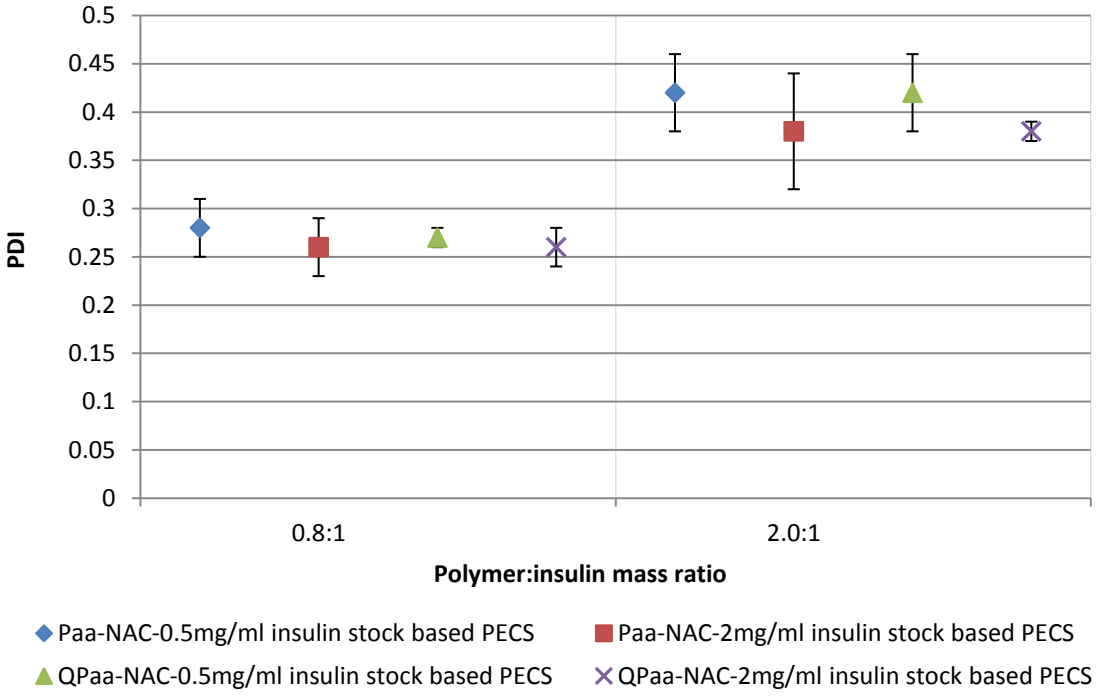

B.

Fig. 38: Hydrodynamic diameter of Paa-NAC and QPaa-NAC insulin PECS prepared in Tris buffer pH 7.4 at different P: I mass ratios using 0.5 and 2mgml^{-1} insulin stock solution (day 0). All values are mean ± S.D. (n=3).

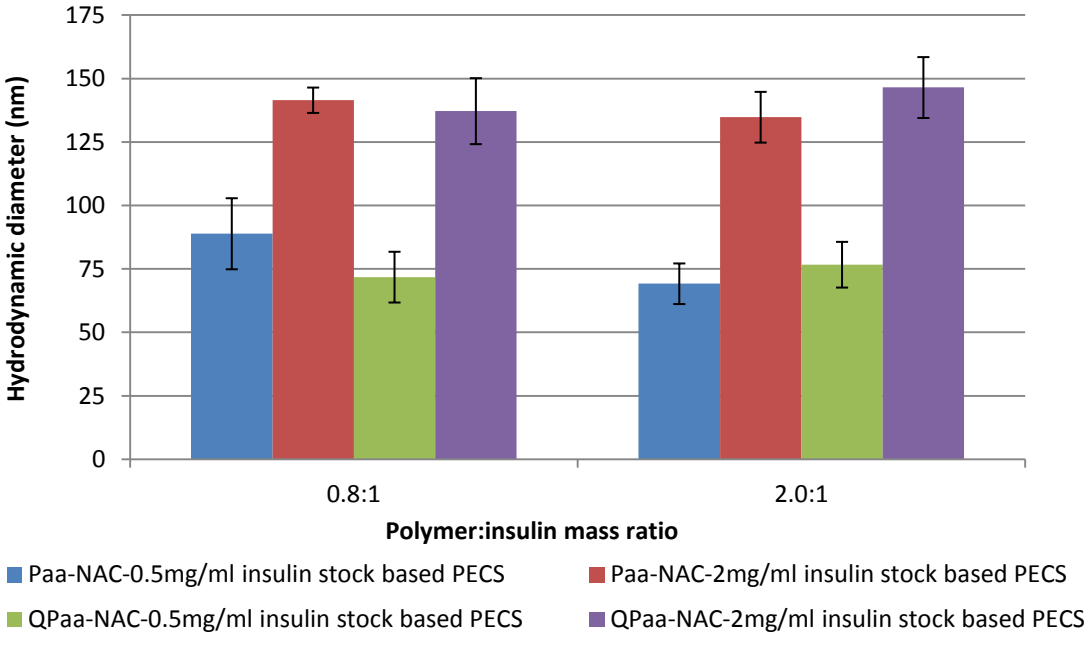

A.

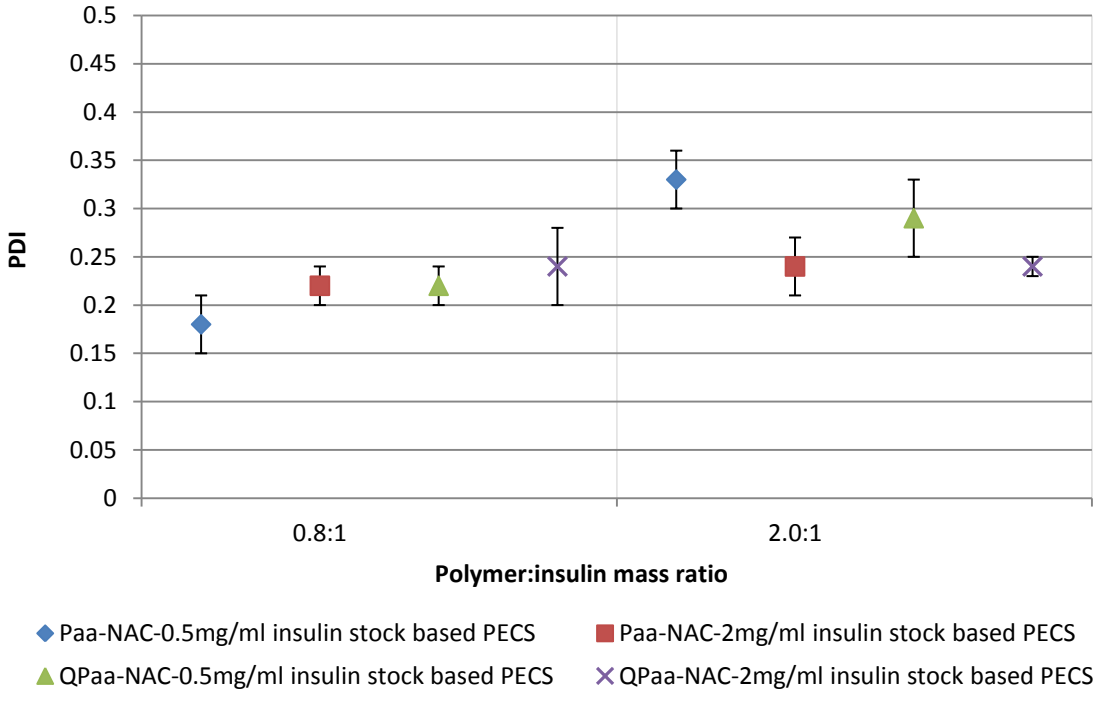

B.

Fig. 39: Hydrodynamic diameter of Paa-NAC and QPaa-NAC insulin PECS prepared in Tris buffer pH 7.4 at different P : I mass ratios using 0.5 and 2mgml^{-1} insulin stock solution (day 3). All values are mean ± S.D. (n=3).

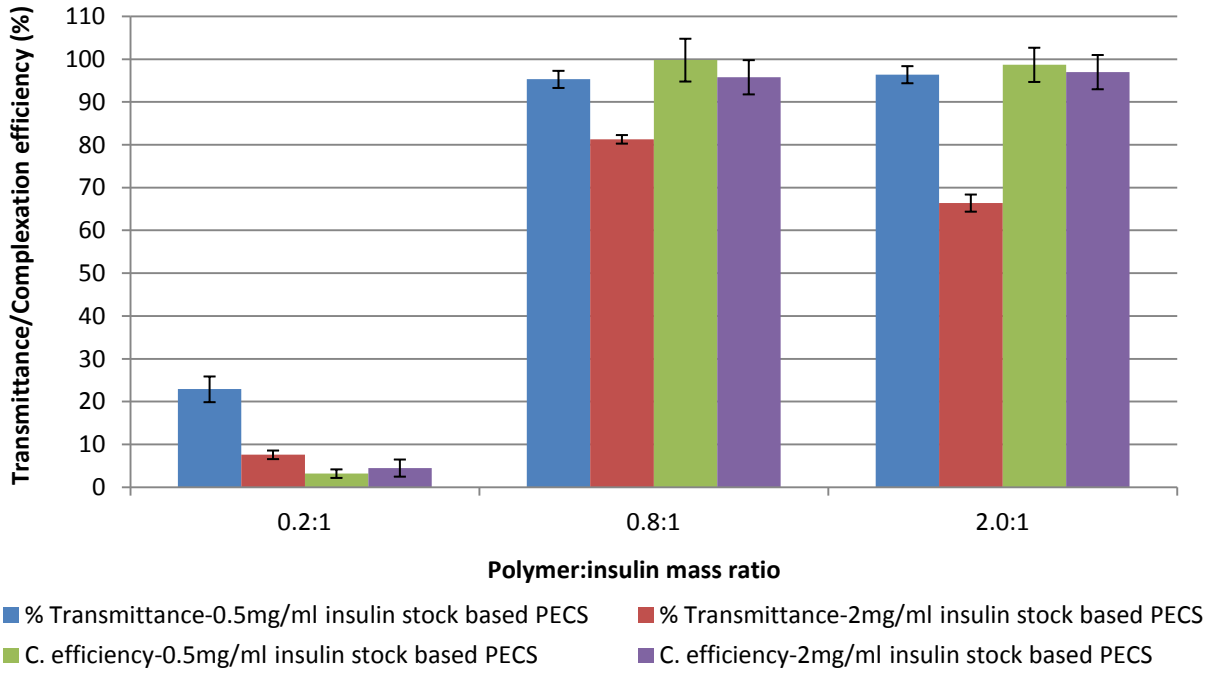

Fig. 40: Transmittance and Complexation efficiency (%) of Paa-NAC, insulin PECS made at various P : I mass ratios using 0.5 and 2mgml^{-1} insulin solutions (day 0) (n= 3; mean ± S.D.)

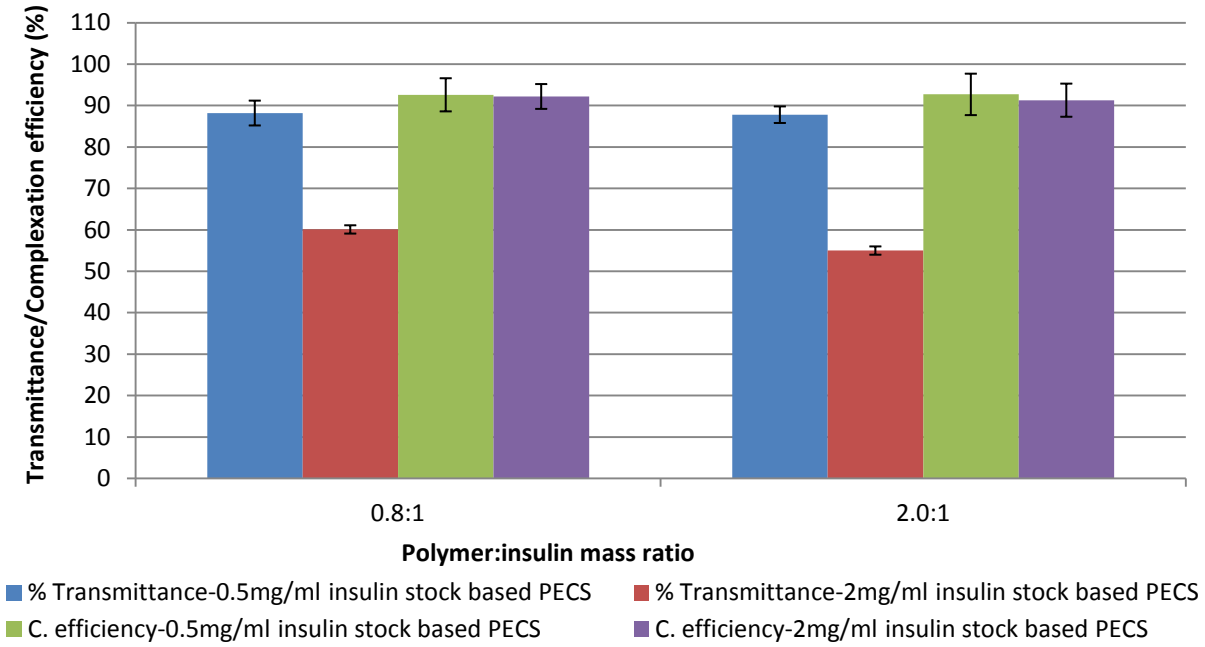

Fig. 41: Transmittance and Complexation efficiency (%) of Paa-NAC, insulin PECS made at varied P : I mass ratios using 0.5 and 2mgml^{-1} insulin solutions (day 3) (n= 3; mean ± S.D.).

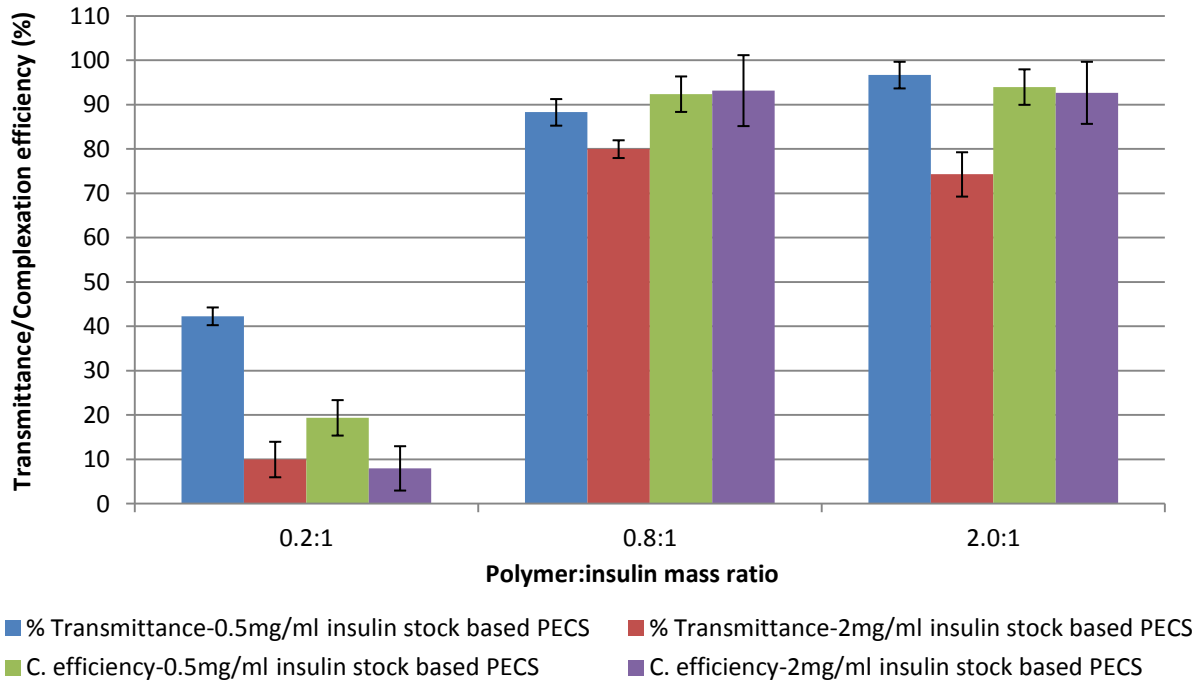

Fig. 42: Transmittance and Complexation efficiency (%) of QPaa-NAC, insulin PECS made at various P : I mass ratios using 0.5 and 2mgml^{-1} insulin solutions (day 0) (n= 3; mean ± S.D.)

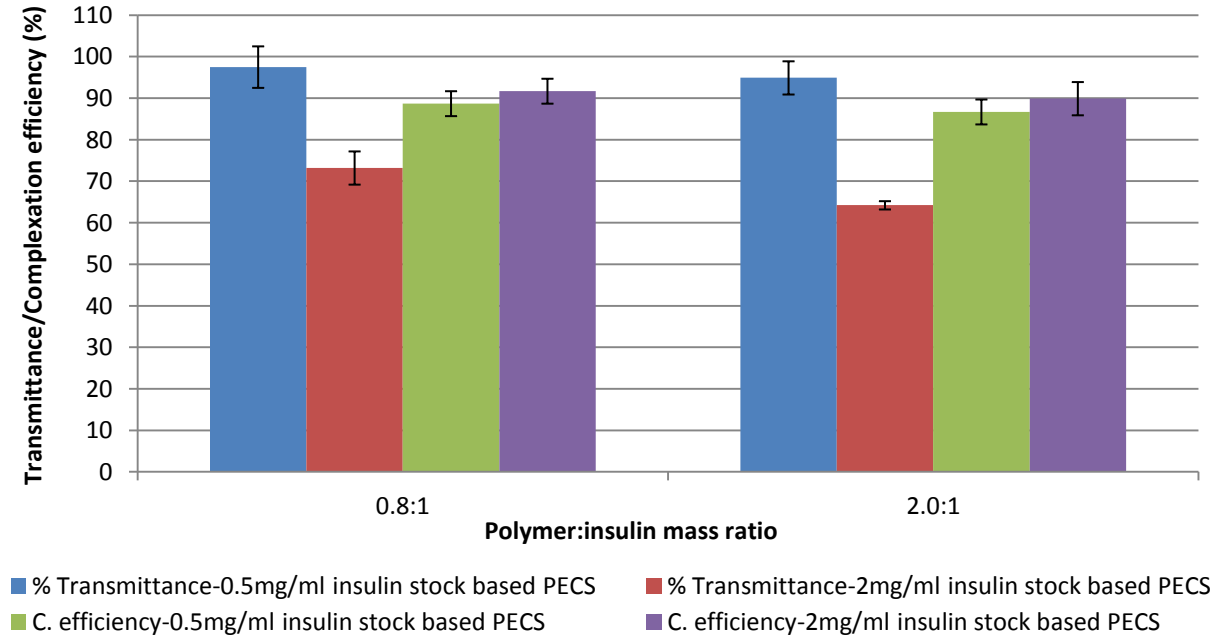

Fig. 43: Transmittance and Complexation efficiency (%) of QPaa-NAC, insulin PECS made at various P : I mass ratios using 0.5 and 2mgml^{-1} insulin solutions (day 3) (n= 3; mean ± S.D.)

Figures 38-43 show that the complexation profiles of insulin PECS prepared with both NAC-conjugates (Paa/QPaa-NAC) were quite similar. For both 0.5 and 2mgml^{-1} insulin stock concentration levels, precipitation and phase separation at 0.2:1 P : I mass ratio was observed to occur almost instantaneously, while PECS prepared at 2:1 P : I mass ratio exhibited more compact sizes and higher transmittance values than their non-thiolated counterpart. Optimal P : I mass ratios for insulin complexation with NAC-based thiomers was found to be between 0.8-2:1 for both insulin stock concentration levels, as complexes prepared at this mass ratios were observed to be stable to aggregation at day 3 (figures 39, 41 and 43).

3.3.1.5. Evaluation of insulin complexation with TBA conjugates

Insulin PECS were prepared in Tris buffer pH 7.4 using both TBA conjugates (Paa-TBA and QPaa-TBA). Complexes were prepared using both thiomers and 0.5 and 2mgml^{-1} insulin stock at mass ratios of 0.2:1, 0.8:1 and 2:1. Complexes from each thiomer were characterised as in section 3.2 at Day 0 (2 hours after PEC preparation) and at day 3 (72 hours after PEC preparation). Zeta potential of complexes was carried out only at day 0 (table 8).

Table 8: Zeta potential (mV) and PDI of Paa-TBA, insulin complexes in Tris buffer pH 7.4 prepared at different P : I mass ratios using the 0.5 and 2mgml^{-1} insulin stock solution. (n= 3; mean ± S.D.).

	0.5mgml^{-1} insulin stock			**2mgml^{-1} insulin stock**		
Mass ratios	**0.2:1**	**0.8:1**	**2:1**	**0.2:1**	**0.8:1**	**2:1**
Paa-TBA	20.1 ± 3	35.1 ± 6	35.4 ± 1	20.1 ± 3	37.7 ± 5	42.0 ± 5
QPaa-TBA	18.4 ± 3	37.0 ± 8	38.3 ± 0	26.4 ± 6	37.0 ± 0	40.9 ± 1

Paa-TBA, insulin and QPaa-TBA, insulin complexes prepared at 0.2:1 P : I mass ratio were excessively precipitated and particle sizes were outside the nano-range. Results were therefore not included in figures 44 and 45 below.

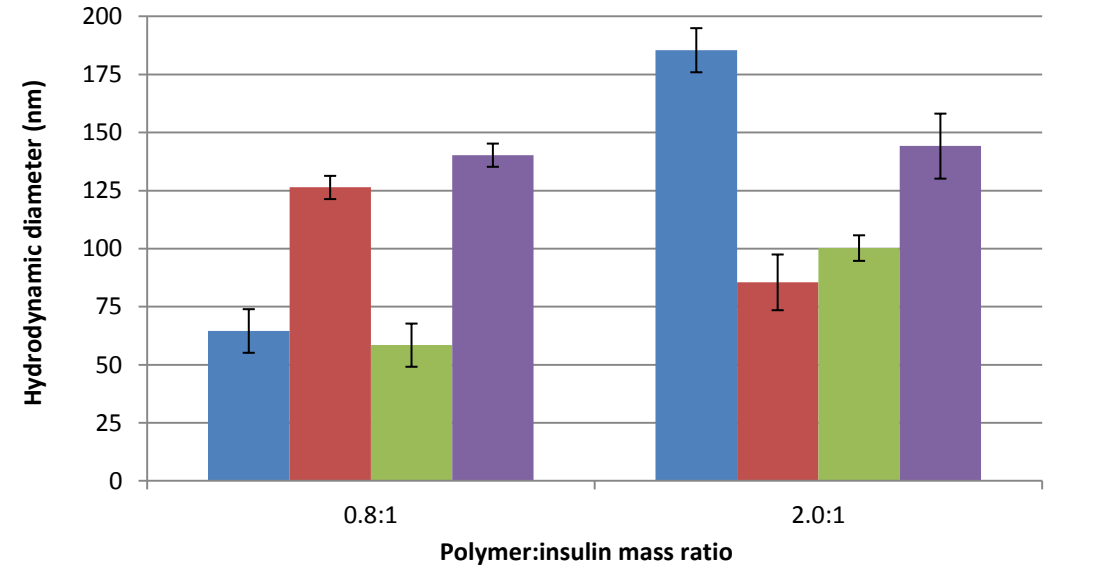

A.

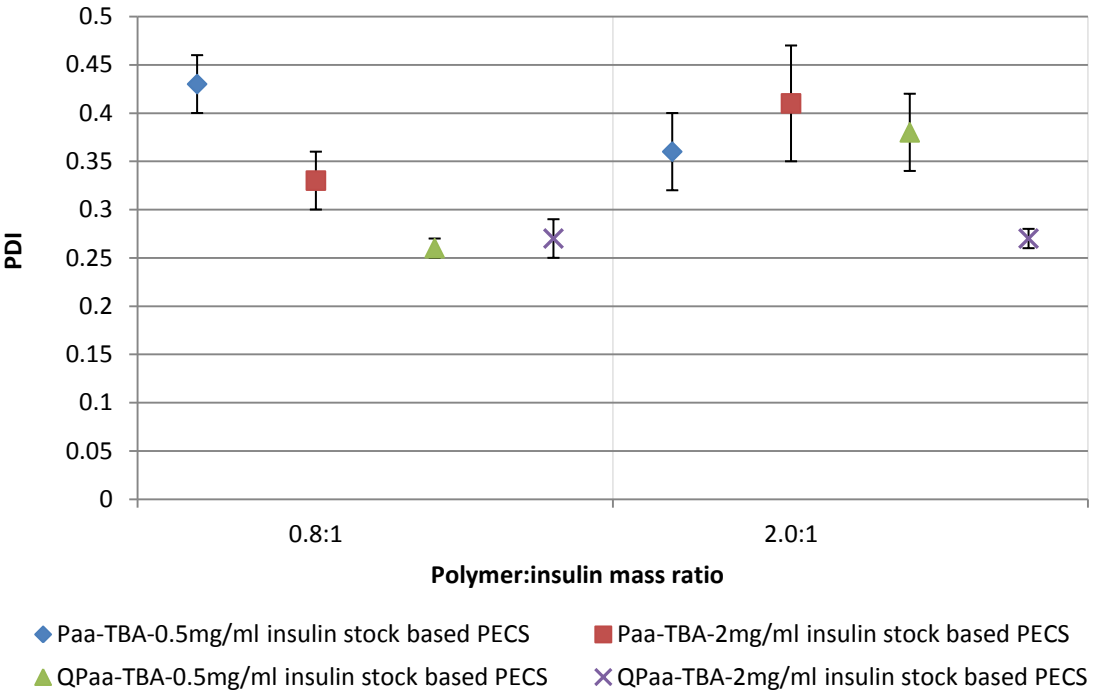

B.

Fig. 44: Hydrodynamic diameter of Paa-TBA and QPaa-TBA insulin PECS prepared in Tris buffer pH 7.4 at different P : I mass ratios using 0.5 and 2mgml^{-1} insulin stock solution (day 0). All values are mean ± S.D. (n=3).

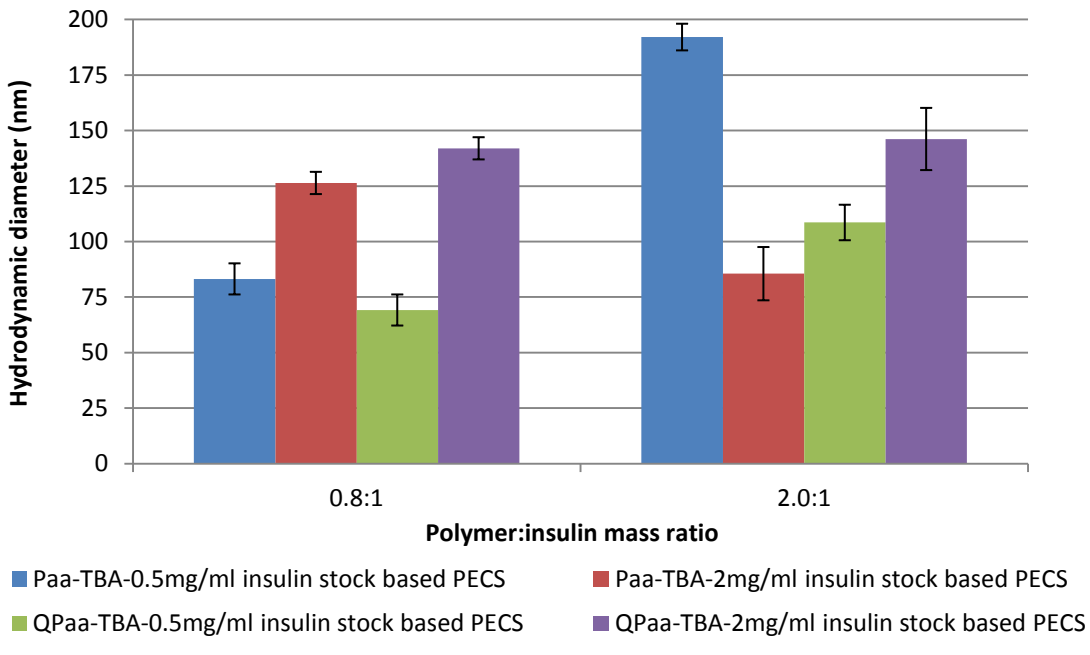

A.

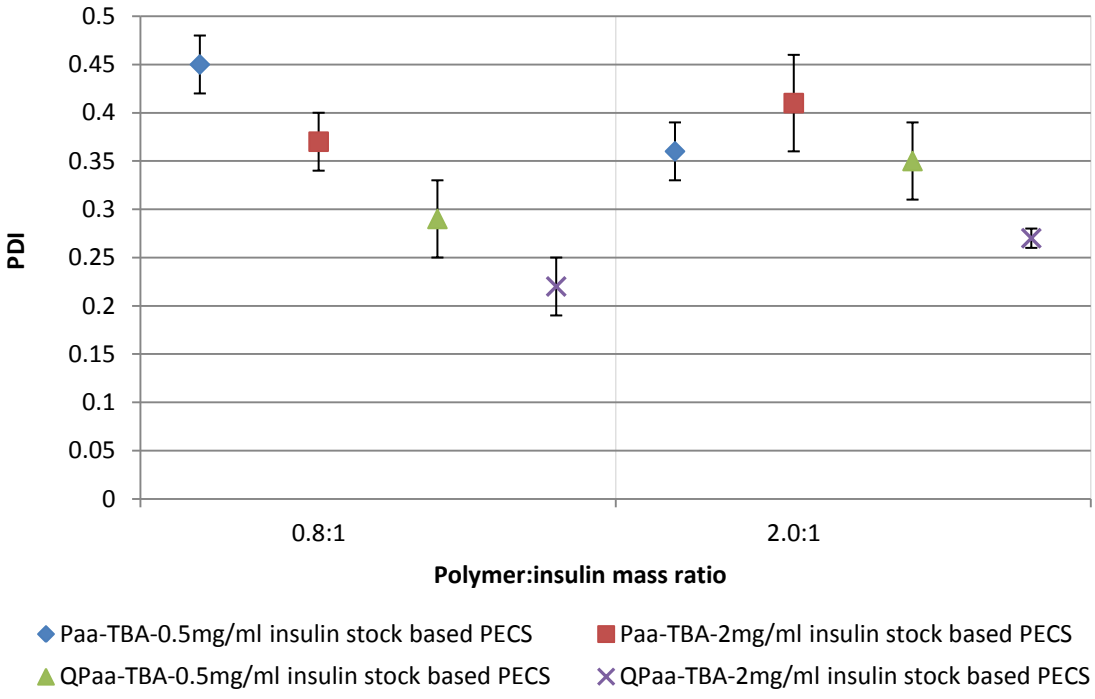

B.

Fig. 45: Hydrodynamic diameter of Paa-TBA and QPaa-TBA insulin PECS prepared in Tris buffer pH 7.4 at different P: I mass ratios using 0.5 and 2mgml^{-1} insulin stock solution (day 3). All values are mean ± S.D. (n=3).

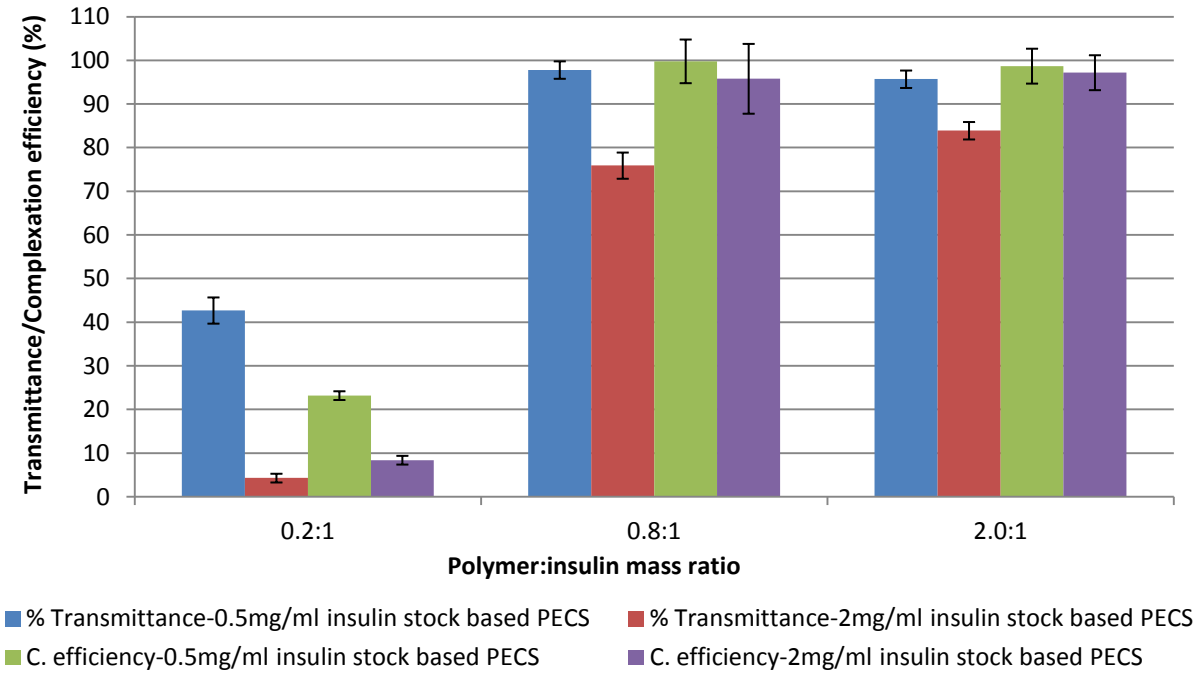

Fig. 46: Transmittance and Complexation efficiency (%) of Paa-TBA, insulin PECS made at various P: I mass ratios using 0.5 and 2mgml^{-1} insulin solutions (day 0) (n= 3; mean ± S.D.)

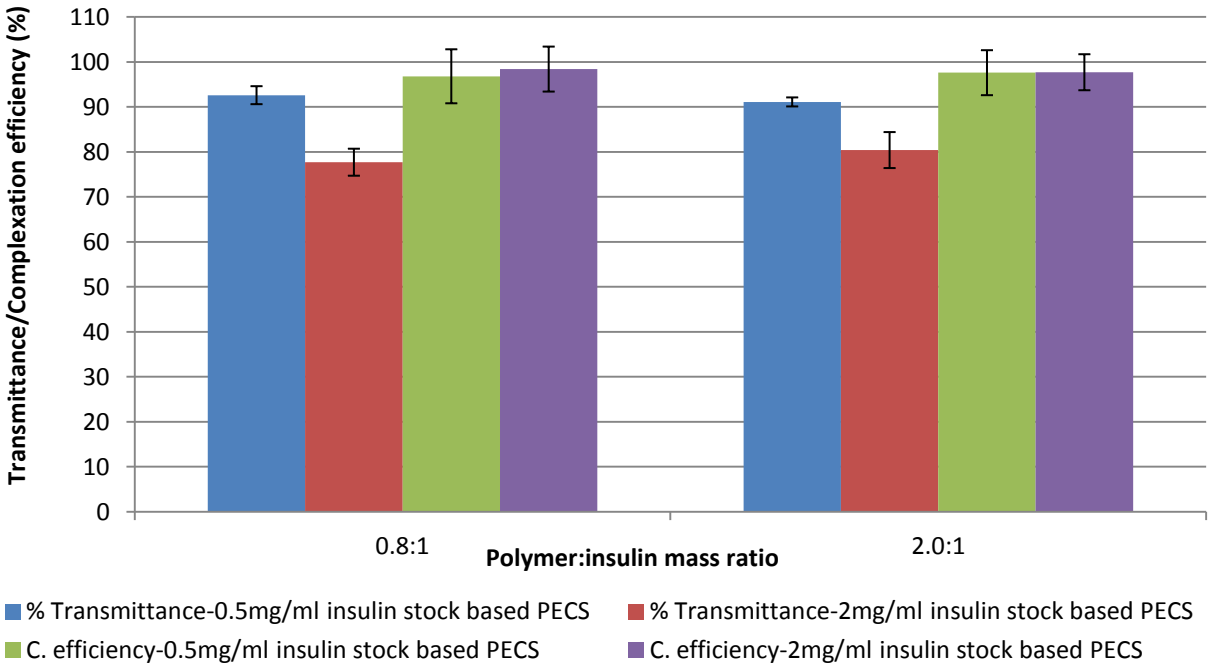

Fig. 47: Transmittance and Complexation efficiency (%) of Paa-TBA, insulin PECS made at various P: I mass ratios using 0.5 and 2mgml^{-1} insulin solutions (day 3) (n= 3; mean ± S.D.).

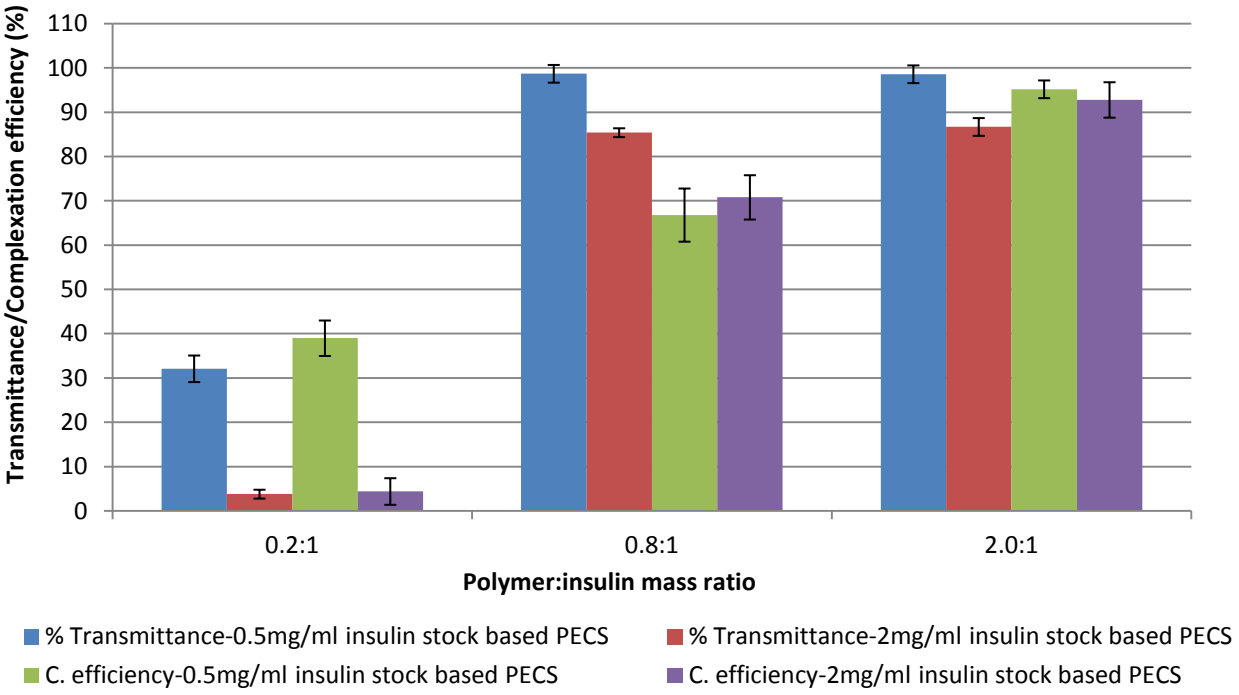

Fig. 48: Transmittance and Complexation efficiency (%) of QPaa-TBA, insulin PECS made at various P: I mass ratios using 0.5 and 2mgml^{-1} insulin solutions (day 0) (n= 3; mean ± S.D.)

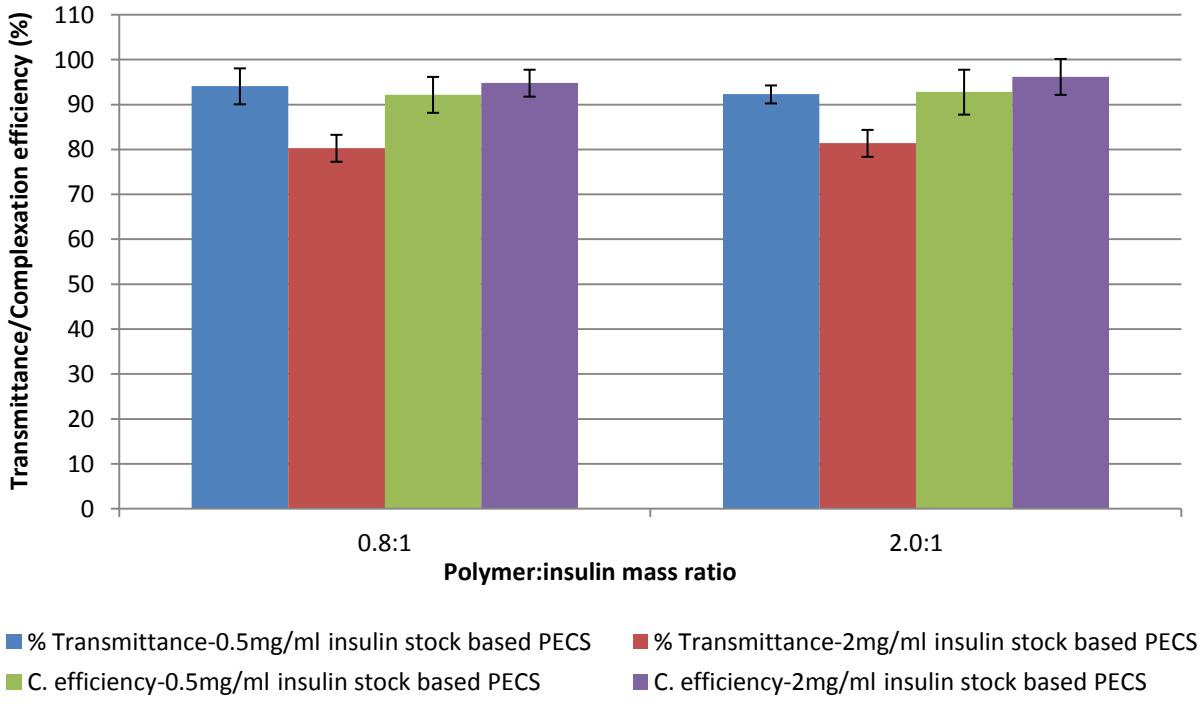

Fig. 49: Transmittance and Complexation efficiency (%) of QPaa-TBA, insulin PECS made at various P: I mass ratios using 0.5 and 2mgml^{-1} insulin solutions (day 3) (n= 3; mean ± S.D.)

Interaction between TBA conjugates and insulin also yielded nano-sized, positively-charged PECS. The size range of Paa/QPaa-TBA insulin complexes was similar to that obtained for the NAC-conjugates with complexes prepared at 0.2:1 P: I mass ratio containing precipitates. For Paa-TBA/QPaa-TBA, insulin complexes prepared at P: I mass ratios above 0.2:1, complexation efficiency results showed that the insulin peak detected by HPLC appeared to be absent in PEC formulations (shown in figures 50 and 51) without any obvious sign of precipitation or instability being observed in the samples. The run time for this analysis was also increased from 10-15 minutes to check if the insulin peak had shifted, but no insulin peak could still be detected within this timeframe.

This led to the assumption that the structure of complexed insulin was altered on complexation with the polymer thereby affecting the normal interaction of the protein with components of the HPLC system specifically the stationary phase. The insulin content (detected by HPLC) of complexes was observed to gradually decline from 100% as the complexes were made to approximately < 10% at the 2hour timepoint, it was presumed that P : I complexation taking place resulted in the decline in the amount of insulin detected by HPLC. Therefore insulin complexation efficiency was expressed as the amount of insulin detected at this time interval (which is presumed to be detected by HPLC because it has not interacted with the polymer) subtracted from total insulin incorporated.

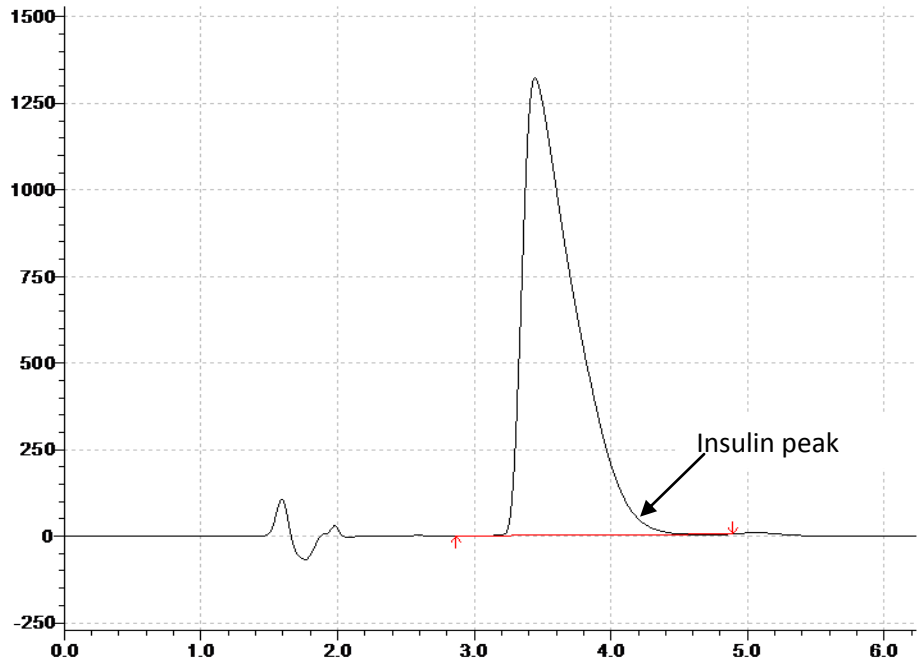

Fig. 50: HPLC Chromatogram of insulin control in Tris buffer pH 7.4 (0.5mgml^{-1})

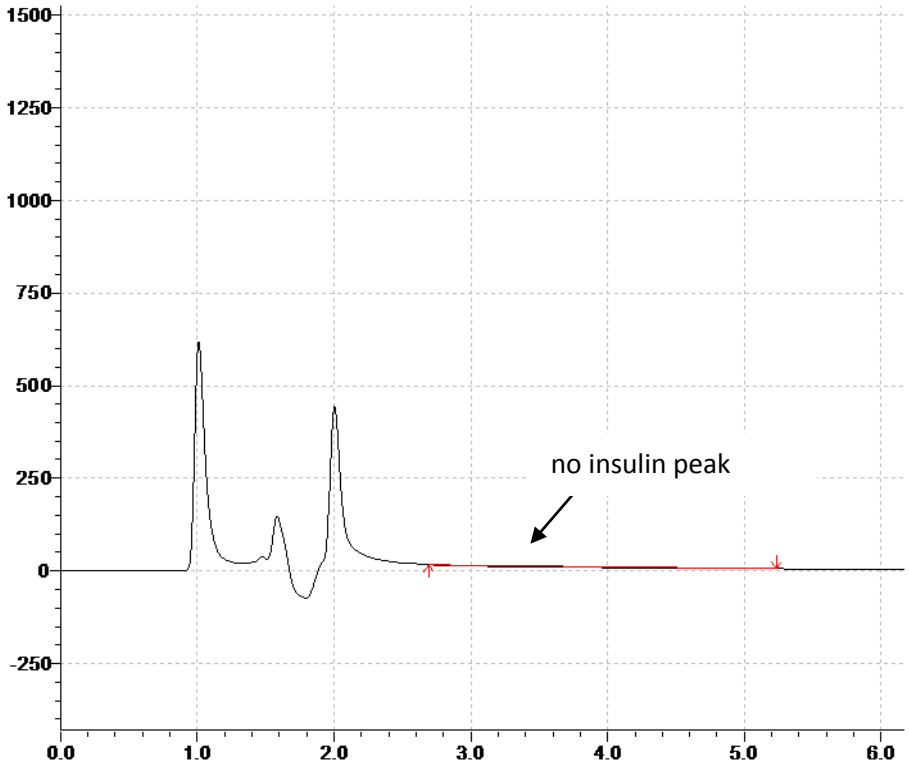

Fig. 51: HPLC Chromatogram of Paa-TBA, insulin complex in Tris buffer pH 7.4 (0.5mgml^{-1} insulin stock, 0.8:1 P: I mass ratio.

It was observed that acidification of Paa/QPaa-TBA insulin complexes using 2M HCl resulted in a distinct insulin peak similar to that obtained on acidification of a similar insulin control solution reappearing on HPLC analysis of the acidified complex formulation (shown in figures 52 and 53).

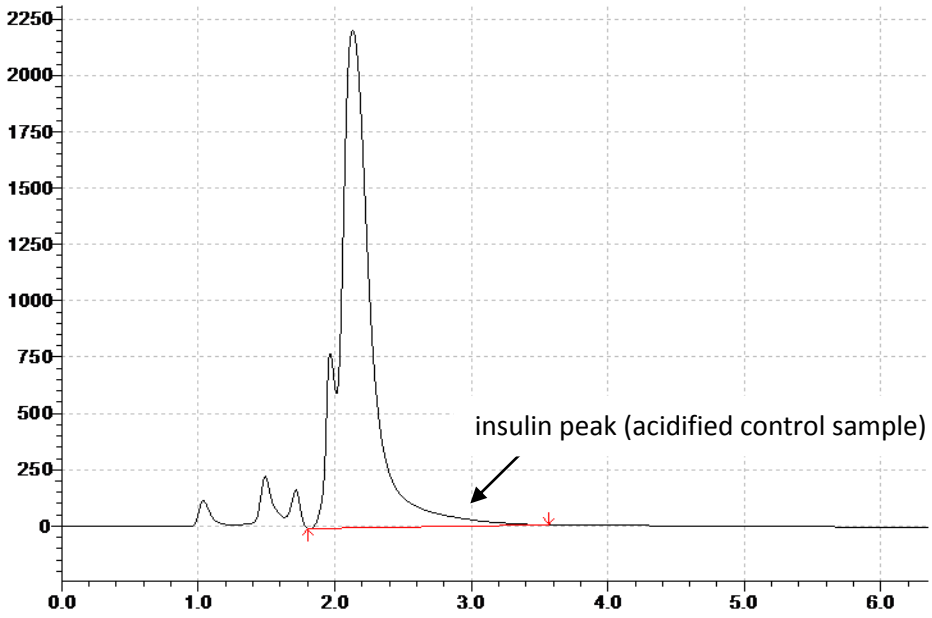

Fig. 52: HPLC Chromatogram of acidified insulin control (Tris buffer pH 7.4)

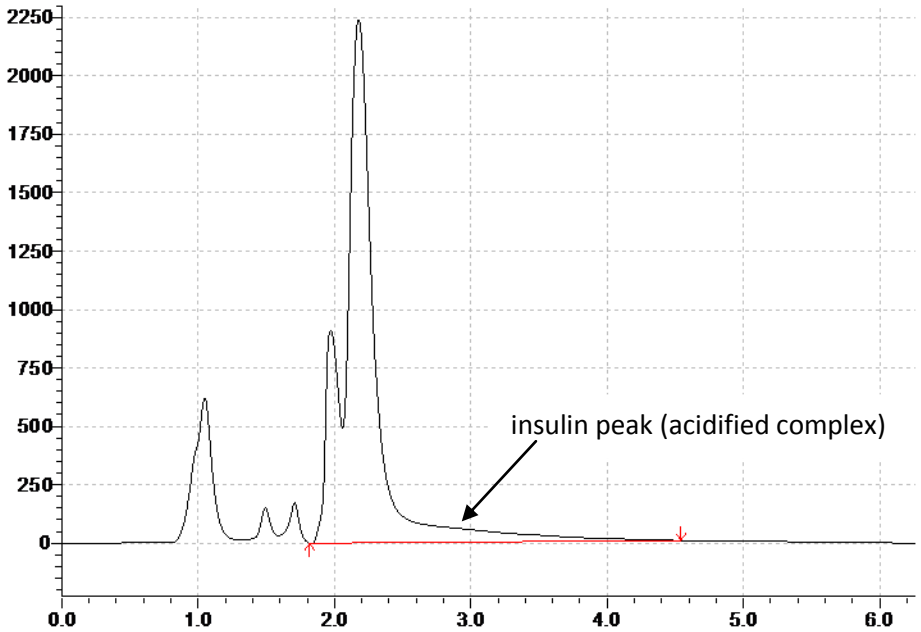

Fig. 53: HPLC Chromatogram of acidified Paa-TBA, insulin PECS (Tris buffer pH 7.4)

This may indicate that the effect of TBA conjugates on complexed insulin may be caused by covalent (thiol-disulphide) bonding between the thiomers and insulin at pH 7.4, which may have been reversed by protonation of reactive thiolate ions on acidification [155].The increased reactivity of the thiol groups on TBA conjugates compared to NAC conjugates may have been brought about by the cationic substructure of the amidine thiol-bearing moiety enhancing the affinity of the polymer thiols for the cysteine groups on insulin. This sort of P : I interaction could have deleterious effects on the conformation of the insulin chains and may affect the ability of the protein to interact with its receptor [180]. Confirmation of this reduction of insulin content of Paa-TBA insulin complexes was carried out using an insulin ELISA kit. Complexes were prepared at 0.8:1 P: I ratio ($0.5mgml^{-1}$ insulin stock) as described in section 3.2 and analysed with an ELISA kit. Results confirmed that after 2 hours, only 11.8 ± 4.2% of insulin was available as opposed to 97.8 ± 0.2% of insulin present in the control. Other techniques like circular dichroism could be used in the future in investigating the nature of conformational change in insulin complexed with TBA-conjugates [140].

3.3.2.. COMPARATIVE EVALUATION OF PHYSICAL AND MORPHOLOGICAL PROPERTIES OF OPTIMAL POLYMER, INSULIN COMPLEXES

Based on results of the formulation optimisation process in 3.1. PECS prepared in Tris buffer pH 7.4 at 0.8:1 P : I mass ratio using the $0.5mgml^{-1}$ insulin stock solution were identified as optimal formulations across all the polymers tested. The properties of insulin complexes of the various polymers formed at 0.8:1 P: I mass ratio ($0.5mgml^{-1}$ insulin stock solution) are summarised in Table 9 below.

Table 9: Hydrodynamic size, PDI, zeta potential (mV), complexation efficiency and % transmittance of polymer, insulin complexes prepared at 0.8:1 P: I mass ratio (0.5mgml^{-1} insulin stock solution) on day 0. (Mean ± S.D.; n=3)

	Hydro-dynamic Size (nm)	PDI	Zeta potential (mV)	Complexation efficiency (%)	Transmittance (%)
Paa	104.0 ± 4	0. 45 ± 0.03	31.2 ± 2	83.68 ± 4	93.34 ± 2
QPaa	75.0 ± 9	0.24 ± 0.05	30.4 ± 1	94.21 ± 5	93.62 ± 3
Paa-NAC	74.8 ± 3	0.28 ± 0.03	29.2 ± 3	98.80 ± 9	95.30 ± 2
QPaa-NAC	71.1 ± 9	0.27 ± 0.01	28.7 ± 3	92.44 ± 12	98.20 ± 2
Paa-TBA	64.6 ± 9	0.43 ± 0.03	35.1 ± 6	94.80 ± 5	97.80 ± 3
QPaa-TBA	54.0 ± 7	0.26 ± 0.04	37.0 ± 2	98.00 ± 10	99.30 ± 1

3.3.2.1. Particle size analysis (Hydrodynamic size and PDI)

Complexation of the various polymers with insulin in Tris buffer pH 7.4 resulted in the production of positively charged, nano-sized PECS at optimal P: I mass ratios. PECS prepared using modified Paa derivatives (quaternised and/or thiolated) were observed to be smaller (<100nm) than unmodified Paa complexes as can be seen in Table 9 above. Therefore suggesting that the processes of quaternisation and thiolation enhanced P: I interaction resulting in more tightly bound, compact complexes. This is expected as quaternisation reinforces the positive charge on the polymer facilitating the process of electrostatically induced P: I complexation. Thiolation results in the formation of disulphide bonds which creates hydrophobic regions within the polymer chains capable of mediating hydrophobic interactions with the insulin molecule hence providing additional forces for P : I complexation [149].

This improvement in complexation was reflected by thiolated QPaa (QPaa-NAC and QPaa-TBA) complexes which benefits from the cumulative effects of quaternisation and thiolation displaying smaller sizes than both QPaa and their thiolated Paa counterparts. Further evaluation of results of particle size analysis in Table 9 above also indicated that complexes prepared from TBA-based thiomers were smaller and hence more compact than complexes from NAC-based thiomers. This could be related to the extra positive charge present on the amidine bond of TBA-conjugates providing a site for additional electrostatic

interaction with insulin and hence condensing PECS even more. QPaa-TBA formulations hence contained the smallest complexes suggesting this polymer interacts closely with insulin molecules.

PDI of complexes gives an idea of the range of size populations of complexes present within the formulation. Apart from Paa and Paa-TBA complexes which exhibited a wider size distribution, the PDI of complexes was found to be quite narrow (0.2- 0.3).

The size of nanocomplexes for oral delivery is very relevant in optimising their intestinal uptake as smaller-sized particles (< 300nm) have been found to be favoured in the processes like transcellular uptake by Peyers patches and paracellular uptake through tight junctional spaces [88, 181]. Particle size has also been found to affect the process of nanoparticle clearance by macrophages; as complexes with smaller sizes (<150nm) have been shown to exhibit a higher level of exocytosis [166, 177].

3.3.2.2. Zeta Potential

The zeta potential of polymer, insulin complexes was observed to be positive and range between approximately 28-38mV. NAC conjugates displayed lowest zeta potential values, Paa and QPaa showed intermediate zeta potential values, while TBA conjugates had the highest magnitude of surface charge. This is in agreement with the charge on their constituent polymer chains shown in Table 2 in chapter 1, which showed there was a reduction in surface charge of NAC-based thiomers due to substitution with the neutral amide bond. However, complexes from TBA-based thiomers exhibited the highest zeta potential probably due to the extra-cationic charge conferred by the protonated amidine bond. The positive surface charge on complexes is beneficial in facilitating complexation with insulin and initiating processes like paracellular transport and mucoadhesion through electrostatic interaction with tight junction proteins and mucin respectively. Surface charge of nanoparticles affects their biodistribution [166]. Nanoparticles with a slight negative charge have been shown to accumulate better in tumor sites, while an elevation of positive surface charge was found to be associated with an increased affinity for the negatively charged cell membrane enhancing cellular uptake of cationic nanoparticles [166].

3.3.2.3. Complexation efficiency

Insulin complexation efficiency did not vary greatly amongst the various polymers, as all complexes showed high insulin complexation efficiency (> 90%). However, as highlighted

earlier the structure of insulin complexed to TBA conjugates was altered in Tris buffer at pH 7.4, making it questionable as to whether it was a viable derivative for future study.

3.3.2.4. Transmittance

Turbidimetric measurements reflect the molecular weight and solubility of complexes present as these properties are directly related to the UV light scattering effects of the formulation [182]. High transmittance values obtained for optimal polymer, insulin PEC formulations displayed in Table 9 above indicated that the nanocomplexes formed were water soluble and discrete showing no turbidity or precipitation in the samples tested.

3.3.2.5. TEM

The morphology of different PECS prepared at 0.8:1 P: I mass ratio using the 0.5mgml^{-1} insulin stock was elucidated using TEM. Paa, insulin complexes were not analysed by TEM .The images are displayed below in figures 54-58 below.

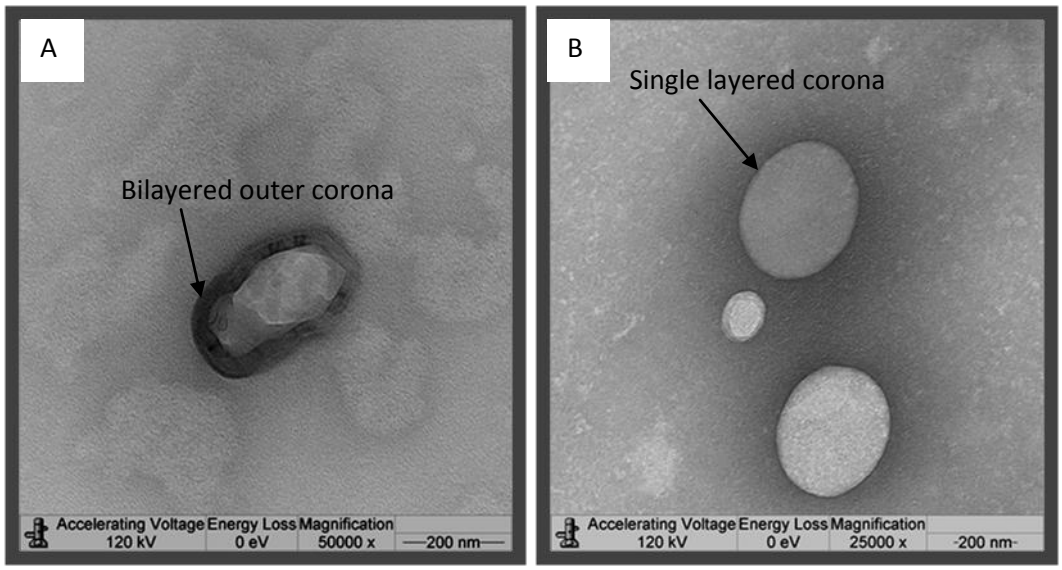

Fig. 54: TEM micrographs of QPaa, insulin complexes A) nanovesicular complex with a bilayered outer corona B) nanoparticles with a single layer outer corona.

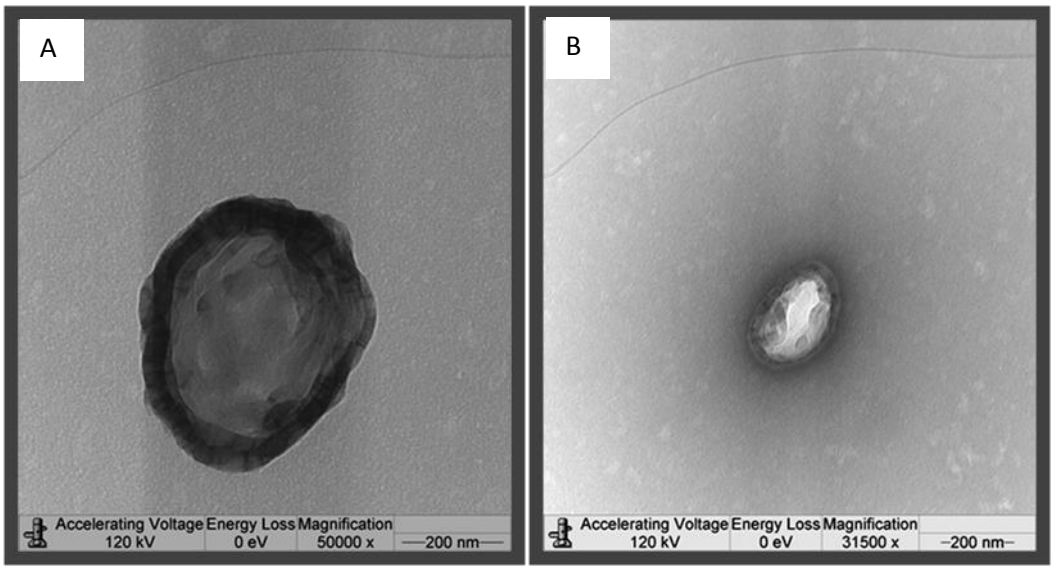

Fig. 55: TEM micrographs of Paa-NAC, insulin complexes A) nanovesicular complex with a bilayered outer corona B) nanovesicles with a single layer outer corona.

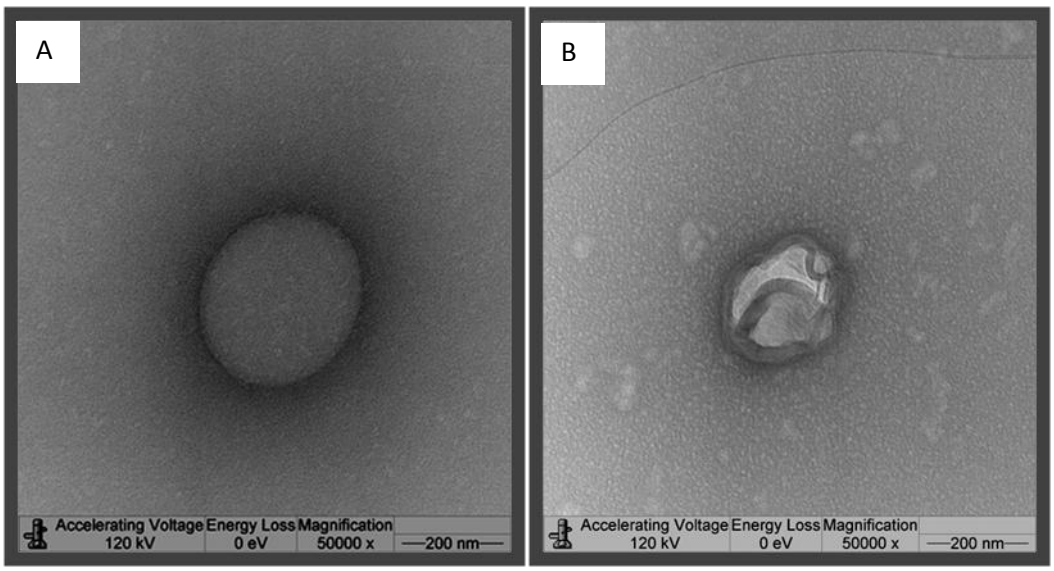

Fig. 56: TEM micrographs of QPaa-NAC, insulin complexes. A) nanoparticle with a single layer outer corona B) nanovesicular complex with a bilayered outer corona.

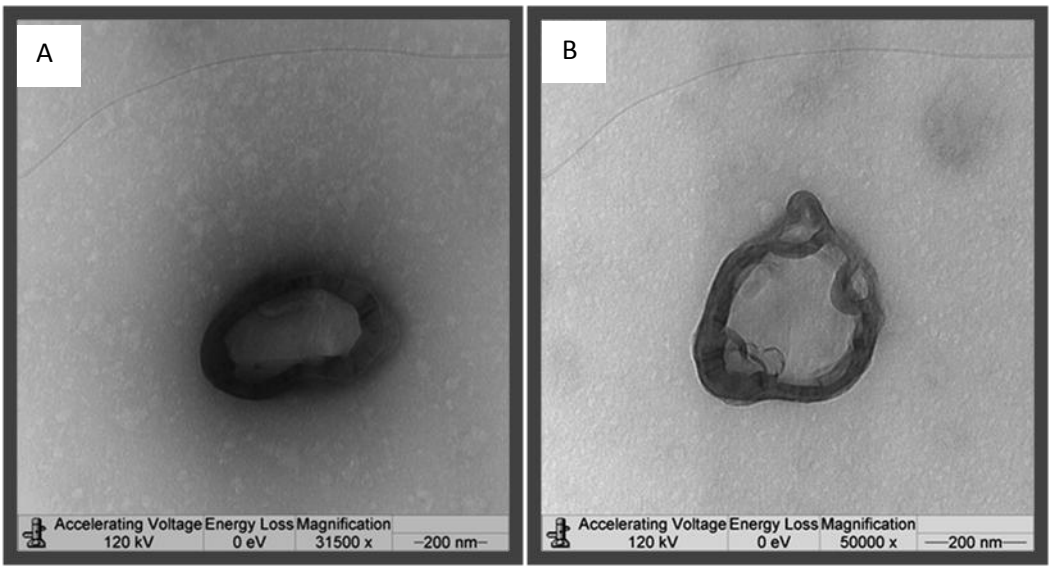

Fig. 57: TEM micrographs of Paa-TBA, insulin complexes A) nanovesicle with a bilayer outer corona B) nanovesicle with a bilayer outer corona magnification.

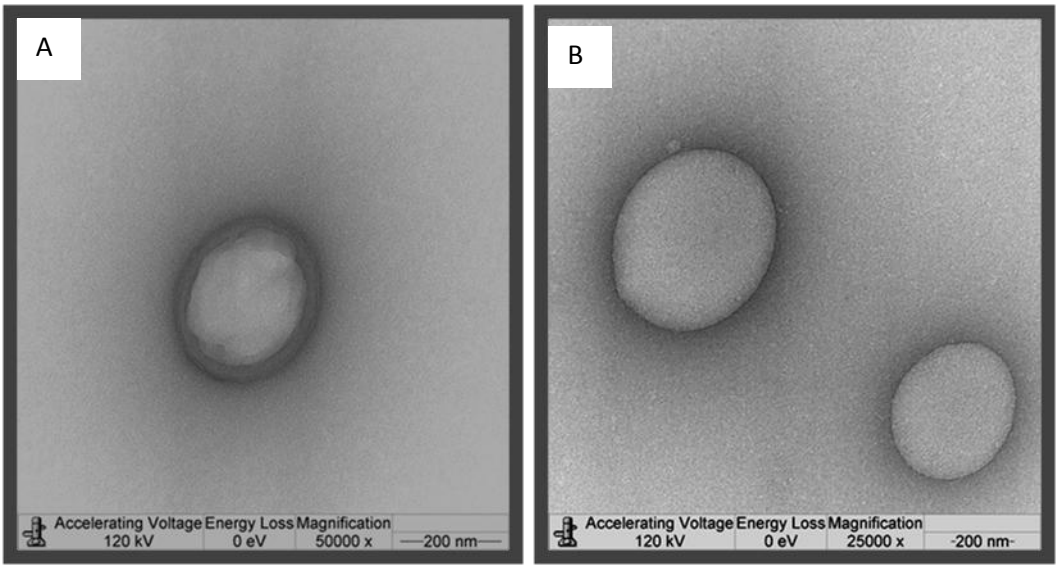

Fig. 58: TEM micrographs of QPaa-TBA, insulin complexes. A) nanovesicle with a bilayer outer corona magnification B) nanoparticle with single outer layer.

The TEM micrographs in figures 54-58 above show that quaternised polymers appeared to be capable of forming nanoparticles having a single layer of polymer chains as their outer corona and nano-sized vesicular structures with a distinctive bilayered outer corona.

However, non-quaternised thiomers (Paa-NAC/Paa-TBA) complexes appeared to form mostly nano-vesicles. These nano-vesicle bilayers appear to show darkened regions which suggests that these areas may have resisted staining indicating they are likely more hydrophobic than other regions of the complex [136].

The formation of bilayer vesicles has been observed to be directly related to the hydrophobic content of the polymer, with nano-vesicular self-assembly being initiated by an attempt to minimise the high energy interaction between hydrophobic groups of the polymer and the aqueous disperse phase while also maximising interfacial area by sustaining low level interactions between hydrophilic groups and the disperse phase [183, 184]. Also, water-soluble oppositely charged polyelectrolytes have been found to promote vesicle formation in non-vesicle forming water-soluble amphiphiles. This phenomenom arises due to partial charge neutralization by the adsorption of one polyelectrolyte onto the bilayer of the polymer of opposite charge, influencing the balance of opposing forces of electrostatic repulsion and hydrophobic interaction in favour of vesicle formation [185]. Considering that modification of Paa by thiolation and quaternisation imparts some level of hydrophobicity to the resultant constructs may suggest that interaction with anionic insulin molecules can promote the formation of the vesicles observed in the TEM micrographs through the aforementioned mechanism.

TEM results further emphasize the role of hydrophobic interactions arising from the intramolecular disulphide bonds formed during the thiolation of the polymers in complexation with insulin.

3.3.3. *IN-VITRO* ENZYMATIC DEGRADATION STUDIES

The ability of QPaa, Paa-NAC and QPaa-NAC complexes (optimal formulations at 0.8:1 P: I mass ratio-0.5mgml^{-1} insulin stock) to protect complexed insulin from degradation by the serine proteases trypsin, α-chymotrypsin and pepsin was assessed. The results were compared to that obtained for a similar control solution of free insulin and are illustrated in figures 59-62 below.

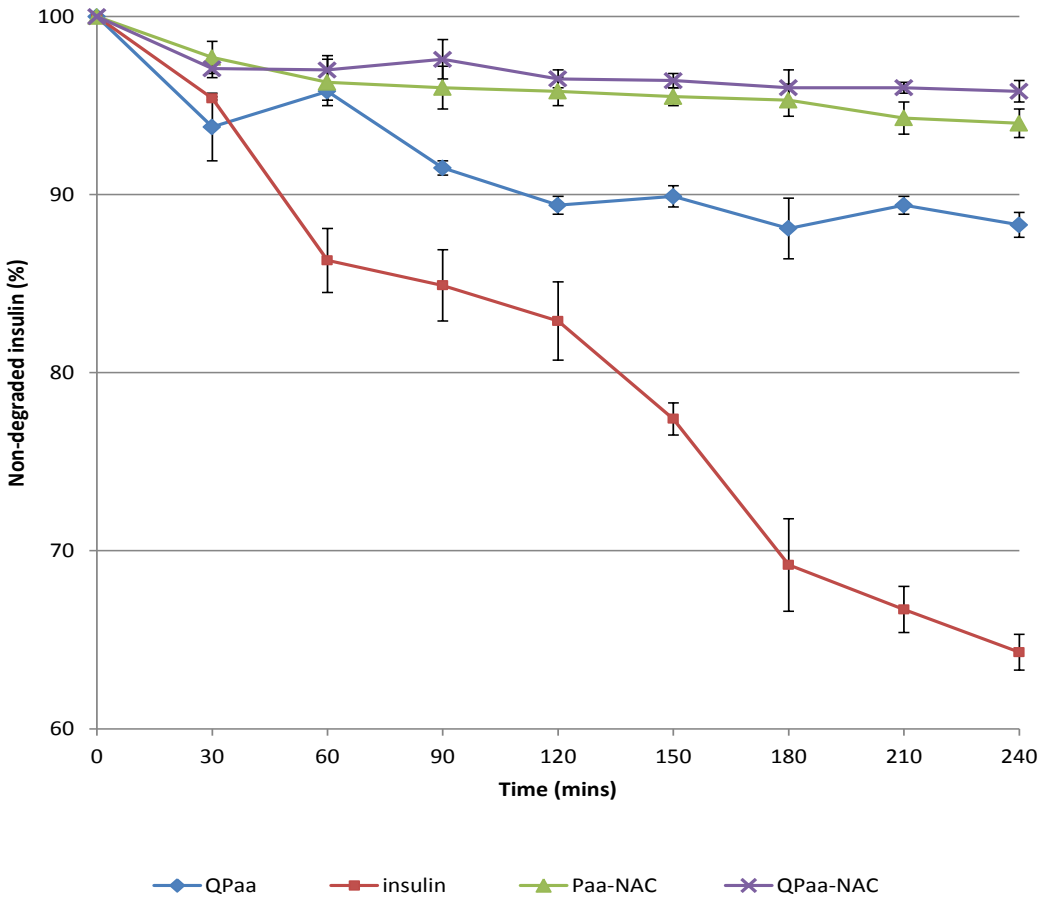

Fig. 59: Degradation curves of insulin and insulin PECS prepared from Qpaa, Paa-NAC and QPaa-NAC exposed to trypsin (mean ± S.D.; n=3).

Results of exposure of polymer, insulin complexes to tryptic degradation showed that > 90% of insulin contained within the complexes was still available after 240 minutes. Taking into consideration the amount of undegraded insulin present within the control sample (64.3%) after 4 hours, approximately 30% of incorporated insulin was left undegraded as a result of complexation of the protein to Paa-NAC and QPaa-NAC. Although, the fact that 88% of undegraded insulin was present in QPaa complexes after 4 hours and 96% insulin available in a similar formulation of QPaa-NAC after exposure to trypsin for the same time interval indicated that thiolation further enhanced enzymatic protection. Paa-NAC and QPaa-NAC complexes exhibited only slight variations in protection of insulin from the effects of trypsin.

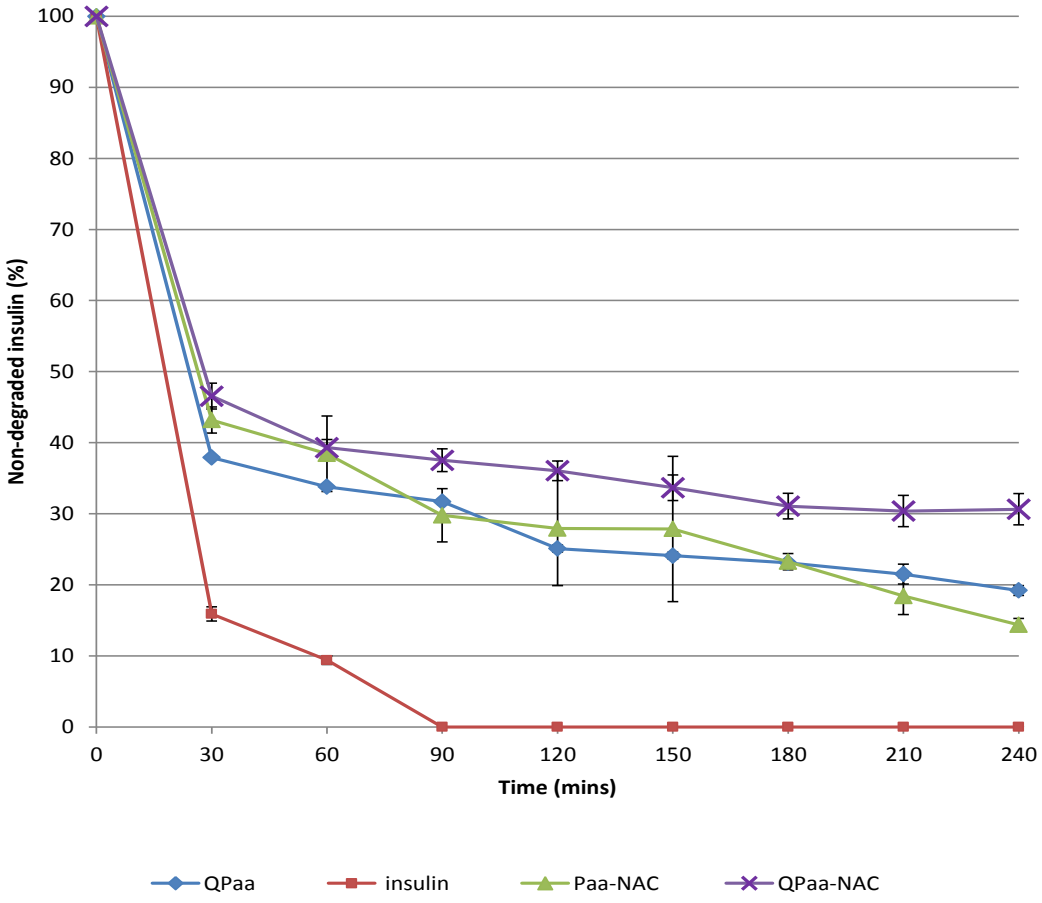

Fig. 60: Degradation curves of insulin and insulin PECs prepared from QPaa, Paa-NAC or QPaa-NAC complexes exposed to α-chymotrypsin (mean ± S.D.; n=3).

Thiomer, insulin complexes showed a different insulin degradation profile on exposure to α-chymotrypsin. Thiolated QPaa (QPaa-NAC) insulin complexes showed increased resistance to degradation by α-chymotrypsin than either QPaa or Paa-NAC complexes. The amount of undegraded insulin available in QPaa-NAC complexes after 4 hours was observed to be 10% more than QPaa complexes, 15% more than Paa-NAC complexes and 30% more than was present in the insulin control. This may show a synergistic effect was obtained from thiolation and quaternisation of the parent polymer, Paa, in terms of protection of insulin from degradation by α-chymotrypsin.

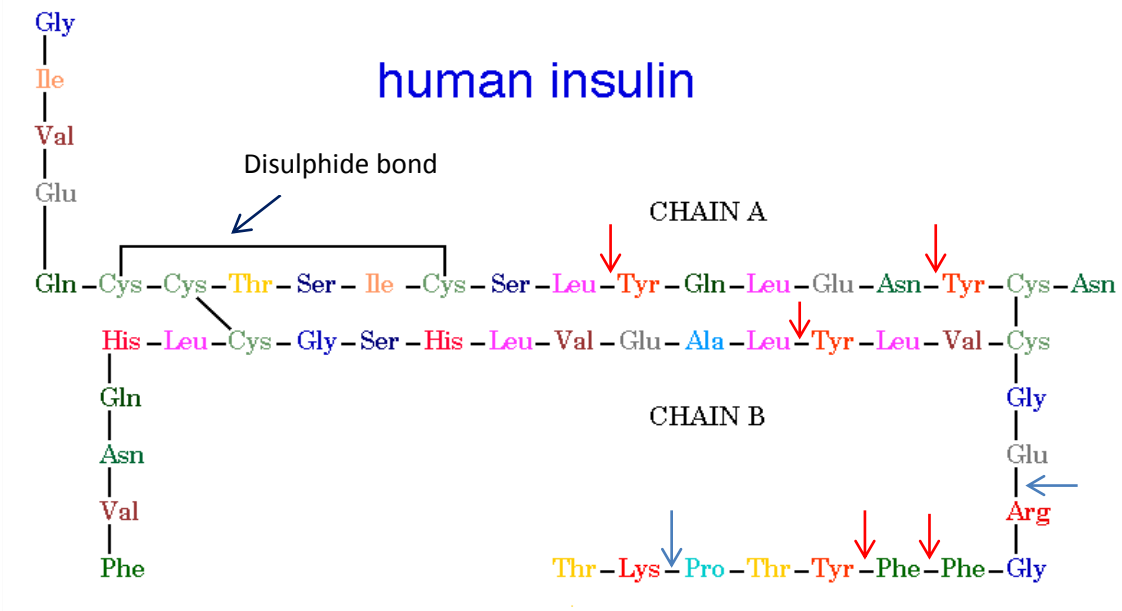

Fig. 61: Structure of insulin showing cleavage sites of trypsin (blue arrows) and α-chymotrypsin (red arrows).

In the three-dimensional structure of insulin, bonds prone to tryptic cleavage which include the carboxyl terminus of B29-Lys and B22-Arg are accessible at the B-chains as shown in figure 61 [186]. These carboxyl groups are deprotonated and hence negatively charged at pH 7.4. It may therefore be that the electrostatic binding of positively charged polymer molecules at this negative terminal shields susceptible bonds at this site from tryptic attack [187]. This sort of enzymatic protection/shielding of insulin by polymer-insulin interactions have previously been reported by researchers working with modified chitosan and Paa [148, 187]. Hence, this protective effect would be limited to sites on insulin which are capable of coulombic interactions with compatible polymer chains. However, two bonds prone to cleavage by α-chymotrypsin are enclosed within the hydrophobic core of the insulin molecule [185] and complexation with a less hydrophobic polymer like QPaa may not allow for interaction of these regions with the polymer chains due to differences in polarity. Hence these areas may not be protected from the attacking protease.

Conversely, polymer thiolation creates hydrophobic regions within the thiomer as seen with the TEM photos displayed in figures 54-58 due to intramolecular disulphide bond formation. Hence, protection of complexed insulin from proteolytic attack by

α-chymotrypsin observed with complexes prepared with NAC-conjugates may be because the thiomers are capable of protecting the bonds located within the hydrophobic core of insulin from degradation due to hydrophobic interactions between the thiomer and insulin occurring at this region. The ability of such hydrophobic intractions to offer improved protection of insulin associated within a PEC delivery system to degradation by serine proteases has been previously reported [138, 148].

Consequently, QPaa-NAC which may incorporate charge-mediated and hydrophobic interactions with insulin on complexation yields a cumulative protective effect , being able to shield more susceptible sites on the insulin molecule from proteolytic degradation by α-chymotrypsin than either QPaa or Paa-NAC. This result is in agreement with previous publications which showed that the ability of PECS formulated from Paa-based polymers to protect complexed insulin from the effects of α-chymotrypsin was enhanced when Paa was functionalised with both hydrophobic and quaternary groups [138].

In addition to the shielding effect provided by the PEC polymeric network, thiomers can also provide enzyme-inhibitory advantages due to their ability to bind Zn^{2+} ions limiting the activity of several zinc-dependent enzymes [76, 173, 188]. Studies have shown that thiolation of polycarbophil (polycarbophil-cysteine conjugates) improved its ability to inhibit the activity of intestinal proteases like α-chymotrypsin, aminopeptidase-N and carboxypeptidases [76, 173]. This effect was attributed to the ability of thiomers to bind metal ion cofactors essential for the activity of intestinal proteolytic enzymes. However *in-vivo* studies was not within the scope of the present research and the ability of these novel Paa-based thiomers to effect enzymatic protection of insulin via metal ion binding could not be evaluated. This may however be the subject of future investigations.

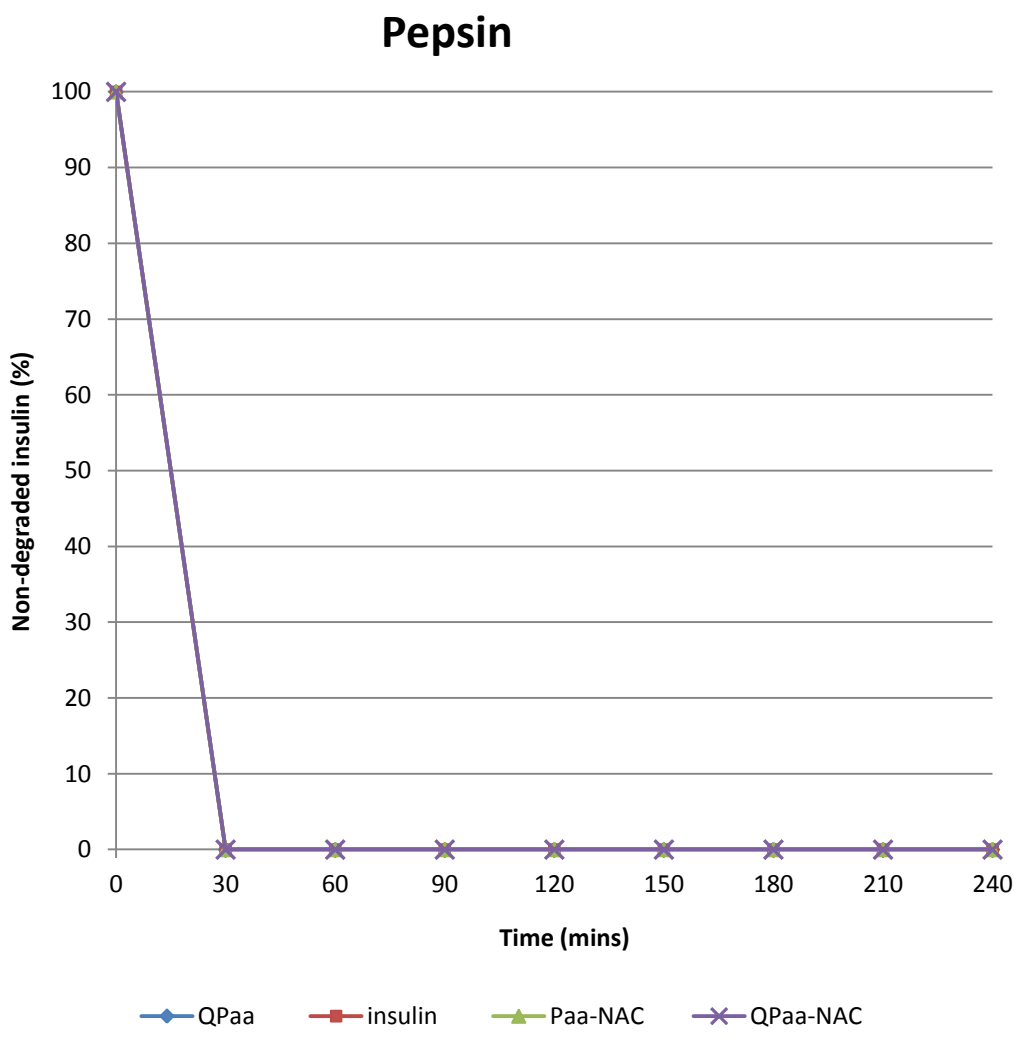

Fig. 62: Degradation curves of insulin and insulin PECs prepared from QPaa, Paa-NAC or QPaa-NAC complexes exposed to pepsin (mean ± S.D.; n=3)

None of the insulin PECS prepared from both quaternised and/or thiolated Paa derivatives offer any protection of complexed insulin from degradation by pepsin, as complete degradation of insulin present in complexes was observed after 30 minutes of exposure of complexes to pepsin. This is likely as a result of the numerous sites on the insulin molecule susceptible to degradation by pepsin. Examples of sites susceptible to peptic degradation include sites before leucine, phenylalanine, tyrosine and tryptophan except if preceded by proline [138, 189]. Although, rapid peptic degradation of complexed insulin may also be accelerated by acidification of the complexes to simulate normal physiological pH conditions for peptic activity thereby making insulin positively charged (below its pI of 5.5) and destabilizing electrostatic polymer insulin interaction. Amphiphillic Paa-insulin

nanocomplexes which benefited from both hydrophobic and electrostatic interactions were observed to show some protective effect from peptic degradation [136, 138]. However, exposure of oral insulin formulations to the effect of pepsin can be prevented by the use of enteric formulations which target the release of insulin to the small intestine and distal parts of the GIT, hence curtailing insulin proteolysis by enzymes operating within the gastric region of the gut [140].

3.3.4. *IN-VITRO* EVALUATION OF MUCOADHESIVE CAPACITY OF COMPLEXES

Assessment of mucin adsorption properties of polymer, insulin complexes prepared in Tris buffer pH 7.4 at 0.8:1 P: I mass ratio using the 0.5mgml^{-1} insulin stock solution (figure 63 below). The results were compared to an insulin control.

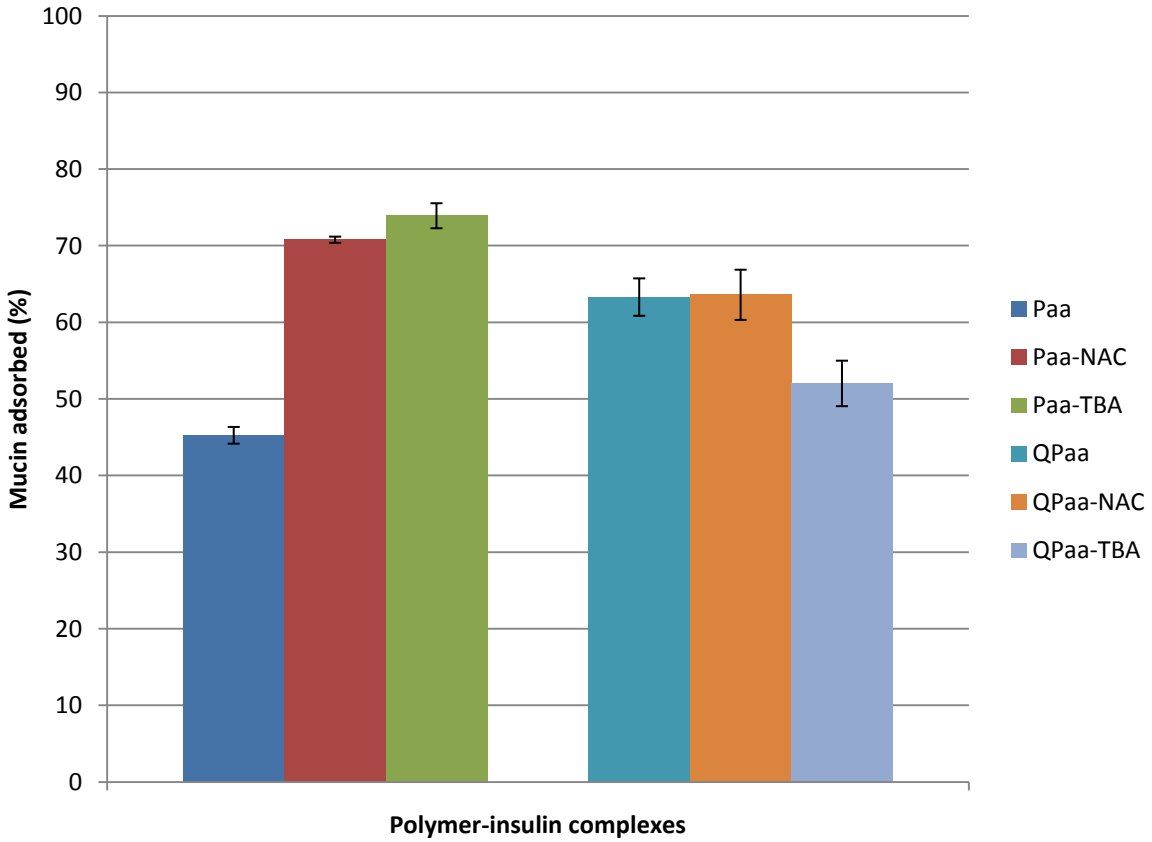

Fig. 63: Mucin adsorption profile of polymer, insulin complexes (mean ± S.D.; n=3)

From figure 63 above, the mucin adsorption profile of insulin PECS was observed to be identical to that obtained for the polymer solutions in section 2.3, with modified Paa-based complexes showing better mucoadhesive properties than the unmodified backbone. This

implies that complexation of the polymers with insulin did not affect the mucoadhesive properties of the polymers. Thiolated Paa (Paa-NAC and Paa-TBA) PECS displayed the greatest mucoadhesive properties, while thiolation of QPaa did not offer any substantial improvement in the mucoadhesive profile of the quaternised backbone or its complexes.

However, comparing the mucin adsorption profile of these complexes with that of the insulin control (mucin adsorption of insulin control was observed to be negligible (≤ 0.00%) shows that complexation of insulin to Paa and its derivatives may create a platform for the application of mucoadhesive interactions in oral insulin delivery.

3.4. CONCLUSION

The data collected from the above processes support the spontaneous formation of spherical, nano-sized PECS with good insulin complexation efficiency on mixing optimal mass ratios of Paa/QPaa and insulin in buffer solutions. The differences in the zeta potential of separate polymer and insulin solutions from that of their complexes indicate the role of electrostatic forces in the formation of these polymer-insulin complexes. Optimisation of the complexation process varying polyelectrolyte stoichiometry and type of buffer used for complex formation showed that most complexes were more stable in Tris than sodium hydroxide buffer and less stable when prepared at higher solute concentration levels of $2mgml^{-1}$ as compared to $0.5mgml^{-1}$ insulin stock levels. Generally, $0.5mgml^{-1}$ insulin stock based complexes prepared between 0.8-1:1 mixing ratio were consistently stable for all polymers, with 0.8:1 showing the best stability profile. Electrostatic –induced polymer, insulin complexation carried out using Paa-based polymers was found to result in the formation of nano-sized, positively-charged complexes. However complexation efficiency data obtained showed that interaction of TBA-based thiomers with insulin in Tris buffer pH 7.4 may have altered the conformation of insulin affecting HPLC analysis of insulin. This was also confirmed by an insulin Elisa assay. QPaa, QPaa-NAC and Paa-NAC insulin complexes could protect insulin from the effects of trypsin and α-chymotrypsin to varying extents. *In-vitro* mucin adsorption profile of polymer, insulin complexes was basically similar to that of the free polymer. All complexes showed good mucoadhesive properties when compared to free insulin, with all modified polymers performing better than the unmodified Paa backbone.

4. BIOCOMPATIBILITY AND CELLULAR UPTAKE OF COMPLEXES

4.1. INTRODUCTION

This chapter evaluates the performance of insulin PEC formulations in biological systems by assessing in-vitro cytotoxicity and cellular uptake of PECS using Caco-2 cell monolayers as a predictive model for human small intestinal epithelial cells.

The biocompatibility of each polymer was evaluated by carrying out MTT assays on Caco-2 cell monolayers treated with dilutions of each polymer in supplemented media. Cell monolayers were either subjected to a 24-hour recovery period in fresh media before the MTT assay (recovery period) or were assayed immediately after treatment with polymer solutions Therefore two IC_{50} values were obtained for each polymer (corresponding to the IC_{50} value of the polymer with/without a recovery period).

Cellular uptake of nanocomplexes by Caco-2 cell monolayers was monitored over different time courses by fluorescence microscopy using PECS prepared by mixing optimal mass ratios (0.8:1) of rhodamine-tagged polymers and FITC-insulin in Tris buffer pH 7.4. Cell monolayers were stained with 4'6'Diamidino -2-phenylindole hydrochloride (DAPI) to determine the location of complexes in relation to the cell nuclei. Uptake of polymers was also quantified by measuring the amount of rhodamine-tagged polymer taken up after solubilisation of the cells by 2% Sodium dodecyl sulphate (SDS).

Further investigations into the mechanism of PEC uptake were carried out using calcium-free media as uptake medium to limit the function of calcium-dependent uptake mechanisms . Cells were also pre-incubated with insulin solution to saturate and so down-regulate, insulin receptors prior to treatment with PECS.

4.2. MATERIALS AND METHOD

4.2.1. MATERIALS

Caco-2 cells were obtained from ECACC, Wiltshire UK (passage number 45-70).Poly (allylamine hydrochloride) (15kDa), rhodamine B isothiocyanate (RBITC), fluorescein isothiocyanate (FITC)-insulin, Eagle's minimum essential medium (EMEM), calcium-free EMEM, 3-(4,5-dimethylthiazol-2-yl)-2,5-diphenyl tetrazolium bromide (MTT), Triton X-100, dimethylsulfoxide (DMSO) HPLC grade, Glycine, Dulbecco's phosphate buffered saline (PBS), SDS and trypan blue were from Sigma Aldrich, UK. L-glutamine (200mM), non-

essential amino acids, trypsin-EDTA (0.05%) and DAPI was from Invitrogen, Scotland. Foetal calf serum-activated (FCS) was obtained from Biosera, UK. All other reagents used were of analytical grade.

4.2.2. *IN-VITRO* CYTOTOXICITY ASSAY

The IC_{50} value of each polymer which refers to the polymer concentration required to reduce cell survival by 50% was determined by MTT assay [1]. Caco-2 cells cultured at 37°C in EMEM containing 10% (v/v) foetal calf serum, 1% (v/v) non-essential amino acids and 1% (v/v) L-glutamine at 5% CO_2 and 95% humidity were trypsinised and used to seed 96-well plates at a cell density of 10,000 cells per well using 200µl of cell suspension per well. The cells were grown at the same conditions for 72 hours, after which the culture media was aspirated and replaced with 200µl of polymer solutions (concentrations ranging between 0.001-0.5 $mgml^{-1}$) prepared in EMEM without FCS. The polymer treatments were made up in EMEM without FCS to prevent interaction of the polymers with the proteinous components of FCS.

The plate was incubated for 24 hours after which 50µl of MTT (5$mgml^{-1}$ in PBS) was added into each well and the plate wrapped in foil (to protect it from light) and incubated for 4 hours. The plate was subsequently retrieved from the incubator and the contents aspirated. Each well was filled with DMSO (200µl) followed by 25µl of glycine buffer (7.5gL^{-1} glycine, 5.9gL^{-1} NaCl, pH 10.5) and the plate read by UV spectrophotometry (SoftMax Pro 5.0, Molecular Devices, U.S) at 570nm. Cell viability (%) was calculated relative to the negative control (cells treated with Triton-X in PBS) and the positive control (untreated cells in EMEM) [137]. This process was repeated for each polymer with the polymer solutions replaced with fresh media (200µl) to allow the cells to recover for a 24-hour period before treating monolayers with MTT. Plots of % cell viability against polymer concentration were used to determine the IC_{50} value of the different polymers without/with a recovery period.

4.2.3. LABELLING OF POLYMERS WITH RBITC

For non-thiolated polymers, 5ml of RBITC in dimethylsulfoxide (1$mgml^{-1}$) was added dropwise over 10 minutes into 95ml of a 0.05% (w/v) solution of polymer in double-distilled water with gentle magnetic stirring. The stirring was continued for one hour and the mixture dialysed (molecular weight cut-off - 7kDa; Medicell UK) against 5L of double-distilled water for 48 hours with 6 water changes every 24 hours [190].

For thiolated polymers, the method was adjusted by replacing DMSO with methanol and keeping the pH of the reaction at 4-5 to limit oxidation of thiol groups to disulphides. Briefly, 5ml of RBITC in methanol (1mgml^{-1}) was added dropwise over 10minutes into 95ml of a 0.05% (w/v) solution of thiomer in double-distilled water acidified with 5M HCl to pH 4-5 [191]. Stirring was done under nitrogen for one hour and the mixture dialysed in the dark (MW cutoff-7kDa; Medicell UK) against 5L of 5mM HCl for 24 hours and 0.4mM HCl for a further 24 hours (6 water changes every 24 hours).

The polymer solution obtained from the dialysis process was freeze dried over 48 hours to yield a deep pink to purple solid. RBITC-tagged Paa and QPaa were stored in dessicators at room temperature, while RBITC-tagged thiomers were stored at -20°C.

4.2.4. CELLULAR UPTAKE STUDIES

4.2.4.1. Assessing cellular uptake of PECS by fluorescence microscopy

Caco-2 cells were seeded at a density of 0.1 X 10^6 cellsml^{-1} in 24 well plates and grown over 3 days at 5%CO_2, 95% humidity and 37°C [192]. The media contained in the wells was aspirated and washed with PBS. Fluorescent complexes were prepared in Tris buffer pH 7.4 by mixing RBITC-labelled polymer with FITC-insulin at P: I mass ratios of 0.8:1 (0.2:0.25mgml^{-1}). The PEC concentrations used for the uptake experiments had to be optimised based on the IC_{50} values of each polymer obtained from MTT assays conducted without a recovery period. Each well was treated with PECS (0.005:0063mgml^{-1} P: I mass ratio for non-quaternised complexes; 0.016:0.020 mgml^{-1} P: I mass ratio for quaternised complexes in FCS-free EMEM) and incubated for time periods of 0.5-4 hours. PEC uptake experiments were repeated reversing the concentration of quaternised polymers used to that of non-quaternised polymers (0.005:0063mgml^{-1}) to enable detection of concentration-based differences in uptake profile. The concentration of non-quaternised polymers used could not be increased to 0.016:0.020 mgml^{-1} P : I mass ratio, as this may lead to excessive damage of the cells during the polymer treatment step.

After incubation with the PECS, treatment was removed and the cell layer subsequently washed (x2) with PBS and treated with Trypan blue to highlight non-viable cells. Uptake of complexes was assessed by examining Caco-2 cell monolayers under a fluorescence microscope (Leica DMI4000B, Leica Microsystems Ltd. UK) (magnification x20) post-treatment with PECS using different filters set at excitation/emission wavelengths for FITC, RBITC and a combination of both. Images were captured on a camera fitted to the

microscope and are indicative of replicate wells. Uptake of control polymer and FITC-insulin solutions at similar concentrations and time intervals was also assessed by fluorescence microscopy.

4.2.4.2. Determination of cellular location of PECS

Caco-2 cells were grown on 24 well plates and the monolayers treated with PECS following the method described in section 4.2.4.1. after which the monolayers were stained with 18.8μgml^{-1} solution of DAPI in PBS for 10 minutes to highlight the nuclear region of the cells [193]. The monolayers were washed(x2) with PBS and treated with Trypan blue and rewashed prior to fluorescence microscopy. This gives an idea of the location of PECS in relation to the cell nuclei and enables the identification of complexes located within the perinuclear region.

4.2.4.3. Investigation of PEC uptake mechanism

Uptake experiments were carried out replacing EMEM (FCS-free) with calcium-free EMEM (FCS-free) as uptake media for 2 hours prior to treatment to inhibit the performance of calcium-dependent uptake mechanisms. Monolayers were also pre-incubated with 3μgml^{-1} of insulin for 1 hour prior to treatment to enable saturation of insulin receptors and so inhibit insulin-receptor mediated uptake mechanisms. Cells from the experiments above were visualised under the fluorescence microscope and the results compared with that obtained from previous uptake experiments done in section 4.2.4.1. [192]

4.2.4.4. Quantification of polymer uptake

Caco-2 cells were cultured and treated with RBITC-labelled polymers (Paa, QPaa, QPaa-NAC and QPaa-TBA) as described for uptake experiments. The cell layer was then washed (x 3) with PBS and the cell layer attached to each well and treated with 1ml of 2% SDS in PBS solution for 30 minutes to lyse cells [147]. The fluorescence intensity of the cell lysate obtained from the above procedure was measured by fluorescence spectrophotometer (Perkin Elmer LS55 Fluorescence Spectrophotometer, Perkin-Elmer, UK) using a 1ml quartz cuvette and excitation/emission wavelength set at 547/590nm for RBITC. The results obtained were input into calibration curves (R^2 = 0.99) prepared using dilutions of the tagged polymers in 2% SDS (concentrations ranging from 0.3-10μgml^{-1}). The values obtained were subsequently used to estimate the percentage of tagged polymer taken up

by the Caco-2 cells within 2 hours of incubation. The process was also repeated using calcium-free media as uptake medium.

4.3. RESULTS AND DISCUSSION

4.3.1. BIOCOMPATIBILITY TESTING

Biocompatibility of each polymer was assessed based on IC_{50} values obtained from MTT assays conducted on Caco-2 cell monolayers treated with increasing concentrations of each polymer (0.001-4mgml^{-1}) in supplemented media. MTT assays assess cellular metabolic activity by measuring the activity of cellular enzymes capable of reducing the dye to an insoluble purple formazan product in living cells [194]. Rapidly dividing cells show a high rate of MTT reduction giving out a deep purple colouration, while a lower rate of MTT reduction may reflect a loss of cell viability (cytotoxic effect) or a shift from the proliferative to the resting or quiescent state (cytostatic effect) [195]. Quiescent cells are usually still viable but metabolically inactive, therefore producing very little formazan.

The toxicity profile of polymers was first evaluated without the inclusion of a cell recovery period and findings are described in the subsequent paragraphs. From the results of MTT assays conducted without a recovery period (WOR), plots of % cell viability versus log polymer concentrations prepared for each polymer is shown in figure 64 below.

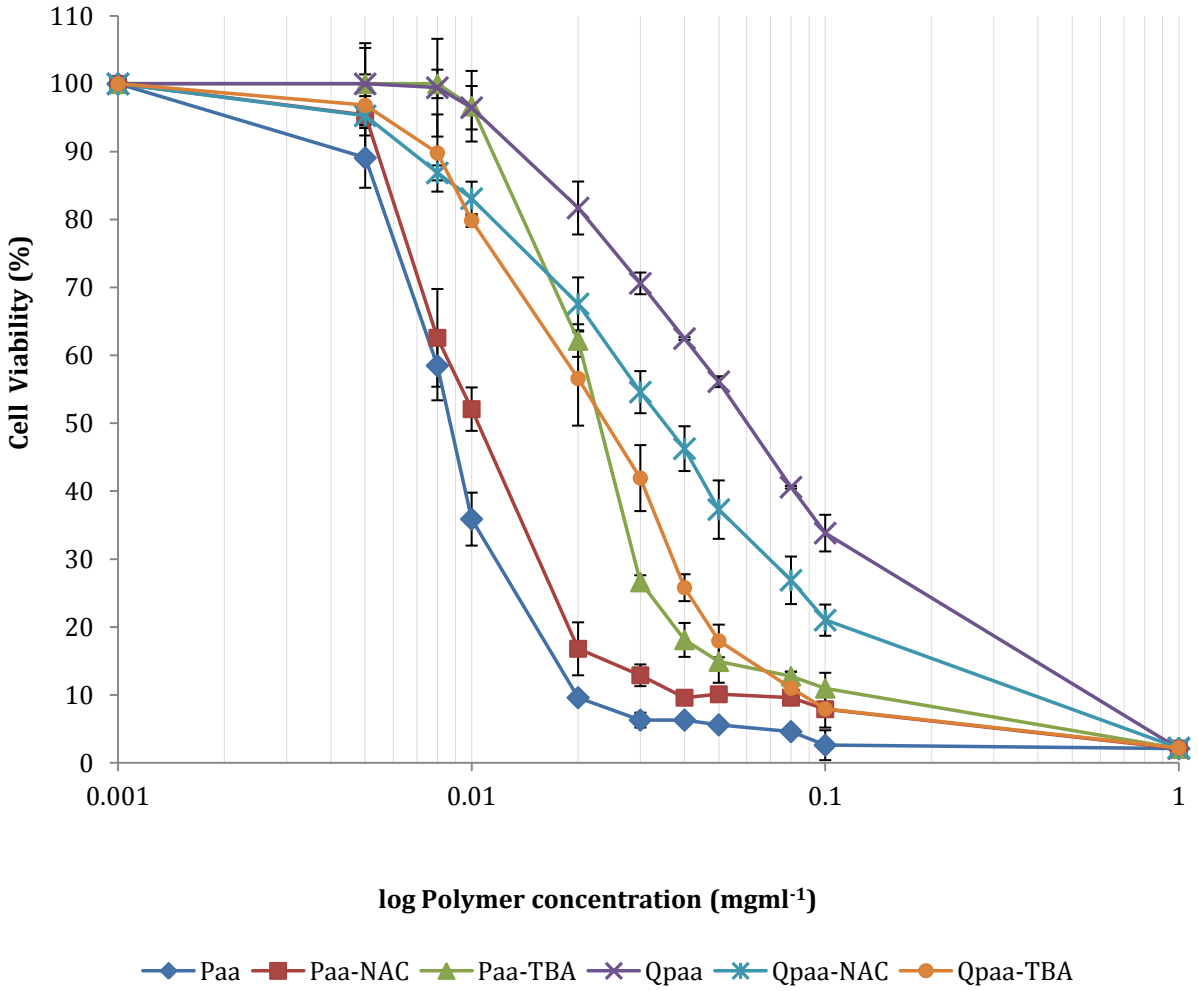

Fig. 64: Caco-2 cell viability (%) as determined by MTT assay after 24 hour exposure to varied concentrations of Paa, QPaa and their thiolated derivatives without a recovery period (n =3; ± S.D.).

IC_{50} values of each polymer obtained from MTT assays conducted without a recovery period are highlighted in Table 10 below.

Table 10: IC_{50} values of Paa, QPaa and thiolated derivatives obtained without a recovery period. Values are mean ± S.D. (n = 3).

	Paa	**QPaa**	**Paa-NAC**	**QPaa-NAC**	**Paa-TBA**	**QPaa-TBA**
IC_{50}(mgml^{-1})	0.009 ± 0.003	0.062 ± 0.001	0.011 ± 0.009	0.036 ± 0.003	0.023 ± 0.002	0.024 ± 0.003

The unmodified Paa backbone showed the highest toxicity having the lowest IC_{50} value of 0.009 ± 0.003mgml^{-1}. This is expected as polycationic polymers like Paa and polylysine have been observed to be quite cytotoxic due to the availability of free protonable amine groups which have the ability to interact with anionic portions of glycoproteins on the cell membrane causing apoptosis [196]. Quaternisation decreases the number of these protonable primary amine groups per molecule improving biocompatibility [197], as may be seen by the marked improvements in IC_{50} exhibited by QPaa when compared to the non-quaternised Paa backbone (Table 10). This is consistent with the results obtained from other research groups where quaternisation of other polycations was observed to be associated with improvements in their toxicity profile [149].

Thiol substitution of the Paa backbone was also observed to result in an increase in IC_{50} values (smaller than was obtained with quaternisation) with Paa-NAC displaying a lower IC_{50} value than Paa-TBA. This could be as a result of the lower level of primary amine substitution found in Paa-NAC (total thiol substitution-320 ± 4.1µmol compared to 1080 ± 28µmol thiol groups found in Paa-TBA) implying that Paa-NAC has a higher level of free protonable primary amine groups to exert cytotoxic effects.

Thiolation of QPaa resulted in a fall in IC_{50} suggesting that the thiol moieties had a negative effect on biocompatibility of the quaternised Paa backbone. Thiols are capable of covalent interactions (thiol-disulphide reactions) with glycoproteins and can consequently damage protein components of cells irreversibly altering their structure/conformation [198]. Quaternisation increased the IC_{50} of Paa-NAC (IC_{50} increased from 0.011 ± 0.009 to 0.036 ± 0.003mgml^{-1}) as shown in figure 64 and table 10, but had no noticeable effect on the IC_{50} of Paa-TBA. Considering that QPaa-TBA had the highest level of total substitution (thiol and quaternary substitution combined) of primary amine groups, it should show the least toxicity. It is therefore surprising that Paa-TBA and QPaa-TBA have approximately the same IC_{50} (0.02mgml^{-1}). This implies that the biocompatibility enhancing effects of the quaternary groups present in QPaa-TBA appear to have been completely mitigated by TBA-based thiol substitution and may suggest that this thiol group has toxic effects on cells. This also highlights the fact that while quaternisation tends to completely mask the highly charged primary amine groups of Paa limiting their ability to damage cells, thiolation may only result in the replacement of one type of reactive groups (in this case free primary amine groups) with another type (thiol groups). The cationic substructure of the amidine linkage also makes it possible for these thiomers to initiate toxic effects associated with

cationic charge as well as effects arising from the actual thiol group as mentioned earlier, making these TBA conjugates more toxic than their NAC-counterparts [199].

The IC_{50} of each polymer was also evaluated after allowing the cells a 24-hour recovery period in supplemented EMEM post-treatment with polymers and similar plots of % cell viability versus log polymer concentrations prepared. The plots are shown in figure 65 below.

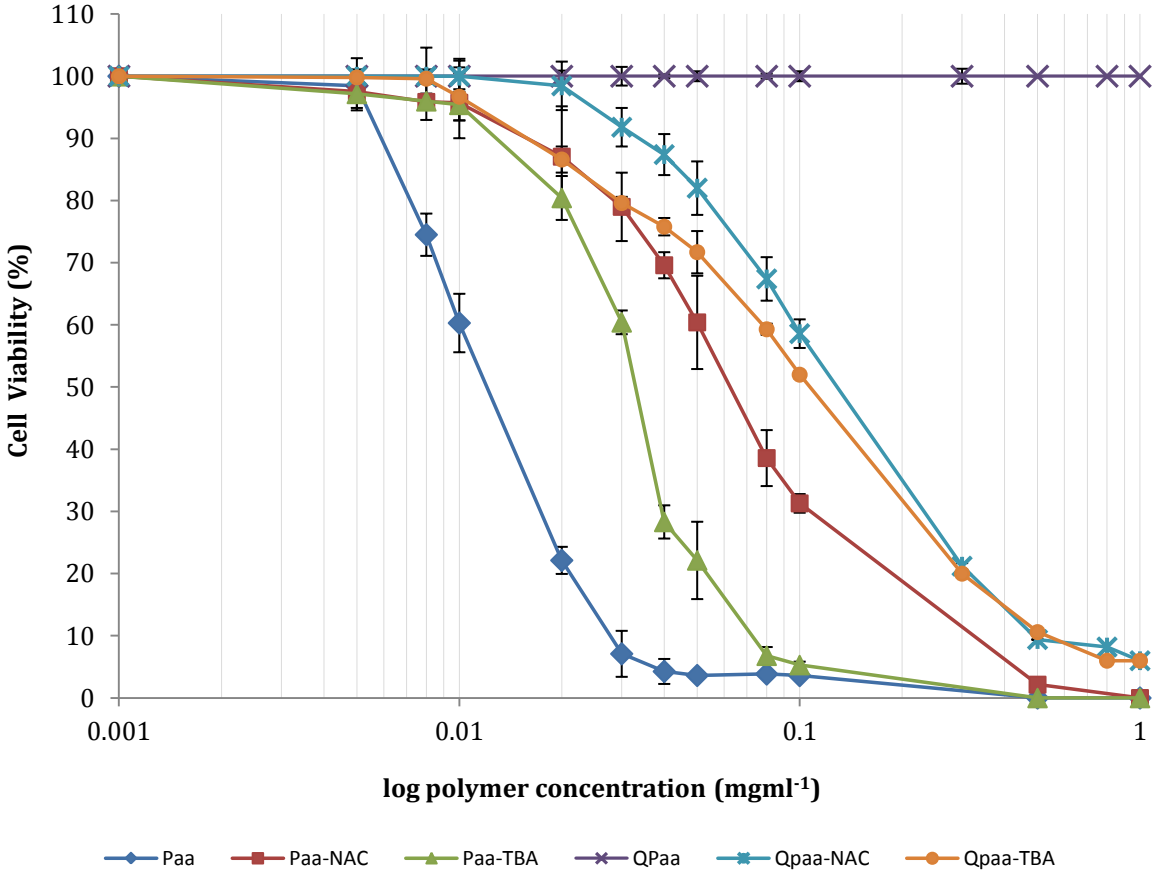

Fig. 65: Caco-2 cell viability (%) as determined by MTT assay post-24 hr recovery period and 24 hour exposure to varied concentrations of Paa, QPaa and thiolated derivatives (n =3; ± S.D.)

IC_{50} values of each polymer obtained from MTT assays conducted with a recovery period are highlighted in Table 11 below.

Table 11: IC_{50} values of Paa, QPaa and their thiolated derivatives post-24 hour recovery period. Values are mean ± S.D. (n = 3)

	Paa	QPaa	Paa-NAC	QPaa-NAC	Paa-TBA	QPaa-TBA
$IC_{50}(mgml^{-1})$	0.013 ± 0.005	No toxicity	0.064 ± 0.002	0.144 ± 0.007	0.033 ± 0.009	0.110 ± 0.003

The purpose of introducing a recovery period is to determine the extent to which cells can recover (their metabolic activity) from the toxic effect of the different polymers. This may give more insight on whether the toxic effect of the polymers on cells are transient/reversible or permanent. Results shown in table 11 above indicate that the inclusion of a recovery period before treating the cells with MTT resulted in an upward shift in IC_{50} for all the polymers tested as may be seen in figure 66 below.

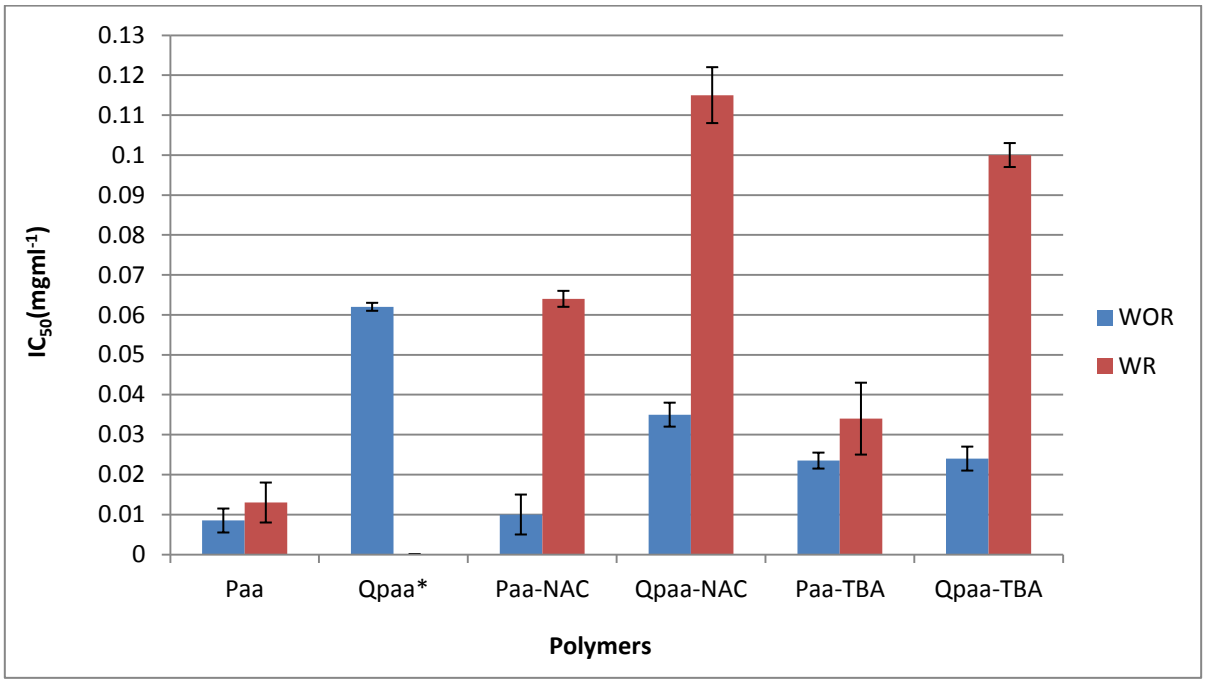

Key: WOR-without recovery period; WR – with recovery period

* Results obtained from the MTT assay of QPaa with a recovery period indicated that the IC_{50} of the polymer was higher than the highest polymer concentration tested ($4mgml^{-1}$).

Fig. 66: $IC_{50}(mgml^{-1})$ of polymers as determined by MTT assay without a recovery period (WOR) and post-24 hour recovery period (WR) (n =3; ± S.D.).

Cells treated with QPaa showed 100% cell viability at concentrations up to 4mgml^{-1}, with the polymer showing no toxicity(and hence no IC_{50} between 0.001-4mgml^{-1}). NAC-based thiomers also showed marked improvements (approximately 6-fold) in their IC_{50} after being subjected to a recovery period (figure 65 and 66). The effects of these polymers on cells appear to have been cytostatic rather than cytotoxic, as most of the cells affected were still viable and were able to recover full metabolic activity on removal of treatments and re-culturing. Hence this suggests that the effects of these polymers on affected cells are largely reversible, and do not result in permanent irreparable damage. This is especially true for QPaa which appears to only show a cytostatic effect as no loss of cell viability was observed (100% cell viability) between the cencentration 0.001-4mgml^{-1} post-recovery (figure 65).

On the other hand, polymers Paa and Paa-TBA showed little improvements in their IC_{50} (about 1.5 fold) with the introduction of a recovery period (figure 66). This indicates that these polymers are largely cytotoxic, and their interactions with cells mostly causes irreparable damage to cells and marked loss in cell viability. This again confirms the highly cytotoxic effect of the primary amine groups in Paa and suggests the amidine thiol substructure of Paa-TBA is a relatively cytotoxic moiety although less toxic than primary amine groups (TBA substitution of Paa improved IC_{50} both with and/or without a recovery period as may be seen in table 10 and 11). Bearing in mind that the difference in level of thiol substitution between Paa-TBA and Paa-NAC may not allow direct comparison of their toxic effects on cells, the presence of a protonable group within the amidine bond as compared to the uncharged amide bonds of Paa-NAC (refer to figure 8 and 9 in chapter 2) could however result in an increase in potential to cause toxic effects. QPaa-TBA also appeared to show cytostatic effects, although IC_{50} values were lower than QPaa and QPaa-NAC. The IC_{50} of QPaa-TBA was improved considerably after the introduction of a recovery period much higher than what was observed with Paa and Paa-TBA, but to a lesser extent to QPaa and QPaa-NAC.

Generally, considering the results of the cytotoxicity assays conducted with and/or without a recovery period the toxicity profile of the parent polymer was found to play a role in determining the biocompatibility of the thiolated derivatives. For non-quaternised thiomers where the parent backbone Paa was cytotoxic, the toxicity profile of the polymers followed this order: Paa > Paa-TBA > Paa-NAC. While for quaternised polymers where the parent backbone QPaa was found to be less-cytotoxic , the toxicity profile of the thiomers followed this order QPaa-TBA > QPaa-NAC > QPaa. This may then indicate that when

developing Paa-based thiomers, using QPaa as the parent polymer rather than Paa improves the biocompatibility of the resultant thiomers.

All substituted polymers showed better biocompatibility profile than the parent polymer, Paa. Also quaternisation improved overall biocompatibility considerably with all quaternised polymers having better IC_{50} and cell recovery rates than non-quaternised polymers. Thiolation improved the IC_{50} of Paa but made QPaa more toxic, while TBA-based thiomers were observed to be more toxic than their NAC-based counterparts. Futher biocompatibility issues to be aware of include the fact that the particulate nature of PEC delivery system may increase its potential to elicit immune responses *in-vivo* and affect its biodistribution/cellular trafficking altering toxicity profile [199, 200].

4.3.2. Cellullar uptake of complexes

4.3.2.1. Determination of uptake profile of optimal polymer, insulin PECS

After a 2 hour treatment with PECS, results of uptake experiments were recorded as images of Caco-2 cells visualised using separate fluorescent filters specific for insulin-FITC, RBITC-tagged polymers and a FITC/RBITC combination filter to identify areas of polymer, insulin colocalisation. Results are shown in figure 67-72 and are indicative of replicate wells. Images were taken of the same region of the cell layer using the brightfield and then the different filter sets.

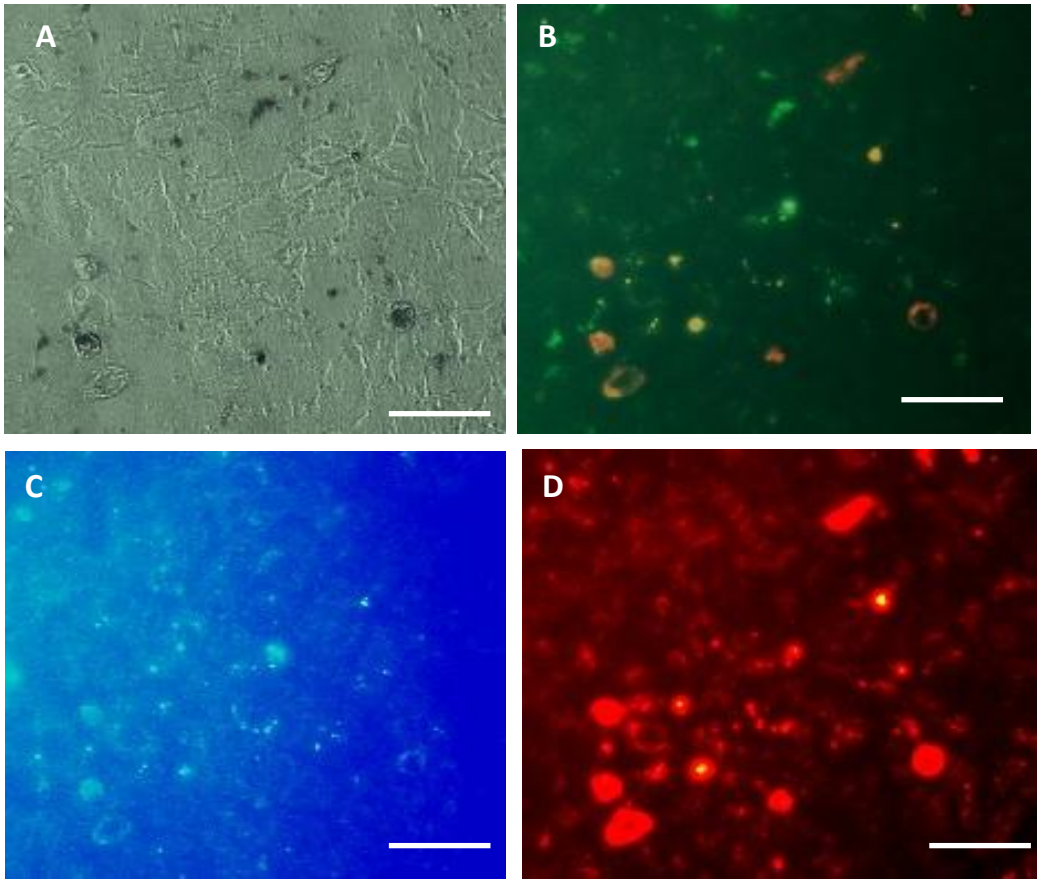

Fig. 67: Fluorescent microscopy images of Caco-2 cells treated with Paa, insulin complexes viewed using A) brightfield B) RBITC/FITC combination filter C) FITC filter D) RBITC filter. Scale bar -50µm.

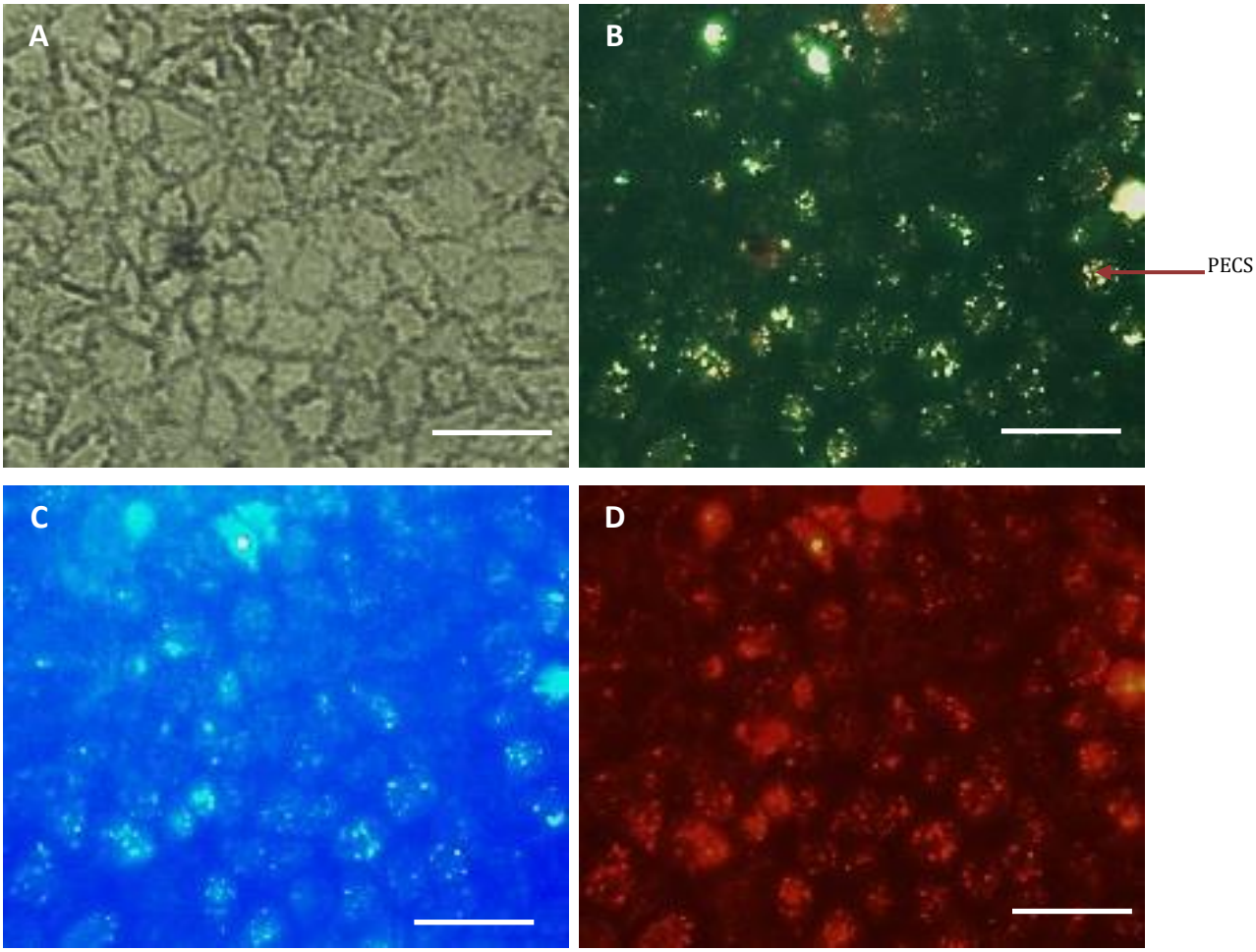

Fig. 68: Fluorescent microscopy images of Caco-2 cells treated with QPaa, insulin complexes viewed using A) brightfield B) RBITC/FITC combination filter C) FITC filter D) RBITC filter. Scale bar -50µm.

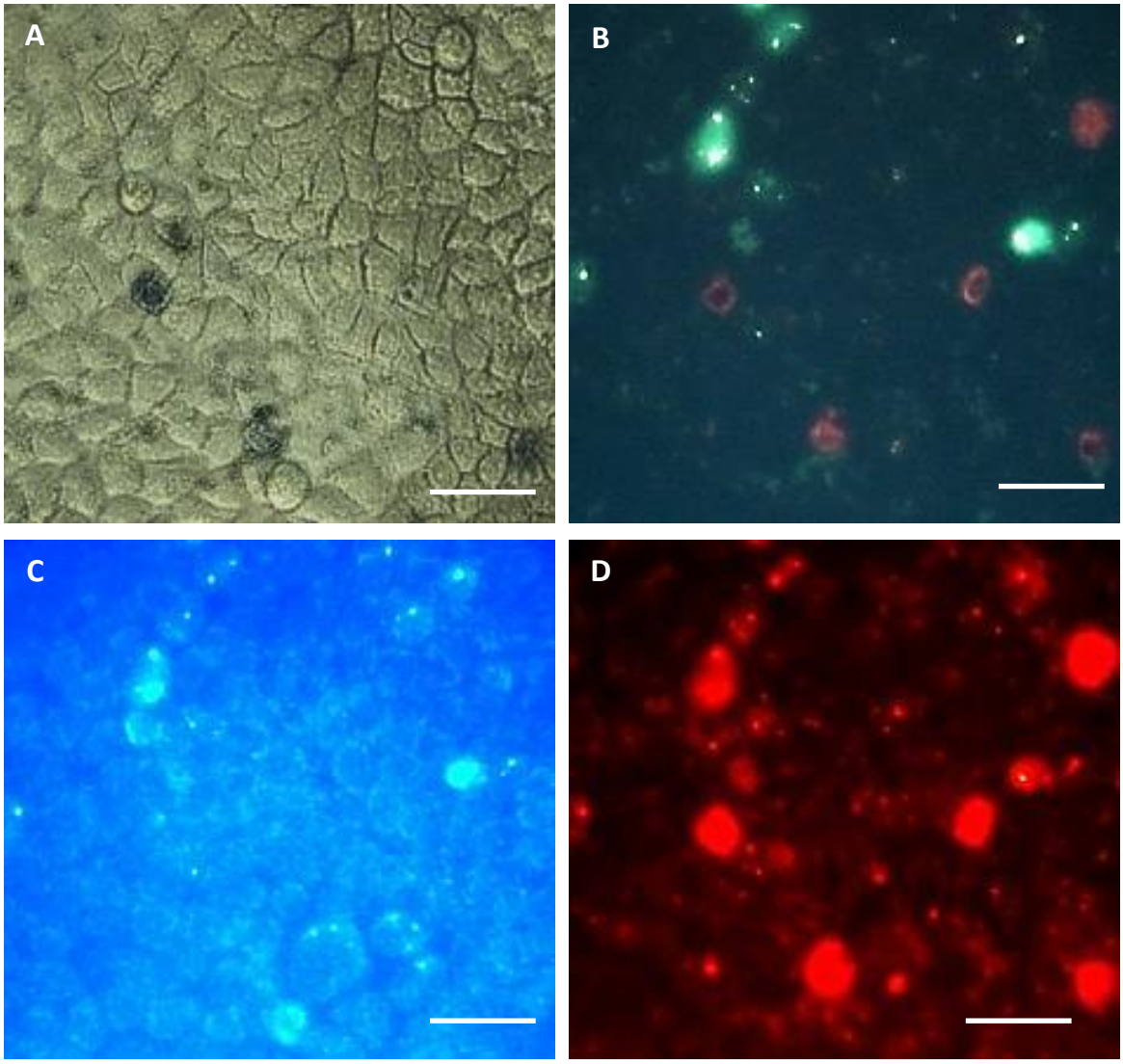

Fig. 69: Fluorescent microscopy images of Caco-2 cells treated with Paa-NAC, insulin complexes viewed using A) brightfield B) RBITC/FITC combination filter C) FITC filter D) RBITC filter. Scale bar -50µm.

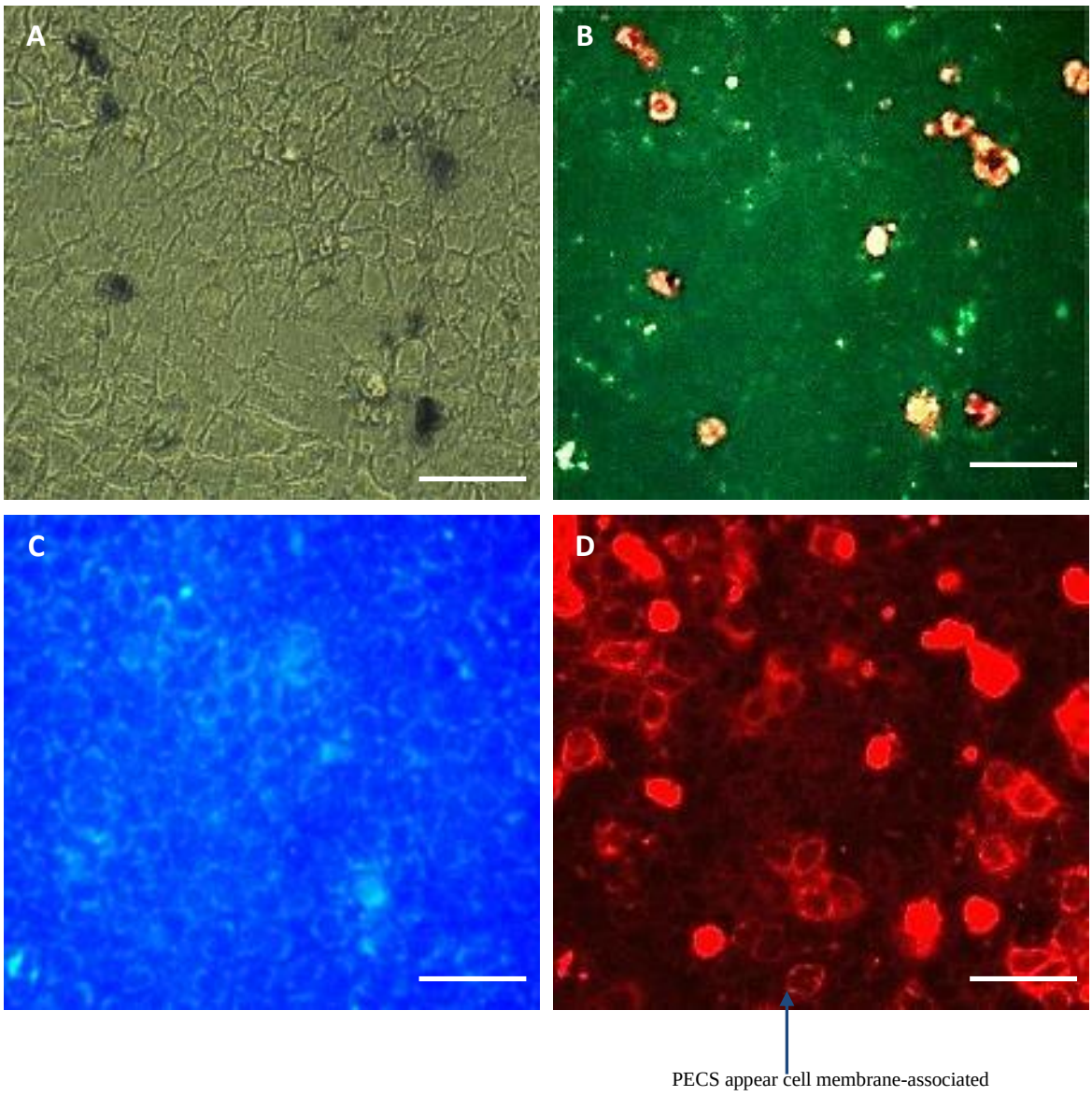

Fig. 70: Fluorescent microscopy images of Caco-2 cells treated with QPaa-NAC, insulin complexes viewed using A) brightfield B) RBITC/FITC combination filter C) FITC filter D) RBITC filter. Scale bar -50µm.

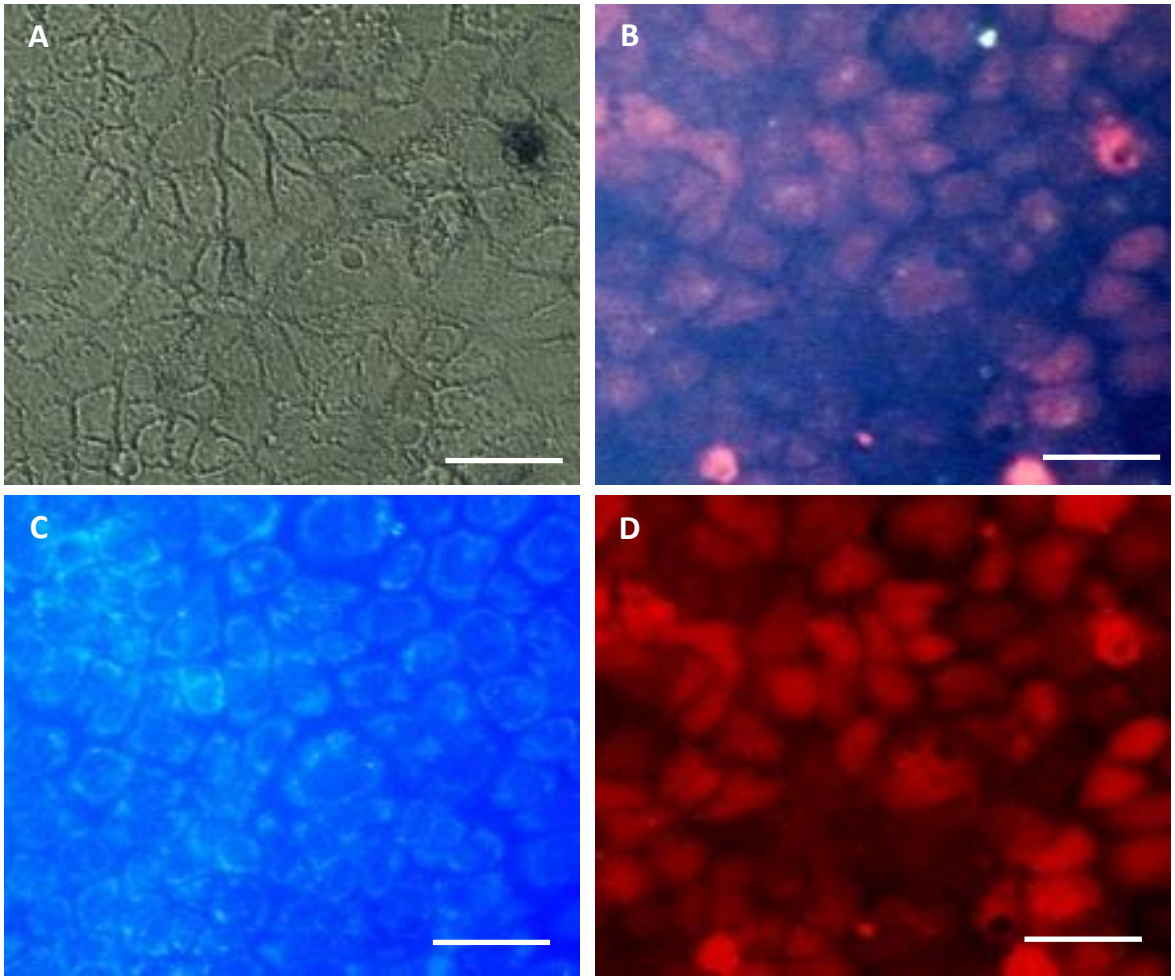

Fig. 71: Fluorescent microscopy images of Caco-2 cells treated with Paa-TBA, insulin complexes viewed using A) brightfield B) RBITC/FITC combination filter C) FITC filter D) RBITC filter. Scale bar -50µm.

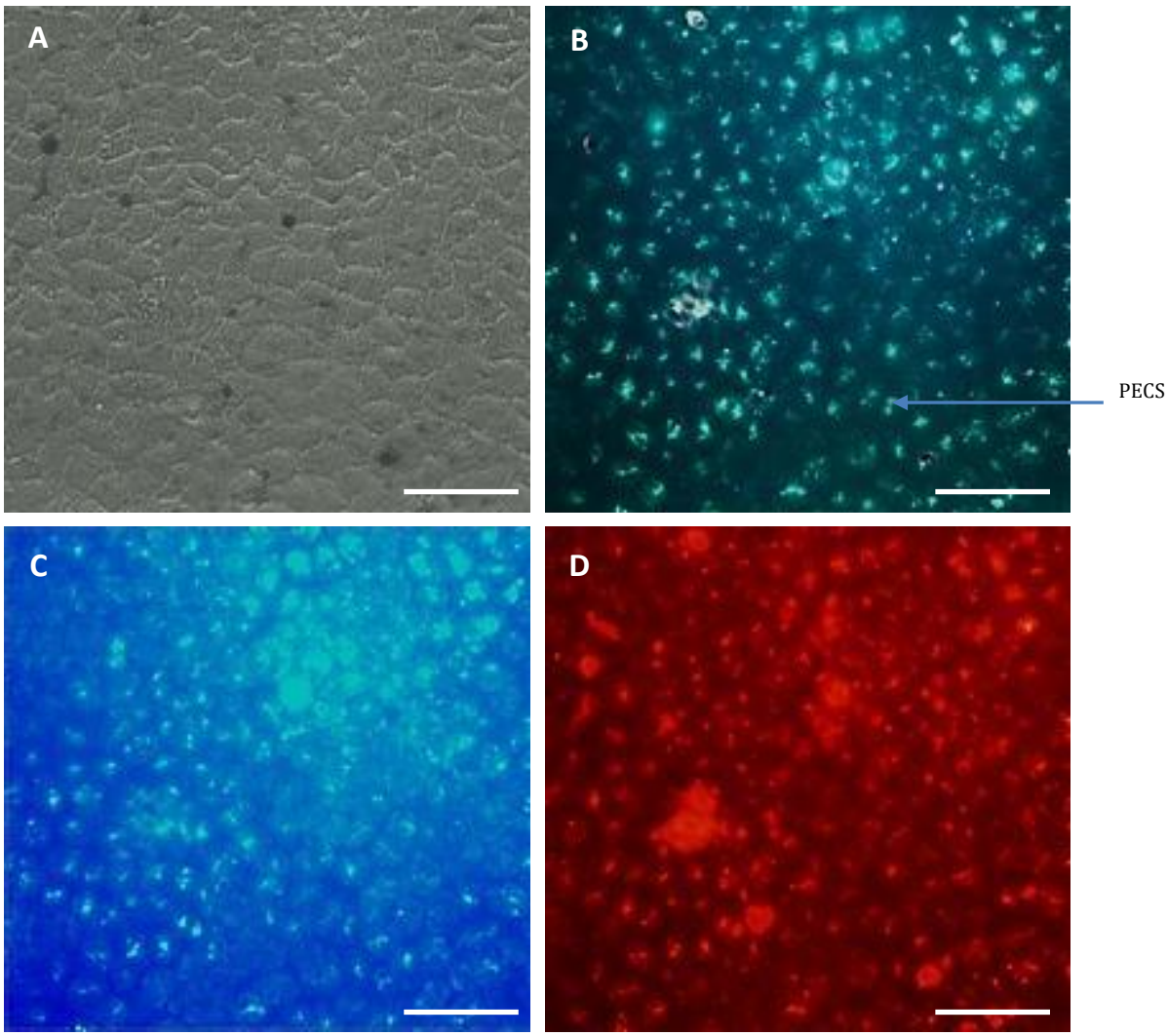

Fig. 72: Fluorescent microscopy images of Caco-2 cells treated with QPaa-TBA, insulin complexes viewed using A) brightfield B) RBITC/FITC combination filter C) FITC filter D) RBITC filter. Scale bar -50µm.

The uptake profile of different PECS by Caco-2 cells was observed to vary with the type of polymer used in the formulation . Results showed that only complexes prepared using QPaa and QPaa-TBA appear to be internalised by cells, with others only being associated with the cell membrane. Polymer, insulin colocalisation was confirmed using the RBITC/FITC combination filter by the appearance of numerous light yellow fluorescent spots within the cell layer as may be seen in figure 68A and 72A above . These spots also show up as red rhodamine and white FITC fluorescence under the separate RBITC and FITC filter respectively. For all results detailed in section 4.3.2.1, the brightfield image of the same section of the cell layer was also examined and imaged to determine cell viability

based on the appearance of the blue/black trypan blue stain which indicates non-viable cells. Cellular uptake of other complexes e.g. QPaa-NAC appeared to be more cell membrane-associated as the red RBITC staining was observed to be limited to the cell membrane area (figure 70D) .

Uptake of complexes was not instantaneous but was observed to be time-dependent, with the cell layer being observed to attain visible intracellular fluorescence (PEC uptake) between 1-4 hours. Figure 73 below shows the progression in QPaa, insulin PEC uptake from 0.5-4 hours as indicated by the increase in the level of fluorescence observed in the cell layer.

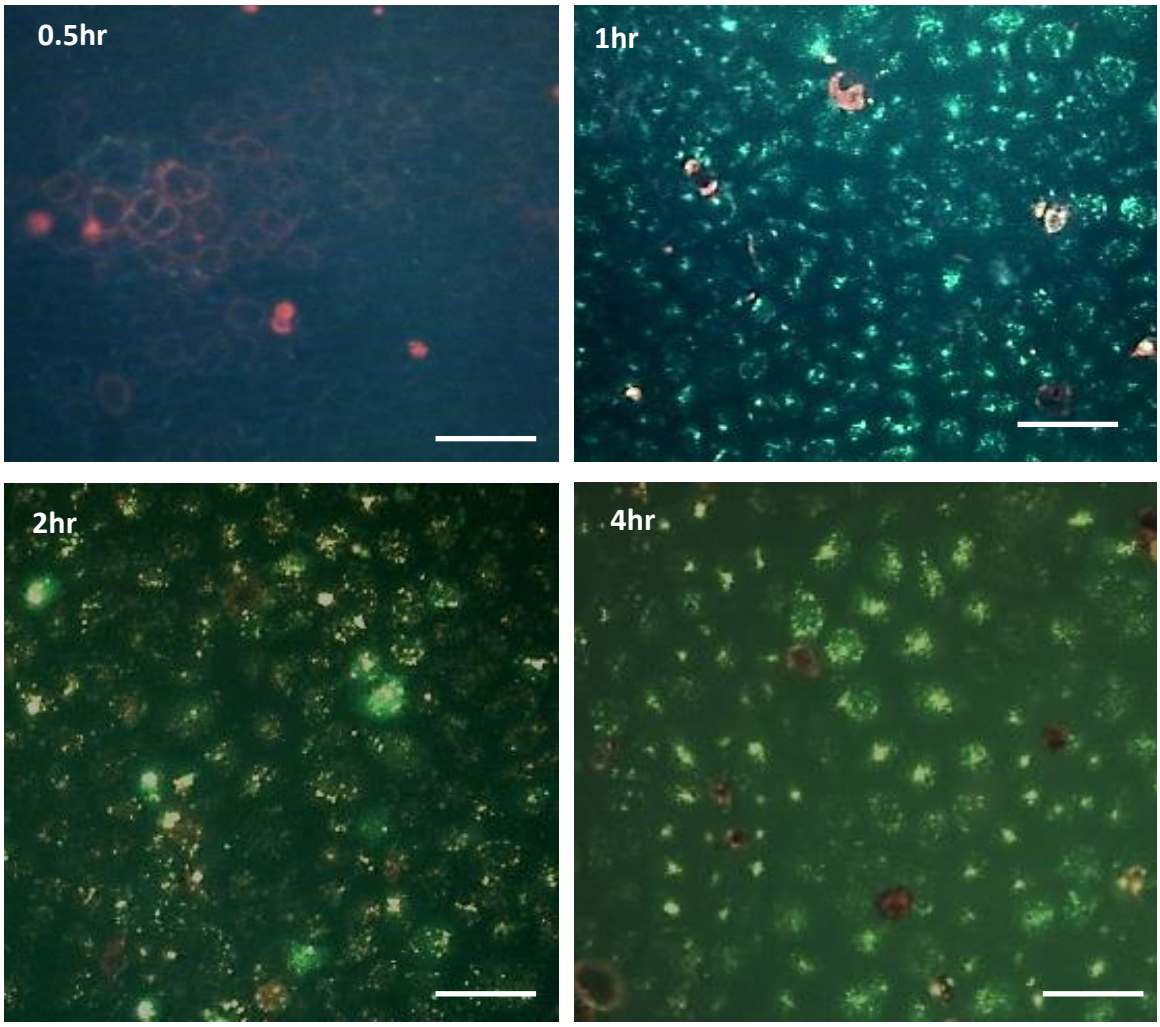

Fig.73: Fluorescent microscopy images of Caco-2 cells treated with QPaa, insulin complexes viewed using RBITC/FITC combination filter to show complex uptake at 0.5, 1, 2 and 4 hours. Scale bar -50µm.

Similar results were obtained between 0.5-2hrs for QPaa-TBA, insulin PECS (Figure 74 below).

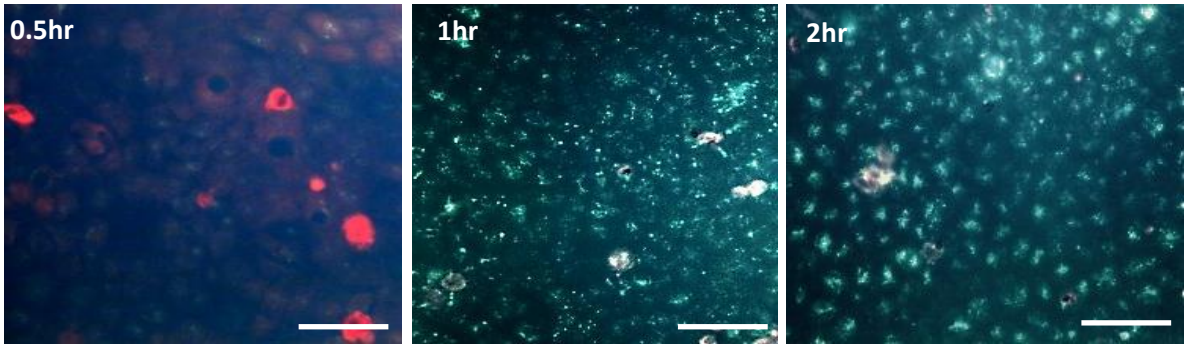

Fig. 74: Fluorescent microscopy images of Caco-2 cells treated with QPaa-TBA, insulin complexes viewed using RBITC/FITC combination filter to show complex uptake at 0.5, 1 and 2 hours. Scale bar -50µm.

The observed differences in the uptake profile of different complexes was also found to be unaffected by the variation between the concentration of quaternised and non-quaternised complexes used for the uptake experiments. Uptake experiments were repeated reducing the amount of QPaa and QPaa-TBA complexes used from 0.016:0.020 to 0.005:0063mgml^{-1} P: I mass ratio to match the concentration used for Paa and non-quaternised thiomers (figures 75 and 76 below).

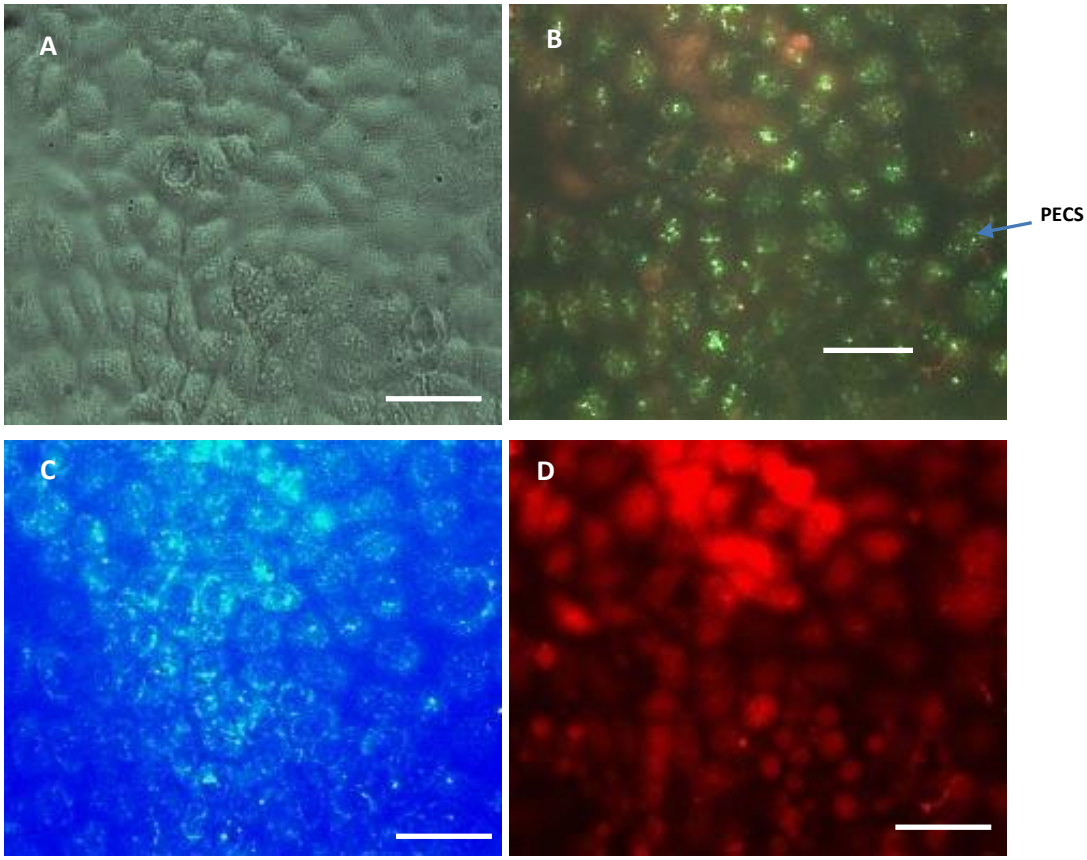

Fig. 75: Fluorescent microscopy images of Caco-2 cells treated with 0.005:0063mgml^{-1} (P: I mass ratio) of QPaa, insulin complexes viewed using A) brightfield B) RBITC/FITC combination filter C) FITC filter D) RBITC filter. Scale bar -50µm.

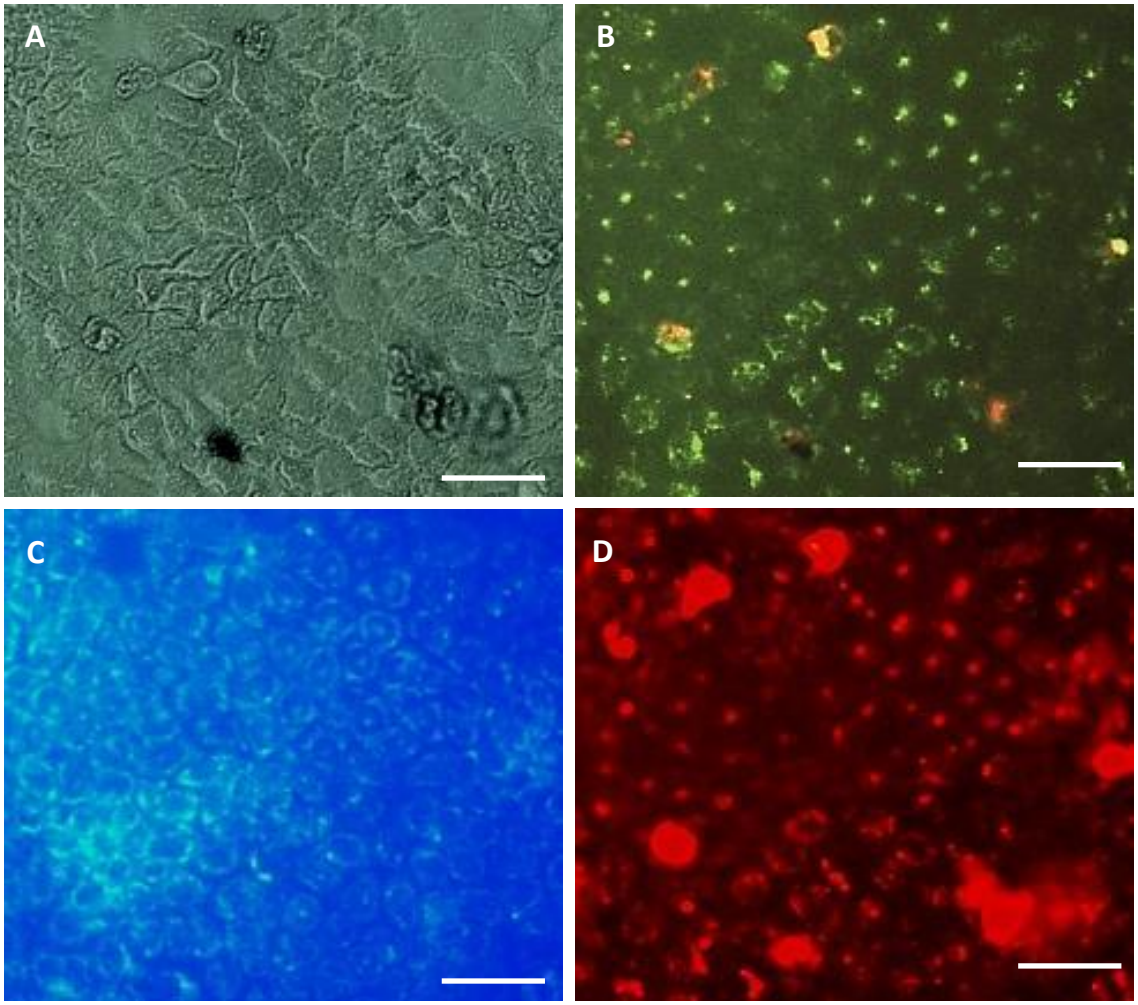

Fig. 76: Fluorescent microscopy images of Caco-2 cells treated with 0.005:0063 mgml^{-1} (P: I mass ratio) of QPaa-TBA, insulin complexes viewed using A) brightfield B) RBITC/FITC combination filter C) FITC filter D) RBITC filter. Scale bar -50µm.

QPaa and QPaa-TBA, insulin PECS were still observed to be taken up by cells even with the lower PEC concentration used (figures 75 and 76). This indicates that uptake of PECS was determined by differences in structure of the polymer used in the PEC formulation rather than the concentration of complexes used for the uptake experiment. The effect of increasing the amount of Paa and non-quaternised complexes used (to match that used for quaternised polymers) could not be evaluated because of the low IC_{50} of non-quaternised polymers.

Determining the precise location of complexes in the cell was carried out using DAPI nucleic acid stain to highlight the perinuclear region (figure 77).

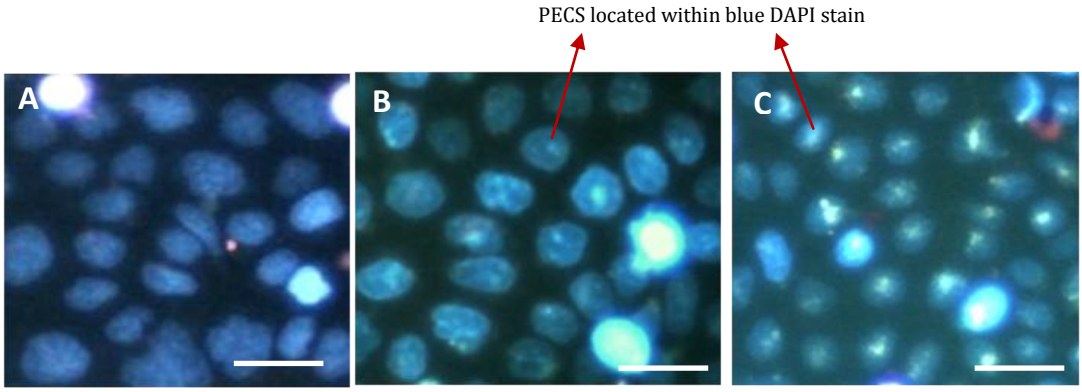

Fig. 77: Fluorescent microscopy images of Caco-2 cells treated with PECS and DAPI. A) Paa PECS on RBITC/FITC combination filter B) QPaa PECS on RBITC/FITC combination filter C) QPaa-TBA PECS on RBITC/FITC combination filter. Scale bar -50µm.

Results indicated that uptake of QPaa and QPaa-TBA complexes was mostly intracellular. For both QPaa and QPaa-TBA complex formulations, distinct regions of polymer, insulin colocalisation could be observed (as bright spots) under the blue DAPI stain, suggesting that these complexes were located within the cell cytoplasm. Paa complexes did not appear to be localised under the blue DAPI stain as can be seen in figure 77A above.

4.3.2.2. Polymer structure-cellular uptake relationship

The nature of the polymer used in PEC formulation was observed to play a vital role in determining the cellular uptake of the resultant complexes. Major factors that may affect the ability of the polymer to facilitate PEC uptake include structural composition of the polymer, charge density, molecular weight, polymer conformation as well as hydrophilic/lipophilic balance [201, 202, 203]. The properties of the original polymer may also be altered after complexation with insulin, resulting in a complex with different physicochemical properties from the parent molecules. Also, for thiomers which have disulphide bonds created during the thiolation process, due to the highly reducing conditions present within the cell cytoplasm these bonds may be reduced when the polymers are taken up into cells [204]. This implies that for thiomers like TBA conjugates which appear to be covalently bound to insulin on complexation (refer to section 3.3.1.5.), insulin may be released intracellularly from the PEC if it is taken up into cells and polymer-insulin disulphide bonds are reduced.

While most quaternised polymers (with the exception of QPaa-NAC complexes) were able to facilitate intracellular uptake of complexed insulin, complexes prepared from non-

quaternised polymers were all poorly taken up by Caco-2 cells, confirming the importance of the quaternary group in promoting the cellular uptake of PECS. Quaternisation enhanced the ability of Paa and Paa-TBA to promote the uptake of insulin complexes, but did not noticeably enhance the uptake profile of Paa-NAC. Cellular uptake of Paa-NAC/QPaa-NAC PECS may have been affected by substitution of cationic primary amine groups of Paa/QPaa with the uncharged amide bond of the thiol moiety resulting in products with a lower charge density when compared to their parent polymers. This can be seen in the relatively lower zeta potential of these NAC conjugates shown in table 2 in section 2.3.4. (35-37mV for NAC conjugates as compared to 40 -48mV for other polymers). Uptake of QPaa-TBA complexes by Caco-2 cells highlights that the cationic substructure of the amidine bond results in retention of cationic charge post-thiolation favouring intracellular uptake of these complexes. These results suggests that quaternisation and TBA-based thiolation which stabilise polycationic charge were fundamental in facilitating the uptake of QPaa and QPaa-TBA insulin complexes, emphasizing that interaction of polymers with anionic glycoproteins present in the cell membrane may play a key role in initiating the process of PEC uptake.

The uptake of polymer control solutions at the same concentration used for each PEC formulation was also assessed and results are shown in figures 78-80 below.

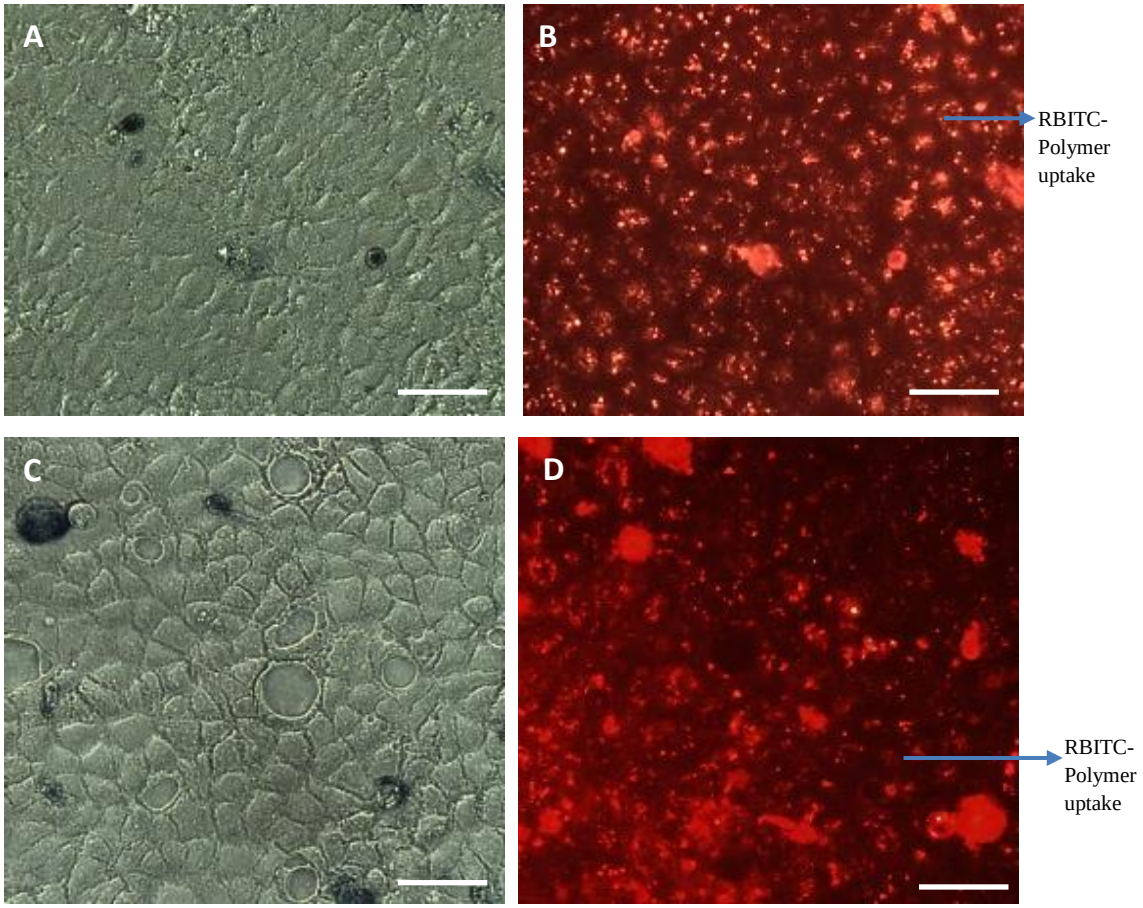

Fig. 78: Fluorescent microscopy images of Caco-2 cells treated with A) QPaa -brightfield B) QPaa-RBITC filter C) QPaa-TBA- brightfield D) QPaa-TBA-RBITC filter. Scale bar -50µm.

These results show that at the 2 hour timepoint, QPaa and QPaa-TBA solutions appear to be taken up intracellularly as with corresponding complexes.

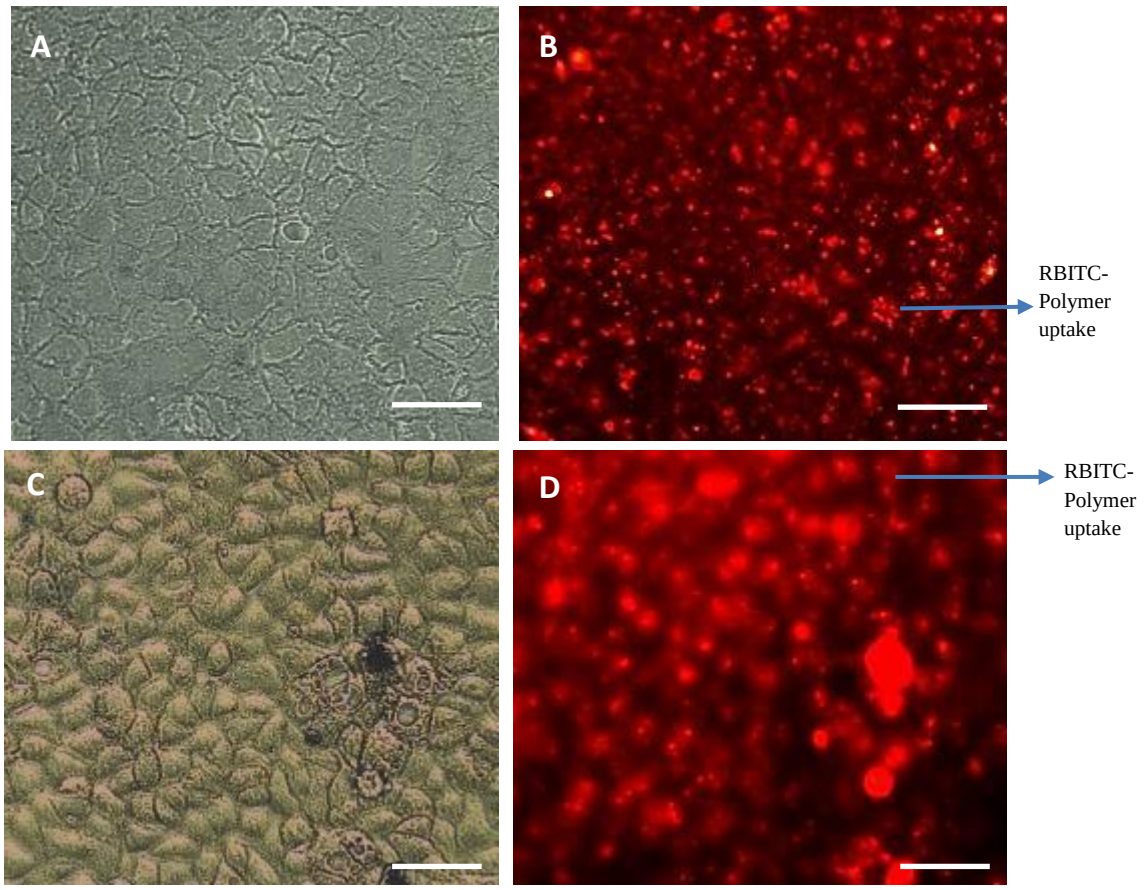

Fig. 79: Fluorescent microscopy images of Caco-2 cells treated with A) Paa -brightfield B) Paa-RBITC filter C) QPaa-NAC- brightfield D) QPaa-NAC-RBITC filter. Scale bar -50µm.

However unlike their PEC formulations, Paa and QPaa-NAC were also taken up by Caco-2 cells as a shown in figure 79 above. This implies that complexation of Paa and QPaa-NAC with insulin may have limited the ability of charged sites on these polymers to interact with the cell membrane and initiate uptake of PECS. This may be due to polymer, insulin complexation rendering charged sites on these polymers unavailable for interaction with the cell membrane. The PEC network may also create a steric barrier that prevents sites on the polymer from accessing compatible cell membrane components thereby limiting uptake [205]. Paa and QPaa-NAC polymers however show better uptake than Paa-TBA and Paa-NAC polymers shown in figure 80 below.

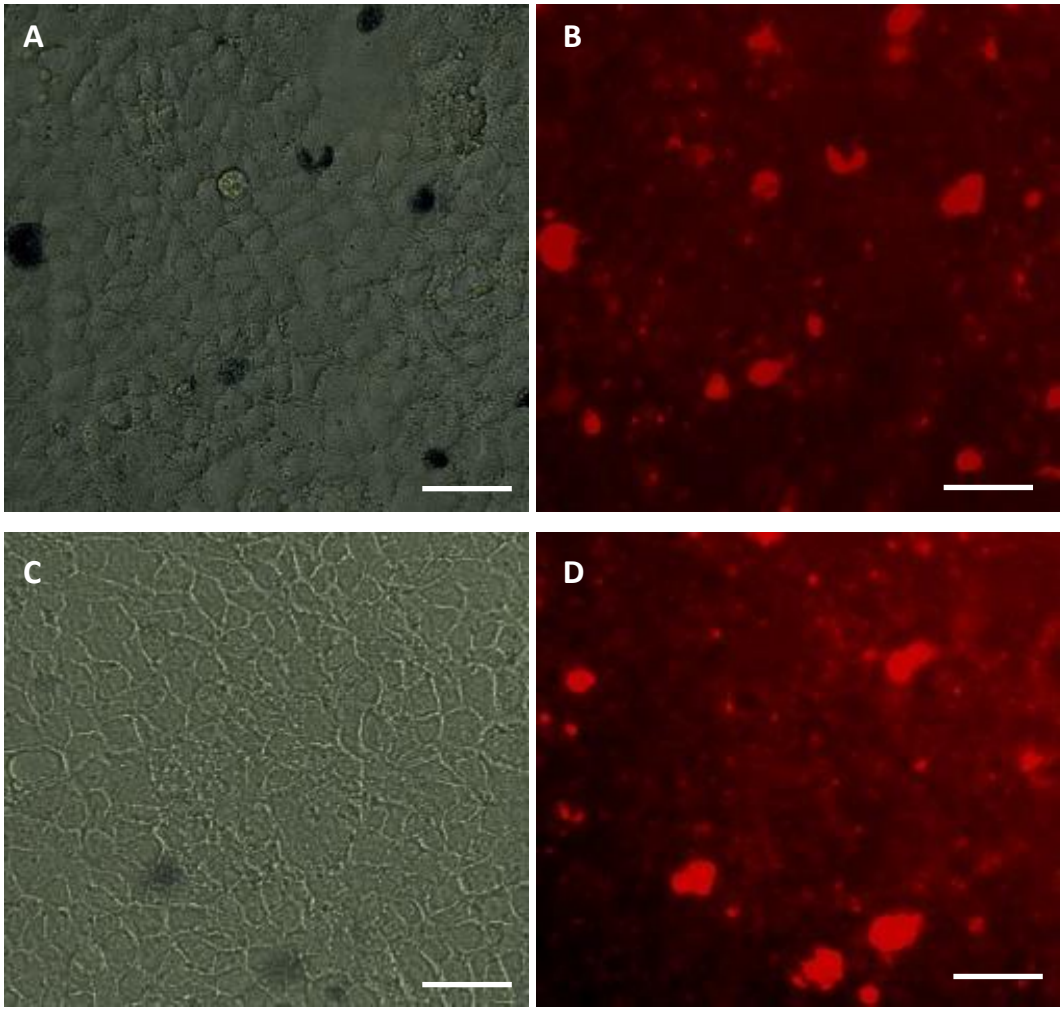

Fig. 80: Fluorescent microscopy images of Caco-2 cells treated with A) Paa – NAC-brightfield B) Paa-NAC-RBITC filter C) Paa-TBA- brightfield D) Paa-TBA-RBITC filter. Scale bar -50µm.

Uptake of Paa-TBA and Paa-NAC was observed to be minimal as was observed with their insulin PECS (figure 80). This is probably because unlike Paa which may benefit from the high charge density and reduced tendency for steric hindrance conferred by the presence of free unsubstituted primary amine groups enabling cellular uptake, interaction of thiolated Paa derivatives with cellular components may be sterically hindered. Also without the benefit of quaternisation, cellular interactions of thiolated Paa derivatives may be affected by fluctuations in the magnitude of their polycationic charge with change in the pH of the cellular environment.

Further work was carried out to quantify the uptake of these polymer control solutions. This was done by solubilising the cell layers with 2% SDS after treating the cells with

polymer solutions for 2 hours as in the uptake experiment in 4.3.2.2. above and measuring the fluorescence of the resultant lysate using fluorimetry. This experiment was carried out for only the following polymer solutions: Paa, QPaa and thiolated QPaa derivatives which were observed to have been taken up by the cells (figures 78 and 79 above). Thiolated Paa solutions were not analysed as their cellular uptake appeared to be poor. The results are detailed in Table 12 below.

Table 12: Percentage uptake of polymers by Caco-2 cells (n = 3; mean ± S.D.)

	Paa	**QPaa**	**QPaa-NAC**	**QPaa-TBA**
% Polymer uptake	12.55 ± 0.83	22.88 ± 1.77	26.48 ± 1.40	28.50 ± 0.38

The results of the quantification experiment shown in Table 12 above are consistent with the results of fluorescence microscopy, showing that all quaternised polymers were taken up by the cells and the percentage of quaternised polymers taken up approximately double the amount of Paa uptake. The analysis was however not done with polymer, insulin complexes due to difficulties in getting a good calibration curve for insulin-FITC with the fluorimeter. However fluorescence microscopy has shown polymer, insulin colocalisation was evident for QPaa and QPaa-TBA. The results of the quantification process also confirm fluorescence microscopy results which show cellular uptake of Paa and QPaa-NAC from their polymer solutions, even though uptake of their insulin PECS appeared to be negligible.

From the cellular uptake studies of polymers and their corresponding insulin PECS, only QPaa and QPaa-TBA showed the best uptake profile both as a simple polymer solution and in association with insulin as a PEC delivery system. Based on these findings, they appear to be the most suitable polymers for use in facilitating oral delivery of insulin and hence these polymers (QPaa and QPaa-TBA) would be the focus of further investigations detailed in the sections below.

4.3.2.3. IDENTIFYING MECHANISMS OF CELLULAR UPTAKE

To clarify the mechanisms involved in the cellular uptake of PECS into the cytoplasm, the cell layers were either pre-incubated for 2hours in calcium free EMEM to inhibit calcium-dependent uptake processes or 1hour in free insulin (3μgml^{-1}) to saturate insulin receptors

and down-regulate insulin receptors prior to treatment with PECS . The cell layers were examined by fluorescence microscopy to evaluate any changes in the uptake of QPaa and QPaa-TBA PECS in response to down-regulation of insulin receptors.

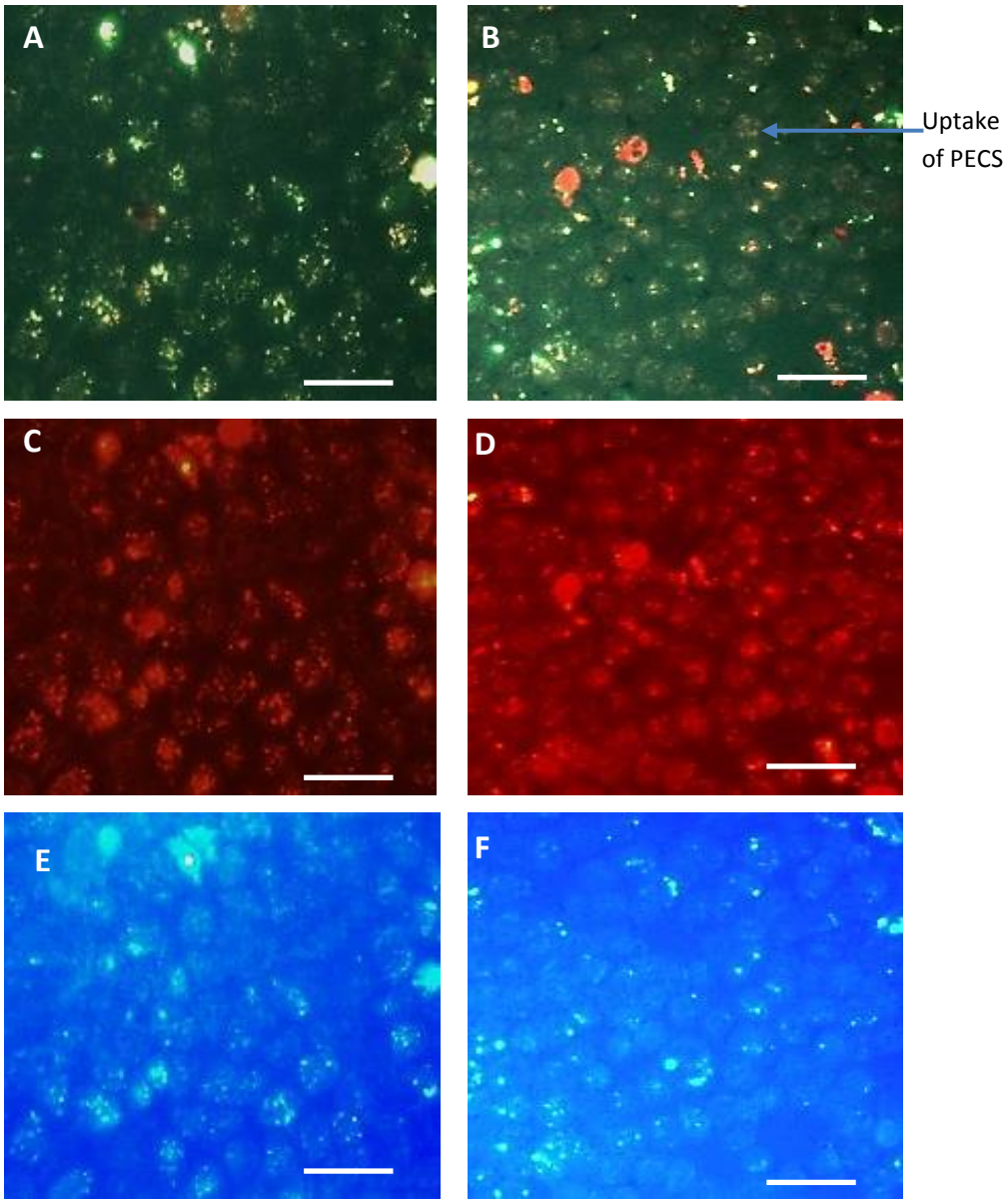

Fig. 81: Fluorescent microscopy images of Caco-2 cells post treatment with QPaa, insulin complexes in A) normal media using RBITC/FITC combination filter B) calcium-free media using RBITC/FITC combination filter C) normal media using RBITC filter D) calcium free media using RBITC filter E) normal media using FITC filter F) calcium free media using FITC filter. Scale bar -50µm.

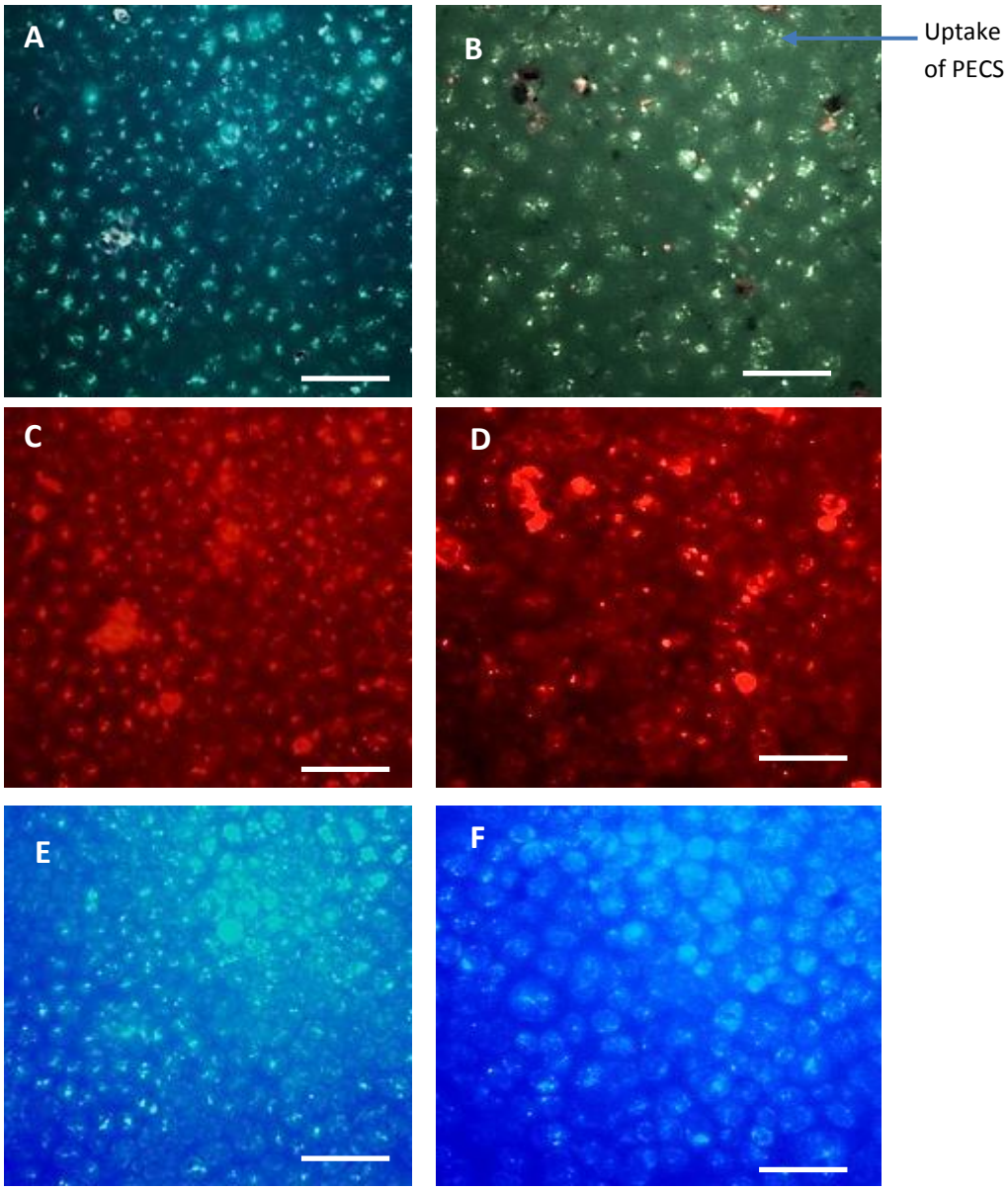

Fig. 82: Fluorescent microscopy images of Caco-2 cells post treatment with QPaa-TBA, insulin complexes in A) normal media using RBITC/FITC combination filter B) calcium-free media using RBITC/FITC combination filter C) normal media using RBITC filter D) calcium free media using RBITC filter E) normal media using FITC filter F) calcium free media using FITC filter. Scale bar -50µm.

Figures 81 and 82 above show the uptake of QPaa and QPaa-TBA, insulin PECS in normal and calcium-free media compared to those from normal uptake conditions (in FCS-free

supplemented EMEM). Cell layers incubated in calcium-free media before treatment with QPaa and QPaa-TBA, insulin PECS were observed to still show uptake similar to the results obtained in normal media as may be seen in figures 81 and 82 above. This may imply that the processes involved in the cellular uptake of both QPaa and QPaa-TBA insulin PECS appear to be independent of calcium-based mechanisms.

The results of the uptake experiments conducted with cells incubated with insulin prior to treatment with QPaa and QPaa-TBA, insulin PECS compared to that obtained from uptake experiments carried out in normal media is shown in figures 83 and 84 below.

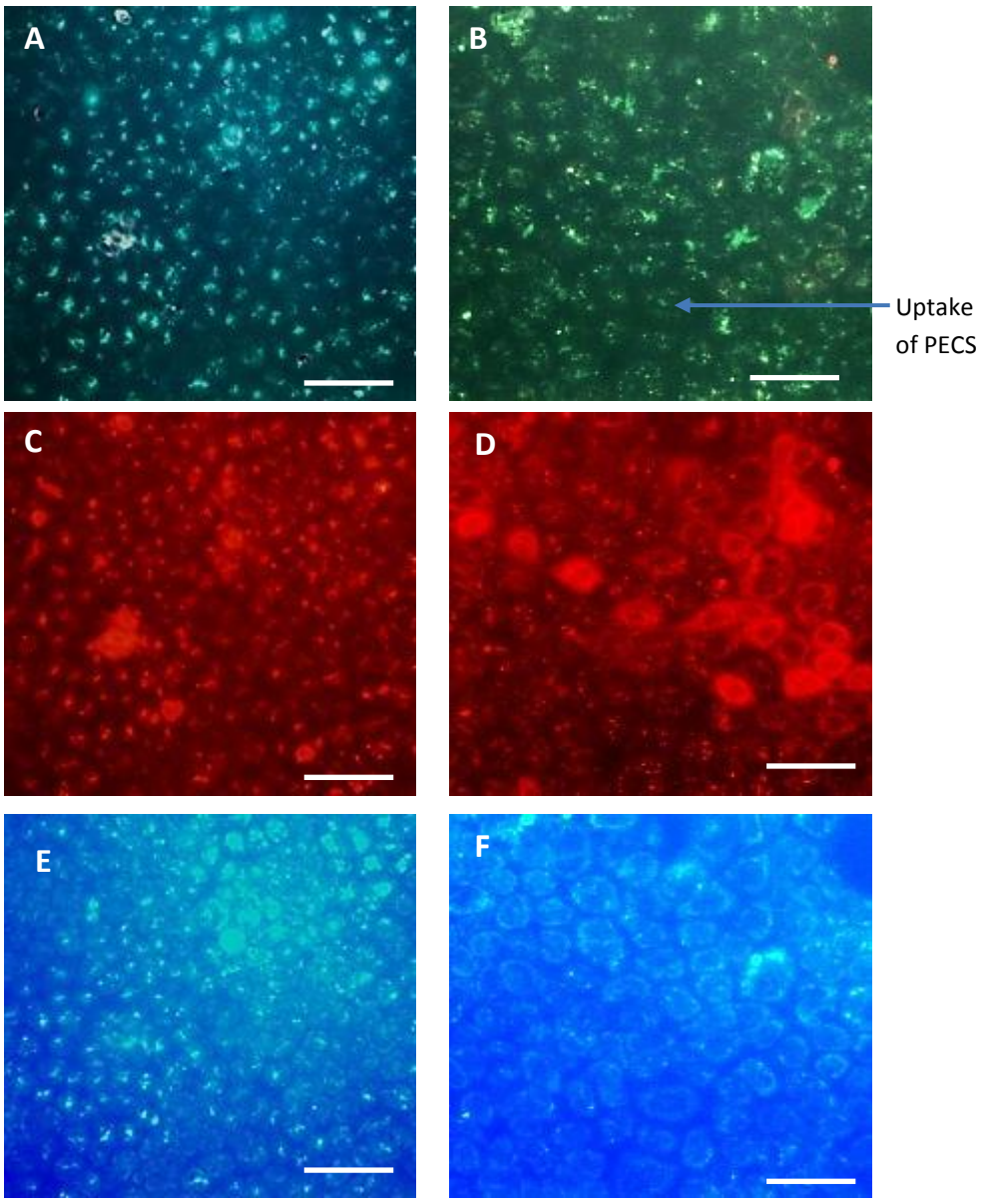

Fig. 83: Fluorescent microscopy images of Caco-2 cells treated with QPaa-TBA, insulin complexes where cells are pre-incubated with A) normal media on RBITC/FITC combination filter B) 3μgml^{-1} insulin on RBITC/FITC combination filter C) normal media on RBITC filter D) 3μgml^{-1} insulin on RBITC combination filter E) normal media on FITC filter F) 3μgml^{-1} insulin on FITC combination filter. Scale bar -50μm.

Pre-saturation of insulin receptors did not affect uptake of QPaa-TBA insulin complexes, which were still observed to be taken up regardless of the down-regulation of insulin receptors as shown in figure 83 above.

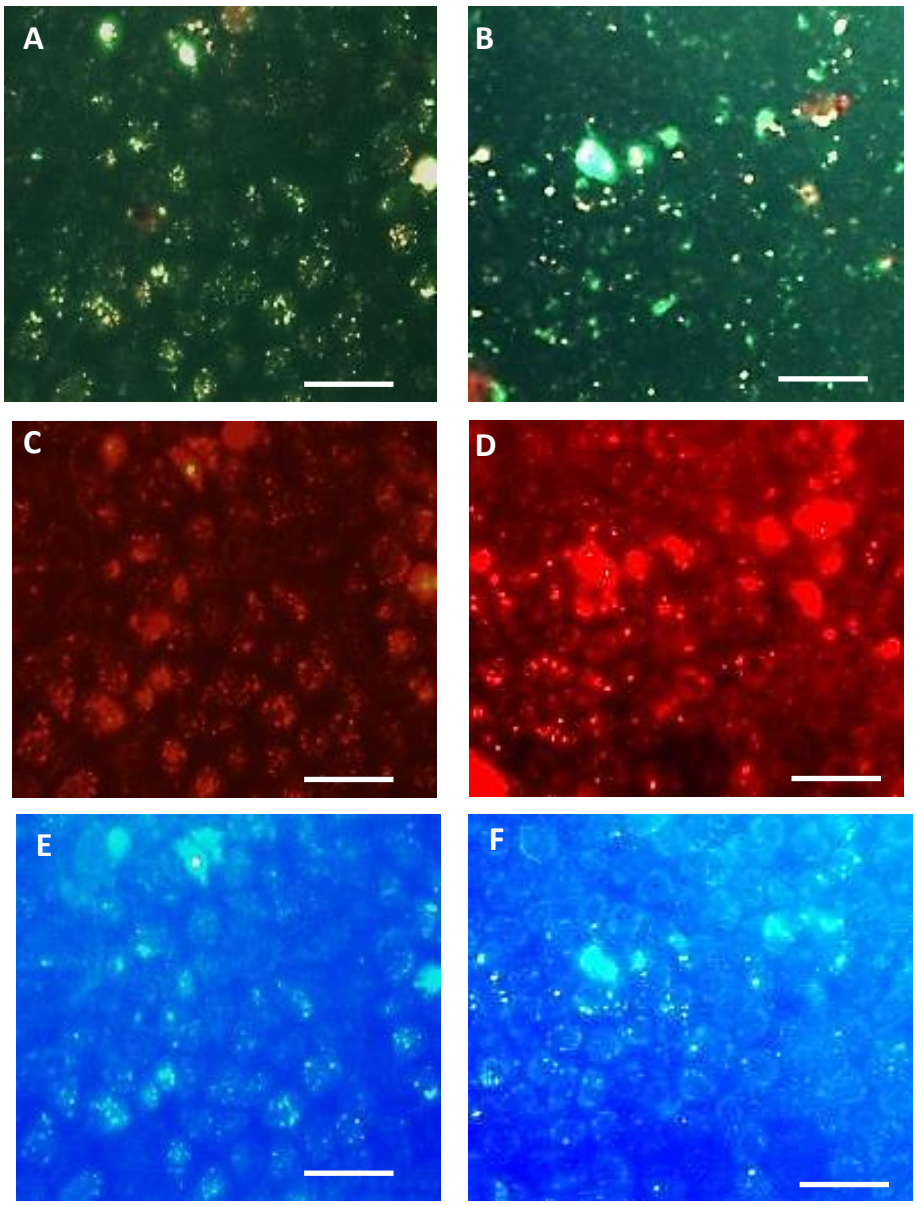

Fig. 84: Fluorescent microscopy images of Caco-2 cells treated with QPaa-TBA, insulin complexes where cells are pre-incubated with A) normal media on RBITC/FITC combination filter B) 3μgml^{-1} insulin on RBITC/FITC combination filter C) normal media on RBITC filter D) 3μgml^{-1} insulin on RBITC combination filter E) normal media on FITC filter F) 3μgml^{-1} insulin on FITC combination filter. Scale bar -50μm.

However, the pre-saturation process appeared to have a noticeable effect on the uptake of QPaa, insulin complexes as figure 84 above show that unlike figure 84 A) where the interior of the cells contains PECS figure 84 B) shows poor uptake of the fluorescent complexes

after pre-incubation with insulin. The images taken with the RBITC and FITC filters also confirm poor uptake of the formulation (figure 84D and 84F respectively), indicating that with QPaa, insulin complexes the uptake process appears to benefit from interaction of complexed insulin with receptors on the cells. Insulin receptors have been found to be present on the luminal surface of the small intestine [206] and several studies have confirmed active transcytosis of insulin through the intestinal epithelial cells [15, 207]. This highlights the active role the insulin receptor may play in the uptake of complexed insulin into the cells.

This implies that the conformation of QPaa allows for complexed insulin to be held on or near the surface of the PEC enabling the insulin molecule adequate interaction with its receptor. Some reviews have however stated that for interaction of insulin with its receptor to take place, insulin has to be in its monomeric state and that insulin hexamer and aggregate formation is promoted by changes in environmental pH *in vivo* [208]. Hence complexation of insulin with QPaa which possesses a quaternary group may limit pH-dependent changes of insulin from the monomeric to the hexameric state enhancing insulin receptor –mediated uptake. The stabilising effect of polymer-insulin linkage on insulin structure has been previously documented by other groups. Linkage of Vit B_{12} or PEG to the Lys-29 residue of insulin was reported to inhibit formation of the insulin hexamer, facilitating interaction of the insulin monomer with insulin receptors on the surface of the epithelial cells and contributing to a marked increase in the oral insulin bioavailability of these formulations [42, 209].

Further work is needed to clarify the exact mechanisms responsible for cellular uptake of these complexes. This may involve the use of specific inhibitors like sodium azide which inhibits metabolic processes as well as cytochalasin D and nocodazole, which are inhibitors of the endocytotic trafficking pathway [192]. Hypothesizing on the fate of the complexes in the cytosol, it is hoped that insulin PEC delivery systems will not only initiate uptake of the protein, but also facilitate transport of complexes across the cells (transcytosis). In an attempt to effect and control PEC uptake and transport in biological systems, future work may be directed at functionalization of PECS using receptor-recognisable ligands to facilitate active receptor-mediated transcytosis as opposed to relying on passive uptake mechanisms depicted in the present work. This concept is already being investigated by groups using the vit B_{12} ligand to produce receptor-mediated transcytosis of nanoparticles via the vit B_{12} receptors [95].

4.4. CONCLUSION

The biocompatibility of the parent polymer Paa was improved by both thiol and quaternary substitution, with quaternisation offering a more substantial improvement in biocompatibility profile than thiolation. Thiolation was observed to lower the IC_{50} of QPaa, although QPaa, Paa-NAC and QPaa-NAC appeared to be largely cytostatic rather than cytotoxic. Cellular uptake of polymer, insulin complexes was observed to be highly dependent on polymer structure, with QPaa and QPaa-TBA showing the best potential for facilitating intracellular uptake of complexed insulin by Caco-2 cells. Uptake of QPaa-TBA insulin PECS was found to be unaffected by both down-regulation of insulin receptors and inhibition of calcium-dependent uptake mechanisms. However, cellular uptake of QPaa, insulin PECS was independent of calcium-based mechanisms but appeared to be affected by down-regulation of insulin receptors.

5. GENERAL CONCLUSIONS

The report has shown that thiolation of Paa and QPaa was possible either through EDAC/NHS mediated coupling of the primary amine groups of the polymer to N-acetylcysteine creating a stable amide bond or by reacting the polymers with 2-iminothiolane which yields the 4-thiobutylamidine derivatives of the parent polymer. Estimation of free thiol and disulphide bond content of each thiolated derivative indicated that the efficiency of the EDAC/NHS mediated coupling process was relatively lower than thiolation using 2-iminothiolane. Subsequent complexation of Paa/QPaa and their thiolated derivatives with insulin in Tris buffer pH 7.4 yielded nano-sized, positively-charged insulin PECS at P: I mass ratios between 0.8-2:1. However, the optimal P: I mass ratio for all PEC formulations was observed to be 0.8 :1. The complexation process was also found to be less efficient at the higher insulin stock concentration of $2mgml^{-1}$ and in sodium hydroxide buffer pH 7.4. Complexation efficiency data showed that interaction of TBA-based thiomers with insulin in Tris buffer pH 7.4 affected HPLC analysis of complexed insulin which may suggest that the conformation of the protein has been altered. TEM images showed that most PECS were in form of bilayered nanovessicular structures or conventional single-layered nanoparticles.

Assessment of the ability of QPaa, QPaa-NAC and Paa-NAC PECS to shield complexed insulin from proteolytic degradation by trypsin, α-chymotrypsin and pepsin showed that all formulations are effective against tryptic degradation with about 30% more undegraded insulin being recovered from complexes than an equivalent sample of free insulin. QPaa-NAC complexes were observed to offer the best protection of complexed insulin from the effects of α-chymotrypsin containing approximately 30% more undegraded insulin than the insulin control solution after 4 hours. PECS were unable to protect insulin from the effects of pepsin. Evaluation of the mucoadhesive ability of the polymers and their corresponding insulin PECS indicated that complexation of the polymers with insulin did not have any effect on their mucoadhesive properties. Quaternisation enhanced the mucoadhesive properties of Paa, although thiolated Paa derivatives (Paa-NAC and Paa-TBA) exhibited the highest mucin adsorption capacity. However, thiolation of QPaa did not yield substantial improvements in mucin adsorption capacity.

Cytotoxicity assays carried out on Paa, QPaa and their thiolated derivatives indicated that an improvement in the biocompatibility profile of Paa was obtained due to thiolation and quaternisation. Qpaa was found to be largely cytostatic within the concentration of 0.001-

4mgml^{-1}. However thiolation of QPaa was found to make the polymer less biocompatible. TBA conjugates were found to be more cytotoxic than their NAC-based counterparts probably as a result of the protonated amidine group substructure. Amongst the novel thiomers synthesized, QPaa-NAC was found to have the best biocompatibility profile. Cellular uptake studies showed that QPaa and QPaa-TBA insulin complexes showed the best uptake profile, with both PEC formulations being taken up intracellularly by Caco-2 cells within 1-2hours. Uptake of both QPaa and QPaa-TBA complexes was found to be independent of calcium-based uptake mechanisms while uptake of QPaa complexes was affected by down-regulation of insulin receptors.

Therefore future work would be focused on further development of PEC formulations prepared from QPaa and QPaa-TBA , which showed the most promising potential in terms of cellular uptake of complexed insulin. For QPaa-TBA, insulin PECS preliminary investigations would be needed to ascertain that insulin complexed to the polymer is pharmacologically active. This may involve *in-vivo* studies to evaluate the physiological response (i.e. induction of hypoglycemia) obtained on parenteral administration of QPaa-TBA, insulin PEC formulations as compared to an equivalent insulin standard. Also, the fate of complexes after being taken up by cells would be investigated. This would help clarify the timing and process of insulin release from the PEC and identify major cellular pathways/ mechanisms that may be involved in the PEC uptake process. Other areas that would be incorporated in future studies include investigating the ability of the thiomer, QPaa-TBA to chelate metal ions required by proteases thereby offering enhanced enzymatic protection *in-vivo* and specific functionalisation of PECS with receptor-recognisable ligands like Vit B_{12} to facilitate the process of active receptor-mediated uptake. Finally, future studies may also look at further modification of polymer structure by the attachment of hydrophobic grafts to the backbone of quaternised thiomers and evaluation of the performance of the new construct in terms of facilitating oral insulin delivery.

The results obtained so far indicate that these Paa-based polymer, insulin PECS specifically QPaa and QPaa-TBA formulations showed considerable potential in promoting the delivery of insulin through the oral route.

REFERENCES

1. Gale, E.M. and Anderson, J.V. (2002) Diabetes mellitus and other disorders of metabolism. In Kumar, P. and Clark, M. [Ed] Clinical Medecine. W.B. Saunders, Toronto, 22-54.
2. Baxter, M.A. (1994) Diabetes mellitus. In Baxter, M. and White, D.A. [Ed] Hormones and Metabolic Control. Edward Arnold, London, 79-92.
3. Wong, W. T. (2010) Design of oral insulin delivery systems. Journal of Drug Targeting, 18(2), 79-92.
4. Belchetz, P. and Hammond, P. (2004) Mosby's Color Atlas and Text of Diabetes and Endocrinology. Spain. Elselvier limited.
5. Carino, G.P. and Mathiowitz, E. (1999) Oral insulin delivery. Advanced Drug Delivery Reviews, 35, 249-257.
6. Dhawan, S., Chopra, S., Kapil, R. and Kapoor, D. (2009) Novel approaches for oral insulin delivery. Pharmaceutical Technology, 33(7).
7. Ehud Arbit, M.D and Kidron, M. (2009) Oral insulin: The rationale for this approach and current developments. Journal of Diabetes Science and Technology, 3(3), 562-567.
8. Narayani, R. (2001) Oral delivery of insulin-making needles needless. Trends in Biomaterials and Artificial Organs, 15 (1), 12-16.
9. Satake, S., Moore, M.C., Igawa, K., Converse, M., Farmer, B., Neal D.W. and Cherrington A.D. (2002) Direct and indirect effects of insulin on glucose uptake and storage by the liver. Diabetes, 51(6), 1663-1671.
10. Bai, J.P.F. and Chang, L.L. (1995) Transepithelial transport of insulin: Insulin degradation by insulin-degrading enzyme in small intestinal epithelium. Pharmaceutical Research, 12, 1171-1175.
11. Soltero, R. and Ekwuribe, N. (2001) The oral delivery of protein and peptide drugs. Innovations in Pharmaceutical Technology, 1, 106-110.
12. Duckworth, W.C. (1988) Insulin degradation: mechanisms, products and significance. Endocrine Reviews, 9(3), 319-345.
13. Ashford, M. (2002) The gastrointestinal tract - physiology and drug absorption. In: M.E. Aulton [2nd Ed]. Pharmaceutics: The science of dosage form design. Churchill livingstone, Edinburgh, 217-233.
14. Morishita, M. and Peppas, A.N. (2006) Is the oral route possible for peptide and protein drug delivery? Drug Discovery Today, 11, 905-910.

15. Bendayan, M., Ziv, E., Gingras, D., Ben-Sasson, R., Bar-on, H. and Kidron, M. (1994) Biochemical and morpho-cytochemical evidence for the intestinal absorption of insulin in control and diabetic rats. Comparison between the effectiveness of duodenal and colon mucosa. Diabetologia, 37, 119-126.
16. Pauletti, G., Gangwar, S., Knipp, G.T., Nerurkar, M.M., Okuma, F.W., Tamura, K., Siahaan, T.J. and Borchardt, R.T.(1996) Structural requirements for intestinal absorption of peptide drugs. Journal of Controlled Release, 41, 3-17.
17. Fix, A.J. (1996) Oral controlled release technology for peptides: status and future prospects. Pharmaceutical Research, 13(12), 1760-1764.
18. Agarwal, V. and Khan, M.A. (2001) Current status of the oral delivery of insulin. Pharmaceutical Technology, 76-90.
19. Ziv, E., Lior, O. and Kidron, M (1987) Absorption of protein via the intestinal walls: A quantitative model. Biochemistry and Pharmacology, 39(7), 1035-1039.
20. Yamamoto, A., Taniguchi, T., Rikyuu, K., Tsuji, T., Fujita, T., Murakami, M. and Muranishiet, S. (1994) Effects of various protease inhibitors on the intestinal absorption and degradation of insulin in rats. Pharmaceutical Research, 11(10), 1496-1500.
21. Narayani, R. and Panduruanga Rao, K. (1995) Hypoglycemic effect of gelatin microspheres with entrapped insulin and protease inhibitor in normal and diabetic rats. Drug Delivery, 2, 29-38.
22. Dileep, K.J., Rowsen, M. L. and Sharma, C.P. (1998) Modulation of insulin release from chitosan/alginate microspheres. Trends in Biomaterials and Artificial Organs, 12(2), 42-46.
23. Lee, V.H.L. (1988) Enzymatic barriers to peptide and protein absorption. Critical Review of Therapeutic Drug Carrier Systems, 5, 69-97.
24. Rao, S. and Ritschel (1995) Colonic delivery of small peptides. STP Pharma Sciences, 5, 19-29.
25. Shah, R.B., Ahsan, F. and Khan, M.A. (2002) Oral delivery of proteins: Progress and prognostication. Critical Review of Therapeutic Drug Carrier Systems, 19, 135-169.
26. Mesiha, M., Plakogiannis, F. and Vejosoth, S. (1994) Enhanced oral absorption of insulin from desolvated fatty acid-sodium glycocholate emulsions. International Journal of Pharmaceutics. 111,213-216.
27. Li, C.L. and Deng, Y.J (2004) Oil-based formulations for oral delivery of insulin. Journal of Pharmaceutical Pharmacology, 56(9), 1101-1107.

28. Eaimtrakarn, S., Ramaprasad, Y.V., Konishi T., Yoshikawa Y., Shibata N., Takada K. and Ohno, T. (2002) Absorption-enhancing effect of labrasol on the intestinal absorption of insulin in rats. Journal of Drug Targeting, 10(3), 255-260.
29. Fasano, A. and Uzzau, S. (1997) Modulation of intestinal tight junctions by zona occludens toxin permits enteral absorption of insulin and other macromolecules in an animal model. Journal of Clinical Investigations, 99, 1158-1164.
30. Kotze, A.F., Leuben, H.L., de Leeuw, B.J., de Boer, B.G., Verhoef, J.C. and Junginger, H.E. (1997b) N-Trimethyl chitosan chloride as a potential absorption enhancer across mucosal surfaces: in-vitro evaluation in intestinal epithelial cells (Caco-2). Pharmaceutical Research, 14(9), 1197-1202.
31. Bayat, A., Dorkoosh, F.A., Dehpour, A.R., Moezi, L., Larijani, B., Junginger, H.E. and Rafiee-Tehrani, M. (2008) Nanoparticles of quarternized chitosan as a carrier for colon delivery of insulin: ex vivo and in vivo studies. International Journal of Pharmaceutics, 356(1-2), 259-266.
32. De Meyts, P., Van Obberghen, E., Roth, J., Wollmer, A., and Brandenburg, D. (1978) Mapping of the residues responsible for the negative cooperativity of the receptor-binding region of insulin. Nature, 273, 504-509.
33. Baker, E. N., Blundell, T. L., Cutfield, J. F., Cutfield, M., Dodson, E. J., Dodson, G. G., Hodgkin , D.C.M., Hubbard, R. E., Isaacs, N. W., Reynolds, C. D., Sakabe, K., Sakabe, N. and Vijayan, N. M. (1988) *The structure of 2zn pig insulin crystals at 1.5a resolution.* In: Philosophical Transactions of the Royal Society. Biological Sciences, 319 (1195). 369-456.
34. Thurow, H. and Geisen, K. (1984) Stabilization of dissolved proteins against denaturation at hydrophobic surfaces. Diabetologia, 27, 212-218.
35. Sato, S., Ebert, C.D. and Kim, S.W. (1983) Prevention of insulin self-association and surface adsorption. Journal of Pharmaceutical Sciences, 72, 228-232.
36. Hovgaard, L., Harvey, J., Dana, E.W. and Kim, S.W. (1996) Stabilization of insulin by alkylmaltosides. B. Oral absorption in vivo in rats. International Journal of Pharmaceutics, 132, 115-121.
37. Hou, Z., Zhang, Z., Zhang, C. and Huang, M (2004) Use of natural plant exudates (Sanguis Draxonis) for sustained oral insulin delivery with dramatic reduction of glycaemic effects in diabetic rats. Journal of Controlled Release, 97, 467-475.

38. Jatzkewitz, H. (1966) Peptamin (glycyl-L-leucyl-mescaline) bound to blood plasma expander (polyvinylpyrrolidone) as anew depot form of a biologically active primary amine (mescaline). Zeitschrift fur Natursforschung, 10b, 27.
39. Abuchowski, A. and Davis, F.F. (1979) Preparation and properties of polyethylene glycol-trypsin adducts. Biochimica et Biophysica Acta, 578, 1, 41-46.
40. Calceti, P., **Salmaso, S., Walker, G. and Bernkop-Schnürch, A.** (2004) Development and in vivo evaluation of an oral insulin-PEG delivery system. European Journal of Pharmaceutical Sciences, 22, 315-323.
41. Basu, A., Yang.K., Wang, M., Liu,S., Chintala, R., Palm, T., Zhao, H., Peng, P., Wu, D., Zhang, Z., Hua, J., Hsieh, M., Zhou, J., Petti, G., Li, X., Janjua, A., Mendez, M., Liu,J., Clifford, L., Zhihua, Z., Mary, M., Virna, B., Manickam V. and David F. (2006) Structure-function engineering of interferon-beta-1b for improving stability, solubility, potency, immunogenicity and pharmacokinetic properties by site-selective mono-PEGylation. Bioconjugate Chemistry, 17, 618-630.
42. Still, J.G. (2002) Development of oral insulin: progress and current status. Diabetes Metabolism Research and Reviews, 18(1), 29-37.
43. Russell-Jones, G.J. (2001) The potential use of receptor-mediated endocytosis for oral drug delivery. Advanced Drug Delivery Reviews, 46, 59-73.
44. Shen, W. (2003) Oral peptide and protein delivery: unfulfilled promises? Drug Discovery Today, 8(14).
45. Wang, J., Shen, D. and Shen, W.C. (1997) Oral delivery of insulin-transferrin conjugate in streptozocin-treated CF/1 mice. Pharmaceutical Research Supplement, 14, 469.
46. Shah, D. and Shen, W.C. (1996) Transcellular delivery of an insulin-transferrin conjugate in enterocyte-like Caco-2 cells. Journal of Pharmaceutical Sciences, 85(12), 1306-1311.
47. Azari, P.R. and Feeney, R.E. (1958) Resistance of metal complexes of conalbulmin and transferrin to proteolysis and thermal denaturation. Journal of Biological Chemistry, 232, 293-302.
48. Banerjee, D., Flanagan, P.R., Cluett, J. and Valberg, L.S. (1986) Transferrin receptors in the human gastrointestinal tract. Gastroenterology, 91, 861-869.
49. Xia, C.Q., Wang, J. and Shen, W.C. (2000) Hypoglycaemic effect of insulin-transferrin conjugate in streptozocin-induced diabetic rats. The Journal of Pharmacology and Experimental Therapeutics, 295, 594-600.

50. Wang, J., Shen, D.,Taub, M.E. and Shen, W.C. (1992) Brefeldin A enhances receptor-mediated transcytosis of transferrin in filter-grown Madin-Darby canin kidney cells. Journal of Biological Chemistry, 267(19), 13446-13450.
51. Xia, C.Q. and Shen, W.C. (2001) Tryphostin-8 enhances transferrin receptor-mediated transcytosis in Caco-2 cells and increases hypoglycemic effect of orally administered insulin-transferrin conjugate in diabetic rats. Pharmaceutical Research, 18(2), 191-195.
52. Vaikunth, C. and Jindrich, K. (2006) Polymer-drug conjugates. In I. F. Uchegbu and A.G. Schatzlein [Ed] Polymers in drug delivery. Taylor and Francis group, Boca Raton, 156-182.
53. Deshayes, S., Morris, M.C., Divita, G. and Heitz, F. (2005) Cell-penetrating peptides: tools for intracellular delivery of therapeutics. Cellular and Molecular Life Sciences, 62, 1839-1849.
54. Schwarz, S.R. and Dowdy, S.F. (2000) In vivo protein transduction: intracellular delivery of biologically active proteins, compounds and DNA. Trends in Pharmacological Sciences, 21, 45-48.
55. Trehin, R. and Merkle, H.P. (2004) Chances and pitfalls of cell penetrating peptides for cellular drug delivery. European Journal of Pharmaceutical Biopharmaceutics, 58, 209-223.
56. Zorko, M. and Langel, U. (2005) Cell-penetrating peptides: mechanisms and kinetics of cargo delivery. Advanced Drug Delivery Reviews, 57, 529-545.
57. Liang, J.F. and Yang, V.C. (2005) Insulin-cell penetrating peptide hybrids with improved intestinal absorption efficiency. Biochemical and Biophysical Research Communications.
58. Derossi, D., Chassaing, G. and Prochiantz, A. (1998) Trojan peptides: the penetratin system for intracellular delivery. Trends in Cell Biology, 8, 84-87.
59. Schwarz, S.R., Dowdy, S.F., Ho, A. and Vocero-Akbani, A. (1999) In vivo protein transduction: delivery of a biologically active protein. Science, 285, 1569-1572.
60. Wang, J., Shen, W.C., Chow, D. and Heiati, H. (2003) Reversible lipidization for the oral delivery of salmon calcitonin. Journal of Controlled Release, 88, 369-380.
61. Qadri, B. and Hoffman, A. (2008) Eligen insulin – a system for the oral delivery of insulin for diabetes. The Investigations Drug Journal, 11(6), 433-441.
62. Yin, L., Fei, L., Cui, F., Tang, C. and Yin, C. (2007) Superporous hydrogels containing poly(acrylic acid-co-acrylamide)/O-carboxymethyl chitosan interpenetrating polymer networks. Biomaterials, 28, 1258-1266.

63. Rahamatullah, S., Singh, R.T., Garland, M.J., Woolfson, D.A. and Donnelly, R.F (2011) Mucoadhesive drug delivery systems. Journal of Pharmacy and Bioallied Sciences, 3(1), 89-100.
64. McBain, J. W and Hopkins D. G. (1925) On adhesives and adhesive action. Journal of Physical Chemistry. 29:188–204.
65. Pritchard W. H. (1970) Aspects of adhesion 6. In: Alder D, editor. 3rd edition ed. London: London University Press. pp. II–23.
66. Deraguin, B.V., Smilga, V. P. And London, M. (1969) Adhesion: Fundamentals and Practice.
67. Jimenez-Castellanos, M. R, Zia, H. And Rhodes, C. T. (1993) Mucoadhesive drug delivery systems. Drug Development and Industrial Pharmacy, 19:143–94.
68. Duchene, D. , Touchard, F. and Peppas, N. A. (1988) Pharmaceutical and medical aspects of bioadhesive systems for drug administration. Drug Development and Industrial Pharm.acy, 14:283–18.
69. Ahuja, A., Khar, R. K. and Ali, J. (1997) Mucoadhesive drug delivery systems. Drug Development and Industrial Pharmacy, 23:489–515.
70. Huntsberger, J. R. (1967) Mechanisms of adhesion. Journal of Pain Technology, 39:199–211.
71. Junginger, H.E. (1990) Bioadhesive polymer systems for peptide delivery. Acta pharmaceutical Technology, 36, 25-37.
72. Park, K. and Robinson, J.R. (1984) Bioadhesive polymers as platforms for oral-controlled drug delivery: method to study bioadhesion. International Journal of Pharmaceutics, 19, 107.
73. Huang, Y., Efremova, N., Peppas, N.A. and Leckband, D.E. (2002) Direct measurement of interactions between tethered PEG chains and adsorbed mucin layers. Langmuir, 18, 836-845.
74. Albrecht, K. and Bernkop-Schnurch, A. (2007) Thiomers: forms, functions and applications to nanomedicine. Nanomedicine 2(1), 41-50.
75. Mourya, V.K. and Inamdar, N.N. (2008) Chitosan-modifications and applications: opportunities galore. Reactive and Functional Polymers, 68, 1013-1051.
76. Bernkop-Schnurch, A., Walker, G. and Zarti, H. (2001) Thiolation of polycarbophil enhances its inhibition of intestinal brush border membrane bound aminopeptidase N. Journal of Pharmaceutical Science, 90, 1907-1914.

77. Whitehead, K., Shen, Z. and Mitragotri, S. (2004) Oral delivery of macromolecules using intestinal patches: application for insulin delivery. Journal of Controlled Release, 98, 37-45.
78. Lehr, C. (2000) Lectin-mediated drug delivery:the second generation of bioadhesives. Journal of Controlled Release, 65, 19-29.
79. Wirth, M., Gerhadt, K., Wurm, C. and Gabor, F.J. (2002) Lectin-mediated drug delivery: influence of mucin on cytoadhesion of plant lectins in vitro. Journal of Controlled Release, 79, 183-191.
80. Byoung-Yun, K., Jeong, J.H., Kinam, P. and Jong-Duk, K. (2005) Bioadhesive interaction and hypoglycemic effect of insulin-loaded lectin-microparticle conjugates in oral insulin delivery system. Journal of Controlled Release, 102, 525-538.
81. Wood, K.M., Stone, M.G. and Peppas, N.A. (2008) Wheat germ functionalized complexation hydrogels for oral insulin delivery. Biomacromolecules, 9, 1293-1298.
82. Guggi, D., Kast, C.E. and Bernkop-Schnurch, A. (2003a) In vivo evaluation of an oral salmon calcitonin-delivery system based ona thiolated chitosan carrier matrix. Pharmaceutical Research, 20, 1989-1994.
83. Hillaireau, H. and Couvreur, P. (2006) Polymeric nanoparticles as drug carriers. In I. F. Uchegbu and A.G. Schatzlein [Ed] Polymers in drug delivery. Taylor and Francis group, Boca Raton, 101-110.
84. Ponchel, G. and Irache, J. (1998) Specific and non-specific bioadhesive particulate systems for oral delivery to the gastrointestinal tract. Advanced Drug Delivery Reviews, 34(2-3), 191-219.
85. Desai, M.P., Labhasetwar, V., Walter, E., Levy, R.J. and Amidon G.L. (1997) The mechanism of uptake of biodegradable microparticles in Caco-2 cells is size-dependent. Pharmaceutical Research, 14, 1568-1573.
86. Damge, C., Michel, C., Aprahamian, M., Couvreur, P. and Devissaguet, J. (1990) Nanocapsules as carriers for oral peptide delivery. Journal of Controlled Release, 13(2-3), 233-239.
87. Damge, C., Vranckx, H., Balschmidt, P. and Couvreur, P. (1997) Poly(alkylcyanoacrylate) nanospheres for oral administration of insulin. Journal of Pharmaceutical Sciences, 86(12), 1403-1409.
88. Brayden, D.J., Jepson, M.A. and Baird A.W. (2005) Keynote review: Intestinal Peyer's patch M cells and oral vaccine targeting. Drug Discovery Today, 10, 1145-1157.

89. Jung, T., Kamm, W., Breitenbach, A., Xiao, J.X., Kissel, T. and Kaiserling, E. (2000) Biodegradable nanoparticles for oral delivery of peptides: is there a role for polymers to affect mucosal uptake? European Journal of Pharmaceutical Biopharmaceutics, 50(1), 147-160.
90. Damge, C., Michel, C., Aprahamian, M., Humbert, W. and Devissaguet, J. (1987) Transmucosal passage of polyalkylcyanoacrylate nanocapsules as a new drug carrier in the small intestine. Biology of the Cell, 61(1-2), 69-76.
91. Pan, Y., Li, Y., Zhao, H., Zheng, J., Xu, H., Wei, G., Hao, J. and Cui, F.D. (2002) Bioadhesive polysaccharides in protein delivery syatem: chitosan nanoparticles improve the intestinal absorption of insulin in vivo. International Journal of Pharmaceutics, 249, 139-147.
92. Ma, Z., Lim, T.M. and Lim, L.Y. (2005) Pharmacological activity of peroral chitosan-insulin nanoparticles in diabetic rats. International Journal of Pharmaceutics, 293(1-2), 271-280.
93. Sarmento, B., Ribeiro, A., Veiga, F., Ferreira, D. and Neufeld, R. Oral bioavailability of insulin contained in polysaccharide nanoparticles. Biomacromolecules, 8(10), 3054-3060.
94. Foss, A.C, Goto, T., Morishita, M, Peppas, N.A. (2004) Development of acrylic based copolymers for oral insulin delivery. European Journal of Pharmaceutical Biopharmaceutics, 57, 163-169.
95. Chalasani, K.B., Russell-Jones, G.J., Akhlesh, K.J., Diwan, P.V. and Jain, K.S. (2007) Effective oral delivery of insulin in animal models using vitamin B12-coated dextran nanoparticles. Journal of Controlled Release, 122, 141-150.
96. Radwan, M.A. (2001) Enhancement of absorption of insulin-loaded polyisobutylcyanoacrylate nanospheres by sodium cholate after oral and subcutaneous administration in diabetic rats. Drug Development and Industrial Pharmacy, 27(9), 981-989.
97. Brange, J. and Langkjaer, L. (1992) Chemical stability of insulin. 3. Influence of excipients, formulation, and pH. Acta Pharmaceutica Nordica, 4(3), 148-158.
98. Ginty, P.J., Howdle, S.M., Rose, R.A.J. and Shakesheff, M.K. (2006) An assessment of the role of polymers for drug delivery in tissue engineering. In I. F. Uchegbu and A.G. Schatzlein [Ed] Polymers in drug delivery. Taylor and Francis group, Boca Raton, 62-80.

99. Pappo, J. and Ermak, T.H. (1989) Uptake and translocation of fluorescent latex particles by rabbit Peyer's patch follicle epithelium: a quantitative model for M cell uptake. Clinical Experimental Immunology, 76, 144-148.

100. Hodges, G.M., Carr, E.A., Carr, K.A. and Hazzard, R.A. (1989) Uptake and translocation of microparticles in small intestine. Digestive Diseases and Science, 40, 967-975.

101. Morishita, M., Goto, T., Peppas, A.N., Joseph, J.I., Torjman, M.C., Munsick, C., Nakamura, K., Yamagata, T., Takayama, K. and Lowman, A.M. (2004) Mucosal insulin delivery systems based on complexation polymer hydrogels: effect of particle size on insulin enteral absorption. Journal of Controlled Release, 97, 115-124.

102. Peppas, N.A. (2004) Devices based on intelligent biopolymers for oral protein delivery.

103. Teply, B.A., Tong, R., Jeong, S.Y., Luther, G., Sherifi, I., Yim, C.H., Khademhosseini, A., Farokhzad, O.C., Langer, R.S. and Cheng, J. (2008) The use of charge-coupled polymeric microparticles and micromagnets for modulating the bioavailability of orally delivered macromolecules. Biomaterials, 29, 1216-1223.

104. Sprangler, R.S. (1990) Insulin administration via liposomes. Diabetes care, 13(9), 911-922.

105. Ubaidulla, U., Sultana, Y., Ahmed, F.J., Khar, R.K. and Panda, A.K. (2007) Chitosan pthalate microspheres for oral delivery of insulin: preparation, characterisation and in vitro evaluation. Drug Delivery, 14(1), 19-23.

106. Gowthamarajan, K. and Kulkarni, G.T.(2003) Oral insulin-fact or fiction? Possibilities of achieving oral delivery of insulin. Resonance, 38-46.

107. Wu Z.H. Ping, Q.N., Song, Y.M., Lei, X.M., Li J.Y. and Cai P.(2004) Studies on the insulin-liposomes double coated by chitosan and chitosan-EDTA conjugates. *Yao Xue Xue Bao,* 39(11), 933-938.

108. Goto, T., Morishita, M., Nishimura, K., Nakanishi, M., Kato, A., Ehara, J. and Takayama, K. (2006) Novel mucosal insulin delivery systems based on fusogenic liposomes. Pharmaceutical Research, 23, 384-391.

109. Takeuchi, H., **Matsui Y., Yamamoto, H. and Kawashima**, Y. (2003) Mucoadhesive properties of carbopol or chitosan-coated liposomes and their effectiveness in the oral administration of calcitonin to rats. Journal of Controlled Release, 86, 235-242.

110. Hoffman, A.S. (2002) Hydrogels for biomedical application. Advanced Drug Delivery Reviews, 11, 109.

111. Jeong, S.H., Huh, K.M. and Park, K. (2006) Hydrogel drug delivery systems. In I. F. Uchegbu and A.G. Schatzlein [Ed] Polymers in drug delivery. Taylor and Francis group, Boca Raton, 49-61.

112. Ichikawa, H. and Peppas, N.A. (2001) Synthesis and characterization of pH-responsive nanosized hydrogels of poly(methacrylic acid-g-ethylene glycol) for oral peptide delivery. In New trends in polymers for oral and parenteral administration: from design to receptors. Baratt, G., Duchene, D.F. and Legendre J.Y. [Eds], Editions de Sante, Paris, France, 261-264.

113. Lowman, A.M., Cowans, B.A. and Peppas, N.A. (2000) Investigation of interpolymer complexation in swollen polyelectrolyte networks by solid state NMR spectroscopy. Journal of Polymer Science and Polymer Physics, 38, 2823-2831.

114. Garcia, M., Torres-Lugo, M., Alonso, M.J. and Peppas, N.A. (2001) Biointeractions of pH-sensitive poly(methacrylic acid-g-ethylene glycol) hydrogel microspheres with the Caco-2 model cell line. In New trends in polymers for oral and parenteral administration: from design to receptors. Baratt, G., Duchene, D.F. and Legendre J.Y. [Eds], Editions de Sante, Paris, France, 386-389.

115. Ichikawa, H. and Peppas, N.A. (2003) Novel complexation hydrogels for oral peptide delivery: In vitro evaluation of their cytocompatibility and insulin-transport enhancing effects using Caco-2 cell monolayers. Journal of Biomedical Materials Research, 67, 609-617.

116. Ito, Y., Casolaro, M., Kono, K. and Imanishi, Y. (1989) An insulin-releasing system that is responsive to glucose. Journal of Controlled Release, 10, 195.

117. Brownlee, M. and Cerami, A. (1979) A glucose-controlled insulin-delivery system: semisynthetic insulin bound to lectin. Science, 206, 1190.

118. Kitano, S. Koyama, Y., Kataoka, K., Okano, T. and Sakurai, Y. (1992) A novel drug delivery system utilizing a glucose responsive polymer complex between poly(vinyl)alcohol and poly(N-vinyl-2-pyrrolidone) with a phenylboronic acid moiety. Journal of Controlled Release, 19, 161.

119. Yin, L., Fei, L., Cui, F., Tang, C. and Yin, C. (2007) Superporous hydrogels containing poly(acrylic acid-co-acrylamide)/O-carboxymethyl chitosan interpenetrating polymer networks. Biomaterials, 28, 1258-1266.

120. Musabayne, C.T., Munjeri, O., Bwititi, P. and Osim, E.E. (2000) Orally administered, insulin-loaded amidated pectin hydrogel beads sustain plasma concentrations of insulin in streptozocin-induced diabetic rats. Journal of Endocrinology, 164, 1-6.

121. Ramkissoon-Ganorkar, C., Liu, F., Baudys, M. and Kim, S. W. (1999) Modulating insulin-release profile from pH/thermosensitive polymeric beads through polymer molecular weight. Journal of Controlled Release, 59, 287-298.
122. Qiu, Y. and Park, K. (2001) Environment-sensitive hydrogels for drug delivery. Advanced Drug Delivery Reviews, 53, 321.
123. Kubisa, P. (2004) Terminology of polymers containing ionizable or ionic groups and of polymers containing ions. IUPAC recommendations (draft 23, December, 2004).
124. Mao, S., Germershaus, O., Fischer, D., Linn, T., Schnepf, R. and Kissel, T. (2005) Uptake and transport of PEG-graft-trimethyl-chitosan copolymer-insulin nanocomplexes by epithelial cells. Pharmaceutical Research, 22, 2058-2068.
125. Hartig, S.M., Carlesso, G., Davidson, J.M. and Prokop, A. (2007) Development of improved nanoparticulate polyelectrolyte complex physicochemistry by nonstoichiometric mixing of polyions with similar molecular weights. Biomacromolecules, 8, 265-272.
126. Kokofuta, E. (1979) Colloid titration behaviour of poly(ethyleneimine). Macromolecules, 12, 350-353.
127. Tsuchida, E. (1994) Formation of polyelectrolyte complexes and their structures. Journal of Macromolecular Science And Pure Applied Chemistry, A31, 1-15.
128. Lankalapalli, S. and Kolapalli, V.R.M. (2009) Polyelectrolyte complexes: A review of their applicability in drug delivery technology. Indian Journal of Pharmaceutical Sciences, 71(5), 481-487.
129. Overbeek, J. T. and Voorn, M. J. (1957) Phase separation in polyelectrolyte solutions: Theory of complex coacervation. Journal of Cellular and Comparative Physiology, 49:7-26.
130. Webster, L. and Huglin, M. B. (1997) Observations on complex formation between polyelectrolytes in dilute aqueous solution. European Polymer Journal, 339:1173-7.
131. Gamzazade, A. I. and Nasibov, S. M. (2002) Formation and properties of polyelectrolyte complexes of chitosan hydrochloride and sodium dextransulfate. Carbohydrate Polymers, 50:339-43.
132. Shiratori, S. S. and Rubner, M. F. (2000) pH-Dependent thickness behavior of sequentially adsorbed layers of weak polyelectrolytes. Macromolecules, 33:4213-9.
133. Herbert, D. (2001) Light scattering studies on polyelectrolyte complexes. Macromolecular Symposia, 162:1-22.

134. Alexander, K. and Monica, O. D. (2004) Precipitation of oppositely charged polyelectrolytes in salt solutions. Journal of Physical Chemistry, 20:404-12

135. Fredheim, G. E. and Christensen, B. E. (2003) Polyelectrolyte complexes: Interactions between lignosulfonate and chitosan. Biomacromolecules, 4:232-9.

136. Thompson, C.J., Ding, C., Qu, X., Yang, Z., Uchegbu, I.F., Tetley, L. and Cheng, W.P. (2008) The effect of polymer architecture on the nano self-assemblies based on novel comb-shaped amphiphillic poly(allylamine). Colloid and Polymer Science, 286, 1511-1526.

137. Thompson, C.J., Tetley, L., Uchegbu, I.F. and Cheng, W.P. (2009B) The complex between novel comb shaped amphiphillic polyallyamine and insulin –Towards oral insulin delivery. International Journal of Pharmaceutics, 376, 216-227.

138. Thompson, C.J., Tetley, L. and Cheng, W.P. (2010) The influence of polymer architecture on the protective effect of novel comb-shaped amphiphillic poly(allylamine) against in vitro enzymatic degradation of insulin- Towards oral insulin delivery. International Journal of Pharmaceutics, 260(2), 229-237.

139. Dailey, L.A., Wittmar, M. and Kissel, T. (2005) The role of branched polyesters and their modifications in the development of modern drug delivery vehicles. Journal of Controlled Release, 101, 137-149.

140. Simon, M., Wittmar, M., Bakowsky, U. and Kissel, T.(2004) Self-assembling nanocomplexes from insulin and water-soluble branched polyesters, poly[(vinyl-3-(diethylamino)-propylcarbamate-co-(vinylacetate)-co-(vinylalcohol)-graft-poly(L-lactic acid): A novel carrier for transmucosal delivery of peptides. Bioconjjugate Chemistry, 15, 841-849.

141. Thanou, M., Verhoef, J.C. and Junginger, H.E. (2001a) Oral drug absorption enhancement by chitosan and its derivatives. Advanced Drug Delivery Reviews, 52, 117-126.

142. Sadeghi, A.M.M., Dorkoosh, F.A., Avadi, M.R., Weinhold, M., Bayat, A., Delie, F., Gurny, R., Larijani, B., Rafiee-Tehrani, M. and Junginger, H.E. (2008b) Permeation enhancer effect of chitosan and chitosan derivatives: comparison of formulations as soluble polymers and nanoparticulate systems on insulin absorption in Caco-2 cells. European Journal of Pharmaceutics and Biopharmaceutics, 70, 270-278.

143. Kotze, A.F., Leuben, H.L., de Leeuw, B.J., de Boer, A.G., Verhoef, J.C. and Junginger, H.E. (1997a) Chitosans for enhanced delivery of therapeutic peptides across intestinal

epithelia: in vitro evaluation in Caco-2 cell monolayers. International Journal of Pharmaceutics, 159, 243-253.

144. Domard, A., Rinaudo, M. and Terrasin, C. (1986) New method for the quaternization of chitosan. International Journal of Biological Macromolecules, 8(2), 105-107.

145. Jonker, C., Hamman, J.H. and Kotze, A.F. (2002) Intestinal paracellular permeation enhancement with quaternized chitosan : in situ and in vitro evaluation. International Journal of Pharmaceutics, 238, 205-213.

146. Hamman, J.H., Schultz, C.M. and Kotze, A.F. (2003) N-trimethyl chitosan chloride: optimum degree of quaternization for drug absorption enhancement across epithelial cells. Drug Development and Industrial Pharmacy.

147. Yin, L., Ding, J., He, C., Cui, L., Tang, C. and Yin, C. (2009) Drug permeability and mucoadhesion properties of thiolated trimethyl chitosan nanoparticles in oral insulin delivery. Biomaterials, 30, 5691-5700.

148. Jintapattanakit, A., Junyaprasert, V.B., Mao, S., Sitterberg, J., Bakowsky, U. and Kissel, T. (2007) Peroral delivery of insulin using chitosan derivatives; a comparative study of polyelectrolyte nanocomplexes and nanoparticles. International Journal of Pharmaceutics, 342, 240-249.

149. Bernkop-Schnurch, A., Hornof, M. and Zoidl, T. (2003) Thiolated polymers-thiomers: synthesis and in vitro evaluation of chitosan-2-iminothiolane conjugates. International Journal of Pharmaceutics, 260(2), 229-237.

150. Vigl, C., Leitner, K., Albrecht, K. and Bernkop-Schnurch, A. (2009) The efflux pump inhibitory properties of (thiolated) polyallylamines. Journal of Drug Delivery Science and Technology, 19 (6), 405-411.

151. Roldo, M., Hornof, M., Caliceti, P. and Bernkop-Schnurch, A. (2004) Mucoadhesive thiolated chitosans as platforms for oral controlled drug delivery: synthesis and in vitro evaluation. European Journal of Pharmaceutics and Biopharmaceutics, 57, 115-121.

152. Modi, J., Joshi, G. and Sawant, K. (2012) Chitosan based mucoadhesive nanoparticles of ketoconazole for bioavailability enhancement: formulation, optimisation, *in vitro* and *ex vivo* evaluation. Drug Development and Industrial Pharmacy, 10, 1-8.

153. Bacalocostantis, I., Mane, V.P., Kang, M.S., Goodley, A.S., Muro, S. and Kofinas, P. (2012) Effect of thiol pendant conjugates on plasmid DNA binding, release and stability of polymeric delivery vectors. Biomacromolecules, 13, 1331-1339.

154. Damink, L.H.H.O., Dijkstra, P.J., Vanluyn, M.J.A., Vanwachem, P.B., Nieuwenhuis, P. and Feijen, J. (1996) Cross-linking of dermal sheep collagen using a water soluble carbodiimide. Biomaterials, 17, 765-773.

155. Bernkop-Schnurch, A., Krauland, A.H., Leitner, K. and Palmberger, T. (2004) Thiomers: potential excipients for non-invasive peptide delivery systems. European Journal of Pharmaceutics and Biopharmaceutics, 58, 253-263.

156. Millotti, G., Samberger, C., Frohlich, E. and Bernkop-Schnurch, A. (2009) Chitosan-graft-6-mercaptonicotinic acid: synthesis, characterisation and biocompatibility. Biomacromolecules, 10, 3023-3027.

157. Cevher, E., Sensoy, D., Taha, M.A.M. and Araman, A. (2008) Effect of thiolated polymers to textural and mucoadhesive properties of vaginal formulations prepared with polycarbophil and chitosan. AAPS Pharmaceutical Science and Technology, 9, 3.

158. Picquart, M., Abedinzadeh, Z., Grajcar, L. and Baron, H.M. (1998) Spectroscopic study of N-acetylcysteine and N-acetylcystine/hydrogen peroxide complexation. Chemical Physics, 228, 279-291.

159. Millotti, G., Bernkop-Schnurch, A., Perera, G., Hombach, J. and Sakloetsakun, D. (2010) The impact of vehicles on the mucoadhesive properties of orally administered nanoparticles: a case study with chitosan-4-thiobutylamidine conjugate. AAPS Pharmaceutical Science and Technology, 11, 3.

160. Yudovin-Farber, I., Golenser, J., Beyth, N., Weiss, E.I.and Domb, A.J. (2010) Quaternary ammonium polyethyleneimine: antibacterial activity. Journal of Nanomaterials, Volume 2010, Article ID 826343, 11 pages doi:10.1155/2010/826343

161. Juntaprama, K., Praphairaksitb, N., Siraleartmukulc, K. and Muangsind, N. (2012) Synthesis and characterisation of chitosan-homocysteine thiolactone as a mucoadhesive polymer. Carbohydrate Polymers, 87, 2399-2408.

162. Hoffman, S. A. (2006) Selecting the right polymer for biomaterial application. In I. F. Uchegbu and A.G. Schatzlein [Ed] Polymers in drug delivery. Taylor and Francis group, Boca Raton, 7-22.

163. Buckton, G. (2002) Solid-state properties In: M.E. Aulton [2nd Ed]. Pharmaceutics: The science of dosage form design. Churchill Livingstone, Edinburgh, 141-151.

164. Billmeyer, F. W. Jr. (1984) *Textbook of Polymer Science*, 3rd Edition. Wiley-Interscience, New York.

165. Rodriguez, F. (1996) *Principles of Polymer Systems*. 4th Edition. Hemisphere, New York.

166. He. C, Hu, Y., Yin, L., Tang, C. and Yin, C. (2010) Effects of particle size and surface charge on cellular uptake and biodistribution of polymeric nanoparticles. Biomaterials, 31, 3657-3666.

167. Longer, M.A and Robinson, J. R. (1986) Fundamental aspects of bioadhesion. Pharmaceutics International, 114-117.

168. Hamman, J.H., Kotze, A.F. and Schultz, C.M. (2003) N-trimethyl chitosan chloride: optimum degree of quaternisation for drug absorption enhancement across epithelial cells. Drug Development and Industrial Pharmacy, 29, 161-172.

169. Hamman, J.H., Kotze, A.F. and Synman, D. (2003) Evaluation of the mucoadhesive properties of N-trimethyl chitosan chloride. Drug Development and Industrial Pharmacy, 29, 59-67.

170. Leitner, V.M., Walker, G.F. and Bernkop-Schnurch, A. (2003) Thiolated polymers: evidence for the formation of disulphide bonds with mucus glycoproteins. European Journal of Pharmaceutics and Biopharmaceutics, 56, 207-214.

171. Cullis, C.F. and Trimm, D.L. (1968) Homogenous catalysis of the oxidation of thiols by metal ions. Discussions of the Faraday Society, 46, 144-149.

172. Eisley, L. (2010) Water: The medium of Life. In: R. Garrett and C.M. Grisham [Ed] Biochemistry. Brooks/Cole, Boston, USA, 28-47

173. Snyder, G.H., Reddy, M. K., Cennerazzo, M. J. and Field, D. (1983) Use of local electrostatic environments of cysteines to enhance formation of a desired species in a reversible disulfide exchange reaction. Biochim Biophys Acta 749, 219–226.

174. Bernkop-Schnurch, A. and Thaler, C.S. (2000) Polycarbophil-cysteine conjugates as platforms for oral polypeptide delivery systems. Journal of Pharmaceutical Science, 89(7), 901-909.

175. Bernkop-Schnurch, A. and Marschutz, M.K. (2002) Thiolated polymers: self-crosslinking properties of thiolated 45-kDa poly(acrylic acid) and their influence on mucoadhesion. European Journal of Pharmaceutical Science, 15, 387-394.

176. Hunter, R.J. (1988) Zeta potential in colloid science, Principles and applications. Academic Press, UK.

177. Attwood, D. (2002) Disperse systems. In: M.E. Aulton [2nd Ed]. Pharmaceutics: The science of dosage form design. Churchill Livingstone, Edinburgh, 70-100.

178. Ravina, L. and Moramarco. N (1993) Everything you need to know about coagulation and flocculation. 4th Ed. Zeta-meter, Inc. Virginia, USA.

179. Dautzenberg, H. (1997) Polyelectrolyte complex formation in highly aggregating systems. 1. Effect of salt: polyelectrolyte complex formation in the presence of NaCl. Macromolcules, 30, 7810-7815.

180. Hamman, J.H., Enslin, G.M.and Kotze, A.F. (2005) Oral delivery of peptide drugs-barriers and developments. Biodrugs, 19 (3), 165-177.

181. Shakweh, M., Besnard, M., Nicolas, V. and Fattal, E. (2005) Poly(lactide-co-glycolide) particles of different physicochemical properties and their uptake by Peyer's patches in mice. European Journal of Pharmaceutical Biopharmaceutics, 61, 1-13.

182. Zimm, B.H. (1948) The scattering of light and the radial distribution function of high polymer solutions. Journal of Physical Chemistry, 16(12), 1093-1099.

183. Wang, W., Tetley, L. and Uchegbu, I.F. (2001) The level of hydrophobic substitution and the molecular weight of amphiphillic poly-L-lysine-based polymers strongly affects their assembly into polymeric bilayer vessicles. Journal of Colloid Interfacial Science, 237, 200-207.

184. Uchegbu, F., Anderson, S. and Brownlie, A.(2006) Polymeric vessicles. In I. F. Uchegbu and A.G. Schatzlein [Ed] Polymers in drug delivery. Taylor and Francis group, Boca Raton, 131-153.

185. Kotz, J., Tiersch, B. and Bogen, I. (2000) Polyelectrolyte-induced vesicle formation in lamellar liquid-crystalline model systems. Colloid Polymer Science, 278, 164-168.

186. Schilling, R.J. and Mitra, A.K (1991) Degradation of insulin by trypsin and alpha-chymotrypsin. Pharmaceutical Research, 8(6), 721-727.

187. Zhang, L., Jang, H., Zhu, W., Lin, W., Song, L., Wu. Q. and Ren. Y. (2008) Improving the stability of insulin in solutions containing intestinal proteases *in vitro*. International Journal of Molecular Sciences, 9, 2376-2387.

188. Sajeesh, S., Bouchemal, K. , Sharma, C. P. and Vauthier, C. (2010) Thiol-functionalized polymethacrylic acid based hydrogel microparticles for oral drug delivery. European Journal of Pharmaceutics and Biopharmaceutics, 74, 209-218.

189. Ibie, C. and Thompson, C. J. (2011) The oral delivery of proteins using interpolymer polyelectrolyte complexes. Therapeutic Delivery, 2(12), 1611-1631.

190. Lin A, Liu Y, Huang Y, Sun J, Wu Z, Zhang X and Ping, Q. (2008) Glycyrrhizin surface-modified chitosan nanoparticles for hepatocyte-targeted delivery. International Journal of Pharmaceutics, 359(1–2), 247–53.

191. Ma, O., Lavertu, M., Sun, J., Nguyen, S., Buschmann, F.M. , Winnik, M.F. and Hoemann, C. D. (2008) Precise derivatization of structurally distinct chitosans with rhodamine B isothiocyanate. Carbohydrate Polymers, 72, 616–624.

192. Thompson, C. J., Pramod, G., Skene, K., Smith, M., Smith, G., Mckinnon, A., Cheng, W.P. and Knott, R. (2011) Uptake and transport of novel amphiphillic polyelectrolyte-insulin nanocomplexes by Caco-2 cells-towards oral insulin delivery. Pharmaceutical Research, 28, 886-896.

193. Tyrer, P., Foxwell, R., Kyd, J., Harvey, M., Sizer, P. and Cripps, A. (2002) Validation and quantitation of an in vitro M-cell model. Biochemical and Biophysical Research Communications, 299, 377–383.

194. Mosmann, T. (1983). "Rapid colorimetric assay for cellular growth and survival: application to proliferation and cytotoxicity assays". Journal of Immunological Methods, 65 (1–2): 55–63.

195. David, M., Morgan, L., Clover, J. and Pearson, J.D. (1988) Effects of synthetic polycations on leucine incorporation, lactate dehydrogenase release and morphology of human umbilical vein endothelial cells. Journal of Cell Science, 91, 231-238.

196. Slita, A.V., Kasyanenko, N.A., Nazarova, O.V., Gavrilova I.I et al (2007) DNA-polycation complexes: effect of polycation structure on physic-chemical and biological properties. Journal of Biotechnology, 127, 679-693.

197. Brownlie, A., Uchegbu, I.F. and Schatzlein, A.G. (2004) PEI based vesicle-polymer hybrid gene delivery system with improved biocompatibility. International Journal of Pharmaceutics, 274, 41-52.

198. Wang, J., Gao, S.J., Zhang, P.C., Wang, S., Mao, H.Q., Leong, K.W. (2004b) Polyphosphoramide gene carriers: effect of charge group on gene transfer efficiency. Gene Therapeutics. 11, 1001–1010.

199. Dwivedi, P. D., Tripathi. A, Ansari. K. M., Shanker, R. and Das, M. (2011) Impact of nanoparticles on the immune system. Journal of Biomedical Nanotechnology, 7(1).193-4.

200. Dufes, C., Uchegbu, I.F. and Schatzlein, A.G. (2004) Dendrimers in drug and gene delivery In I. F. Uchegbu and A.G. Schatzlein [Ed] Polymers in drug delivery. Taylor and Francis group, Boca Raton, 199-235.

201. Fischer, D., Li, Y.X., Ahlemeyer, B., Krieglstein, J., Kissel, T., 2003. In vitro cytotoxicitytesting of polycations: influence of polymer structure on cell viability and haemolysis. Biomaterials 24, 1121–1131.

202. Malik N, Wiwattanapatapee R, Klopsch R, Lorenz K, Frey H, Weener JW, Meijer EW, Paulus W, Duncan R (2000) Dendrimers: relationship between structure and biocompatibility in vitro, and preliminary studies on the biodistribution of 125I-labelled polyamidoamine dendrimers *in vivo*. Journal of Controlled Release, 65(1-2), 133-148.

203. Florence, A.T., Sakhivel, T. and Toth, I. (2000) Oral uptake and translocation of a polylysine dendrimer with a lipid surface. Journal of Controlled Release, 65(1-2), 253-259.

204. Lundstrom-Ljung, J. and Holmgren, A. (1998) in Prolyl Hydroxylase, Protein Disulfide Isomerase, and Other Structurally Related Proteins, ed. Guzman, N. A. (Dekker, New York), pp. 297–314.

205. Harris, J.M. and Chess, R.B. (2003) Effect of pegylation on pharmaceuticals. Nature Review Drug Discovery, 2(3), 214-221.

206. Buts, J.P., De Keyser, N., Marandi, S. et al. (1997) Expression of insulin receptors and of 60-kDa receptor substrate in rat mature and immature enterocytes. American Journal of Physiology, Gastrointestinal and Liver Physiology, 273, G217-G226.

207. King, G.L. and Johnson, S. (1985) Processing and transport of insulin by vascular endothelial cells. Effects of sulfonylureas on insulin receptors. Science, 227, 183-1586.

208. Russell-Jones, G. (2011) Intestinal receptor targeting for peptide delivery: an expert's personal perspective on reasons for failure and new opportunities. Therapeutic Delivery, 2(12), 1575-1593.

209. Petrus, A.K. Fairchild, T.J. and Doyle, R.P. (2009) Traveling the Vit B_{12} pathway: oral delivery of protein and peptide drugs. Angew. Chem. Int. Ed. Engl., 48, 1022-1028.

SUPPORTING STUDIES

- Attainment of the post graduate certificate in research methods 2009-2010.
- Presentation at the Robert Gordon University research student symposium, 2010.
- Attendance at Northern Research Partnership Symposium, December 2010.
- Attendance and poster presentation at the Institute for Health and Welfare Research Showcase, May 2012.
- Academy of Pharmaceutical Scientists of Great Britain (APSGB) - PhD project Abstract accepted for poster award at 2013 conference.

COMMUNICATIONS ASSOCIATED WITH THE THESIS

- Thompson, C. and Ibie, C. (2011) The oral delivery of proteins using interpolymer polyelectrolyte complexes. Therapeutic Delivery 2(12), 1611-1631.